# Identifying novel biocontrol agents from New Zealand kiwifruit orchards

Javier Martínez Pérez

John Innes Centre

Norwich, September 2022

© A thesis submitted in fulfilment of the requirements for the degree of Doctor of Philosophy at the University of East Anglia. This copy of the thesis has been supplied on condition that anyone who consults it is understood to recognise that its copyright rests with the author and that use of any information derived therefrom must be in accordance with current UK Copyright Law. In addition, any quotation or extract must include full attribution.

# **CONTENTS**

ABSTRACT	7
ACKNOWLEDGEMENTS	8
LISTS OF FIGURES	10
LIST OF TABLES	16
APPENDIX	18
ABBREVIATIONS	20
CHAPTER 1: INTRODUCTION	23
1.1. Psa: a global problem	23
1.2. Dispersion and infection of <i>Psa</i>	25
1.3. The economic impact of <i>Psa</i> in New Zealand	26
1.4. Current control methods of <i>Psa</i>	26
1.5. A future perspective: biocontrol agents	28
1.6. The kiwifruit microbiome	29
1.7. Pseudomonas spp. as a biocontrol toolbox	30
1.8. Natural products: key in crop protection	31
1.9. Aims and objectives	33
1.9.1. Research objectives:	33
CHAPTER 2: MATERIALS AND METHODS	36
2.1. Growing media	36
2.1.1. LB medium	36
2.1.2. KB medium	36
2.1.3. CFC medium	36
2.1.4. SFM medium	36
2.1.5. FP medium	37
2.1.6. DNA medium	37
2.2. Bacterial sample collection and isolation	37
2.2.1. Orchards location	37
2.2.2. Samples collection	38
2.2.3. Samples processing	39

2.2.4. Bacterial isolation and collection preparation	41
2.2.5. Shipping of bacterial collection	41
2.2.6. Samples sorting	42
2.3. Bacterial phenotyping assays	42
2.3.1. Colony morphology	43
2.3.2. Siderophore production	43
2.3.3. Hydrogen cyanide production	44
2.3.4. Protease production	44
2.3.5. Swarming motility	45
2.3.6. Congo Red binding	46
2.3.7. Streptomyces scabies suppression	46
2.3.7.1. Liquid-culture overlay for <i>Psa</i> suppression	47
2.3.8. Copper sulphate resistance	48
2.3.9. Streptomycin resistance	48
2.3.10. Kasugamycin resistance	49
2.4. Bacterial genotyping and data analysis	50
2.4.1. Genomic DNA extraction	50
2.4.1.1. Storage and quality check	51
2.4.2. PCR and gel electroporation	52
2.4.2.1. PCR	52
2.4.2.2. Gel electroporation	53
2.4.2.3. Illumina® whole genome sequencing	53
2.4.3. Genome mining for NPs clusters	54
2.4.3.1. AntiSMASH	54
2.4.4. Phylogenetics and bioinformatic analyses	55
2.4.4.1. Genotyping of Pseudomonas spp.	55
2.5. Genetic manipulation of <i>Pseudomonas</i> spp.	55
2.5.1. Electrotransformation	55
2.5.2. Transposon screening	56
2.5.3. Chemically competent cells	57

2	2.5.4. Conjugation	57
2.6	. Extraction and concentration of bioactive metabolites	57
2.7	. Plant experiments	58
2	2.7.1. Dip-inoculation pathogenicity assays	58
2	2.7.2. In planta biocontrol assays with model plants	59
2	2.7.3. In planta biocontrol assays with kiwifruit vines	60
	2.7.4.1. Assessment	61
2.8	. Statistical analysis	62
2	2.8.1. Correlation analysis	62
2	2.8.2. ANOVA test	62
2	2.8.3. Statistical analysis of kiwifruit biocontrol results	63
2.9	. Bacteria spore harvesting	63
	2.9.1. Streptomyces spp	63
СН	APTER 3: BACTERIAL ISOLATION AND CHARACTERISATION	65
3.1	. Introduction	65
3.2	. Aims	67
3.3	. Results	67
3	3.3.1. Isolation of kiwifruit-associated bacteria from infected and uninfected orchards	67
3	3.3.2. High-throughput phenotypical screening of bacteria	68
	3.3.2.1. Colony morphology	68
	3.3.2.2. Siderophore production	69
	3.3.2.3. Hydrogen cyanide production	70
	3.3.2.4. Protease production	71
	3.3.2.5. Swarming motility	72
	3.3.2.6. Congo Red binding	73
	3.3.2.7. Streptomyces scabies suppression	74
	3.3.2.8. Streptomyces venezuelae suppression	75
	3.3.2.9. Psa suppression	76
	3.3.2.10. Copper resistance	77
	3.3.2.11. Streptomycin resistance	78

3.3.2.12. Kasugamycin resistance	79
3.3.3. Phenotypic correlations	81
3.3.3.1. Phenotypic correlation for isolates from all four locations	81
3.3.3.2. Phenotypic correlation per location	81
3.3.3.3. Phenotypic correlation between <i>Psa</i> -infected and uninfected orchards	82
3.3.3.5. Phenotypic correlation between visually symptomatic and asymptomatic samples	82
3.3.3.6. Phenotypic correlation between <i>Psa</i> -inhibitory and non-inhibitory strains	83
3.4. Genome sequencing	85
3.4.1. Phylogenetic trees	85
3.5. Discussion	88
CHAPTER 4: GENOME MINING AND BIOINFORMATIC ANALYSIS OF AGROCHEMICAL RESIST. GENES	
4.1. Introduction	91
4.2. Aims	92
4.3. Results	93
4.3.1. Correlation analysis of copper and streptomycin resistance genes	93
4.3.2. Phylogenetic tree	94
4.3.3. Investigating the distribution of copper and streptomycin resistance genes	97
4.4. Discussion	.101
CHAPTER 5: BIOCONTROL AND PATHOGENICITY EXPERIMENTS	.105
5.1. Introduction	.105
5.2. Aims	.106
5.3. Results	.106
5.3.1. Pathogenicity assay by dip-inoculation	.106
5.3.2. Biocontrol assays with model plants	.109
5.3.4. Biocontrol assays with kiwifruit vines	.112
5.4. Discussion	.116
CHAPTER 6: GENETIC MANIPULATION, AND IDENTIFICATION OF BIOSYNTHETIC G	
6.1. Introduction	.120
6.2 Aims	121

5.3. Results	21
6.3.1. Transposon mutagenesis library	21
6.3.1.1. Identification of potential BGCs responsible for <i>Psa</i> biocontrol in strain 4H1212	21
6.3.1.1.1. Preliminary results of next steps with 4H1212	27
6.3.1.2. Identification of potential BGCs responsible for <i>Psa</i> biocontrol in strain 5G913	30
6.3.1.3. Identification of potential BGCs responsible for <i>Psa</i> biocontrol in strain 8H713	32
6.3.1.4. Identification of potential BGCs responsible for <i>Psa</i> biocontrol in strain 10A513	34
6.3.2. AntiSMASH analysis for identification of BGCs	36
S.4. Discussion	39
7. GENERAL DISCUSSION AND FUTURE PERSPECTIVES14	43
7.1. Marked differences exist between strains' phenotypic profiles and orchard's locations14	43
7.2. Published copper and streptomycin resistant genes are missing from most copper and streptomyc	in
esistant <i>Pseudomonas</i> strains	14
7.3. <i>Pseudomonas</i> strains strongly suppress <i>Psa</i> biovar 3 infection <i>in planta</i>	45
7.4. Kiwifruit <i>Pseudomonas</i> harbour a high diversity of NPs and biocontrol potential14	46
7.5. Final remarks, industrial applications, and future directions14	47
APPENDIX14	18
REFERENCES	37

#### **ABSTRACT**

Pseudomonas syringae pv. actinidae (Psa) biovar 3 is a major threat to New Zealand's kiwifruit industry. With more than 90% of the production area infected, cumulative losses amount to well over NZ\$1 billion since 2010. The most effective and commonly used treatments for Psa infection are copper compounds and bactericides. However, following the identification of Psa variants resistant to these treatments their long-term efficacy might be in danger. Therefore, there is an urgent need for effective and environmentally friendly treatment options against Psa.

By examining how the naturally-occurring population of kiwifruit-associated *Pseudomonas* strains respond to *Psa* infection, we aimed to discover and characterise novel anti-*Psa* treatments. *In vitro* characterisation of over 1,000 strains helped identify phenotypic traits associated with *Psa*-inhibition, such hydrogen cyanide, siderophore and protease production, and suppression of Gram-positive pathogens such as *Streptomyces scabies*. This characterisation also identified an extremely high correlation between copper and streptomycin resistance. Further analysis determined that genes previously published as essential for copper and streptomycin resistance were missing from most copper and streptomycin resistant strains. Whole genome sequencing and transposon mutagenesis identified phylogenetic clustering among copper and streptomycin resistant strains and several potential novel copper resistant genes.

Thirty-three *Pseudomonas* strains were identified that strongly suppressed *Psa in vitro*. *In planta* biocontrol experiments with these *Psa*-inhibitory *Pseudomonas* highlighted four biocontrol candidates that reduced *Psa* infection in model plants by almost 99%. Further work on kiwifruit vines under greenhouse conditions showed three biocontrol candidates were able to provide effective protection against *Psa*, with G59 performing as well as a commercially available biopesticide. Finally, whole genome sequencing, transposon mutagenesis and automated genome mining helped to unlock the soil *Pseudomonas* biosynthetic potential. We identified and started to characterise Cluster 17, a novel biosynthetic gene cluster (BGC), alongside genes predicted to contribute to other novel biosynthetic gene clusters.

## **Access Condition and Agreement**

Each deposit in UEA Digital Repository is protected by copyright and other intellectual property rights, and duplication or sale of all or part of any of the Data Collections is not permitted, except that material may be duplicated by you for your research use or for educational purposes in electronic or print form. You must obtain permission from the copyright holder, usually the author, for any other use. Exceptions only apply where a deposit may be explicitly provided under a stated licence, such as a Creative Commons licence or Open Government licence.

Electronic or print copies may not be offered, whether for sale or otherwise to anyone, unless explicitly stated under a Creative Commons or Open Government license. Unauthorised reproduction, editing or reformatting for resale purposes is explicitly prohibited (except where approved by the copyright holder themselves) and UEA reserves the right to take immediate 'take down' action on behalf of the copyright and/or rights holder if this Access condition of the UEA Digital Repository is breached. Any material in this database has been supplied on the understanding that it is copyright material and that no quotation from the material may be published without proper acknowledgement.

#### **ACKNOWLEDGEMENTS**

To my family. For your unconditional love and support. Especially to my grandparents, Daniel, Isabel, Pepe, and Carmen. You are the power of my life, happiness, and relentless inspiration. Thank you, mum, and dad, for tirelessly encouraging me, supporting me thought my entire education, and trusting in me. Without you, I would have not made it.

To Jacob Malone, for your exemplar support and tireless guidance. As my line manager, you have been a role model for me, and you will always be. To Andy Truman and Joel Vanneste. Thank you, I had the best research experience of my life. You have inspired and encouraged me on passionately pursuing scientific goals. Thank you to the best lab anyone would dream work at, the "Malone lab". Thank you to all the members and past members that have helped me though these four years. With your technical assistance, life advice, and mental support. I cannot express well enough how amazing has been working with all of you. Special thanks to Alba for keeping me updated on reggaeton trends, Rosaria for accepting my overflow of cakes, to Pla for your enormous help and kindness and Ainelen for your 24/7 help and availability. You guys are one of the main reasons why doing a PhD was such a great fun. To Zespri International Ltd. (sponsors of this PhD project), thank you for supporting research, and proving the future generation of scientists with the economic resources needed. Without your funding I would have not been able to make my dream become true: become a doctor.

Thank you to the Molecular Microbiology department. I had a fantastic time with you all. Coffees, parties and much more beyond your scientific and mental support. To the media kitchen for your relentless patience with my pickiness and the incredible support you provide with media and smiles. To Govind Chandra, for your support, and incredible help with bioinformatics. To Gary Wortley, for being so nice to me despite my continuous avalanche of complaints. To Javier Santos Aberturas, for sharing your wisdom with me as well as your terrible humour. I will never recover. To the students I had the pleasure to supervise. Olivia Johnson, Patsy Whiteman, Ruben Martinez Cuesta and Hazel Surtees, thank you for your help, fresh input of motivation and energy towards learning. To my proof-readers, Alex Durrant, Ainelen Piazza, Juan Falcon Hernandez, Rosaria Campilongo, Catriona Thomson, Alba Pacheco Moreno and Natalia Miguel Vior. You have earned a place in heaven!

To Joel Vasnneste lab, thank you for taking care of me during the first few weeks of my PhD, especially for all you taught me. You were key at the time I was building the motivational foundation of this PhD project. I will always remember you with lots of love. Thank you again, Joel, but also to Deirdre, Janet and Toan.

To all UEA staff that somewhat inspired me through this journey. To Harriet Jones and Tracey Chapman for their confidence and opportunity given to me as demonstrator, allowing me to build new skills through seminars, lab practical and group discussions. To Maria Vardakou for your great charisma and the opportunity you gave me to showcase my science to prospective students.

A big thank you to my external scientific friends. To Victoria Bueno Gonzalez, for your scientific advice, support, and memes. To Ana Martinez Gascueña, for the amazing meals and exploring trips we have done together. To Jake Cridge, for providing me with the best parties in London and a constant flow of memes since 2019. To Alex Durrant for introducing me to Little Britain. You have created a monster. To my Norwich friends from improvisation theatre. You have done so much good to me! You are amazing people and will always bring you in my heart. Thank you, Rosaria, for introducing me to the group and Alastair and Therese for those fun weekends exploring Norfolk. If I was around, of course.

To anyone that I may have forgotten. Thank you for being such amazing human beings. I am lucky to have you.

# LISTS OF FIGURES

Figure 1. Relevant Pseudomonas spp. NPs which are known to have a biocontrol effect against plant
pathogens. Molecules and NP families are shown (Jahanshah, Yan et al. 2019, Santos Kron, Zengerer
et al. 2020, Dagher, Nickzad et al. 2021)
Figure 2. Geographical location of the six orchards from which the 6,123 isolates were isolated. (1)
Karaipiro, (2) Ohaupo, (3) Kaimai Mt, (4) Te Puke, (5) Te Puke and (6) Motueka
Figure 3. Representation of different kiwifruit samples. (A) Mature symptomatic leaf, (B) mature non-
symptomatic leaf, (C) young symptomatic leaf, (D) young non-symptomatic leaf, (E) symptomatic lea
with over 5% necrotic leaf area and (F) non-symptomatic bud (left) and symptomatic bud40
Figure 4. CFC-agar plate with a high number of Pseudomonas spp. isolates, representation of how a
non-biased selection of a section of the plates was chosen and patched on a 24 isolates pattern on KB-
agar41
Figure 5. On the left, dip-inoculation pathogenicity assay. Representation of tomato plants drying after
being inoculated, separated by treatment. On the right, an example of necrotic spots on a tomato plant
inoculated with Psa biovar 3, 7 dpi
Figure 6. Example of high-throughput screening for morphology. In the picture, several hundred strains
48 hpi
Figure 7. Percentage of yellow-pigmented strains across locations. Scoring belongs to (0) white and (1)
yellow colour. Different lowercase letters indicate a significant difference according to one-way analysis
of variance (ANOVA) (p < 0.05), n = 1,05669
Figure 8. Example of high-throughput screening for siderophore production. In the picture, severa
hundred strains under UV illumination69
Figure 9. Percentage of siderophore-producing strains collected from each location. (0) No fluorescent
strains and (1) fluorescent strains under UV illumination. Different lowercase letters indicate a significant
difference according to one-way analysis of variance (ANOVA) ( $p < 0.05$ ), n = 1,05670
Figure 10. Example of high-throughput screening for HCN-producing strains 48 hpi. In the picture, blue
stained filter paper is due to volatile HCN. The darker the blue colour, the higher the amount of HCN
produced by the isolate70
Figure 11. Percentage of HCN-producing isolates. Ordinal values assigned to strains: (0) No production
(1) low level of production and (2) strong production of HCN. Different lowercase letters indicate a
significant difference according to one-way analysis of variance (ANOVA) ( $p < 0.05$ ), n = 1,05671
Figure 12. Example of high-throughput screening for protease-producing strains 48 hpi. In the picture
96 Pseudomonas colonies are shown, with protease-producing isolates surrounded by a (dark)
transparent halo71
Figure 13. Percentage of protease-producing isolates per orchard. Ordinal values assigned to strains
(0) no halo, (1) small/medium halo and (2) large halo. Different lowercase letters indicate a significant
difference according to one-way analysis of variance $(\Delta NOV/\Delta) (n < 0.05), n = 1.056$

Figure 14. Example of high-throughput screening for swarming motile strains 7 hpi. In the picture, several
highly motile strains can be seen swarming across the agar72
Figure 15. Percentage of swarming motile isolates per orchard. Ordinal values assigned to strains: (0)
No swarming motility, (1) low/moderate swarming motility and (2) strong swarming motility. Different
lowercase letters indicate a significant difference according to one-way analysis of variance (ANOVA) (p
< 0.05), n = 1,056
Figure 16. Example of high-throughput screening for exopolysaccharide-producing strains 48 hpi. In the
picture, strains with intense red coloration show greater production of Congo Red binding
exopolysaccharides
Figure 17. Percentage of Congo Red isolates per orchard. Ordinal values assigned to strains: (0) No
Congo Red binding, (1) low/moderate Congo Red binding and (2) strong Congo Red binding. Different
lowercase letters indicate a significant difference according to one-way analysis of variance (ANOVA) (p
< 0.05), n = 1,056
Figure 18. Example of high-throughput screening for S. scabies-inhibitory strains 72 hpi. In the picture,
inhibitory isolates are surrounded by a transparent (dark) halo74
Figure 19, Example of high-throughput screening for S. venezuelae-inhibitory strains 72 hpi. In the
picture, inhibitory isolates are isolates surrounded by a transparent (dark) halo75
Figure 20. Percentage of Streptomyces spp. inhibitory isolates per orchard. On the left, S. scabies
inhibitory isolates and on the right, S. venezuelae inhibitory isolates. Ordinal values assigned to strains:
(0) No inhibition, (1) low/moderate inhibition and (2) strong inhibition against S. scabies. Different
lowercase letters indicate a significant difference according to one-way analysis of variance (ANOVA) (p
< 0.05), n = 1,056
Figure 21. Example of high-throughput screening for Psa-inhibitory strains 48 hpi. Inhibition is shown by
the presence of (dark) transparent haloes surrounding isolates
Figure 22. Percentage of isolates able to supress Psa biovar 3 per orchard. On the left, 10627 inhibitory
strains and on the right, RT596 inhibitory strains. Ordinal values assigned to strains: (0) No inhibition, (1)
$low/moderate\ inhibition\ and\ (2)\ strong\ \textit{Psa}\ inhibition.\ Different\ lowercase\ letters\ indicate\ a\ significant$
difference according to one-way analysis of variance (ANOVA) ( $p < 0.05$ ), n = 1,05677
Figure 23. Example of high-throughput screening for copper resistant strains 48 hpi. In the top left corner,
in read boxes: 10627 (copper sensitive) and RT594 (copper resistant)
Figure 24. Percentage of copper-resistant isolates per orchard. Ordinal values assigned to strains: (0)
No resistance, (1) low/moderate resistance and (2) strong resistance to copper sulphate at 500 ppm.
Different lowercase letters indicate a significant difference according to one-way analysis of variance
(ANOVA) (p < 0.05), n = 1,056
Figure 25. Example of high-throughput screening for streptomycin-resistant strains 48 hpi. In the top left
corner, in read boxes: 10627 (streptomycin sensitive) and RT594 (streptomycin resistant)78
Figure 26. Percentage of streptomycin-resistant isolates per orchard. Ordinal values assigned to strains:
(0) No resistance, (1) low/moderate resistance and (2) strong resistance to streptomycin at 100 ppm.

Different lowercase letters indicate a significant difference according to one-way analysis of variance
(ANOVA) ( $p < 0.05$ ), n = 1,05679
Figure 27. Example of high-throughput screening for kasugamycin-resistant strains 48 hpi79
Figure 28. Percentage of kasugamycin-resistant isolates per orchard. Ordinal values assigned to strains:
(0) No resistance, (1) low/moderate resistance and (2) strong resistance to kasugamycin at 100 ppm.
Different lowercase letters indicate a significant difference according to one-way analysis of variance
(ANOVA) (p < 0.05), n = 1,05680
Figure 29. Percentage of kasugamycin-resistant isolates per orchard. Ordinal values assigned to strains:
(0) No resistance, (1) low/moderate resistance and (2) strong resistance to kasugamycin at 20 ppm.
Different lowercase letters indicate a significant difference according to one-way analysis of variance
(ANOVA) (p < 0.05), n = 1,05680
Figure 30. Comparison of Psa biovar 3 inhibitory isolates from Psa-infected orchards isolated from
symptomatic (inf.) and non-symptomatic (no-inf.) samples (leaves and buds). (0) No inhibition, (1)
ow/moderate inhibition and (2) strong inhibition83
Figure 31. Correlation analysis with all phenotypic assays and orchards together from four locations. In
order, margins abbreviations are infected orchard, infected sample, colour, UV or siderophore
production, HCN production, swarming motility, protease production, Congo Red binding, S. scabies,
S. venezuelae, Psa (10627) and Psa (RT594) inhibition and copper sulphate, streptomycin and
kasugamycin resistance. Values between -1 and 1 indicate negative and positive correlations (Pearson's
correlation coefficient)84
Figure 32. Maximum likelihood phylogenetic NJ tree of 103 Pseudomonas spp. with 1,000 bootstraps,
based on a concatenation of atpD, dnaE, guaA, gyrB and rpoD housekeeping genes. Ten reference
pacterial genomes are included for comparison. Strains are coloured according to their orchard of origin,
as shown in the legend. Tree scale units represent represents the evolutionary time between nodes. 86
Figure 33. Maximum likelihood phylogenetic NJ tree of 103 Pseudomonas spp. with 1,000 bootstraps,
based on a concatenation of atpD, dnaE, guaA, gyrB and rpoD protein encoding genes with key
phenotypic traits. Labels are dip-inoculation assay, pathogenic, sample origin, sample health, presence
of irrigation, siderophore and HCN production, motility, protease production, inhibition against $\mathcal{S}$ .
scabies, S. venezuelae, Psa 10627 and RT594 and copper, streptomycin and kasugamycin resistance.
Filled, coloured circles represent presence of the trait. Tree scale units represent represents the
evolutionary time between nodes
Figure 34. Correlation analysis between czc/cusABC and copABCD and other relevant genes involved
n chemical resistance together with copper, and streptomycin phenotypic traits. Values between -1 and
1 indicate negative and positive correlations (Pearson's correlation coefficient)95
Figure 35. Maximum likelihood phylogenetic analysis based on a concatenation of atpD, dnaE, guaA,
gyrB and rpoD protein encoding genes with presence/absence of genes known to be responsible for
arsenic, copper, streptomycin and kasugamycin resistance together with Psa biovar 3 inhibition, copper
resistance, streptomycin and kasugamycin phenotypic traits. Coloured circles represent presence of the

scale units represent represents the evolutionary time between nodes96
Figure 36. Maximum likelihood phylogenetic NJ tree of 103 <i>Pseudomonas</i> strains with 1,000 bootstraps,
based on a concatenation of atpD, dnaE, guaA, gyrB and rpoD protein housekeeping genes. Ten
reference bacterial genomes are included for comparison. Labels are copper phenotypic data, genes hit
by transposon mutants sensitive to copper in 10A5, streptomycin phenotypic data and genes hit by transposon mutants sensitive to both copper and streptomycin in 10A5. Filled, coloured circles represent
presence of the trait or gene. Tree scale units represent represents the evolutionary time between nodes.
Figure 37. Correlation analysis with copper and streptomycin genes targeted by transposon
mutagenesis in 10A5. In order, margins abbreviations are copper phenotypic data, genes targeted by
transposon mutants sensitive to copper in 10A5, streptomycin phenotypic data and genes targeted by
transposons mutants sensitive to both copper and streptomycin in 10A5. Values between -1 and 1 $$
indicate negative and positive correlations (Pearson's correlation)101
Figure 38. Gels run with gDNA extracted from the 103 Pseudomonas strains where several of them
showed presence of predicted plasmids. Arrows show example of a strain detected with three small
potential plasmids. Reference band: Quick-Load® 1 kb Extend DNA ladder103
Figure 39. Screening representation to determine the minimum inhibitory concentration (MIC) of copper
with a biocontrol candidate (8H7). On the top (0-500), amount of copper in ppm used to supplement
KB-agar. Horizontally I on the left, method used to screen. Dilution (spreading 100 $\mu L$ of a 10-9 dilution
of the biocontrol candidate) or streaking (from overnight culture at 1 = $OD_{600}$ ) on 90 mm-wide plates 48
hpi. Growth cannot be seen at 500 ppm of copper sulphate
Figure 40. MIC of gentamicin, copper, and tetracycline for 22 biocontrol candidates and Psa (10627)
between streaking and plating dilutions ( $\mu g/mL$ ). On the x axis are shown the 22 biocontrol candidates
and <i>Psa</i>
Figure 41. Colony-forming units (CFU) per cm² leaf tissue recovered from tomato plants 1- and 5-days
post inoculation (dpi). Horizontal axis contains 22 non-pathogenic Psa-inhibitory Pseudomonas strains
(left side, 3.C5 to 11.F1), 8 non <i>Psa-</i> inhibitory <i>Pseudomonas</i> strains (horizontal blue line) and <i>Psa</i> biovar
3 as a negative control at the right end of the graph. Different lowercase letters indicate a significant
difference at 5 dpi according to one-way analysis of variance (ANOVA, $p < 0.05$ ). Values are given as
mean ± s.d
Figure 42. Representation of biocontrol assays on tomato plants 7 dpi. A) Uninoculated (control), B) Psa-
inhibitory Pseudomonas strain (8H7 biocontrol candidate), C) Non-inhibitory Pseudomonas strain
(negative control) and D) Psa biovar 3 only. Tomato leaves showing leaf brown spots (necrosis) with a
thin yellow halo around it (chlorosis) are due to Psa biovar 3 infection
Figure 43. Exp 22-7. Disease incidence (%) on Hort16A kiwifruit vines 4 weeks post inoculation (wpi)
assessed by Leaf Doctor. Boxes show median (horizontal lines inside the boxes), mean (crosses),
observations (circles) and maximum and minimum values (whiskers). Letters on top of the whiskers

0.05)
Figure 44. Exp 22-8. Disease incidence (%) on Hort16A kiwifruit vines 4 wpi assessed by Leaf Doctor
Boxes show median (horizontal lines inside the boxes), mean (crosses), observations (circles) and
maximum and minimum values (whiskers). Letters on top of the whiskers represent a pairwise
comparison. Same letters represent no significant difference of the means ( $p = 0.05$ )114
<b>Figure 45</b> . Exp 22-9. Disease incidence (%) on Hayward kiwifruit vines 4 wpi assessed by Leaf Doctor
Boxes show median (horizontal lines inside the boxes), mean (crosses), observations (circles) and
maximum and minim values (whiskers). Letters on top of the whiskers represent a pairwise comparison
Same letters represent no significant difference of the means ( $p = 0.05$ )
Figure 46. Exp 22-12. Disease incidence (%) on Hayward kiwifruit vines 4 wpi assessed by Leaf Doctor
Boxes show median (horizontal lines inside the boxes), mean (crosses), observations (circles) and
maximum and minim values (whiskers). Letters on top of the whiskers represent a pairwise comparison
Same letters represent no significant difference of the means $(p = 0.05)$
Figure 47. Exp 22-13. Disease incidence (%) on Hayward kiwifruit vines 3 wpi assessed by Leaf Doctor
Boxes show median (horizontal lines inside the boxes), mean (crosses), observations (circles) and
maximum and minim values (box extremes). Letters on top of the whiskers represent a pairwise
comparison. Same letters represent no significant difference of the means ( $p = 0.05$ )
Figure 48. Graphic representation of Cluster 17. Above, first identified Cluster 17 (Krzyzanowska
Ossowicki et al. 2016, Matuszewska, Maciąg et al. 2021). Bellow, Cluster 17 found in <i>P. putida</i> 4H12
Arrows represent gene organisation and strand direction
Figure 49. AntiSMASH 6.0 identified secondary metabolite regions in 4H12 using strictness 'relaxed
analysis
Figure 50. Structure of the multidrug transporter MFS-type EmrAB-TolC. A) Transmission electron
microscopy (TEM) image of the EmrAB-TolC complex showing densities corresponding to TolC, EmrA
and $\it EmrB$ . Distances between these components are indicated in nm. The grey arrow indicates the $\alpha$
helical coiled-coil domains of EmrA. B) Representation of the single-component efflux transporter as an
independent multidrug/H+ antiporters which transport the drugs from the cytoplasm to the periplasm
Substrate of the transporter is indicated as a purple-coloured double triangle. Adapted from: (Alav
Kobylka et al. 2021, Yousefian, Ornik-Cha et al. 2021)125
Figure 51. Colony-forming units (CFU) of Psa biovar 3 per cm <sup>2</sup> recovered from tomato plants 1- and 7
dpi. Horizontal axes represent different treatments: 4H12 sprayed before $\textit{Psa}$ biovar 3 (left, $\Delta 2734$ (Treatments)
31), a 4H12 transposon mutant sprayed before $Psa$ biovar 3 (centre) and $Psa$ biovar 3 alone as a
negative control (right). Different lowercase letters indicate a significant difference at 7 dpi according to
one-way analysis of variance (ANOVA, p < 0.05). Values given as mean $\pm$ s.d. (n=6)128
Figure 52. Biocontrol assay in vitro. Three times concentrated treatments (organic phase only) were
tested against Psa used as overlay. Treatments were KB liquid media (negative control), 4H12 only

4H12 with Psa, Psa only (negative control) and acetonitrile (ACN) (negative control). Biggest inhibition
zone was appreciated with 4H12 only and a mild inhibition in the 4H12 with <i>Psa</i> co-culture129
$\textbf{Figure 53}. \ \textbf{Mass spectra showing } \textit{in vitro} \ \textbf{assays with 4H12 only (first and second chromatogram), } \ \Delta 2734 \ \textbf{Mass spectra showing } \ $
only (third and fourth chromatogram), 4H12 grown together with Psa (fifth and sixth chromatogram),
Psa only (seventh and eighth chromatogram) and KB only (nineth and tenth chromatogram). Red arrows
point at the only condition (two repetitions) that have two major peaks, both missing in the rest of
conditions
Figure 54. Example of screening with two 5G9 transposons mutants. In the left, a mutant that produced
as much Psa-inhibition as the wildtype in vitro. In the right, a mutant that had its ability to inhibit Psa
reduced in vitro.
Figure 55. Targeted operons by pALMAR3 in 5G9. Orange stars next to genes represent transposon
insertions
<b>Figure 56</b> . Targeted operons by Tn5 in 8H7. Orange stars next to genes represent transposon insertions.
Figure 57. Targeted operons by Tn5 in 10A5. A) Gene targeted in Tn 55 was 2836, a dut-like protein,
B) Gene targeted in Tn 56 was 607, a hypothetical protein and C) Gene targeted in Tn 57 was 5364, a
hypothetical protein. Arrows represent gene organisation and strand direction. Unnamed genes are
hypothetical proteins. Arrows at different levels show partial parallel gene overlap. Orange stars next to
genes represent transposon insertions
Figure 58. Identified secondary metabolite regions in 10A5 using strictness 'relaxed' analysis. Region 1
shows contig 1 while second number of the region is the position within the contig136
Figure 59. Maximum likelihood phylogenetic analysis combined with AntiSMASH analysis of 33 Psa-
inhibitory <i>Pseudomonas</i> , 70 additional non- <i>Psa</i> inhibitory with reference strains. On the top margin, first
two labels belong to the strains' ability to suppress Psa biovar 3 in vitro, together with the main families
of NP or BGCs identified. In order, Acinetobactin, Arylpolyene, Arthofactin, Anikasin, Bacilomycin,
Bacteriocin, Bananamides, Bicornutin, Butyrolactone, Chichofactin, Cichopeptin, Corpeptin,
Cupriachelin, Cyanopeptin, Daptomycin, Delftibactin, Ectoine, Enduracidin, Enterobactin, Fengycin,
Fragin, FR900359, Glidopeptin, Hserlactone, Jessenipeptin, Lankacidin, Luminmide, Mangotoxin,
Fragin, FR900359, Glidopeptin, Hserlactone, Jessenipeptin, Lankacidin, Luminmide, Mangotoxin, Mitomycin, Mycosubtilin, NAGGN, Nostamide, Nunamycin, Orfamide, Pseudomonine, Poaeamide
Mitomycin, Mycosubtilin, NAGGN, Nostamide, Nunamycin, Orfamide, Pseudomonine, Poaeamide
Mitomycin, Mycosubtilin, NAGGN, Nostamide, Nunamycin, Orfamide, Pseudomonine, Poaeamide Pyochelin, Pyoverdine, Putisolvin, Puwainaphycins, Rhizomide A/B/C, Roseaoflavin, Ralsolamycin,
Mitomycin, Mycosubtilin, NAGGN, Nostamide, Nunamycin, Orfamide, Pseudomonine, Poaeamide Pyochelin, Pyoverdine, Putisolvin, Puwainaphycins, Rhizomide A/B/C, Roseaoflavin, Ralsolamycin, Ristocetin, Rimosamide, Safracin, Serobactins, Siderophore, Stenothricin, Syringafactin, Syringolin A,
Mitomycin, Mycosubtilin, NAGGN, Nostamide, Nunamycin, Orfamide, Pseudomonine, Poaeamide Pyochelin, Pyoverdine, Putisolvin, Puwainaphycins, Rhizomide A/B/C, Roseaoflavin, Ralsolamycin, Ristocetin, Rimosamide, Safracin, Serobactins, Siderophore, Stenothricin, Syringafactin, Syringolin A, Syringomycin, Taiwachelin, Teixobacting, Terpene, Thanamycin, Thiazostatin, Thiopeptide, Tolaasin,

# LIST OF TABLES

Table 1. Psa biovars in order of identification, countries where is or was present and presence (+) or
absence (-) of key phytotoxins in the different Psa biovars
Table 2. Location of the kiwifruit orchards from where samples were collected, region, address, GPS
coordinates and altitude
Table 3. Additional orchard information was gathered during the collection of samples in November and
December 2018
Table 4. Numerical scale for assessing colony morphology 48 hpi.    43
Table 5. Numerical scale for assessing colony siderophore production 48 hpi.      43
Table 6. Numerical scale for assessing hydrogen cyanide production 48 hpi.
Table 7. Numerical scale for assessing protease production 48 hpi.
Table 8. Numerical scale for assessing swarming motility assay 6 hpi.
Table 9. Numerical scale for assessing Congo Red binding 48 hpi.
Table 10. Numerical scale for assessing S. scabies suppression 3 dpi.    47
Table 11. Numerical scale for assessing Psa suppression 48 hpi.
Table 12. Numerical scale for assessing copper sulphate resistance 48 hpi.   48
Table 13. Numerical scale for assessing streptomycin resistance 48 hpi.
Table 14. Numerical scale for assessing kasugamycin resistance 48 hpi.
Table 15. List of ladders used in this thesis from New England BioLabs Inc., UK
Table 16. Reference strains used in this study and source.   55
Table 17. Results of blasting analysis with copABCD. In order, genes used as query, number of strains
with the queried genes, number of strains that are copper resistant in vitro, and percentage of strains
with the queried genes that are copper resistant in vitro.
Table 18. Transposon candidates for potential copper and streptomycin resistant genes. Gene function
predictions were derived based on BLAST using PROKKA. Cut-off for sequence similarity was $80\%97$
Table 19. Dip-inoculation visual assessment 7 dpi of 33 biocontrol Pseudomonas spp. candidates
Values of 0 represent absence of necrotic spots and 1 presence of necrotic spots108
Table 20. 4H12 mutants with Tn5 that have lost bioactivity. In order, qname: transposon reference
hname: targeted contig, hstart: start of the sequenced region within the contig, hend: end of the
sequenced region within the contig, hstrand: direction of the transposon insertion (-1, to the left, 1 to the
right), fracid: fraction of the positions in the alignment which are identical in the two compared
sequences, inGene: locus number of targeted gene and inProduct: targeted gene name according NCB
database122
Table 21. Annotation of genes from Cluster 17 found in 4H12.    123
Table 22. Genes targeted by the pALMAR3 transposon In order, qname: transposon reference, hname
targeted contig, hstart: start of the sequenced region within the contig, hend: end of the sequenced
region within the contig. hstrand: direction of the transposon insertion (-1, to the left, 1 to the right)

fracid: fraction of the positions in the alignment which are identical in the two compared sequences,
inGene: locus number of targeted gene and inProduct: targeted gene name according NCBI database.
131
Table 23. Genes targeted by the Tn5 Transposon. In order, qname: transposon reference, hname:
targeted contig, hstart: start of the sequenced region within the contig, hend: end of the sequenced
region within the contig, hstrand: direction of the transposon insertion (-1, to the left, 1 to the right),
fracid: fraction of the positions in the alignment which are identical in the two compared sequences,
inGene: locus number of targeted gene and inProduct: targeted gene name according NCBI database.
Table 24. Genes targeted by the Tn5 transposon in 10A5. In order, qname: transposon reference,
hname: targeted contig, hstart: start of the sequenced region within the contig, hend: end of the
sequenced region within the contig, hstrand: direction of the transposon insertion (-1, to the left, 1 to the
right), fracid: fraction of the positions in the alignment which are identical in the two compared
sequences, inGene: locus number of targeted gene and inProduct: targeted gene name according NCBI
datahase 135

# APPENDIX

Supplementary 1. List of primers used for genetic manipulations, arbitrary PCR, and sequencing....149 Supplementary 2. Correlation analysis with all phenotypic assays from Moteka. In order, margins abbreviations are infected sample, colour, UV or siderophore production, HCN production, swarming motility, protease production, Congo Red binding, S. scabies, S. venezuelae, Psa (10627) and Psa (RT594) inhibition and copper sulphate, streptomycin and kasugamycin resistance. Values between -1 and 1 indicate negative and positive correlations (Pearson's correlation coefficient)......151 Supplementary 3. Correlation analysis with all phenotypic assays from Kaimai. In order, margins abbreviations are infected sample, colour, UV or siderophore production, HCN production, swarming motility, protease production, Congo Red binding, S. scabies, S. venezuelae, Psa (10627) and Psa (RT594) inhibition and copper sulphate, streptomycin and kasugamycin resistance. Values between -1 and 1 indicate negative and positive correlations (Pearson's correlation coefficient)......152 Supplementary 4. Correlation analysis with all phenotypic assays from Ohaupo. In order, margins abbreviations are infected sample, colour, UV or siderophore production, HCN production, swarming motility, protease production, Congo Red binding, S. scabies, S. venezuelae, Psa (10627) and Psa (RT594) inhibition and copper sulphate, streptomycin and kasugamycin resistance. Values between -1 Supplementary 5. Correlation analysis with all phenotypic assays from Te Puke. In order, margins abbreviations are infected sample, colour, UV or siderophore production, HCN production, swarming motility, protease production, Congo Red binding, S. scabies, S. venezuelae, Psa (10627) and Psa (RT594) inhibition and copper sulphate, streptomycin and kasugamycin resistance. Values between -1 and 1 indicate negative and positive correlations (Pearson's correlation coefficient).......154 Supplementary 6. Correlation analysis with all phenotypic assays from the infected orchards (Te Puke, Kaimai and Ohaupo). In order, margins abbreviations are infected orchard, infected sample, colour, UV or siderophore production, HCN production, swarming motility, protease production, Congo Red binding, S. scabies, S. venezuelae, Psa (10627) and Psa (RT594) inhibition and copper sulphate, streptomycin and kasugamycin resistance. Values between -1 and 1 indicate negative and positive Supplementary 7. Correlation analysis with all phenotypic assays from visually infected samples. In order, margins abbreviations are infected sample, colour, UV or siderophore production, HCN production, swarming motility, protease production, Congo Red binding, S. scabies, S. venezuelae, Psa (10627) and Psa (RT594) inhibition and copper sulphate, streptomycin and kasugamycin resistance. Values between -1 and 1 indicate negative and positive correlations (Pearson's correlation coefficient)......156 Supplementary 8. Correlation analysis with all phenotypic assays from visually healthy samples from infected orchards. In order, margins abbreviations are infected sample, colour, UV or siderophore production, HCN production, swarming motility, protease production, Congo Red binding, S. scabies, S. venezuelae, Psa (10627) and Psa (RT594) inhibition and copper sulphate, streptomycin and

kasugamycin resistance. Values between -1 and 1 indicate negative and positive correlations (Pearson's
correlation coefficient)
Supplementary 9. Correlation analysis with all phenotypic assays from Psa-inhibitory strains. In order,
margins abbreviations are infected sample, colour, UV or siderophore production, HCN production,
swarming motility, protease production, Congo Red binding, S. scabies, S. venezuelae, Psa (10627) and
$^{ m Ps}a$ (RT594) inhibition and copper sulphate, streptomycin and kasugamycin resistance. Values between
-1 and 1 indicate negative and positive correlations (Pearson's correlation coefficient)158
Supplementary 10. Correlation analysis with all phenotypic assays from non-inhibitory Psa strains. In
order, margins abbreviations are infected sample, colour, UV or siderophore production, HCN
production, swarming motility, protease production, Congo Red binding, S. scabies, S. venezuelae, Psa
(10627) and Psa (RT594) inhibition and copper sulphate, streptomycin and kasugamycin resistance.
Values between -1 and 1 indicate negative and positive correlations (Pearson's correlation coefficient).
Supplementary 11. Presence and absence of published essential copper resistant genes within the
copper resistant <i>Pseudomonas</i> strains
Supplementary 12. Transposon insertion locations within Pseudomonas 10A5 in contig 1. In blue, copper
sensitive transposons and in orange, dual copper, and streptomycin sensitive transposons161
Supplementary 13. Transposon insertion locations within Pseudomonas 10A5 in contig 2. In blue, copper
sensitive transposons
Supplementary 14. Biocontrol strains used for biocontrol assays in planta with model plants, bacteria
recovered (CFU/cm²) 1 and 5 dpi, and their standard deviations (s.d.)163
Supplementary 15. Kiwifruit cultivar, inoculum used per treatment (CFU/mL) of the kiwifruit biocontrol
assay, disease incidence measured by Leaf Doctor (%) and standard deviation164
Supplementary 16. Antagonism assay between 4H12, inoculated as a water overlay ( $OD_{600} = 0.01$ ), and
BH7 as a 10 $\mu$ L drop in the middle of the 90 mm plate (OD <sub>600</sub> = 1) 72 hpi165
Supplementary 17. Correlation matrix summary from 103 Pseudomonas strains and all the predicted
BGCs by AntiSMASH. Values between -1 and 1 indicate negative and positive correlations (Pearson's
correlation coefficient)166

#### **ABBREVIATIONS**

CFC

ACAD Acyl-CoA dehydrogenase

antiSMASH Antibiotics and Secondary Metabolite Analysis Shell

ANOVA Analysis of Variance
ATP Adenosine triphosphate

BBCH Biologische Bundesanstalt, Bundessortenamt and CHemical industry

BCAs Biological control agent
BGC Biosynthetic gene cluster

CAGR Compound annual growth rate cAMP Cyclic adenosine monophosphate

CFU Colony forming units
CLP Cyclic lipopeptide

DEFRA Department for Environment, Food & Rural Affairs

Cetrimide-fucidin-cephalosporin

DMSO Dimethyl sulfoxide

DNA Deoxyribonucleic acid
DNA DIFCO™ Nutrient Agar

EDTA Ethylenediaminetetraacetic acid
EFSA European Food Safety Authority
EPS Extracellular polymeric substances

FAD Fatty acid desaturase

FAO Food and Agriculture Organization of the United Nations

gDNA Genomic DNA HCN Hydrogen cyanide

HGT Horizontal gene transfer HMM Hidden Markov Model

HPLC High-performance liquid chromatography

HR Hypersensitivity response
HTS High-throughput screening

ICE Integrative conjugative element

iTOL Interactive tree of life

LC-MS Liquid chromatography-mass spectrometry

MFP Membrane fusion protein
MFS Major facilitator superfamily
MGE Mobile genetic element

MPI Ministry for Primary Industries

NADPH Nicotinamide adenine dinucleotide phosphate oxidase

NCBI The National Center for Biotechnology Information

NMR Nuclear magnetic resonance

NP Natural product

NRPS Non-ribosomal peptides
OAT Organic anion transporter

OEP Outer membrane efflux protein

ORF open reading frame

P&FR Plant and Food Research
PCR Polymerase Chain Reaction

PE Paired ends

Pfm Pseudomonas syringae pv. Actinidia

PGR Plant growth regulator

Psa Pseudomonas syringae pv. actinidifoliorum

RH Relative humidity

RiPP Ribosomally synthesized and post-translationally modified peptide

RND Resistance-nodulation-division

SDR Short-chain dehydrogenase/reductase

SDS Sodium dodecyl sulphate

SFM Soya Flour Mannitol
TAE Tris-acetate-EDTA

TIIISS Type III secretion system NJ Neighbour-joining tree

NCBI National Centre for Biotechnology Information database

VLS Verified Laboratory Services

VWR Van Waters and Rogers Chemicals

# CHAPTER 1 INTRODUCTION

#### **CHAPTER 1: INTRODUCTION**

#### 1.1. Psa: a global problem

Pseudomonas is a bacterial genus that comprises over 190 species (Euzéby, 1997). Among it, the Pseudomonas syringae complex currently comprises over 60 different pathovars and 13 phylogenetic groups (Baltrus, McCann et al. 2017). One of these pathovars is Pseudomonas syringae pv. actinidiae (Psa), a gram-negative, obligate aerobe and non-sporing rod-shaped bacterium (Takikawa Y 1989). Psa is the causal agent of bacterial canker of kiwifruit, as named by Takikawa in 1989 (Bull, De Boer et al. 2010) and is currently the major threat to the worldwide kiwifruit industry. Typical symptoms comprise necrotic spots on leaves, canker and dieback on canes and trunks, twig wilting, and blossom necrosis.

At present, six different *Psa* biovars are known (1-6), named in chronological order of detection. All are closely related but genetically distinct (Zhao, Chen et al. 2019). Moreover, distinct kiwifruit cultivars such as *Actinidia deliciosa* (green flesh), *Actinidia chinensis* (golden flesh) or *Actinidia arguta* (kiwi berries) show different susceptibility to kiwifruit pathogens (Purahong, Orru et al. 2018). *Psa* was first reported in China and Japan in the 1980s, and detected in 2008 when a severe outbreak of *Psa* began to spread from Italy to other countries (Balestra, Mazzaglia et al. 2009). Just two years later, *Psa* biovar 3 was found in New Zealand being the movement of *Psa*-infected plant material the main vector that contributed to the long-distance dispersal of the pathogen in less than a decade (McCann, Li et al. 2017).

Strains of biovar 1 are moderately aggressive and systemic. They possess a phaseolotoxin (a non-host-specific toxin) gene cluster located in the chromosome, acquired by horizontal gene transfer (HGT) that contributes to the formation of chlorotic halo lesions (Sawada, Suzuki et al. 1999, Donati, Buriani et al. 2014). This biovar has been reported in Japan and Italy (**Table 1**) and was responsible for the 1992 outbreak in this last mentioned country (Tamura, Imamura et al. 2002, Scortichini, Marcelletti et al. 2012).

Strains of biovar 2 are moderately aggressive and systemic. They produce coronatine, a polyketide toxin structurally similar to the plant hormone jasmonic acid (Geng, Jin et al. 2014). Among other effects, contrasts stomata closure (Han, Koh et al. 2003, Melotto, Underwood et al. 2006). This biovar has only been reported in South Korea (**Table 1**) and interestingly, both *Psa* biovar 1 and *Psa* biovar 2 have not been detected in the country since 1998 (Han, Koh et al. 2003, Loreti, Cunty et al. 2018).

*Psa* strains of biovar 3, also referred to as *Psa-V*, are responsible for the global outbreak (Kim, Lee et al. 2020). First reported in Italy in 2008, is the most aggressive *Psa* biovar known to date (Ferrante and Scortichini 2010, Abelleira, Ares et al. 2015). Strains of this biovar are systemic, have neither phaseolotoxin nor coronatine synthesis gene clusters and do not produce any known toxins. They can infect vines without causing a high immune response (Sawada and Fujikawa 2019). However, these strains have caused devastating economic consequences putting on a critical position the global kiwifruit

industry (Vanneste 2017). On 2017, 99% of the kiwifruit production came from countries where *Psa* biovar 3 was present (FAO 2017). In New Zealand, fortunately, *Psa* biovar 3 is restricted to North Island only, although comparatively little kiwifruit cultivation occurs on South Island (Martinez Perez 2020).

**Table 1.** *Psa* biovars in order of identification, countries where is or was present and presence (+) or absence (-) of key phytotoxins in the different *Psa* biovars.

Biovar	Countries where are identified	Phaseolotoxin	Coronatine
1	Japan and Italy	+	-
2	South Korea	-	+
3	China, Italy, France, Portugal, Spain, Slovenia, Switzerland, Greece, Turkey, Georgia, Chile, Argentina, Japan, South Korea, and New Zealand	-	-
4	New Zealand, Australia, France, and Spain	-	-
5	Japan	-	-
6	Japan	+	+

Sources: (Serizawa, Ichikawa et al. 1989, Takikawa Y 1989, Scortichini 1994, Balestra, Mazzaglia et al. 2008, Balestra 2008, Balestra, Renzi et al. 2010, Abelleira, Lopez et al. 2011, Everett, Taylor et al. 2011, ProMed 2011, Vanneste, Poliakoff et al. 2011, Bastas and Karakaya 2012, Dreo, Pirc et al. 2014, EPPO 2014, Abelleira, Ares et al. 2015, Cunty, Poliakoff et al. 2015, M. C. Holeva 2015, Kim, Kim et al. 2016, Meparishvili, Gorgiladze et al. 2016, G. M. Balestra 2018, Garcia, Moura et al. 2018).

Strains of biovar 4, reclassified as *Pseudomonas syringae* pv. *actinidifoliorum* (*Pfm*), shows mild aggressiveness and economically do not cause a relevant impact (Chapman, Taylor et al. 2012, Vanneste 2013, Cunty, Poliakoff et al. 2015). These strains can cause leaf spotting but do not cause systemic infections or plant death (Vanneste, Yu et al. 2013). Strains of biovar 4 have been present in Australia since 1992, mistaken for *Pseudomonas viridiflava*, for almost 20 years as well as in New Zealand (Vanneste, Yu et al. 2013, EPPO 2014, Cunty, Cesbron et al. 2016). Interestingly, it was detected for the first time outside these countries in 2014 in France. Furthermore, phylogenetic data suggest that *Psa* biovar 4 has been present in France since the beginning of the global outbreak in 2010 (Cunty, Poliakoff et al. 2015).

Strains of biovar 5, closely related to biovar 2, have neither coronatine biosynthetic genes, nor phaseolotoxin biosynthetic genes such as biovar 3 and are found only in Saga Prefecture, a limited local area of Japan (Fujikawa and Sawada 2016, Firrao, Torelli et al. 2018, Flores, Prince et al. 2018, Garcia, Moura et al. 2018). These strains are mildly aggressive (Kim, Chae et al. 2019). Their potential impact outside the Japanese region is unknown.

Finally, strains of biovar 6 have both coronatine and phaseolotoxin gene clusters acquired from other bacteria through HGT (Sawada and Fujikawa 2019). Strikingly, they produce both mentioned phytotoxins during the early stages of host infection (Flores, Prince et al. 2018, Fujikawa and Sawada 2019, Sawada and Fujikawa 2019). To date, no other phytopathogenic bacteria are known to produce two phytotoxins (Hirose, Ishiga et al. 2020). In 2015, strains of biovar 6 were found but only in Nagano

Prefecture on Honshu Island, a small local area of Japan (Fujikawa and Sawada 2016, Sawada, Kondo et al. 2016). Their potential impact outside the Japanese region is unknown.

### 1.2. Dispersion and infection of Psa

Psa does not get naturally dispersed as well as other bacteria. This type of bacterium is non-spore forming. Therefore, it does not become air-borne without physical assistance such as wind, rain, or anthropomorphic input. Importation of propagative plant material by nurseries are considered the main mean of long-distance dispersal of the pathogen (Froud, Everett et al. 2015). Evidence suggests that this mean caused the spread of the bacterium among most European countries where *Psa* biovar 3 has been detected (Balestra, Renzi et al. 2010, Abelleira, Lopez et al. 2011, Vanneste, Giovanardi et al. 2011). Nowadays scientists strongly believe that the strain that caused the outbreak in New Zealand originates from China (Mazzaglia, Studholme et al. 2012, Butler, Stockwell et al. 2013, McCann, Li et al. 2017). Proving that the movement of kiwifruit plant material plays a key role in the dispersion of the pathogen. Strains of biovar 3 have been detected on all physiological parts of the kiwifruit vine: leaves, trunk, buds, flowers, fruits, pollen, and roots (Balestra, Mazzaglia et al. 2009, Everett, Taylor et al. 2011, Gallelli, Talocci et al. 2011, Vanneste, Giovanardi et al. 2011, Biondi, Galeone et al. 2013, Abelleira, Ares et al. 2014). Import of Psa-contaminated plant material (kiwifruit pollen) from China seems to be the strongest hypothesis that explains how Psa biovar 3 arrived at North Island in 2010 (Mazzaglia, Studholme et al. 2012, Butler, Stockwell et al. 2013, Vanneste, Yu et al. 2013, Froud, Everett et al. 2015).

Once plant material is infected, *Psa* can surprisingly survive in dead plant material such as plant litter and twigs, for more than two months (Scortichini, Marcelletti et al. 2012, Aguín, Ares et al. 2015). Similarly, there is evidence that transmission of *Psa* can take place via infected pollen in artificially pollinated kiwifruit (Tontou, Giovanardi et al. 2014, Kim, Lee et al. 2020). Artificial pollination with Chinese imported pollen used to be a common practice in New Zealand. It seems that the 2010 *Psa* outbreak in New Zealand started by those means. Additionally, natural means such as wind, rain and pollinator insects may contribute to the dispersal of *Psa* (Pattemore, Goodwin et al. 2014, Vanneste, Yu et al. 2015). For example, bleeding sap from kiwifruit cankers is disseminated by rain-splash and wind-driven rain (Scortichini, Marcelletti et al. 2012, Biondi, Galeone et al. 2013).

Under favourable conditions, strains of *Psa* biovar 3 can drastically reduce crop yields and even cause plant death (Balestra, Mazzaglia et al. 2009, Scortichini, Marcelletti et al. 2012, Vanneste 2012, Gao, Huang et al. 2016). But how does *Psa* manage to cause such devastating crop losses? To cause disease, the pathogen must first enter the plant and does so via natural openings such as stomata or wounds on leaf surfaces (Xin, Kvitko et al. 2018, Donati, Cellini et al. 2020). Here, flagella play a key role by helping bacteria swim into the stomata (motility) and toward high concentrations of nutrients (chemotaxis). Once inside, the pathogen uses its extensive virulence arsenal to attack the plant. *Psa*, like many gram-negative pathogenic bacteria, has a type III secretion system (a needle-like protein) to

sense the presence of eukaryotic cells to directly secrete effector proteins (toxins and immunosuppressive factors) into the host; a near perfect weapon to escape from the plant immune response (Lindeberg, Cunnac et al. 2012). If those effector proteins damage the host, the pathogen causes a virulent effect while if the interaction are incompatible or there is incompatibility such as when the host harbours the complementary *R* gene, the pathogen causes an avirulent effect (Surico 2013).

Other key genetic features that contribute to the virulence of the *Pseudomonas syringae* complex are phytotoxins production such as phaseolotoxin (produced by several enzyme-coding genes, such as *amtA*, *desl*, *argD and argK*, of the *argK*-tox cluster), hormone signalling manipulation, exopolysaccharides production (mainly involved in biofilm formation), degrading enzyme eliciting cell death and/or starting biochemical activity on plant protein targets (Cunnac, Lindeberg et al. 2009, Xin, Kvitko et al. 2018).

#### 1.3. The economic impact of Psa in New Zealand

Psa biovar 3 was first identified in Te Puke, Bay of Plenty, in 2010 and has infected more than 3,000 kiwifruit orchards, above 90% of the kiwifruit production area, leading to cumulative losses well over NZ\$ 1 billion since the outbreak began (Vanneste 2017). During the following years, New Zealand's kiwifruit yields were reduced by 13% compared with 2010 although yellow kiwifruit was increased due to the introduction of Zespri's Gold3 cultivar (FAO 2017). Just in New Zealand, 85% of golden flesh kiwifruit vines (Zespri's Hort16A) were removed between 2010 and 2014 because of the high susceptibility to Psa biovar 3 (McCann, Li et al. 2017). However, positively, Psa biovar 3, so far it is restricted to North Island and growers by shifting to new and more Psa-resistant kiwifruit cultivars such as Zespri's G3 and G9, have managed to generate higher incomes (Butler, Stockwell et al. 2013).

The economic consequences have been devastating for the national kiwifruit industry (Greer and Saunders 2012). Kiwifruit is the major horticultural export earner of New Zealand. Since the 1950s, New Zealand has been the biggest kiwifruit exporter in the world and thousands of full-time jobs depend on this industry. Just Zespri, the largest kiwifruit marketer in the country but also in the world, reached NZ\$2.3 billion global operating revenue (2021/2022 season). Therefore, protecting this industry is vital. Since *Psa* biovar 3 was identified in New Zealand, Zespri and Kiwifruit Vine Health have invested several million dollars into research to fight against this devastating disease.

#### 1.4. Current control methods of Psa

Chemical and biological control options, orchard management and breeding programmes are being employed to control *Psa* and guaranteeing the world kiwifruit supply and protecting this multi-billion industry (Cameron and Sarojini 2014). However, thus far, not completely effective, and environmentally friendly agrochemicals have been released to control *Psa* on kiwifruit (Purahong, Orru et al. 2018). To this issue is added agrochemical overuse which may promote resistance emergence and genetic material transfer between bacteria.

Currently, one of the most common practices among growers to control *Psa* is spraying copper-based agrochemicals such as Nordox 75 WG (750 g/kg copper present as cuprous oxide), Kocide Opti (300 g/kg copper present as copper hydroxide) or Tri-Base Blue (190 g/L copper present as tribasic copper sulphate). However, their application is conditioned to the phenological stage of the vines and below-label rates increase the risk of developing resistance. Therefore, over the years, copper formulates might not be a long-term solution to control *Psa*, especially when copper-resistant strains of biovar 3 have already been detected in the country (Vanneste and Voyle 2003, Colombi, Straub et al. 2017). Not to mention continuous spraying may lead to copper bioaccumulation in the soil which can affect the ecosystem's health as well as fruit quality (Khan and Nafees 2017). In summary, spraying copper formulates is currently considered the best option available in protecting against *Psa* but this is only a short-term solution for New Zealand kiwifruit growers (Vanneste, Poliakoff et al. 2011, Collina, Donati et al. 2016).

Similarly, under very extreme situations and only when *Psa* is out of control, spraying restricted bactericides such as Key-Strepto (170 g/kg streptomycin as sulphate salt) or Kasumin (20 g/L kasugamycin as hydrochloride hydrate salt) can be authorised. However, it has been confirmed that prolonged exposure of *Psa* to streptomycin promotes resistance (Han, Nam et al. 2003, Cameron and Sarojini 2014, Tancos and Cox 2017). Since 2008, streptomycin resistant *Pseudomonas* spp. were isolated from lakes and rivers in New Zealand (Vanneste, Cornish et al. 2008). Additionally, spraying bactericides in agriculture represents a potential hazard for humans and the environment although its use is strictly conditioned to the phenological stage of the vines (Chang, Wang et al. 2015, Cycoń, Mrozik et al. 2019).

Elicitors are an additional and very useful 'weapon' that is part of the kiwifruit grower's 'toolbox' against *Psa*. These chemical substances such as methyl jasmonate, jasmonic acid, salicylic acid, or hydrogen peroxide, induce the plant's defence mechanisms allowing them to fight infection. Their effectiveness is moderated and is meant to be used in addition to the copper treatments (Vanneste, Giovanardi et al. 2011). The only product that holds a full label claim for foliar applications in New Zealand is Actigard (500 g/kg acibenzolar-s-methyl).

Plant growth regulators (PGRs) are chemicals that can work as shoot growth suppressors, return bloom increasers, fruit excess removers, or as crop protection agents. Only for green flesh, kiwifruit growers have available Ambitious 10SL (10 g/L forchlorfenuron or CPPU). CPPU is a highly active synthetic cytokinin PGR that may enhance kiwifruit physiological response to disease through salicylic acid responses and promote chlorophyll biosynthesis (Antognozzi, Famiani et al. 1993, KVH 2016, Zeng, Yang et al. 2016). However, it provides low to moderate *Psa* control and is expected to be used in conjunction with other treatments.

Lastly, biological control agents (BCAs) are another resource available to kiwifruit growers, especially to those doing organic agriculture. The main product available with a protectant activity against *Psa* is Aureo<sup>®</sup>Gold (4·10<sup>9</sup> CFU/g *Aureobasidium pullulans* YBCA5). It has a field efficacy range of 40-60%, 7-

14 days application intervals and its use is strictly conditioned to the phenological stage of the vines (de Jong, Reglinski et al. 2019). It can be used in combination with kasugamycin or elicitors but not copper.

#### 1.5. A future perspective: biocontrol agents

A sustainable and efficient solution in controlling *Psa* can be BCAs. They are the most successful alternative to agrochemicals and genetically modified crops (Heimpel and Mills 2017). BCAs is the term for living organisms which are used as natural enemies to suppress a target population (Le Hesran, Ras et al. 2019). In recent years, their use have increased against plant pathogens due to the increasing public awareness towards sustainable and conservation agriculture and the environmental hazards of agrochemicals (Nguyen, Nguyen et al. 2019). In some areas of the world such as Europe, the demand of organic product is so strong that their institutions and governments are experiencing a complete shift in their agricultural policies and have more generous research budgets and stricter food safety controls (Pollex 2017). Evidence of this trend is the recently approved 'European Green Deal' that aims by 2030 a 50% reduction in agrochemicals use and a 25% increase in organic farming (European Commission 2020).

Pseudomonas spp. are wildly known for their potential as BCAs against pathogenic bacteria such as Pseudomonas putida, Pseudomonas asplenii, Pseudomonas fluorescens and Pseudomonas protegens (Akter et al., 2016, Durairaj et al., 2017, Michavila et al., 2017 and Sun et al., 2017). If used smartly, BCAs in agriculture do not require the introduction of new non-endemic organisms into an ecosystem. By doing that, it is drastically reduced the potential of non-target effects (effects on organisms other than the target organisms). BCAs, if isolated from the same environment where the disease is present, would be well adapted to the local climate conditions and its host (Rojas, Sapkota et al. 2019). The use of bacteria in agriculture as BCAs gives a whole range of potential additional benefits, including enhancement of the symbiotic or associative rhizosphere, inducing systemic plant resistance and growth promotion (Gao, Wu et al. 2013, Pieterse, Zamioudis et al. 2014). Several epiphytic bacterial species isolated from the plant phyllosphere have been reported to be strong competitors against plant pathogens, thus acting as BCAs (Völksch and May 2001).

Furthermore, BCAs reduce agrochemical use and the risk of bacteria transferring genetic material to other species causing agrochemical resistance. This resistance is commonly conferred because of mobile elements such as insertion sequences, transposons, plasmids, and integrative conjugative elements (ICEs) (Butler, Stockwell et al. 2013). ICEs are self-transmissible modular mobile genetic elements (MGEs) integrated into a host genome (Johnson and Grossman 2015). They encode the machinery to transfer genetic elements into a new host by conjugation and can participate in HGT (Sawada and Fujikawa 2019). HGT often contributes by providing resistance or an adaptation to some environmental factor of their host. It has been confirmed that HGT played an important role in New Zealand, conferring *Psa* copper and streptomycin resistance (Colombi, Straub et al. 2017).

#### 1.6. The kiwifruit microbiome

Biocontrol agents are categorised into those that are applied directly to the plant's infection site, those that are applied in a single region of the plant such as seeds, and those with persistent benefits after a single or multiple applications. Naturally occurring kiwifruit *Pseudomonas* spp. from New Zealand's orchards may help controlling *Psa* but first, understanding how the plant pathogen shapes the kiwifruit microbiome is essential. The plant microbiome is a vital part of the plant. It has received a lot of research attention in recent years due to its role in controlling the development, productivity and maintenance of plant health (Compant, Samad et al. 2019). Because of recent advances in high-throughput technologies, it has been able to reveal the interactions between complex communities and their hosts. Plants can adapt to the environment, enhanced by their unique microbial signatures (Turner, James et al. 2013, Dastogeer, Tumpa et al. 2020).

On kiwifruit, the scientific community has dedicated an enormous effort to studying and understanding the interaction between *Psa* and the native phyllosphere microbiome of the host. Before *Psa* enters the host tissues, it develops an epiphytic growth phase on the leaves and flowers which interacts with the phyllosphere bacterial community. This interaction will mark the development of the disease and will shape the structure and biodiversity of the phyllosphere bacterial community (Purahong, Orru et al. 2018). Researchers have studied how *Psa* can affect the leaf and flower microbiomes on two different kiwifruit cultivars, *Actinidia chinensis* cv. Hort16A (golden kiwifruit) and *Actinidia deliciosa* cv. Hayward (green kiwifruit).

It was identified that healthy male and female kiwifruit leaves share an almost identical bacterial population profile (Ares, Pereira et al. 2021). However, one of the most fascinating observations by the research community was that the presence of *Psa* incurs profound changes in the kiwifruit microbiome. Especially in *A. deliciosa*, where a depletion in the relative abundance of previously prominent genera was identified (Purahong, Orru et al. 2018, Ares, Pereira et al. 2021). Similarly, it was found that healthy male and female leaves experience profound changes between seasons, where the relative abundance of *Methylobacterium* spp. considerably increased. In contrast, the impact of *Psa* was less prominent within the male phyllosphere across seasons, revealing the potential of the naturally-occurring bacteria as BCAs (Ares, Pereira et al. 2021). Also, other researchers studied the microbial diversity in kiwifruit pollen from New Zealand, China, and South Korea. Surprisingly, results revealed that the bacterial phyla in the different pollens were mainly and consistently Proteobacteria, Actinobacteria and Firmicutes. However, dissimilarities were appreciated in terms of microbial community structures. For example, samples from New Zealand were more diverse, being *Pseudomonas* spp. the most abundant specie (Kim, Jeon et al. 2018).

Additionally, the presence of *Psa* has been associated with the presence of a multi-pathogenic bacterial group that includes the strains of *P. syringae* pv. *syringae* and *P. viridiflava*. Suggesting that the establishment of a pathogenic consortium could lead to a higher degree of virulence (Purahong, Orru et al. 2018). This pathogenic consortium was noted for the first time on kiwifruit; however, it is a

phenomenon that has been reported centuries ago in other plant diseases. In recent years, the number of reports where synergistic pathogen–pathogen interactions are mentioned have increased, probably due to the recent technological advances in diagnostics (Lamichhane and Venturi 2015).

#### 1.7. Pseudomonas spp. as a biocontrol toolbox

Pseudomonas spp. are one of the most abundant bacterial genera of the kiwifruit phyllosphere and, in many plants, its abundance is correlated with plant health (Purahong et al., 2018). The Pseudomonas complex is one of the best characterised bacterial genera but naturally occurring kiwifruit-associated Pseudomonas spp. is underexplored, as well as their metabolic profile and its natural products (NPs) biosynthetic potential. NPs have a key role in the suppression of plant pathogens. Whole genome sequencing and automated genome mining for NPs clusters can help unlocking Pseudomonas spp. potential. In microbial interactions, to compete for nutrients, territory and suppress other organisms, bacteria biosynthesise competitive metabolites such as NPs, siderophores, phenols, antibiotics, bacteriocins and even toxins, conferring a competitive advantage to those organisms that produce them (Ongena and Jacques 2008, Chen, Jiang et al. 2015, Stringlis, Zhang et al. 2018).

On one hand, bacteria compete for territory and nutrient resources. Biocontrol bacteria tend to be good colonisers by quickly conquering as much surface as possible and advantageously taking any nutrients available. Especially, as the growth of epiphytic bacteria is generally carbon-limited (Mercier and Lindow 2000, Lindow and Brandl 2003). To succeed, for example, bacteria biosynthesise siderophores. These high-affinity iron-chelating compounds solubilise and transport iron across cell membranes. Also, to succeed in colonising a new territory as an epiphyte, the flagellum plays a key role in swarming motility chemosensing, and chemotaxis (McAtee, Brian et al. 2018). The naturally occurring associated kiwifruit *Pseudomonas* spp. niche has a huge potential for discovering bacteria which may biosynthesise novel and efficient NPs against *Psa*. One of the first steps for screening bacterial candidates is understanding the genotypic and phenotypic correlation of these bacteria. Moreover, from the point of view of agriculture, to determine how these correlations may be linked to agriculture practices and climate could give kiwifruit growers a highly valuable input (Mauchline, Chedom-Fotso et al. 2015, Mauchline and Malone 2017).

On the other hand, *Pseudomonas* spp. secrete toxic secondary metabolites such as cyclic lipopeptides, biosynthesised by non-ribosomal peptide synthetases, to kill or suppress the growth of competitor organisms (Durairaj, Velmurugan et al. 2017, Geudens and Martins 2018). For example, cyclic lipopeptides (CLPs) such as surfactins, iturins and fengycins, are self-assembling molecules that may have strong antimicrobial activity, including against bacteria, fungi, and oomycetes (Raaijmakers, De Bruijn et al. 2010, Bonnichsen, Bygvraa Svenningsen et al. 2015, Meena and Kanwar 2015). CLPs produced by *Pseudomonas* spp. constitute a varied class of bioactive NPs compounds as a biological Swiss-army knife (Geudens and Martins 2018). One of them is viscosin, a biosurfactant produced by *Pseudomonas* spp. known to have antimicrobial activity but also known for facilitating surface motility

and influence biofilm formation. This is essential for bacteria to access host tissues through natural openings such as stomata and multiply in the apoplast (Lindow and Brandl 2003, Alsohim, Taylor et al. 2014, Bonnichsen, Bygvraa Svenningsen et al. 2015).

#### 1.8. Natural products: key in crop protection

Antimicrobial peptides produced by living organisms *in planta* seem to be a good alternative to conventional antibiotics for controlling pathogenic bacteria (Aldayel 2019). They have shown promising applications in crop protection and could contribute to expanding the agrochemical control toolbox against *Psa* (Cameron and Sarojini 2014). Therefore, screening bacteria from underexplored ecosystems such as the unique diversity of New Zealand could be a smart strategy.

Since 1950s, NPs have received special scientific attention. They are an extraordinarily diverse group of chemicals, well known for their varied bioactivity, produced by living organisms. In recent years, processes such as high-throughput screening (HTS) technologies, separation science (e.g., nuclear magnetic resonance (NMR) spectroscopy or high-performance liquid chromatography (HPLC) fractionation) to determine molecular structures and efficient processes of chemicals purification have promoted natural products research to gain more importance (Sarker and Nahar 2012). These processes combined with whole genome sequencing and automated genome mining for NPs clusters may provide a strong scientific path to isolate and analyse *Pseudomonas* spp. that biosynthesise novel and efficient NPs against phytopathogens *in planta*. The Renaissance of NPs discovery may be about to begin.

In *Pseudomonas* spp., there are 119 known NPs belonging to 30 different molecule families (Gross and Loper 2009, Nguyen, Melnik et al. 2016). These molecule families are composed of molecules that exhibit the diversity of strains within the species. Some of the main classes of biosynthetic compounds that are produced by *Pseudomonas* spp. are polyketides, ribosomally synthesised post-translationally modified peptides (RiPPs), lipopeptides, non-ribosomal peptides (NRPS) and cyclic lipopeptides (CLPs) (Figure 1).

The polyketides group is composed of a wide variety of biologically active compounds. Some of these are commonly used as antifungal agents and antibiotics (Staunton and Weissman 2001, Majumder, Kongbrailatpam et al. 2014). NRPS are a highly diverse group of NPs with an extremely broad range of biological activities and pharmacological properties such as toxins or siderophores (Hennessy, Phippen et al. 2017). Unlike NRPS that require large multimodular enzyme complexes, through the extensive post-translational modifications of ribosomal-based precursor peptides, RiPPs can access a wide range of chemical diversity (Hug, Krug et al. 2020, Alam, Islam et al. 2021). Ultimately, CLPs are of particular interest for their biocontrol potential abilities.

Cyclic lipopeptides (CLPs) are a diverse class of natural compounds that are produced by various bacterial genera, such as *Bacillus*, *Pseudomonas*, and *Streptomyces*. These compounds have received

particular interest in recent years due to their biocontrol ability in plants. One of the main reasons why CLPs are of interest for their biocontrol ability is that they have been shown to possess a broad-spectrum antifungal activity. CLPs can inhibit the growth and development of various plant pathogenic fungi, including *Fusarium*, *Botrytis*, and *Phytophthora* species. This antifungal activity is thought to be due to the ability of CLPs to disrupt fungal cell membranes and inhibit fungal spore germination. In addition to their antifungal activity, CLPs have also been shown to have other beneficial effects on plants. For example, some CLPs have been found to stimulate plant growth, enhance plant root development, and improve plant tolerance to abiotic stress, such as drought and salinity. These effects are thought to be due to the ability of CLPs to promote plant hormone production, increase nutrient uptake, and activate plant defence mechanisms (Jahanshah, Yan et al. 2019).

**Figure 1**. Relevant *Pseudomonas* spp. NPs which are known to have a biocontrol effect against plant pathogens. Molecules and NP families are shown (Jahanshah, Yan et al. 2019, Santos Kron, Zengerer et al. 2020, Dagher, Nickzad et al. 2021).

Overall, the broad-spectrum antifungal activity and beneficial effects on plant growth and development make CLPs an attractive option for use as biocontrol agents in plant protection. Additionally, since CLPs are naturally produced by bacteria, they are environmentally friendly and sustainable alternatives to synthetic pesticides.

#### 1.9. Aims and objectives

A highly promising source of treatments for crop pathogens such as *Psa* are the NPs produced by non-pathogenic *Pseudomonas* strains. These microbes live side-by-side with *Psa* and are locked in a continual struggle for resources and survival. To successfully colonise the plant surface, *Pseudomonas* strains produce a diverse array of secreted NP molecules to kill or suppress competing microorganisms. These NPs take many forms, from molecules that enable efficient plant colonisation and nutrient acquisition to specialised antibiotics and bactericidal peptides. Depending on the conditions, the plant-associated *Pseudomonas* population selects from its huge NP potential to produce the most effective response to the environment. If we can define the NP clusters that contribute to biocontrol and determine how this change between infected and not-infected orchards, we will be able to identify NPs that are selected by *Psa* infection. This will allow us to identify NPs and/or biocontrol agents that are particularly effective at combating plant pathogens in the field environment (Pacheco-Moreno, Stefanato et al. 2021).

In the first stage of the project, sampling of plant material took place. From *Psa*-infected and uninfected New Zealand orchards and were isolated approximately 6,000 *Pseudomonas* strains from them using selective media. Once isolated, colonies were stored at -80 °C, selected 1,000 *Pseudomonas* strains and tested them using high-throughput lab-bench assays for the ability to suppress *Psa* alongside with other relevant phenotypes (swarming motility, siderophore production, etc.). Following initial characterisations, approximately 50 suppressive and 50 non-suppressive isolates were whole-genome sequenced and subjected to rapid, automated annotation using a bioinformatic pipeline. This annotation process enabled us to identify a wide range of important phenotypic output genes and NP gene clusters quickly and easily and will be used to create a database of genes present in each *Pseudomonas* isolate in the study.

Then, a statistical analysis of the phenotypic and genomic data to identify correlations between genes, phenotypes and the metadata was carried out. At this stage, there were used molecular techniques to identify NP clusters that correlate with *Psa* suppression. If beneficial, environmental *Pseudomonas* are actively fighting *Psa* for control of the plant environment, then NPs that are particularly effective at suppressing *Psa* are likely to be selected in the population. Based on the findings at this stage, with the promising NP-producing *Pseudomonas* isolates, a combination of genetics and biochemistry was used. Finally, preliminary *in planta* assays for *Psa* biocontrol and mass spectrometry analysis were carried out to examine the impact of key BGCs against *Psa* by using transposon mutants.

#### 1.9.1. Research objectives:

1. Isolation of a representative number of *Pseudomonas* isolates from infected and non-infected New Zealand kiwifruit orchards and characterisation of several hundreds of them.

- 2. Selection and genome sequencing of a representative population subset (approximately 50% *Psa*-suppressive and 50% non-suppressive isolates). Annotation of the genome data and identification of relevant NP as well as other relevant genes.
- 3. Conduction a statistical analysis of the phenotypic and genome data. Identification of correlations between phenotypes, genotypes, and the metadata.
- 4. Identification of biocontrol candidate strains from the *Pseudomonas* isolate collection. Conduct *in vitro* and *in planta* biocontrol experiments with these with model plants and on kiwifruit with the best candidates.
- 5. Identification of the potential genes responsible to produce *Psa*-suppressive NPs by the *Pseudomonas* biocontrol candidates. Conduct *in planta* biocontrol experiments with mutants to confirm NPs gene clusters responsible for *Psa* control.

CHAPTER 2
MATERIALS AND METHODS

## **CHAPTER 2: MATERIALS AND METHODS**

# 2.1. Growing media

Depending on the experiment and the microorganism, different media were used. Additionally, according to each location, the recipes of the same media were also slightly different. Below, the different ingredients, and media-making protocols can be found.

#### 2.1.1. LB medium

LB Miller agar was prepared with powder provided by Formedium, UK. The ingredient dosage per litre was: 10 g of peptone from casein (tryptone), 5 g of yeast extract, 10 g of sodium chloride (NaCl) and 11 g of agar.

#### 2.1.2. KB medium

For experiments carried out at P&FR (Ruakura, NZ) was used KB as described by King et al., 1954. The composition employed per litre was: 10 g of proteose peptone, 1.5 g of magnesium sulphate, 1 g of potassium phosphate, 16 g of agar and 6 mL of glycerol. After autoclaving, and when the media were below 50 °C, sterile filtered cycloheximide was added at 1 g per 100 mL of media.

For experiments carried out at the John Innes Centre, the following recipe was used per litre: 20 g of proteose peptone No 3 (Becton Dickinson, France), 1.5 g of di-potassium hydrogen phosphate (K<sub>2</sub>HPO<sub>4</sub>) (VWR Chemicals, France) and 10 mL of glycerol (Fisher, UK). With a magnetic bar, the solution was mixed and adjusted to a 7.2 pH by using 5M HCl. Then, 15 g of AGA03 agar (Formedium, UK) were added. After autoclaving, 6 mL of 1 M magnesium sulphate stock solution were added.

#### 2.1.3. CFC medium

CFC stands for cetrimide-fucidin-cephalosporin media. It is a selective media for the isolation of *Pseudomonas* species. It was made by using ready-made CM0559 dehydrated culture media, the Pseudomonas agar base (Oxoid, UK) at a rate of 24.2 g of powder per 500 mL of de-ionised water and 5 mL of glycerol. After the media were autoclaved and cooled down to 50 °C, it was supplemented with SR0103 CFC supplement (Oxoid, UK), a vial that combines a mixture of lyophilised cetrimide (10 mg/L), fucidin (10 mg/L) and cephalosporin (50 mg/L).

#### 2.1.4. SFM medium

Soya Flour Mannitol media were made following Hopwood *et al.*, 2000 preparation method. The formulation per litre was: 20 g of D-mannitol (Sigma, UK), 20 g of soy flour (Holland and Barrett, UK), 15 g of No 1 agar (Formedium, UK) and 1 L of tap water from the John Innes Centre.

# 2.1.5. FP medium

First, six 500 mL stock solutions were prepared:

- 1. 20 g of calcium chloride (CaCl<sub>2</sub> 2H<sub>2</sub>O) from Sigma, UK.
- 2. 20 g of magnesium sulphate (MgSO<sub>4</sub> 7H<sub>2</sub>O) from Fisher, UK.
- 3. 15 g of potassium phosphate monobasic (KH<sub>2</sub>PO<sub>4</sub>) from Sigma, UK.
- 4. 22.5 g of di-sodium hydrogen phosphate dodecahydrate (Na<sub>2</sub>HPO<sub>4</sub> 12H<sub>2</sub>O) from VWR Chemicals, France).
- 5. 1.25 g of ferric citrate (C<sub>6</sub>H<sub>5</sub>FeO<sub>7</sub>) from Sigma, UK. To bring it into solution, it requires heat and, later, light protection is required as it is photo sensitive.
- 6. Gibson's Trace: 1.43 g of boric acid (H<sub>3</sub>BO<sub>3</sub>) from Sigma, UK, 1.02 g of manganese sulphate (MnSO<sub>4</sub> 4H<sub>2</sub>O) from BDH, UAE, 0.11 g of zinc sulphate (ZnSO<sub>4</sub> 7H<sub>2</sub>O) from BDH, UAE, 0.04 g copper sulphate pentahydrate (CuSO<sub>4</sub> 5H<sub>2</sub>O) from BDH, UAE and 0.04 g of molybdic acid (H<sub>2</sub>MoO<sub>4</sub>) from Sigma, UK.

Then, for every 1 L of media, the following substances were added from the stock solutions: 2.5 mL of calcium chloride, 3 mL of magnesium sulphate, 3.33 mL of potassium phosphate monobasic, 3.33 mL of di-sodium hydrogen phosphate dodecahydrate, 2 mL of ferric citrate, 1 mL of Gibson's trace and 5 g of agar No 1 (Formedium, UK).

# 2.1.6. DNA medium

For 1 L, 23g of DIFCO™ Nutrient Agar was used (Becton Dickinson, France) were mixed into 1 L of deionised water and then shaken until all the powder was dissolved. Pre-autoclaving, no pH adjustment was needed.

#### 2.2. Bacterial sample collection and isolation

#### 2.2.1. Orchards location

Samples from six different orchards were collected (**Figure 2**). Orchards were located across the main kiwifruit production areas in New Zealand, as well as in areas where *Psa* was known to have and have not been detected, such as South Island —which remains to date *Psa*-free—. Orchards were exposed to a wide range of different climates and altitudes, worked under different agricultural practices and treated with or without irrigation. Altogether, they became part of the representative November and December 2018 sampling area for isolating kiwifruit-associated *Pseudomonas* spp. in New Zealand (**Table 2**).

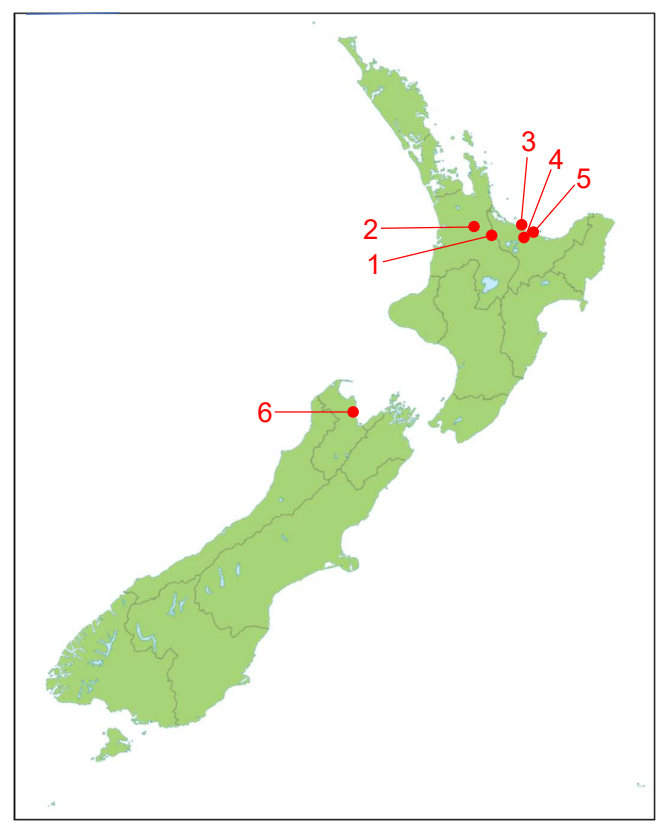


**Figure 2**. Geographical location of the six orchards from which the 6,123 isolates were isolated. (1) Karaipiro, (2) Ohaupo, (3) Kaimai Mt, (4) Te Puke, (5) Te Puke and (6) Motueka.

**Table 2**. Location of the kiwifruit orchards from where samples were collected, region, address, GPS coordinates and altitude.

No	Orchard	Region	Address	GPS location	Altitude (m)	
1	Karapiro	Waikato	995 Maungatautari Rd	-37.958302,	96	
	'			175.566599		
2	Ohaupo	Waikato	584 Ngahinapouri Rd	-37.9175060,	53	
_				175.2639820		
3	Kaimai	Bay of Plenty	585 McLaren Rd	-37.8374020,	261	
	ramiai		000 1110201011110	176.0624810	201	
4	Te Puke Bay of Plenty 288 No 3		288 No 3 Rd	-37.799250,	60	
'	TO T GIVE	Bay of Flority	2001100110	176.297000		
5	Te Puke	Fe Puke Bay of Plenty 950 No 3 Rd		-37.842849,	203	
	10 1 dito	Day of Flority	555 115 6 11d	176.264797	230	
6	Motueka	Nelson-Tasman	55 Old Mill Rd	-41.096463,	15	
	motacha		oo ola Mili Na	172.973581	. 0	

# 2.2.2. Samples collection

In total, 100 samples were collected per orchard, except from Motueka (orchard No 6) from which only 50 samples were collected. Samples were all collected by me, except those from Motueka, which were

collected by P&FR staff and kindly sent overnight by express courier services in a polystyrene box containing ice.

From each location, 80% of the samples were leaves and 20% buds, except from Te Puke's Gold 3 vines (orchard No 5) and Motueka's orchard, where only leaves were collected. This was due to the advanced phenological stage of kiwifruit vines (BBCH  $\geq$  69) (Salinero *et al.*, 2009), where buds were not present anymore. Then, from those orchards where *Psa* was known to be present, 50% of the samples were visually non-infected and 50% visually infected. From Motueka, where *Psa* was not present, all samples collected were considered visually non-infected. Non-biasedly, a total of 650 plant samples were collected.

To have a wide range of samples at different growth stages, young and mature leaves were collected. Similarly, visually infected, and non-visually infected samples from *Psa*-infected orchards were collected as shown in **Figure 3** (A-D). Symptomatic samples were required not to have a high number of necrosis areas as shown in **Figure 3** (E). Otherwise, an excessive amount of *Psa* colonies may appear on the agar plate post isolation. Additionally, visually infected, and non-visually infected kiwifruit buds were collected, when possible, at the phenological stage shown in **Figure 3** (F).

# 2.2.3. Sample processing

Plant samples were collected, labelled, and kept individually in zip plastic bags. They were transported along with ice in polystyrene boxes until their arrival to P&FR Ruakura, where samples were kept at 4 °C, while they were being processed, to minimise any microbiome change. As soon as samples arrived at the laboratory, they were all photographed.

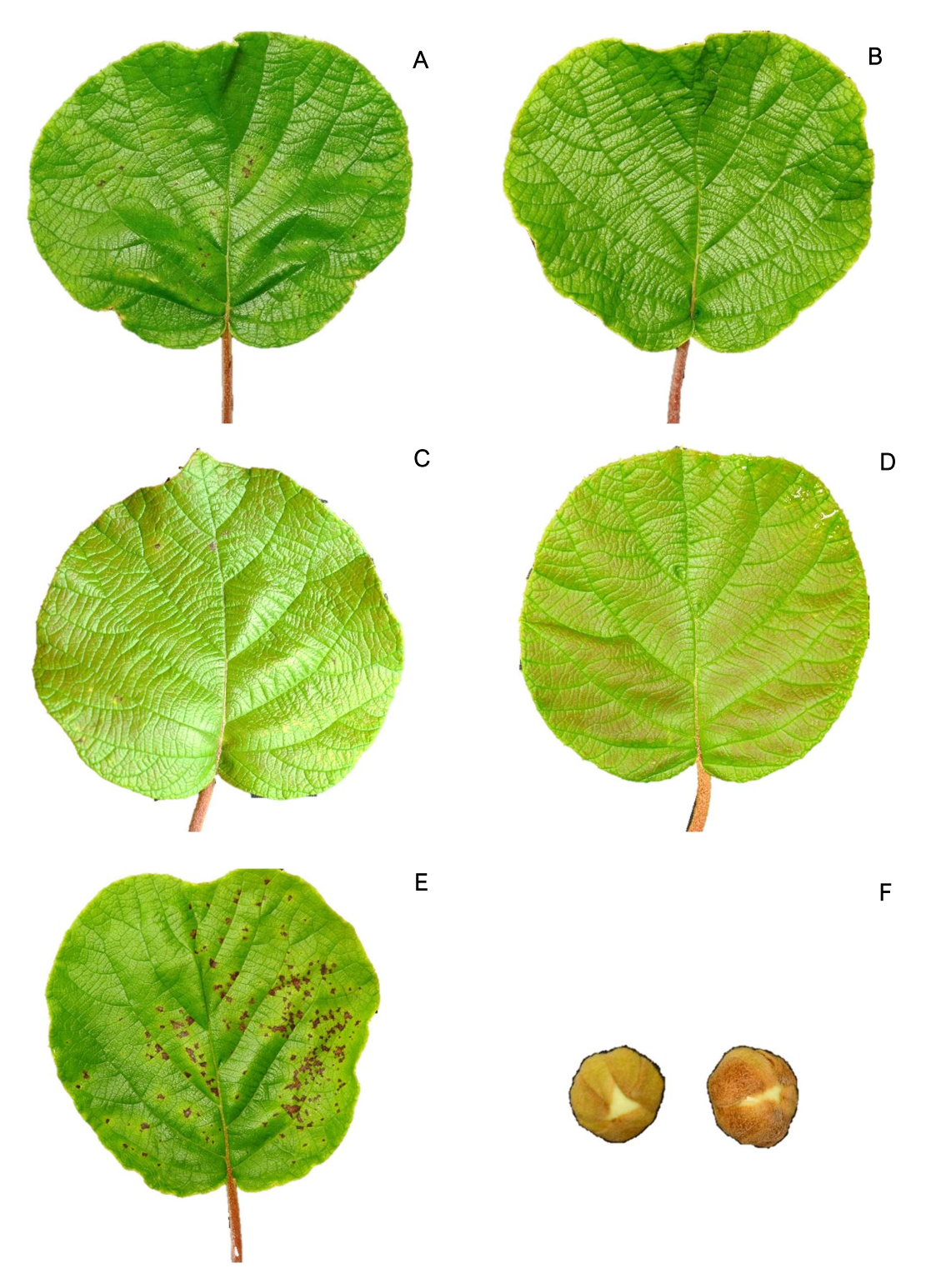


**Figure 3.** Representation of different kiwifruit samples. (A) Mature symptomatic leaf, (B) mature non-symptomatic leaf, (C) young symptomatic leaf, (D) young non-symptomatic leaf, (E) symptomatic leaf with over 5% necrotic leaf area and (F) non-symptomatic bud (left) and symptomatic bud.

# 2.2.4. Bacterial isolation and collection preparation

Epiphytic bacteria from leaves and buds were individually extracted by washing each sample inside its distinct zip plastic bag. Leaves and buds were washed with 10 mL and 5 mL of sterile di-ionised water, respectively. Bags were gently rubbed by hand, one by one, for 60 seconds on both sides and let sat for 15 minutes. Per sample, three 9 cm wide CFC-agar plates were required; one for the undiluted washing and two for two-fold dilutions (1/10 and 1/100). Per plate, 100 μL were widespread with help of a glass spreader. Then, the plates were incubated at 28 °C for 48 hours. At this stage, *Psa* would have grown less compared to other bacteria on the plates and making it easier for visual identification and exclusion. *Psa* single colonies were notoriously smaller than the rest of the isolates and phenotypically transparent-like.

To make the isolation non-biased, when the number of colonies per plate topped 24 (without counting *Psa*-looking isolates), portions of plates were randomly selected, and colonies within that portion were patched from the CFC-agar plates onto the KB-agar plates on a 24-isolates pattern (**Figure 4**).

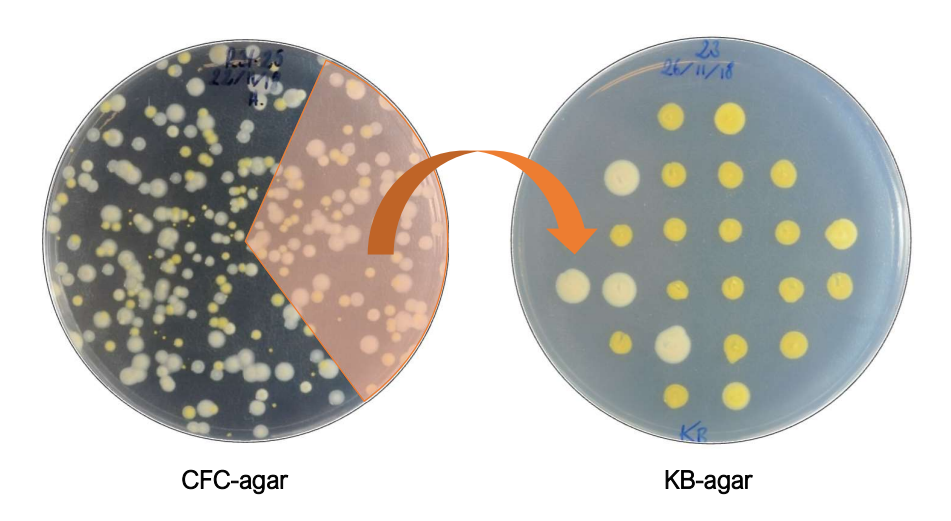


**Figure 4.** CFC-agar plate with a high number of *Pseudomonas* spp. isolates, representation of how a non-biased selection of a section of the plates was chosen and patched on a 24 isolates pattern on KB-i agar.

were streaked. This procedure was repeated for up to 100 isolates if no mixed colonies were found. Secondly, if the number of mixed colonies was too high, streaking of all isolates before patching from KB-agar to the 96-well pattern was considered. Streaking was done on KB-agar plates, incubated at 28°C and assessed after 48 hours. Additionally, to ensure that only non-*Psa* isolates were being patched onto KB-agar plates, isolates were randomly checked by PCR. For that, primers PsaF1 and PsaR2 were used (**Supplementary 1**).

# 2.2.5. Shipping of bacterial collection

A total of 1,056 bacterial isolates were unbiasedly selected from the Kaimai, Ohaupo, Motueka and Te Puke orchards. All of them were grafted with Hayward. From each orchard, 288 isolates were chosen, except from Motueka (*Psa*-free orchard), of which192 were selected. Similarly, 50% of the isolates came from non-symptomatic samples and 50% from symptomatic ones, except for Motueka, where there were no symptomatic samples.

Bacterial colonies were shipped to the United Kingdom in 11 double-contained CFC-agar 96-well plates. Bacterial colonies were sitting upright and inside the personal hand luggage, as for transporting non-pathogenic bacteria no special permit or licence was required. A total of 100 µl of CFC-agar medium per well were added.

# 2.2.6. Samples sorting

In New Zealand, 6,123 collected isolates were stored at -80 °C (**Table 3**). A mixture of KB broth, as described in section 2.1.2., supplemented with sterile 100% glycerol was used for freezing the isolated colonies at a ratio of 85:15, respectively. Colonies were replicated from a master copy incubated for 48 hours on KB-agar. At the John Innes Centre, two copies of the 1,056 isolates collection were stored at -80 °C; One copy as working stock and another one as a backup. Colonies were incubated at 28 °C for 20 hours with L media in 96-well plates. After incubating, 10% of dimethyl sulfoxide, a cryoprotective agent commonly known as DMSO (Sigma-Aldrich Company Ltd., Gillingham, UK), was added, and shaken at low speed for five minutes. When freezing any other samples, the same protocol was followed but using KBB media instead.

**Table 3**. Additional orchard information was gathered during the collection of samples in November and December 2018

December 2010.						
Orchard No	Psa present	Rootstock	Graft	Irrigated	BBCH	No isolates
1	Yes	Bruno	Hayward	Yes	60-65	738
2	Yes	Bruno	Hayward	Yes	53	980
3	Yes	Bruno	Hayward	No	53	1181
4	Yes	Bruno	Hayward	No	71	1096
5	Yes	Bruno	Gold G3	No	69-71	1034
6	No	Bruno	Hayward	Yes	-	1094

# 2.3. Bacterial phenotyping assays

Unless specified, all assays were carried out in 500 cm<sup>2</sup> big square plates (Thermo Scientific, UK) with 200 mL of KB-agar and dried for 45 minutes. Similarly, plates were inoculated with a 96-pin replicator, which loads approximately 2 µL of overnight culture per pin, dried for two minutes with the lid open inside the laminar flow hood, until drops were completely absorbed by the agar, and incubated upside-down at 28 °C for 48 hours post inoculation (hpi). Each phenotypic assay was repeated three times.

# 2.3.1. Colony morphology

Plates were inoculated and assessed by following a numerical scale. Zero for white or whitish colonies and one for all the other colours such as intense yellow (**Table 4**).

Score Representation

0

**Table 4**. Numerical scale for assessing colony morphology 48 hpi.

# 2.3.2. Siderophore production

Plates were inoculated and assessed by following a numerical scale. Zero for non-fluorescent colonies and one for fluorescent colonies (**Table 5**). Bacteria produce siderophores to scavenge iron from their environment. Iron is an essential nutrient that is required for many important cellular processes, including respiration and DNA synthesis. However, iron is often scarce in the environment, so bacteria have evolved various mechanisms to acquire iron. One of these mechanisms is the production of siderophores (Ahmed and Holmström, 2014).

Siderophores are small molecules that bind tightly to iron and facilitate its uptake into the bacterial cell. Some siderophores, such as pyoverdine, also have the ability to fluoresce under certain conditions. This fluorescence is thought to be a by-product of the chemical structure of the siderophore molecule. The exact mechanism by which siderophores fluoresce involve the interaction of the molecule with light because of energy transfer between the iron-bound siderophore and other molecules in the bacterial cell, such as flavins or porphyrins (Behnsen and Raffatellu, 2016).

Score Representation

0

**Table 5**. Numerical scale for assessing colony siderophore production 48 hpi.

# 2.3.3. Hydrogen cyanide production

For this assay, three mm Whatman™ filter paper (GE Healthcare, UK) was needed. Small sheets that could fit a 96-well plate lid (approximately 100 cm²) were manually cut, placed on an envelope and dry sterilised. Then, each sheet was impregnated with 2 mL of freshly made Feigl-Anger solution (Feigl and Anger, 1966). The proportions of the Feigl-Anger solution were 100 µg of copper ethyl acetoacetate (Sigma-Aldrich, UK), 100 µg of 4-4'-methylene-bis-N, N-dimethylaniline (Sigma-Aldrich, UK) and 30 mL of chloroform (Thermo Fisher Scientific, UK).

While the impregnated sheets were drying, non-treated CytoOne® 96-well plates (STARLAB, Germany) were filled with 150  $\mu$ L of King's B liquid media per well. Then, each well was subsequently inoculated with 2  $\mu$ L of overnight culture with the help of a replicator. Then, assisted by sterile tweezers, the impregnated sheet was gently placed on top of the inoculated plates and non-hermetically closed with the lid; this step was essential to avoid condensation, which would erase the results. Plates were incubated, as usual, only that, in this case, for the first 24h were shaken and for the next 24 hours, were placed statically on a shelf. When assessed, numerical scores between zero and two were given to each isolate. Zero for no change of colour in the paper, one for very low or low blue pigmentation and two for strong or very strong blue pigmentation (**Table 6**).

Score Representation

1
2

**Table 6.** Numerical scale for assessing hydrogen cyanide production 48 hpi.

## 2.3.4. Protease production

For this assay, KB-agar supplemented with 1 % (w/v) instant dried skimmed milk powder (Tesco, UK) was used. To prepare it, for 200 mL of medium, in a separate sterile Duran®, 2 g of the milk powder were dissolved in 20 mL of cold sterile water and then heated up in a water bath for no more than 5 minutes, to bring it to the media temperature and avoid lamps and caramelisation of milk sugars. Then, 20 mL of the melted media were discarded, replaced with the 20 mL milk hot solution, and mixed carefully, as otherwise, many bubbles would appear.

Then the medium is poured onto the plates, dried, inoculated and incubated. When bacteria produce proteases in vitro on KB-agar supplemented with milk, a clear halo around bacteria colonies can be appreciated. This is called milk proteolysis, where casein proteins are broken down. When assessed, scores between zero and two were given to each colony; zero when no milk degradation halo is present, one when a very little or little halo is present and two when a big and clear halo is present (**Table 7**).

Score Representation

1

2

**Table 7**. Numerical scale for assessing protease production 48 hpi.

# 2.3.5. Swarming motility

For this assay, 0.5 % agar KB medium was used. Plates were dried and inoculated as usual. However, for incubation, plates were only incubated and assessed after six hours. Otherwise, some isolates may overgrow. When assessed, numerical scores between zero and two were given to each isolate; zero for those colonies that did not show any swarming motility, one for those with very little or little swarming motility and two when colonies were very or extremely motile (**Table 8**).

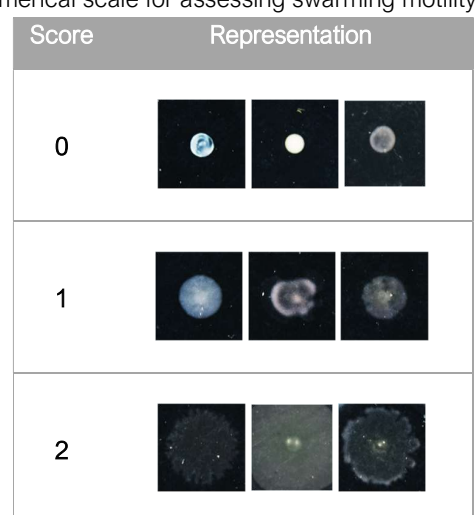


**Table 8**. Numerical scale for assessing swarming motility assay 6 hpi.

# 2.3.6. Congo Red binding

For this assay, it was used KB-agar supplemented with sterile filtered Congo Red at a final concentration of 0.005 %. Plates were dried, inoculated, and incubated as usual. When assessed, numerical scores between zero and two were given to each isolate based on their red binding intensity; zero for those colonies that did not show red binding, one for those that showed very low or low red binding and two for those colonies that showed a strong or very strong Congo Red binding (**Table 9**).

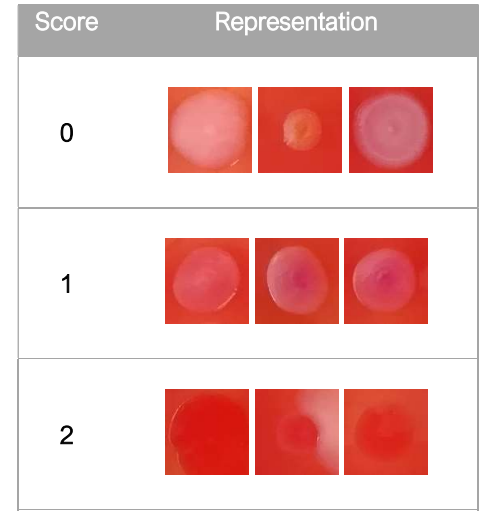


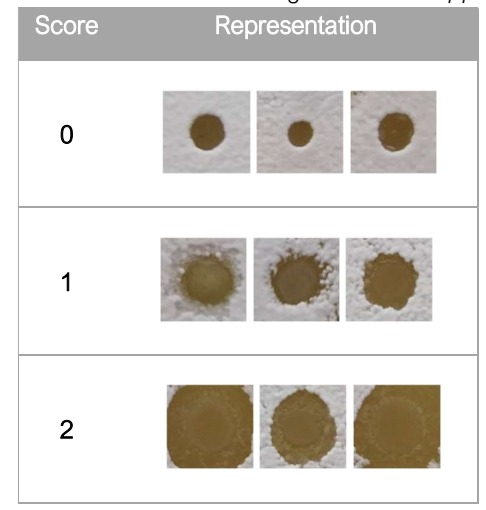
**Table 9**. Numerical scale for assessing Congo Red binding 48 hpi.

# 2.3.7. Streptomyces scabies suppression

For this assay, 140 mm diameter circular plates (Thermo Scientific, UK) with 70 mL of SFM media were used. For the overlay inoculation, 200 µL of 1:4 *Streptomyces scabies* spore suspension (see section 2.11. for stock preparation) along with 1x PBS was evenly spread until fully absorbed by the agar. It was essential to use sterile filtered tips throughout this assay to avoid contamination.

After inoculating the plates with *S. scabies*, they were dried for 10 minutes inside the cabinet, and then inoculated with the isolates of interest, following the standard procedure. Plates were incubated at 30 °C and assessed after three- and five-days post inoculation (dpi). When assessed, numerical scores between zero and two were given to each isolate; zero for those colonies that did not show any growth suppression against *S. scabies*, one if small or little suppression was observed and two for colonies that strongly suppressed *S. scabies* growth and where a clear halo was present around the bacterial colony (**Table 10**).

**Table 10**. Numerical scale for assessing *S. scabies suppression* 3 dpi.



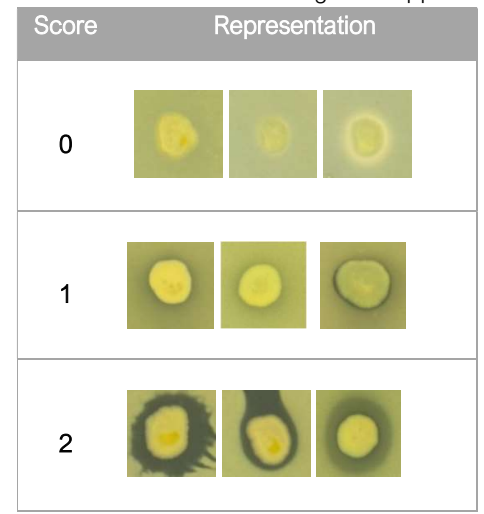
# 2.3.7.1. Liquid-culture overlay for Psa suppression

Two different *Psa* pathovars were used for this assay: *Psa* biovar 3, 10627 and *Psa* biovar 3, RT594. The first one (10627), being the outbreak strain, was isolated from *Actinidia chinensis* wood in 2010 by Dr Joel Vanneste at Te Puke, New Zealand (Vanneste *et al.*, 2013). The second one (RT594), a naturally-resistant strain to copper and streptomycin at farming spraying rates, was isolated from *Actinidia chinensis* var. *chinensis* in 2015 by VLS in Te Puke, New Zealand (Cornish, Schipper et al. 2017).

Plates were prepared and dried as usual. Simultaneously, a water inoculum suspension of Psa biovar 3 was prepared. Starting from a Psa biovar 3 overnight culture —at an adjusted  $OD_{600}$  of 1, 500  $\mu$ L were added to a mixture of 90 mL of sterile purified water, along with 10 mL of 100 mM of MgCl<sub>2</sub> to reduce the osmotic pressure of the cells, reaching a final  $OD_{600}$  of 0.005. Then, some of this solution was poured in excess on the plates, gently rotated to evenly distribute the inoculum solution. Afterwards, the excess was removed with an electronic pipette.

Plates were left to dry for 15 minutes, or until the whole surface was dry. Occasional rotation made the drying more homogenous. Next, plates were inoculated and incubated as usual. When assessed, numerical scores between zero and two were given to each isolate; zero for colonies that did not show any growth suppression against *Psa*, one if a small or very small suppression halo was seen and two for those colonies that strongly suppressed the bacteria, and where a clear halo was present (**Table 11**).

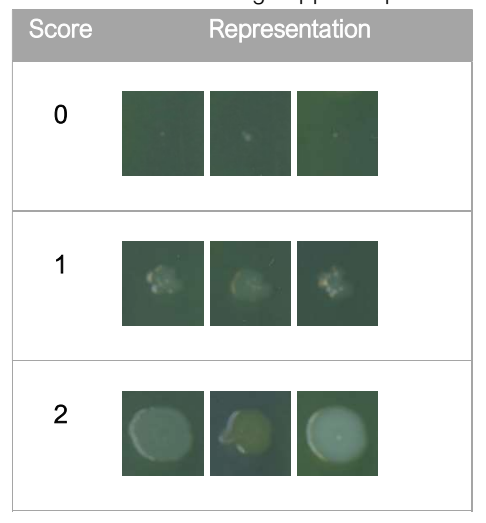
**Table 11**. Numerical scale for assessing *Psa* suppression 48 hpi.



# 2.3.8. Copper sulphate resistance

For this assay, media were supplemented with 500 mg/L of copper (II) sulphate pentahydrate (CuSO<sub>4</sub>·5H<sub>2</sub>O) (Sigma-Aldrich, UK) to mimic field applications for kiwifruit vines against *Psa* biovar 3 in New Zealand (Vanneste and Voyle 2003, Vanneste, McLaren et al. 2005). Plates were dried, inoculated, and incubated as usual. When assessed, numerical scores between zero and two were given to each isolate; zero for those colonies that did not grow, one for colonies that experienced very little or little growth and two when colonies had the expected growth (**Table 12**).

Table 12. Numerical scale for assessing copper sulphate resistance 48 hpi.



# 2.3.9. Streptomycin resistance

For this assay, medium was supplemented with streptomycin sulphate salt (Sigma-Aldrich, Germany) at 100 ppm to mimic field applications for kiwifruit vines against *Psa* biovar 3 in New Zealand (Vanneste, McLaren et al. 2005), such as the commercially available bactericide Key Strepto<sup>TM</sup> from Key Industries

Ltd., New Zealand. The antibiotic was added to the media when it was below 50 °C from a sterile-filtered stock solution on water. Plates were dried, inoculated, and incubated as usual. When assessed, numerical scores between zero and two were given to each isolate; zero for those colonies that did not grow, one for colonies that experienced very little or little growth and two when colonies had the expected growth (Table 13).

Score Representation

0

1

2

**Table 13**. Numerical scale for assessing streptomycin resistance 48 hpi.

# 2.3.10. Kasugamycin resistance

For this assay, medium was supplemented with 100 mg/L of kasugamycin hydrochloride (Sigma-Aldrich, Germany) mimicking field applications for kiwifruit vines against *Psa* biovar 3 in New Zealand such as the commercially available bactericide Kasumin® from UPL Ltd., New Zealand. The antibiotic was added to the medium when it was below 50 °C from a sterile-filtered stock solution on water. Plates were dried, inoculated, and incubated as usual. When assessed, numerical scores between zero and two were given to each isolate; zero for those colonies that did not grow, one for colonies that experienced very little or little growth and two when colonies had the expected growth (**Table 14**).

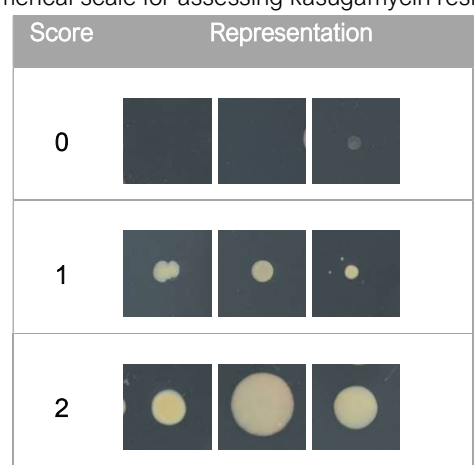


**Table 14**. Numerical scale for assessing kasugamycin resistance 48 hpi.

# 2.4. Bacterial genotyping and data analysis

#### 2.4.1. Genomic DNA extraction

For genomic DNA (gDNA) extraction, a selection of 103 *Pseudomonas* isolates from the 1,056 UK collection were picked. These isolates were actively chosen based on their phenotypic profile such as resistance to copper sulphate, resistance to streptomycin or biocontrol ability against *Psa* biovar 3. All *Psa*-suppressive *Pseudomonas* were included in the batch, however, non-*Psa* suppressive, copper sulphate resistant and streptomycin-resistant *Pseudomonas* were randomly chosen across the isolates that strongly showed the above-mentioned characteristics.

Bacteria were streaked out from the -70 °C stock onto individual KB-agar plates. Plates were incubated at 28 °C for 48 hours. After that time, single colonies were picked with an inoculation loop, inoculated in 30 mL glass universal tubes with 5 mL of LB-liquid media and incubated whilst shaken overnight at 250 rpm and 28 °C for 20 hours.

For the actual gDNA extraction, GenElute Bacterial Genomic DNA Kit (Sigma-Aldrich, USA) was used. Most of the protocol steps were followed as described by the manufacturer, but further procedures were added to optimise the environmental *Pseudomonas* gDNA extraction.

As described here, 11 steps were followed. Unless specified, steps were carried out at room temperature:

- 1. First, the Dri-Block® DB-2D heating block (TECHNE, UK) was preheated to 55 °C.
- 2. For each *Pseudomonas* isolate, 1.5 mL of overnight culture were pelleted in a 2 mL microfuge tube (SARSTEDT, Germany) by centrifuging with a Heraeus Pico 17 centrifuge (Thermo Fisher, UK) for 2 minutes at 12,000 x g. Then, bacteria culture media were completely removed and discarded. A pipette was used when needed as rests of liquid media may reduce the efficiency or partially inhibit the following reactions.
- 3. Pellets were resuspended in 180  $\mu$ L of lysis solution T and, with the help of pipette tips, the bottom of the different microfuge tubes was gently scratched to facilitate resuspension of the harvested cells. Next, 20  $\mu$ L of RNase A solution was added as RNA-free gDNA is desired. Samples were vortexed at 2,500 rpm for 10 seconds and left incubating for 2 minutes at room temperature.
- 4. Afterwards,  $20 \,\mu\text{L}$  of  $20 \,\text{mg/mL}$  proteinase K solution were added, vortexed at 2,500 rpm for 5 seconds and incubated for 30 minutes at 55 °C.
- 5. When finished, 200  $\mu$ L of lysis solution C were added, vortexed at 2,500 rpm for 15 seconds, and incubated at 55 °C for 10 minutes until a homogeneous mixture was obtained. Simultaneously, the elution solution was placed on top of the heating block to start warming it up at 55 °C.

- 6. While samples were incubated, the binding columns were prepared. They were assembled in 2 mL collection tubes, and  $500 \,\mu\text{L}$  of column preparation solution were added to be then centrifuged at 12,000 x q for 1 minute. The follow-through liquid was discarded, and the collection tube was retained.
- 7. To prepare for binding, once incubation was finished, 200 µL of ethanol absolute (VWR Chemicals, France) was added to the lysate, so DNA binding would occur. Samples were then vortexed for 10 seconds until obtaining a homogeneous mixture.
- 8. The entire content of the 2 mL microfuge tubes was transferred into the prepared binding columns to be then centrifuged at 8,000 x g for 1 minute. The follow-through liquid and the collection tube were discarded, and the binding columns were transferred into new 2 mL collection tubes.
- 9. To proceed with the first wash,  $500~\mu L$  of wash solution 1 were added to the binding column and centrifuged at 8,000~x~g for 1 minute. The follow-through liquid was discarded, and collection tubes were retained.
- 10. For the second wash, 500  $\mu$ L of wash solution (20 mL of wash solution concentrate in 80 mL of ethanol absolute) were added to the columns and centrifuged for 3 minutes at 12,000 x g to dry the column. The follow-through liquid was discarded, and the collection tubes were retained. Tubes were centrifuged again for an additional 1 minute at 12,000 x g. The follow-through liquid and the collection tubes were discarded, and the binding columns were transferred into new 2 mL collection tubes.
- 11. Before eluting the DNA, to ensure columns were ethanol free, the new collection tubes with the binding columns were incubated with lids open at  $55\,^{\circ}$ C for 5 minutes. Then, to remove the contaminants, 100  $\mu$ L of the elution solution, tris-EDTA, were added. They were applied directly onto the centre of the columns, incubated at  $55\,^{\circ}$ C for 5 minutes and centrifuged first at  $0.3\,x$  g for 1 minute and then at  $8,000\,x$  g for 1 minute. The follow-through liquid and the collection tubes were kept, and binding columns were transferred into new 2 mL collection tubes to repeat the same procedure for a second and separate elution.

### 2.4.1.1. Storage and quality check

For short-term storage, samples were stored up to 72 hours at 4 °C while absorbance, quantity, size and quality of the gDNA were measured. Afterwards, all samples were stored at -20 °C before being prepared for sequencing. Additionally, with an ND-1000 NanoDrop<sup>TM</sup> spectrophotometer (Thermo Fisher Scientific, France) gDNA purity was measured (Simbolo, Gottardi et al. 2013, Kapp, Diss et al. 2015). It was calibrated by using di-ionised sterile water and elution solution as blank. Each measurement was done with a 2  $\mu$ L sample to avoid the appearance of bubbles. For the absorbance reading at 260/280 nm, a ratio of 1.7-1.90 was established as a minimum to pass the quality standard. Similarly, to ensure that samples were pure nucleic acid, for the 260/230 ratios, values of 2 or more were looked for (Lucena-Aguilar, Sanchez-Lopez et al. 2016).

If readings were not as expected, gDNA was re-isolated or re-precipitated. However, due to the solution's acidic pH and the equipment accuracy, readings were expected to vary by 0.2-0.3 (Wilfinger, Mackey et al. 1997). For those samples where the ratio 260/230 was below 2, their gDNA was re-precipitated to help remove the contaminants. However, doing so resulted in the loss of some nucleic acid.

For reprecipitation, the followed protocol was adapted from QIAGEN:

- 1. First, the heating block was preheated to 60 °C.
- 2. To the 100  $\mu$ L DNA samples, 10  $\mu$ L of 3 M Na-acetate at pH 5.2, and 200  $\mu$ L of ice-cold ethanol absolute were added.
- 3. The samples were then mixed and stored at –20 °C for 1 h to precipitate the DNA.
- 4. Then, DNA was recovered by centrifuging for 20 minutes at 13,000 x g.
- 5. Next, the ethanol supernatant was carefully poured off.
- 6. Pellets were washed twice with room-temperature 70 % ethanol and, again, the ethanol supernatant was carefully poured off. A pipette was used when needed as rests of ethanol may reduce the efficiency or partially inhibit the following processes on which this DNA was to be used.
- 7. Then, pellets were dry at 60 °C for 5 minutes or until no liquid was remaining.
- 8. Finally, pellets were re-suspended in the elution buffer.

With Qubit<sup>TM</sup> 2.0 Fluorometer (Thermo Fisher Scientific, USA), the quantity of gDNA was measured (Simbolo, Gottardi et al. 2013). The fluorometer was calibrated by using Qubit dsDNA HS standards (Invitrogen<sup>TM</sup>, USA) and Qubit Assay Tubes (Invitrogen<sup>TM</sup>, China) were used for the readings. Samples were prepared by mixing 1  $\mu$ L of gDNA with 199  $\mu$ L of the master solution. The master solution was achieved by mixing 199  $\mu$ L Qubit<sup>TM</sup> dsDNA BR buffer (Invitrogen<sup>TM</sup>, USA) with 1  $\mu$ L Qubit concentrated assay reagent (Invitrogen<sup>TM</sup>, USA) and vortexed for 3 seconds. Samples were prepared away from direct light, as Qubit concentrated assay reagent was photosensitive.

To determine the size and quality of the extracted gDNA, gel electrophoresis was carried out (Sambrook, Russell et al. 2001) as described in section 2.4.2.

## 2.4.2. PCR and gel electroporation

## 2.4.2.1. PCR

Colony PCRs was carried out with GoTaq® Green Master Mix (Promega, UK) and, unless specified, following the manufacturer's protocol recommendations. Similarly, unless specified, desired genes were amplified by placing the reaction mixture in the thermocycler for an initial denaturation of 95 °C for 3 min, followed by 30 cycles at 95 °C for 15 s (denaturing), 60 °C for 30 s (annealing) and 72 °C for 1 min 30 s (elongation). Final elongation lasted 5 min at 72 °C and was then brought and kept to 4 °C until required.

#### 2.4.2.2. Gel electroporation

For 1 L of 50x TAE electrophoresis buffer, 242 g of Tris-base (Severn Biotech Ltd., UK) were dissolved in approximately 700 mL of di-ionised water; carefully, 57.1 mL of glacial acetic acid (Fisher Scientific, UK) and 100 mL of 0.5 M EDTA (Formedium<sup>TM</sup>, UK) at pH 8 were added. Then, the solution was brought to a final volume of 1 L. If the pH of the buffer was not adjusted, it was done so to 8.5 and stored at room temperature for further use when required. The final concentration in the gel was 40 mM Tris, 20 mM acetic acid, and 1 mM EDTA when diluting 20 mL of 50x TAE in a final volume of 1 L.

For gel electrophoresis, two gel chambers were used. A small Mini-Sub Cell GT (BIO-RAD, UK) and a bigger one (Fisher Scientific, UK), with PowerPac Basic as a power supply (BIO-RAD, UK). The small one had the capacity for 50 mL agarose gels, while the big one for 120 mL agarose gels. For agarose gels, 1x Tris-borate-EDTA diluted from a 10x solution (Severn Biotech Ltd., UK) and agarose (Melford, UK) were used at a final 0.9% agarose concentration.

When cooled down, a 0.5% of RedSafe™ nucleic acid staining solution at 20,000x was added (Chembio Ltd., UK) in P&FR Rakaura or ethidium bromide solution (Sigma-Aldrich, UK) at 8 µL per 100 mL of agarose gel at John Innes Centre, UK. When gels were solidified, at P&FR Rakaura, the electrophoresis units were filled with 1x TAE while at John Innes Centre, electrophoresis units were filled with 1x Trisacetic acid-EDTA diluted from a 50x solution (Formedium Ltd., UK), until gels were completely covered.

Power supply was set at 90 V for 80 minutes. Gels were loaded with 5  $\mu$ L of a ladder depending on the test (**Table 15**. List of ladders used in this thesis from New England BioLabs Inc., UK.).

Table 15. List of ladders used in this thesis from New England BioLabs Inc., UK.

Ladder name	Size range (kb)
Quick-Load® 1 kb Extend DNA ladder	0.5 - 48.5
Quick-Load® Purple 1 kb DNA Ladder	0.5 - 10
Quick-Load® Purple 100 bp DNA Ladder	0.1 – 1.5

If the reaction required loading dye, purple 6x without sodium dodecyl sulfate (SDS) for sharper results (New England BioLabs Inc., UK). Reactions and dye were mixed well and loaded into the gel at a rate of  $5 \mu L$  of loading dye per  $25 \mu L$  of reaction.

#### 2.4.2.3. Illumina® whole genome sequencing

A total of 103 *Pseudomonas* spp. strains were sent to Earlham Institute (Norwich, UK) for whole genome sequencing. The concentration of the samples was normalised to 30 ng/µL by using elution buffer and in total, 20 µL per sample were sent for sequencing.

Library construction was done with LITE (5-10% expected failure) and sequenced in one lane with NovaSeq 6000 SP flow cell, giving a theoretical output of 150 paired-ends (PE) reads (325 million reads per lane for each direction sequenced). *Pseudomonas* spp. were known to have a genome size of around 6 Mb. Therefore, a 30x coverage per sample was expected.

Later, a batch of 33 *Pseudomonas* spp. strains within those 103 initial ones were sent for a higher indepth whole genome sequencing to Novogene (Hong Kong, China). Per sample,  $30 \,\mu\text{L}$  with at least  $2\mu\text{g}$  of gDNA were sent. DNA library preparation was carried out with 400-450 bp insert size and sequencing with NovaSeq 6000 giving a theoretical output of 250 PE reads. Assembly was done by Govind Chandra (John Innes Centre, UK) using the 3.13.1 SPAdes with its default settings (Prjibelski, Antipov et al. 2020). From the assemblies, nucleotide sequences of encoding genes were mined using a combination of various BLAST tools and Perl scripts which relied heavily on the BioPerl collection of Perl modules (Stajich, Block et al. 2002).

Finally, another sequencing company whose services were sporadically employed was MicrobesNG (Birmingham, UK). Per sample, 50 µL of gDNA at 30 ng/µL were sent. Strains were sequenced by using standard Nextera protocols, from gDNA, generating a sequencing-ready library with longer insert sizes for sequencing (300bp - 1.5kb target insert size) while producing a 30x coverage (Seth-Smith, Bonfiglio et al. 2019). Reads were trimmed by Govind Chandra (John Innes Centre, UK) using Trimmomatic and the quality was assessed using in-house scripts combined with SAMtools (Li, Handsaker et al. 2009), BEDTools (Quinlan and Hall 2010) and BWA-MEM (Li 2013). Assembly metrics were provided by MicrobesNG and calculated using QUAST (Gurevich, Saveliev et al. 2013). Similarly, MicrobesNG provided top families and genera by using the Kraken (Wood and Salzberg 2014).

Additionally, a more enhanced service was utilised where Illumina® sequencing (2x250 bp) is combined with Oxford Nanopore sequencing to produce top-quality genome assemblies. For this service,  $5 \times 10^9$  of bacteria cells were sent, the equivalent of 10-12 ml of overnight culture at an OD<sub>600</sub> of 1. The reads were trimmed using Trimmomatic and the quality was assessed using in-house scripts combined with SAMtools, BEDTools and BWA-ME; the assembly metrics were calculated using QUAST, and the top families and genera that the reads map to were calculated using the Kraken.

#### 2.4.3. Genome mining for NPs clusters

#### 2.4.3.1. AntiSMASH

For genome mining, antibiotics and Secondary Metabolite Analysis Shell (antiSMASH) 5.0 (Blin, Shaw et al. 2019) and antiSMASH 6.0 (Blin, Shaw et al. 2021) were mainly used. A web server that searches for biosynthetic gene clusters to identify and characterize new chemical compounds was employed.

# 2.4.4. Phylogenetics and bioinformatic analyses

# 2.4.4.1. Genotyping of *Pseudomonas* spp.

For phylogenetic analysis, the tool used was BioEdit 7.2 (Hall, Biosciences et al. 2011), in order to align and concatenate the *atpD*, *dnaE*, *guaA*, *gyrB* and *rpoD* housekeeping genes of 103 *Pseudomonas* spp. strains together with 10 reference strains (**Table 16**.).

**Table 16**. Reference strains used in this study and source.

Name	Reference
Cellvibrio japonicus Ueda107	(DeBoy, Mongodin et al. 2008)
Pseudomonas jensenii GM48	(Brown, Utturkar et al. 2012)
Pseudomonas koreensis Pf0-1	(Varivarn, Champa et al. 2013)
Pseudomonas corrugata F113	(Redondo-Nieto, Barret et al. 2013)
Pseudomonas chlororap 06	(Kang, Anderson et al. 2018)
Pseudomonas protegens Pf-5	(Jing, Cui et al. 2020)
Pseudomonas fluorescens SBW25	(Rainey and Bailey 1996)
Pseudomonas syringae DC3000	(Xin and He 2013)
Pseudomonas putida KT2440	(Martins dos Santos, Timmis et al. 2004)
Pseudomonas aeruginosa PA01	(Labaer, Qiu et al. 2004)

Alignment settings were as follows: Accessory Application > clustal multiple alignment > ClustalW example application (for aligning any number of homologous nucleotide or protein sequences) with no 1,000 bootstraps neighbour-joining (NJ) tree. Output was uploaded on txt. format to the online phylogenetic tree viewer iTOL v6 (Letunic and Bork 2021).

For the construction of the tree on ITOL, *C. japonicus* Ueda107 was chosen as the start of the phylogenetic tree by selecting it > editing tree structure > re-rooting the tree here and displaying the tree on rectangular mode for a better visual presentation.

#### 2.5. Genetic manipulation of *Pseudomonas* spp.

# 2.5.1. Electrotransformation

Overnight 50 mL cultures were set with L medium, inoculated with 500  $\mu$ L of stock overnight culture and grown to and OD<sub>600</sub> of 0.8-1.2. This culture was transferred to a 50-mL Falcon tube and centrifuged at 3,000 x g for 8 minutes. The supernatant was removed by decanting, and, with a pipette, the excess was removed. The pellet was re-suspended into 1 mL of 300 mM sterile filtered sucrose with a 0.22  $\mu$ m

syringe filter (Starlab Ltd., UK) and transferred to a microcentrifuge tube. Cells were centrifuged at 11,000 x g for 1 minutes and the supernatant was removed. Gently, with a pipette, the white gunky layer on top of the cell pellet was removed. This is extracellular polymeric substances such as polysaccharides, proteins, extracellular DNA, and lipids (Jachlewski et al. 2015). Then, sucrose washes were repeated two more times. Once finished, cells were re-suspended into 200  $\mu$ L 300 mM sterile filtered sucrose.

Next, 500 ng of *plJ11282*, a cloning vector for gene expression extracted from *Escherichia coli* with a standard mini prep, were added (Frederix et al., 2014). It was mixed carefully and let to rest for 2 minutes at room temperature while a 'no DNA' control was also prepared. When finished, mixtures were added to 2 mm electroporation cuvettes (Geneflow Ltd., UK), ensuring cells were within the lower part of the cuvette that will receive the current. To electroporate the cells it was used an Eppendorf Eporator® (Eppendorf UK Ltd., UK) set at 2500 V. Immediately after, 1 mL of LB-medium was added directly into the cuvette and transferred into a 15-mL falcon tube where an additional 2 mL of LB-medium were added to help bacteria recover from the electroshock. Cells were recovered shaking obliquely —to enable expression of antibiotic resistance genes— at 28 °C for 3 hours.

In the meantime, fresh L-agar plates supplemented with 10  $\mu$ g/mL of tetracycline were made. When incubation was finished, samples were centrifuged at 3,000 x g for 5 minutes and the supernatant removed. With a pipette the extracellular polymeric substances were removed. Each pellet was resuspended with 100  $\mu$ L of supernatant and 100  $\mu$ L were spread onto each L-agar plate. Plates were incubated for 72 h at 28 °C and single colonies were re-streaked for single colonies, again on L-agar plates supplemented with 10  $\mu$ g/mL tetracycline.

#### 2.5.2. Transposon screening

Some bacteria were electrotransformed into two different transposon plasmids. Based on bacteria natural resistance to tetracycline o kanamycin, either *pALMAR3* —a mariner plasmid that provided tetracycline resistance—, or Tn5 —a transposon that provides kanamycin resistance— were employed (Malone, Jaeger et al. 2010, Tran, Stevenson et al. 2018)

After electrotransforming, cells were plated as usual on selective media. Single colonies were picked and patched onto KB-agar. Single colonies were tooth picked onto L-agar supplemented with the desired antibiotic, grown at 28 °C and used for screening against the desired phenotype. Those plates were used as master plates and used to screen against the desired phenotype. Positive candidates were confirmed via two random PCRs. Arbitrary-primed PCR methods use primers specific to the ends of the transposon and primers of random sequence that may anneal to chromosomal sequences near a transposon insertion. First round, by using Arb 1b and Tn5 ext (**Supplementary 1**). Then Tn5 seq and Arb 1 (**Supplementary 1**). A total of 25  $\mu$ L reaction mix was prepared per sample, purified with 15  $\mu$ L of deionised water as elution buffer, following the manufacturers recommendations for plasmids of low copy

number, from which  $2.5~\mu L$  were used for the second PCR to then be purified and run  $5~\mu L$  of the final elution in an agarose gel. Finally, PCR products were cleaned up re-using the same miniprep columns and following the same steps as described previously in this section. Then, samples were check on a gel and the yield measured with a ND-1000 NanoDrop<sup>TM</sup> spectrophotometer.

# 2.5.3. Chemically competent cells

Cells of *E. coli* S17-1 cells were used. From a fresh plate, one 50 mL LB flask was inoculated and supplemented with 80 ppm streptomycin. Cells were grown at 37 °C until they reached an  $OD_{600}$  = 0.4. During this time, it was put down 100 mM MgCl<sub>2</sub> and 100 mM CaCl<sub>2</sub> on ice. Also, a 50 mL conical centrifuge tube was placed on ice. When the desired OD600 was reached, cells were centrifuged at 4 °C using a conical centrifuge tube and a speed of 4,500 rpm for 8 minutes. Gently, cells were resuspended into 100 mL of ice-cold 100 mM MgCl<sub>2</sub>, finally occupying two 50 mL conical centrifuge tubes. Tubes were centrifuged at 4,500 rpm for 8 minutes. Bacterial pellets were re-suspended into 100 mL ice-cold 100 mM CaCl<sub>2</sub> and the suspension was incubated on ice for 20 minutes. Then, the suspension was centrifuged at 4,500 rpm for 8 minutes. Finally, the cell pellet was re-suspended into 5 mL of ice-cold sterile 100 mM CaCl<sub>2</sub> with 20% (w/v) glycerol. Depending on the purpose, the mixture was dispensed in 200 µL aliquots and stored at -70 °C, unless wanted to use them fresh that were kept on ice.

#### 2.5.4. Conjugation

Conjugation was used to transfer transposon plasmids to other bacteria through direct contact. Both donor (transformed S17-1 cells with the desired plasmid) and recipient bacteria were grown overnight. In microfuge tubes,  $100 \,\mu\text{L}$  of the donor were mixed with  $900 \,\mu\text{L}$  of the recipient, spined down at  $13,000 \, \text{x}$  g for 2 minutes and re-suspended in  $100 \, \mu\text{L}$  of KB liquid medium. Mixtures were plated together on KB-agar with no antibiotic supplementation for 24 hours at  $28 \, ^{\circ}\text{C}$ . Then, grown cultures were taken out with help of a streaking loop and re-suspended in fresh liquid media and diluted to  $10^{-8}$  of  $OD_{600}$ . Next, part of the dilution was spread on selective media and grown for  $78 \, \text{hours}$  at  $28 \, ^{\circ}\text{C}$ . All grown colonies should be transposon mutants if control plates were ungrown. As control, the same process was carried out in parallel without the donor strain.

# 2.6. Extraction and concentration of bioactive metabolites

Overnight cultures of the strain of interest were prepared. Psa biovar 3, 10627, any biocontrol strains desired and their mutants in 5 mL tubes of L liquid medium. Overnights were made from fresh strains taken from the -70 °C freezer to agar two days before they were used. For this assay there were used two 50 mL flasks of KB liquid medium per treatment. From the overnight cultures, flasks were inoculated with 100  $\mu$ L of the strain of interest or not inoculated for the control. It was ensured that all liquid KB medium belonged to the same batch. Flasks were incubated at 28 °C for 24 hours at 250 r.p.m.

To check if bioactivity was preserved after 24 hours in incubation, 2 mL from each flask were pipetted into 2 mL Eppendorf tubes and centrifuged at 13,000 x 5 minutes; carefully, without re-suspending any material, right after the centrifuge finished, under sterile conditions, the supernatant was filtered through a 0.2 µm syringe filter. The filtered supernatant was placed in a new 2 mL Eppendorf tube and tested for biocontrol *in vitro* against *Psa*. While bioactivity of the supernatants was checked, the rest of the supernatants were placed in 50 mL centrifuge tubes. Fifty percent overnight culture, 50% with 100% ACN. Tubes were shaken at 13,000 x g for 30 minutes at 8 °C. Then, aqueous phase and ACN phase were separated to be later evaporated with Genevac (SP Scientific, UK) using program No 8, for HPLC, at 30 °C. Finally, samples were recovered using the appropriate solvent to re-suspend and tested for biocontrol *in vitro* against *Psa*. If successful, samples were ready for HP-LC.

# 2.7. Plant experiments

## 2.7.1. Dip-inoculation pathogenicity assays

Solanum lycopersicum var. moneymaker provided by Premier Seeds Direct, UK, in batches of 200 seeds. When seeds were received on site, they were stored at 4 °C and before use, not surface sterilised. However, to standardise growth, tomato seedlings were vernalised for 7 days.

For this assay, the plant model used was: four-weeks old tomato plants, germinated after a week of vernalisation at 4 °C and transplanted into 24 cells seedling trays. Per tray, 24 plants were inoculated, 12 plants per treatment. However, the top four and bottom plants were left untreated as border plants. The assay was carried out only with *Psa* 10627 inhibitory isolates. LB-broth overnight cultures of 50 mL were set in 250 mL flasks the night before the experiment. The next morning, overnight cultures were centrifuged at 4,000 x g for 8 minutes in 50 mL conical centrifuge tubes (Corning™ Falcon™, UK) and pellets were re-suspended in 20 mL of 10 mM MgCl₂.

In parallel, a mixture of 10 mM sterile MgCl<sub>2</sub> with 0.05% Silwet L-77 (De Sangosse, UK) —an organosilicon non-ionic wetting agent— was prepared. It was important to let it set for a few minutes before mixing it with the bacterial inoculum. Otherwise,  $OD_{600}$  were not accurate due to the murkiness of the water. Then, inoculum aliquots of 500 mL were prepared at  $OD_{600}$  of 0.2. Lastly, dip-inoculation spraying solutions were kept under sterile conditions until the start of the assay, when they were individually transferred to dishwasher-clean beakers.

One hour before plants were inoculated, tomato plants were generously sprayed with tap water all over the canopy. Then, plants were covered with a big transparent plastic bag to guarantee 100% relative humidity (RH), promote stomata opening and facilitate bacterial colonisation. Additionally, before dip-inoculating the plants, to avoid cross-contamination by run-off, laboratory absorbent paper was placed all over the working surface. To dip-inoculate plants, 250 mL beakers were used, filled at 75% the volume with the bacterial inoculum. Plants were immersed upside-down one by one in the solution and holding

the stem between the middle and ring fingers to prevent any substrate from falling into the bacterial suspension. Gently, plants were introduced in and out for 5 seconds. Then, tomato plants were let dry for 20 minutes (**Figure 5**) (Ishiga, Ishiga et al. 2011, Ishiga, Sakata et al. 2020).



**Figure 5**. On the left, dip-inoculation pathogenicity assay. Representation of tomato plants drying after being inoculated, separated by treatment. On the right, an example of necrotic spots on a tomato plant inoculated with *Psa* biovar 3, 7 dpi.

As a positive control, *Pseudomonas syringae* pv. *tomato* DC3000 was used and as negative control 10 mM MgCl<sub>2</sub> and 0.025% Silwet L-77 were utilised. Assessments were visually carried out after 7 days. *Pseudomonas* spp. strains were considered pathogenic if after 7 days dark necrotic spots with a yellowish necrotic halo around them were present (**Figure 5**).

#### 2.7.2. *In planta* biocontrol assays with model plants

One day before starting the experiment, an overnight culture of Psa biovar 3 was prepared. Single colonies were used to set overnight cultures of 10627  $\Delta plJ11282$  in 50 mL L-medium flasks, supplemented with 10  $\mu$ g/mL of tetracycline, as well as the biocontrol candidate strains —but just in L-medium—. Biocontrol strains were those that showed strong inhibition *in vitro* against 10627 only. Bacteria were incubated at 28 °C for 24 hours or until reaching an  $OD_{600}$  of 2. Then, cells were pelleted at  $4,000 \times g$  for 8 minutes and re-suspended in 10 mM  $MgCl_2$  with 0.025% Silwet L-77 at an  $OD_{600}$  of 0.2.

Plants used were four-weeks old 'Moneymaker' tomato plants germinated after one week of vernalisation and transplanted to 24 cells seedling trays. One hour before spraying plants with *Pseudomonas* spp., plants were generously sprayed with tap water until reaching the entire canopy. Plant trays were covered with a lid to create a humid environment and facilitate stomata opening. After an hour, for each treatment, 12 plants were inoculated with a 100-mL hand sprayer (upper and back sides of leaves) and let dry for

20 minutes. As a positive control, 10627 only was used and, as negative control, 10 mM MgCl<sub>2</sub> with 0.025% Silwet L-77. Two hours later, plants were sprayed again with tap water over the entire canopy. Then, 10627 Δ*plJ11282* was sprayed over all tomato plants (upper and back sides of leaves), reaching the entire canopy. Assessments were done 1 hour (day 0), 2, 5 and 7 dpi. Pictures of 6 randomly collected leaves per treatment were taken at 7 dpi.

Bacterial recovery was carried out with 50% of the plants each sampling day (excluding four border plants per treatment). Two leaf disks with corer No 3 (0.384 cm²) were harvested randomly per plant, 0.768 cm² in total. Each couple of leaf disks was placed in 2 mL tubes with 200  $\mu$ L 10 mM MgCl₂ and two sterile glass beads. Then, samples were ground using a SPEX homogeniser and cell lyser (SamplePrep, USA) twice at 1,700 for 1 minute, with a break of 1 minute in between. Grounded leaf disks were transferred to 96-well plated and fold-diluted with 10 mM MgCl₂ to 1/10,000, ensuring a final volume of 200  $\mu$ L per fold-dilution. In 10 cm square L-agar plates, supplemented with 10  $\mu$ g/mL of tetracycline and 25  $\mu$ g/mL nystatin, 10  $\mu$ L from each well were plated twice. Plates were wrapped in aluminium foil and incubated for 72 hours at 28 °C. Then, the number of colonies (CFU) was counted to quantify the number of bacteria that colonised the phyllosphere per cm², by using the following formula:

$$CFU/cm^2 = (E \cdot Df) \cdot 1/cm^2 punched$$

Where,

 $E=Number\ of\ colonies\ /\ volume\ plated\ (\mu L)$  Dilution factor (Df) = Grinding volume ( $\mu L$ )  $\cdot$   $10^d$   $d=Fold\ dilution\ number$ 

Lastly, results were converted into a log10 scale, and the standard deviation was calculated. Log10 was calculated by using the Microsoft Excel command =LOG10 and the standard deviation =STDEV.

#### 2.7.3. In planta biocontrol assays with kiwifruit vines

Bacteria were grown on KB-agar for 72 hours prior to each experiment. With a sterile cotton bud, bacterial cultures were swab and brought into solution. Final aimed concentration was 109 CFU/mL on 50 mL of sterile water and vortexed vigorously. From there, 30 mL were taken into 270 mL to reach a final concentration of 108 CFU/mL. As control, Aureo®Gold was used at 106 CFU/mL, as recommended by the manufacturer. It is a commercially available bio-bactericide against *Psa* that contains a blend of yeast-like fungus *Aureobasidium pullulans* isolated from apricot.

Vines used were green and yellow fleshed kiwifruit. They were grown from tissue culture into soil and then used for experiments after three months. Per vine, seven or eight leaves were sprayed per plant, depending on the number of leaves available to be used but never less than 6 leaves. For treating the vines, manual sprayers were used. Each treatment contained 0.3% of surfactant. When spraying, it was done inside a plastic spraying cabinet with a collection tray beneath. Vines were sprayed leaf by leaf until

run-off was seen. Then, they were put aside for two hours on the floor to then be transferred to a table filled with water and later covered in plastic. Between treatments, the plastic spraying cabinet is disinfected with Virkon<sup>™</sup>. Twenty-four hours later, *Psa* biovar 3 (10628) was sprayed. The temperature inside the cages was monitored until the end of the experiment. Also, each tray was exposed to one single treatment and each treatment was applied to two trays; in each tray, there were three 1 L pots. Per repetition, a total of 6 different treatments were applied. These were the following: water, *Psa*, Aureo®Gold and the three biocontrol candidates. With the spare spraying solution, serial dilution colony counting was done.

Disease assessment was performed by Leaf Doctor, a pathometry phone application for quantitative assessment of plant disease intensity (Pethybridge and Nelson 2015). All the experiments —but the one started on the 30/06/2022— were at a 1:1 ratio for biocontrol candidate: *Psa* biovar 3 (10627). From the 30/06/2022, the biocontrol candidate were 10 times higher compared to the pathogen (10:1). This probably makes more sense as it is a more realistic scenario in nature, where the biocontrol product is sprayed in orchards at grater concentrations than the pathogen would be.

Vines used for the experiments with biocontrol candidate strains, they were grown from clonal tissue-culture obtained from Multiflora Laboratories, Auckland, New Zealand. Individual plantlets were planted into 1 L pots containing a 50:50 ratio of potting mix and perlite. Potting mix was sourced from Daltons Limited (coated extend 3-month starter 1 kg/m³; Dolomite 2 kg/m³; Gypsum Coarse 2 kg/m³; Lime – Ag Grade 2 kg/m³; Microplus 0.5 kg/m³; Osmocote Exact 8/9 Standard Start 5 kg/m³; Permawet 0.75 kg/m³). The plants were placed in the glasshouse at 16–24 °C, with a day length of approximately 16 hours achieved using high-pressure sodium lamps when necessary. Plantlets were watered once daily.

#### 2.7.3.1. Assessment

Assessment of the biocontrol assays was carried out with Leaf Doctor —a smartphone application that uses pictures to distinguish diseased from healthy plant tissues and calculate percentage of disease severity— (Pethybridge and Nelson 2015). Before starting, pictures were edited with PixIr, a free, online image editing program, by reproducing the following steps:

- 1. Load website in your browser Photo Editor: Pixlr X free image editing online (https://pixlr.com/x/),
- 2. Select "open image",
- 3. Navigate to raw photo image and open. \*Important to keep track of which leaf/plant/treatment you are selecting,
- 4. Use "Full HD" on pre-resize image window and apply,
- 5. Select cut out tool on left hand pane,
- 6. Select magic cut-out tool and change mode to remove and set softness to medium. Set tolerance to ~80. Select background around leaf. You should now have an image only of your leaf and no background. \*Please take care when removing background we want everything removed completely

so that when analysing in Leaf Doctor the background is ignored. If there is even a little speckle/corner which has not been removed this will be picked up in the app and must be redone,

- 7. Click on layout and template on left hand pane,
- 8. Select background and click white box on left. Change colour to black. Your image should now have a black background,
- 9. Click save on bottom right corner. Save as a jpeg image under high quality. Make sure you save the image under the correct folder e.g., "edited photos for leaf doctor" giving the image a leaf number under the respective treatment and plant folders and
- 10. Close out of image and move onto editing next leaf.
- 11. Open the Leaf Doctor app

Then, to process the pictures with Leaf Doctor, the following protocol was followed:

- 1. After taking individual leaf photos at 3- or 4-weeks post inoculation, pictures where then edited using PixIr, a free online picture editing tool, to create a black background. No flash was used when taking photos to minimise reflected light on leaf surfaces.
- 2. Photos were then categorically copied onto a tablet, and one-by-one loaded into the image gallery on the leaf doctor app. Using the analyse function, up to 10 different healthy areas within the leaf photo were selected to represent healthy tissue or leaf tissue which was not *Psa* (e.g., botrytis, phytotoxicity, leaf damage). The threshold slider was then adjusted to obtain the maximum distance from a healthy colour, or until only diseased leaf tissue was selected.
- 3. Once satisfied with what had been selected, the app then uses an algorithm to analyse the leaf image and computes a percentage for both healthy and diseased leaf tissue. Both results were entered into an excel spreadsheets for all leaves for further analysis.

# 2.8. Statistical analysis

# 2.8.1. Correlation analysis

Using Microsoft Excel data analysis package or the function PEARSON, correlation analysis was carried out with the phenotypic data. Data was compared as a whole set and as subsets, divided by traits, locations, or conditions. By using conditional formatting, red to blue colour scales, data was easily visualised for better analysis.

## 2.8.2. ANOVA test

Using Microsoft Excel analysis package, an ANOVA test was carried out with two-samples assuming unequal variances for analysing discrete and categorical data (Nevill et al., 2002). Treatments and p-values were compared for significance.

# 2.8.3. Statistical analysis of kiwifruit biocontrol results

Leaf averages and plant averages were calculated for all treatments, as well as standard deviations and standard error of the mean (n=6). Raw data was processed by Duncan Hedderley, statistician of P&FR, to determine significant differences between treatments using a binomial generalised linear model. To compare the plant averages across different treatments, analysis of variance was considered; however, the Nil treatment was less variable than the others. Instead, a binomial generalised linear model was used, assuming the percentages were a proportion out of 100, and estimating the variability. Each trial was analysed separately. To help understand which treatments were different from each other, a series of pairwise comparisons were done between the means (on the logit scale, which the binomial generalised linear model uses), and letters put next to means; two means from the same trial with the same letter next to them did not differ significantly (p = 0.05, no adjustment for multiple testing).

#### 2.9. Bacteria spore harvesting

#### 2.9.1. Streptomyces spp.

Small plates ( $\varnothing$ : 9 cm) with 25 mL of SFM were inoculated with 100  $\mu$ L undiluted *Streptomyces scabies* spore suspension. Plates were incubated at 30 °C and harvested after 10 days post-inoculation. To harvest 1 mL of spore suspension, 3 mL of 20 % sterile glycerol was applied on a sterile cotton pad and with the help of sterile tweezers, the plate surface was scratched. Then, with a sterile syringe, the solution imbibed in the cotton pad was extracted and frozen at -20 °C. With every 3 mL of 20% glycerol, 2 mL were recovered.

# CHAPTER 3 BACTERIAL ISOLATION AND CHARACTERISATION

#### CHAPTER 3: BACTERIAL ISOLATION AND CHARACTERISATION

#### 3.1. Introduction

The phylum Proteobacteria is composed of a wide variety of species that are known to be ubiquitous in the environment. Among these is the bacterium known as *Pseudomonas* spp. (Wu, Monchy et al. 2011). Within that genus, we find more than 100 species and between them we find *Pseudomonas fluorescens*. *P. fluorescens* is a Gram-negative, straight, or slightly curved rod and is a saprophytic bacillus (everything it ingests passes through its cytoplasmic wall). It can be found both in soil and in water and is unable to form spores and grows aerobically, its optimum temperature for growth being between 25 and 30 °C. *P. fluorescens* strains tend to be effective antagonists and are only identified after extensive screening of large collections of plant disease-associated strains. This suggests that only a small number of strains in the group provide biological control (Loper, Hassan et al. 2012). What we certainly know is that the success of a biological control strain depends on its ability to colonise plant surfaces and produce secondary metabolites that are toxic to the targeted pathogens (Haas and Défago 2005).

Pseudomonas spp. are highly diverse entities. It is not surprising that they have varying abilities to suppress plant disease, but the genetic determinants of this beneficial activity are only partially understood (Pacheco-Moreno, Stefanato et al. 2021). The diversity of the various characteristics of Pseudomonas spp. metabolic, ecological, and biochemical properties extend to the genome level. The number of predicted protein-coding genes in each genome is approximately 6,000, with only around 1,300 core genes present in all strains, suggesting that the genome of this group of bacteria is very heterogeneous. Comparative genomics showed a small core genome for the P. fluorescens complex but a large pan-genome, composed of more than 30,000 orthologous coding sequences, providing more evidence for the ecological and genomic diversity of the group (Loper, Hassan et al. 2012, Garrido-Sanz, Meier-Kolthoff et al. 2016).

Over the years, the scientific community has linked certain phenotypes with specific functions or abilities such as biocontrol activity against plant pathogens (Loper, Hassan et al. 2012). For example, the characteristics of a colony (shape, size, pigmentation, etc.) are relevant to identify phenotypic variation among bacteria (Sousa, Machado et al. 2013). Similarly, swarming motility enables the rapidly colonisation of advantageous locations, allowing bacteria privileged access to nutrients (Fan, Zhang et al. 2017). This multicellular surface movement, common to root-associated bacteria, is promoted by rotating flagella (Henrichsen 1972). Operationally, effective root colonisation can translate into growth limitation or suppression of the surrounding bacteria. For this reason, and as studies have shown, highly motile *Pseudomonas* spp. tend to be good BCAs candidates that can mitigate plant disease infections (Gao, Wu et al. 2016).

Another important phenotype within BCAs is biofilm formation as they control plant diseases only if they can successfully colonise plant surfaces. Biofilms are communities of microorganisms that adhere to surfaces and form a matrix of extracellular polymeric substances (EPS) that protects them from

environmental stressors, such as desiccation, UV radiation, and antimicrobial agents. In biocontrol applications, the ability of bacteria to form biofilms can be advantageous for several reasons. First, biofilms can enhance the persistence and survival of bacterial populations in the target environment, such as on plant surfaces or in soil. This increased survival allows for a more extended period of time for the bacteria to establish themselves and compete with the target pathogen for nutrients and space. Second, biofilms can provide a physical barrier that prevents the adhesion and colonisation of pathogenic microorganisms. This barrier can limit the growth and spread of the pathogen and help to protect the plant from infection. In addition, the EPS matrix of the biofilm can contain antimicrobial compounds that can directly inhibit the growth of the pathogen.

Lastly, biofilms can enhance the biocontrol activity of the bacteria by promoting communication and cooperation between individual cells. This cooperative behaviour can lead to increased production of biocontrol agents, such as antibiotics or siderophores, that can further inhibit the growth of the pathogen. For example, *Burkholderia* sp. FP62, a BCA against *Botrytis cinerea*, forms biofilm structures in the phyllosphere. When FP62 transposon mutants deficient in biofilm formation were used in an in vitro biofilm assay, they lacked the capacity to control *B. cinerea* when applied to plants (Elnashar 2010).

Additionally, bacteria can produce toxic secondary metabolites to kill competitor microorganisms. Hydrogen cyanide (HCN) plays a key role *Pseudomonas* biocontrol activity (Haas and Défago 2005, Weller 2007). HCN is a potent inhibitor of cytochrome c oxidase (terminal component of the respiratory chain in many organisms) and several other enzyme proteins such as metalloenzymes (Blumer and Haas 2000, Atwood 2017). Thus, it is important to screen for cyanogenic plant disease-suppressive *Pseudomonas* spp. strains. Other potent enzymes secreted by bacteria are proteases. Proteases are known to have antibacterial activity against several gram-positive bacteria, fungi, and nematodes by breaking down proteins of cell walls (Siddiqui, Haas et al. 2005, Mota, Gomes et al. 2017, Deng, Huang et al. 2018). Bacteria with protease activity are used in agriculture to help with organic matter decomposition and plant growth promotion, but also as BCAs in disease suppression (Passari, Mishra et al. 2016).

Exopolysaccharides such as alginate, cellulose or hyaluronic acid are produced by bacteria to survive in harsh environmental conditions. For example, *P. aeruginosa* produces alginate during infections in cystic fibrosis patients to protect the bacteria from adversity in its surroundings (e.g., antibiotic treatments) and to enhance adhesion to solid surfaces (Boyd and Chakrabarty 1995, Remminghorst, Hay et al. 2009). In plant pathogens, these exopolysaccharides are known to cause wilting and inflammation in the xylem vessels, and they can also help in the invasion, growth, and survival of pathogens in plant tissues (Leigh and Coplin 1992, Donot, Fontana et al. 2012, Krishna, Woodcock et al. 2021). On the other hand, in biocontrol strains a strong positive correlation has been identified between biocontrol ability against plant pathogens and the production of exopolysaccharides, enhancing the biocontrol capacity of the producer bacteria (Upadhyay, Kochar et al. 2017). Lastly, siderophores are molecules that allow microbes to bind and transport iron (Behnsen and Raffatellu 2016). *Pseudomonas* spp. that produce these iron-chelating

molecules are associated with preventing bacterial infection and are thought to exert a biocontrol effect by competing with phytopathogens for trace metals (Peek, Bhatnagar et al. 2012). An example of siderophore is enterobactin, the strongest known siderophore, which can chelate iron from environments where the concentration of iron is extremely low such as living organisms or ferrioxamine B (Ahmed and Holmström 2014). Other positive effects of using siderophore-producing strains as BCAs is that these bacteria may also promote plant growth (Passari, Mishra et al. 2016).

In response to the presence of heavy metal ions in their habitats, bacteria have evolved to adapt (laneva 2009). Copper compounds are some of the main agrochemicals used by kiwifruit growers for *Psa* control in New Zealand. If overused, copper can promote the appearance of copper resistant *Psa* strains (Nakajima, Goto et al. 2002, Colombi, Straub et al. 2017). Streptomycin, historically used in human health to treat bacterial infection, was the first antibiotic discovered that belongs to the group of aminoglycosides. Its mode of action consists in inhibiting the protein synthesis at the level of the 30s subunit of the ribosome (Woodcock 2016). Its use in New Zealand is restricted to exceptional circumstances and requires strict risk assessments. Unfortunately, despite efforts to use the bactericide ethically and responsibly, some strains of *Psa* have developed resistance (Marcelletti, Ferrante et al. 2011). Finally, kasugamycin is used in agriculture in several countries around the world. It has never been used in human or animal health. It functions in a similar way to streptomycin by targeting the ribosome and disrupting protein synthesis (Mankin 2006). To date, there are no confirmed cases by publication of the identification of kasugamycin-resistant *Psa* strains from kiwifruit orchards in New Zealand.

# 3.2. Aims

In this chapter, the following biological questions will be addressed:

Can we identify differences in the phenotypic profiles of *Pseudomonas* strains between orchards?

Can we understand how Psa influences the naturally occurring Pseudomonas population?

Can we identify which phenotypic traits are linked to biocontrol ability against Psa biovar 3?

Can we identify correlations between different phenotypic traits?

Can we identify correlations between genotypes, phenotypic traits, and the metadata?

# 3.3. Results

3.3.1. Isolation of kiwifruit-associated bacteria from infected and uninfected orchards

A collection of 6,123 strains were isolated from infected and uninfected New Zealand kiwifruit orchards. Strains were isolated from visually infected and visually healthy leaves and buds as described in section.

Next, a representative, unbiased subpopulation of 1,056 strains were transported to the John Innes Centre for phenotypic characterisation using a series of high-throughput benchtop assays.

While collecting the kiwifruit tissue samples, marked health differences were seen within the orchards. For instance, in Te Puke, plants close to the road border seemed visually to have a higher disease incidence. This may have occurred due to greater exposure to the wind compared to central vines within the same orchard, *Psa* necrotic spots were hardly seen. Additionally, another challenge to be considered is the high variability in the age of the kiwifruit vines. Some orchards have some of the oldest vines in New Zealand, planted during the early 60s as well as two-year-old grafted vines. To date, there is no research published regarding how kiwifruit vines' age may influence plant-microbe interactions. Therefore, to ensure representative and unbiased collection, the leaves and buds to be collected were planned and agreed in advance of sampling.

# 3.3.2. High-throughput phenotypical screening of bacteria

For the screening, the same media were used for all assays when possible. It is known that results are highly likely to vary when different media were used. For example, different media will activate different NP production pathways or even the concentration of media ingredients may condition the copper resistance ability of bacteria *in vitro* (Cornish, Schipper et al. 2017). For more details see Chapter 2.

# 3.3.2.1. Colony morphology

The objective of this assay was to record in photograph the morphology of the 1,056 strains collection (shape and size) as well as their colour for further study (**Figure 6**).

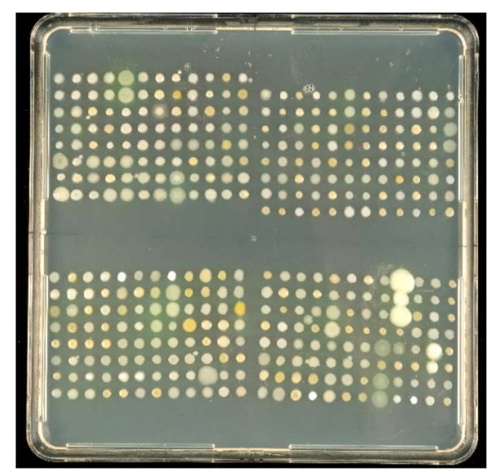


**Figure 6.** Example of high-throughput screening for morphology. In the picture, several hundred strains 48 hpi.

After comparing the orchard's locations no marked differences were found between them except Ohaupo that was significantly different from the rest (ANOVA test *p*-value>0.05) (**Figure 7**). Initial observations showed that little variation existed in the distribution of yellow-like colonies across locations, with the lowest concentrations being in Kaimai (30.21%), Motueka (28.65%) and Te Puke (37.15%) with Ohaupo the location containing the highest abundance of yellow-pigmented strains (42.01%).

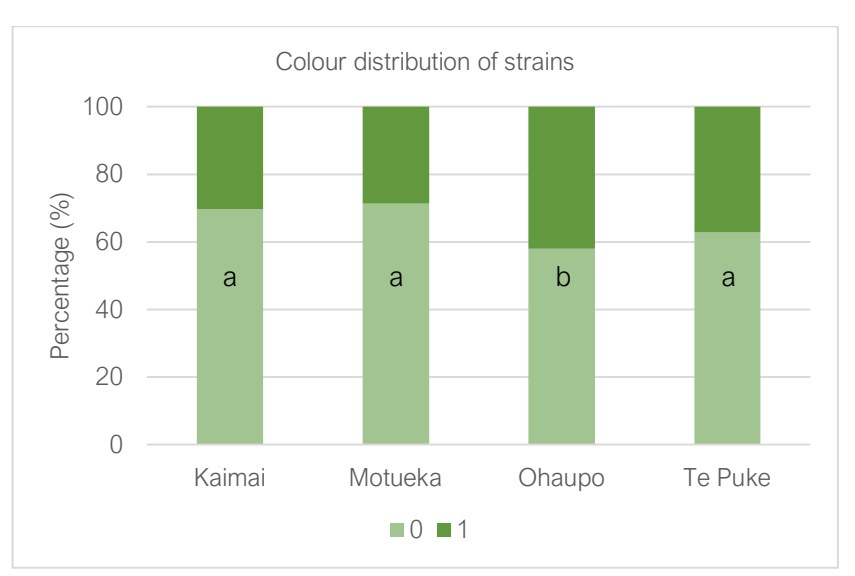


**Figure 7**. Percentage of yellow-pigmented strains across locations. Scoring belongs to (0) white and (1) yellow colour. Different lowercase letters indicate a significant difference according to one-way analysis of variance (ANOVA) (p < 0.05), n = 1,056.

# 3.3.2.2. Siderophore production

The objective of this assay was to identify which isolates were able to produce UV fluorescent siderophores (**Figure 8**). However, it is necessary to keep in mind that not all siderophores are necessarily fluorescent (Embaby, Heshmat et al. 2016).



Figure 8. Example of high-throughput screening for siderophore production. In the picture, several hundred strains under UV illumination.

Te Puke's orchard had the highest population of siderophore-producing strains (42.71%), followed by Kaimai's orchard (38.89%). On the other hand, Ohaupo's orchard had the lowest percentage of siderophore-producing colonies (16.32%) similar to Motueka's orchard (26.04%). ANOVA analysis showed that Motueka's and Ohaupo's orchards were significantly different to Kaimai's and Te Puke's orchards (p < 0.05) (**Figure 9**).

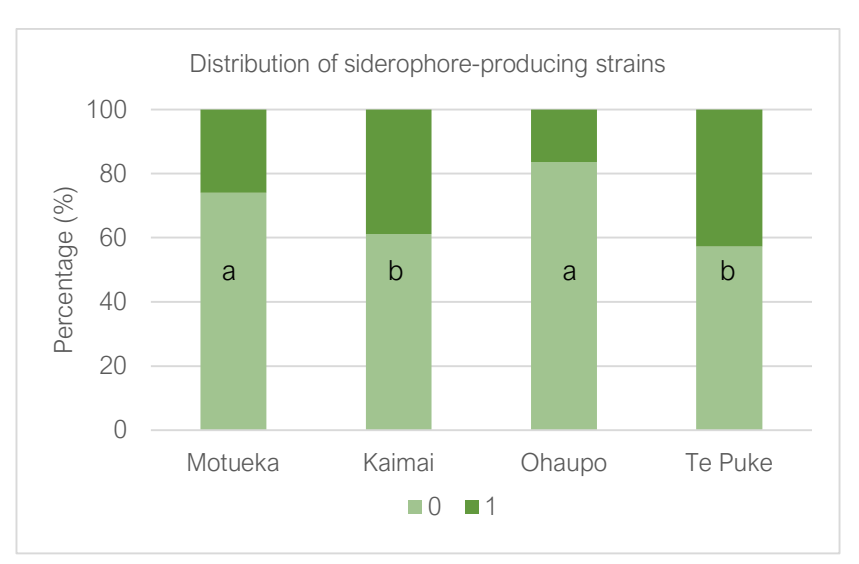


**Figure 9**. Percentage of siderophore-producing strains collected from each location. (0) No fluorescent strains and (1) fluorescent strains under UV illumination. Different lowercase letters indicate a significant difference according to one-way analysis of variance (ANOVA) (p < 0.05), n = 1,056.

# 3.3.2.3. Hydrogen cyanide production

The principle of this assay resides in causing a bright blue colour change in the filter paper treated with Feigl-Anger solution when exposed to bacteria producing HCN (**Figure 10**). This assay qualitatively measured the amount of volatile HCN produced by bacteria.

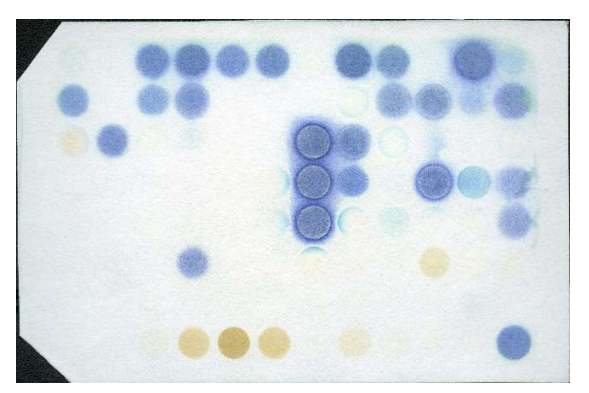


**Figure 10**. Example of high-throughput screening for HCN-producing strains 48 hpi. In the picture, blue stained filter paper is due to volatile HCN. The darker the blue colour, the higher the amount of HCN produced by the isolate.

Unexpectedly, some wells were distinguished for not producing HCN but for producing a different chemical volatile that turned filter paper a brown colour instead. This phenomenon has been observed in the past and has been identified as hydrogen sulphide, another volatile produced by some *Pseudomonas* spp. (Feigl and Anger 1966, Neale, Deshappriya et al. 2017). No further formal assessment was carried out in this regard.

Interestingly, not a single isolate from Motueka's orchard produced HCN (**Figure 11**). Ohaupo's and Kaimai's orchards had low numbers as well, with 1.04% and 4.17%, respectively. The only orchard that had a significant number of HCN-producing isolates was Te Puke's orchard, with 15% of the isolates

scoring for this metric. ANOVA analysis showed that Te Puke's orchard was significantly different from the other three orchards as well as Kaimai's orchard (p < 0.05), and Motueka's and Ohaupo's orchards were not significantly different among them (p > 0.05).

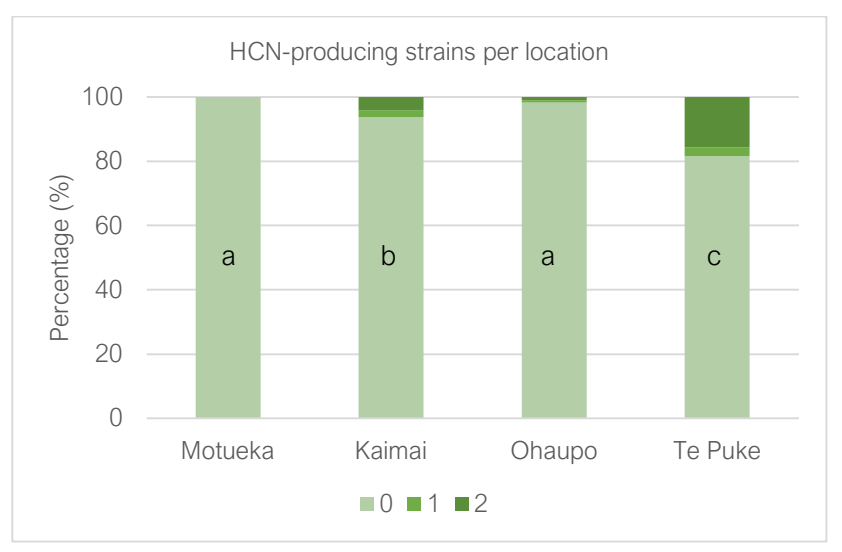


**Figure 11**. Percentage of HCN-producing isolates. Ordinal values assigned to strains: (0) No production, (1) low level of production and (2) strong production of HCN. Different lowercase letters indicate a significant difference according to one-way analysis of variance (ANOVA) (p < 0.05), n = 1,056.

## 3.3.2.4. Protease production

The objective of this assay was to identify which strains could produce proteases (Figure 12).

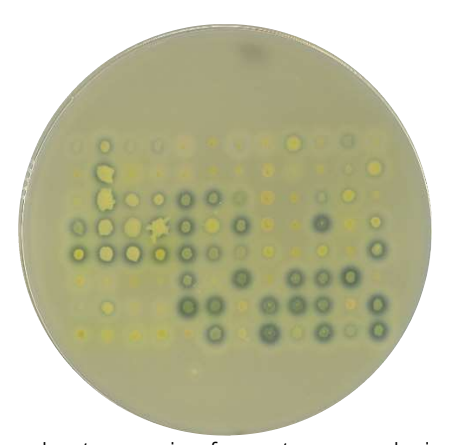


**Figure 12**. Example of high-throughput screening for protease-producing strains 48 hpi. In the picture, 96 *Pseudomonas* colonies are shown, with protease-producing isolates surrounded by a (dark) transparent halo.

In Te Puke's orchard we observed the highest proportion of protease-producing isolates (53.47%). In contrast, Motueka's (22.39%), Kaimai's (28.47%) and Ohaupo's orchards (29.86%) had similar proportions (**Figure 13**). Statistically, both Motueka and Te Puke's orchards were significantly different from the rest of orchards (p > 0.05), while Kaimai's and Ohaupo's orchards were not significantly different from each other (p < 0.05).

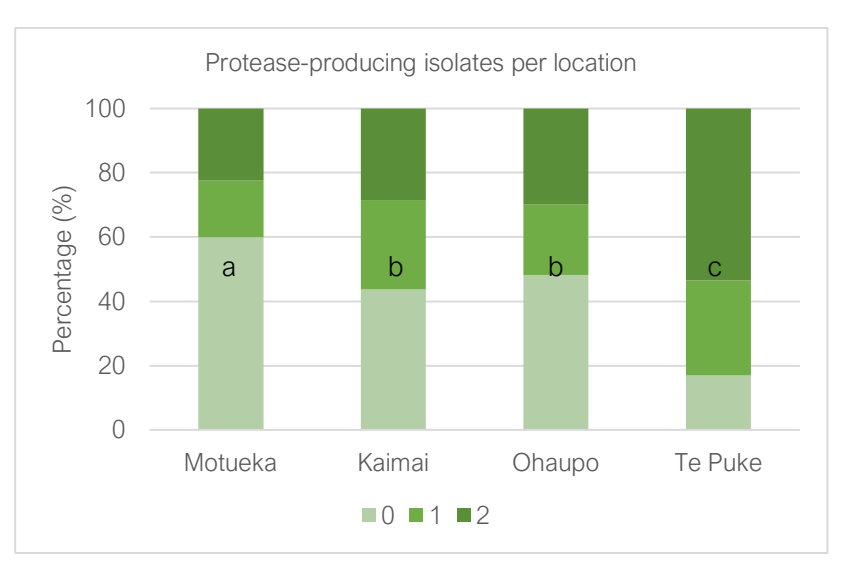


**Figure 13**. Percentage of protease-producing isolates per orchard. Ordinal values assigned to strains: (0) no halo, (1) small/medium halo and (2) large halo. Different lowercase letters indicate a significant difference according to one-way analysis of variance (ANOVA) (p < 0.05), n = 1,056.

# 3.3.2.5. Swarming motility

The objective of this assay was to identify bacteria that were surface motile on semi-solid agar plates, indicative of swarming motility (**Figure 14**).

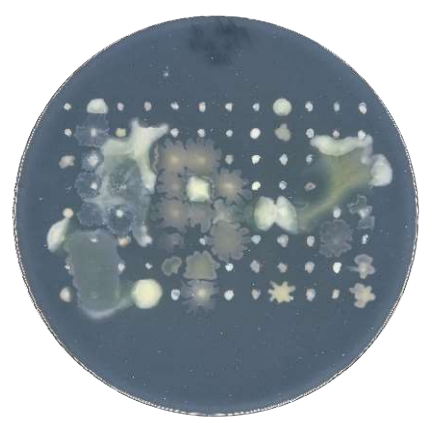


**Figure 14**. Example of high-throughput screening for swarming motile strains 7 hpi. In the picture, several highly motile strains can be seen swarming across the agar.

Isolates from Te Puke were significantly more motile than those from the rest of locations (p > 0.05), with 30.21% of the isolates showing strong swarming motility. Then, Kaimai's and Ohaupo's orchards with 4.51% and 3.12% strong swarmers respectively were significantly similar between each other (p < 0.05). In contrast, Motueka's orchard had the lowest proportion of motile isolates (1.56%) which at the same time, this orchard was significantly different from the other orchards (p > 0.05) (**Figure 15**).

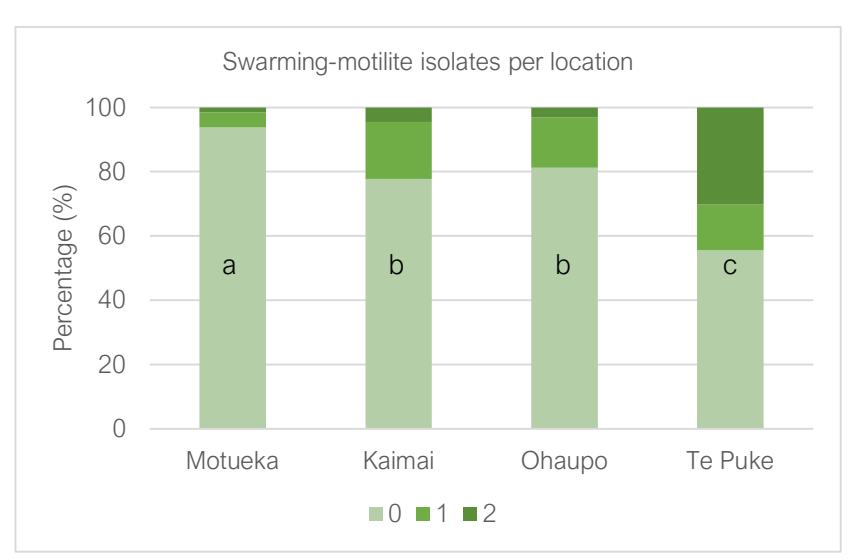


**Figure 15**. Percentage of swarming motile isolates per orchard. Ordinal values assigned to strains: (0) No swarming motility, (1) low/moderate swarming motility and (2) strong swarming motility. Different lowercase letters indicate a significant difference according to one-way analysis of variance (ANOVA) (p < 0.05), n = 1,056.

# 3.3.2.6. Congo Red binding

The objective of this assay was to identify exopolysaccharide and proteinaceous adhesin-producing strains (Figure 16).



**Figure 16**. Example of high-throughput screening for exopolysaccharide-producing strains 48 hpi. In the picture, strains with intense red coloration show greater production of Congo Red binding exopolysaccharides.

After processing the phenotypic results, we can see that only a few strains are able to bind to Congo Red, an average of 10% (**Figure 17**). However, strains coming from Kaimai and Motueka had the lowest distribution of strong Congo Red binding isolates, with 5.72% and 8.68% respectively. On the other hand, Ohaupo (12.15%) and Te Puke (17.01%), which were significantly similar (ANOVA test p>0.05), had the highest proportion of Congo Red binding strains.

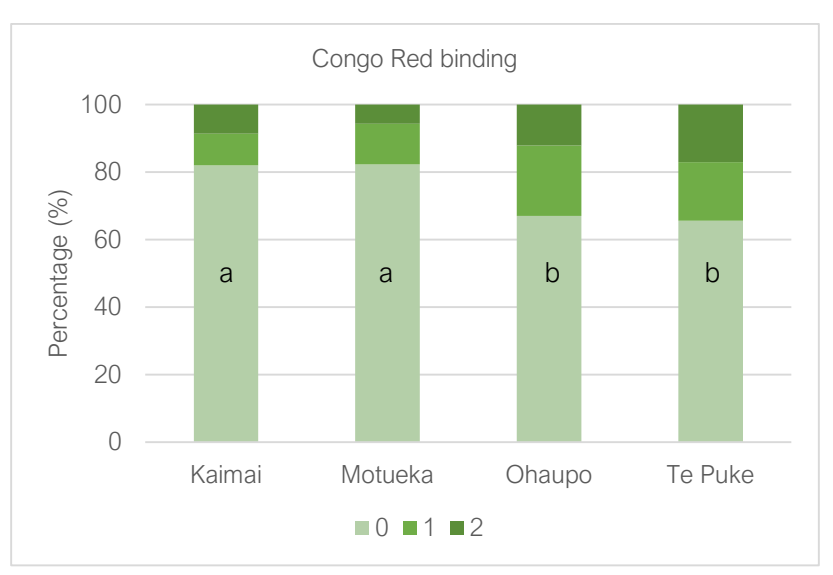


**Figure 17**. Percentage of Congo Red isolates per orchard. Ordinal values assigned to strains: (0) No Congo Red binding, (1) low/moderate Congo Red binding and (2) strong Congo Red binding. Different lowercase letters indicate a significant difference according to one-way analysis of variance (ANOVA) (p < 0.05), n = 1,056.

# 3.3.2.7. Streptomyces scabies suppression

The objective of this assay was to identify isolates that could inhibit *S. scabies* under *in vitro* conditions on SFM-agar (**Figure 18**). *S. scabies* is a plant pathogen that causes lesions and yield loss on tubers and root crops. It is the causal agent of common scab of potatoes and can be controlled by different bacterial BCAs including *Pseudomonas* spp. strains (Arseneault, Goyer et al. 2016, Nahar, Goyer et al. 2018).



**Figure 18.** Example of high-throughput screening for *S. scabies*-inhibitory strains 72 hpi. In the picture, inhibitory isolates are surrounded by a transparent (dark) halo.

In this assay, significant differences between all four orchards were seen (p > 0.05). In descending order, Te Puke's orchard had the highest proportion of *S. scabies* inhibitory isolates with 40.97%, followed by Kaimai (22.57%), Ohaupo (13.54%) and finally, with only 3.64%, Motueka (**Figure 20**).

### 3.3.2.8. Streptomyces venezuelae suppression

The objective of this assay was to screen and identify isolates that could inhibit *S. venezuelae* under in vitro conditions on SFM-agar, as well as showing any potential difference with the closely related *S. scabies* (**Figure 19**). *S. venezuelae* produces chloramphenicol, the first antibiotic to be manufactured synthetically on a large scale (Teixeira, Sanchez-Lopez et al. 2018).

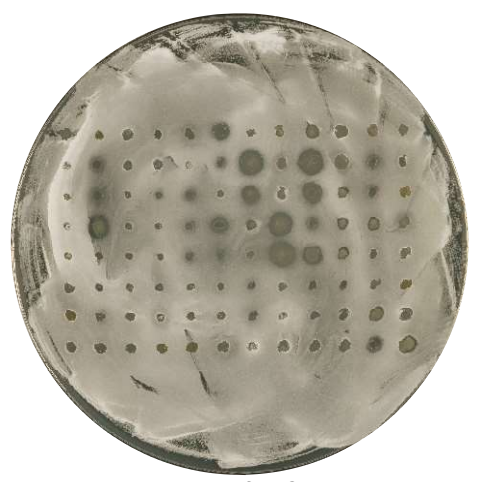


**Figure 19**, Example of high-throughput screening for *S. venezuelae*-inhibitory strains 72 hpi. In the picture, inhibitory isolates are isolates surrounded by a transparent (dark) halo.

Motueka was the orchard with the lowest proportion of strong *S. venezuelae*-inhibitory strains, with 7.29%, quite distanced from Te Puke, where 20.14% of the isolates were *S. venezuelae*-inhibitory. Significance, calculated by using ANOVA test showed that Te Puke's orchard was significantly different from the other three orchards as well as Kaimai's orchard (p < 0.05), and Motueka's and Ohaupo's orchards were not significantly different from each other (p > 0.05) (**Figure 20**).

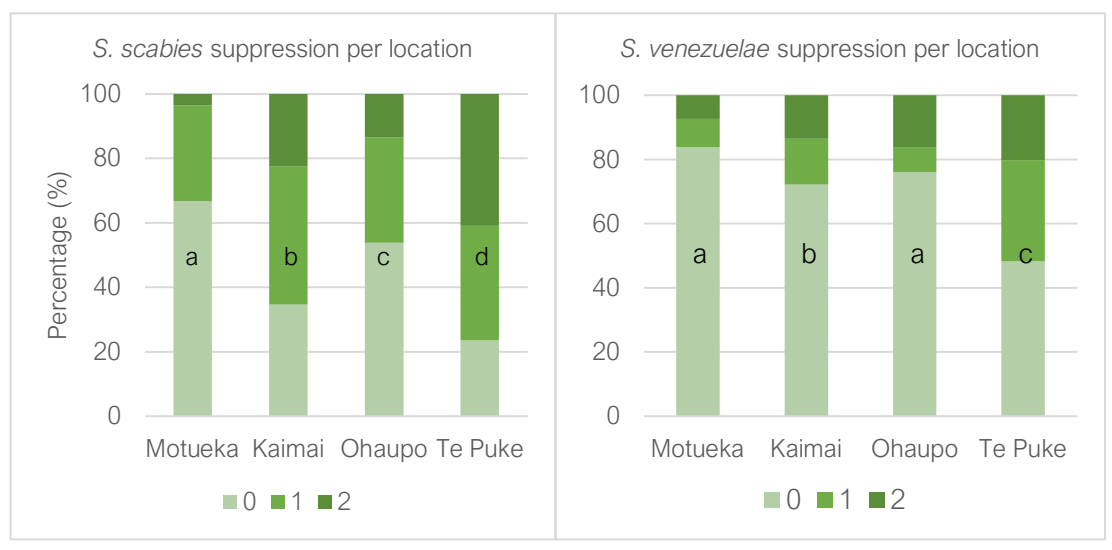


**Figure 20**. Percentage of *Streptomyces* spp. inhibitory isolates per orchard. On the left, *S. scabies* inhibitory isolates and on the right, *S. venezuelae* inhibitory isolates. Ordinal values assigned to strains: (0) No inhibition, (1) low/moderate inhibition and (2) strong inhibition against *S. scabies*. Different lowercase letters indicate a significant difference according to one-way analysis of variance (ANOVA) (p < 0.05), p = 1,056.

### 3.3.2.9. Psa suppression

The objective of this assay was to identify which isolates can effectively fight back against two *Psa* biovar 3 strains *in vitro* (**Figure 21**). For the *Psa* suppression assay, 10627 and RT594 *Psa* strains were analysed.

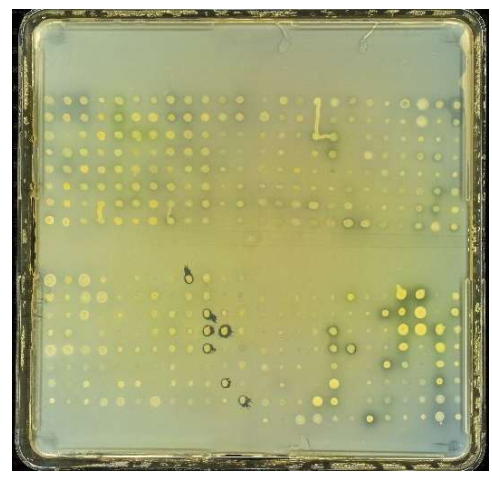


**Figure 21**. Example of high-throughput screening for *Psa*-inhibitory strains 48 hpi. Inhibition is shown by the presence of (dark) transparent haloes surrounding isolates.

Significant differences were found between locations for Psa 10627 (p > 0.05). In decreasing order, 11.46% of Ohaupo's isolates strongly inhibited Psa 10627, 5.21% Kaimai's isolates, 1.39% of Te Puke's isolates and none of Motueka's isolates. However, it also needs to be highlighted that a high number of isolates from Ohaupo showed a low/moderate suppression against Psa.

It was significantly higher (p > 0.05) in comparison with any other orchard's isolates (**Figure 22**). Interestingly, assays conducted with RT594 showed no significant differences between orchards (p > 0.05). Here, Ohaupo was the orchard with more Psa biovar 3 (RT594) inhibitory colonies (7.29%), followed by Kaimai's orchard with 5.21%, Te Puke's orchard with 4.17% and lastly, Motueka's orchard with 3.65% (**Figure 22**).

It is fascinating that no isolates from Motueka could inhibit 10627 but when RT594 strain was used, almost 4% of the isolates could inhibit it. Additionally, the similarity in the number of RT594 inhibitory colonies across orchards, even in Motueka where *Psa* biovar 3 is not present was striking and supports further investigation.

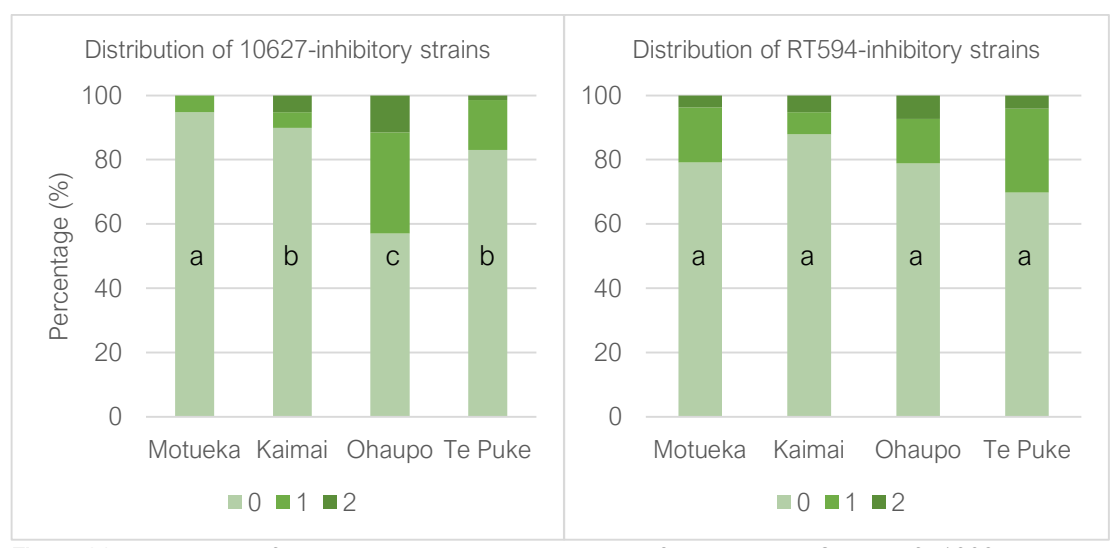


**Figure 22**. Percentage of isolates able to supress Psa biovar 3 per orchard. On the left, 10627 inhibitory strains and on the right, RT596 inhibitory strains. Ordinal values assigned to strains: (0) No inhibition, (1) low/moderate inhibition and (2) strong Psa inhibition. Different lowercase letters indicate a significant difference according to one-way analysis of variance (ANOVA) (p < 0.05), n = 1,056.

# 3.3.2.10. Copper resistance

The objective of this assay was to understand how copper resistant bacteria were distributed across locations and to identify resistant isolates for further characterisation by mimicking field spraying rates of copper formulates (**Figure 23**).



**Figure 23**. Example of high-throughput screening for copper resistant strains 48 hpi. In the top left corner, in read boxes: 10627 (copper sensitive) and RT594 (copper resistant).

Statistically, no significant differences were found between Kaimai's and Ohaupo's orchards (p<0.05) with 14.23% and 11.45% of strong copper sulphate resistant isolates while Motueka's (27.08%) and Te Puke's (73.95%) orchards were significantly different from any other orchard (p<0.05) (**Figure 24**). A remarkably high proportion of copper resistant isolates were found in Te Puke. Te Puke was the *Psa* biovar 3 'ground zero' in November 2010, suggesting that this area may have seen a longer and more sustained exposure to copper since the initial *Psa* outbreak.

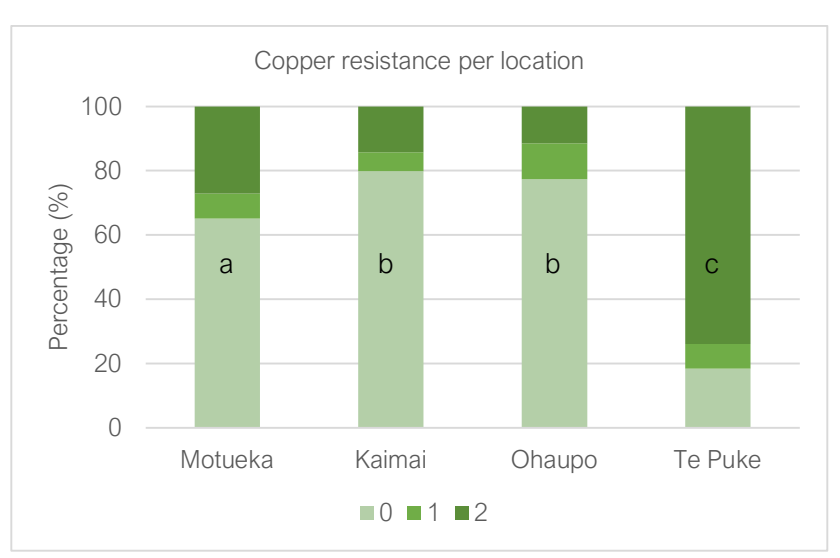


**Figure 24**. Percentage of copper-resistant isolates per orchard. Ordinal values assigned to strains: (0) No resistance, (1) low/moderate resistance and (2) strong resistance to copper sulphate at 500 ppm. Different lowercase letters indicate a significant difference according to one-way analysis of variance (ANOVA) (p < 0.05), n = 1,056.

Curiously, a similar but less marked phenomenon was observed for isolates from Motueka, despite this region being *Psa* biovar 3-free. It might be worth remembering that *Psa* biovar 4 has been present is South Island for more than 20 years (Vanneste 2013). Copper compounds could have been sprayed routinely in the area. Additionally, Motueka's orchard belongs to one of the research stations of P&FR and it is unknown what spraying programmes have been in place in the past. Access to the spraying diaries might help to shed some light on these questions.

### 3.3.2.11. Streptomycin resistance

The objective of this assay was to identify isolates that were resistant to streptomycin under *in vitro* conditions at the spraying rate according to the label recommendation of the commercially available bactericide (**Figure 25**).

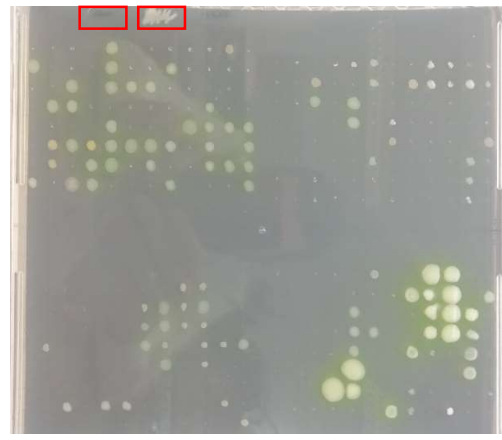


**Figure 25**. Example of high-throughput screening for streptomycin-resistant strains 48 hpi. In the top left corner, in read boxes: 10627 (streptomycin sensitive) and RT594 (streptomycin resistant).

No significant differences were found between Kaimai's and Ohaupo's orchards with 12.84% and 7.64% of streptomycin-resistant isolates respectively (p > 0.05). They were followed by Motueka with 28.64%, which was different from the other orchards as well as Te Puke with 69.10% of this orchard's isolates resistant to streptomycin (**Figure 26**). A similar explanation to the Te Puke copper-resistance results also applies here. Perhaps these kiwifruit vines were exposed for a longer time than other locations to streptomycin since the initial *Psa* outbreak.

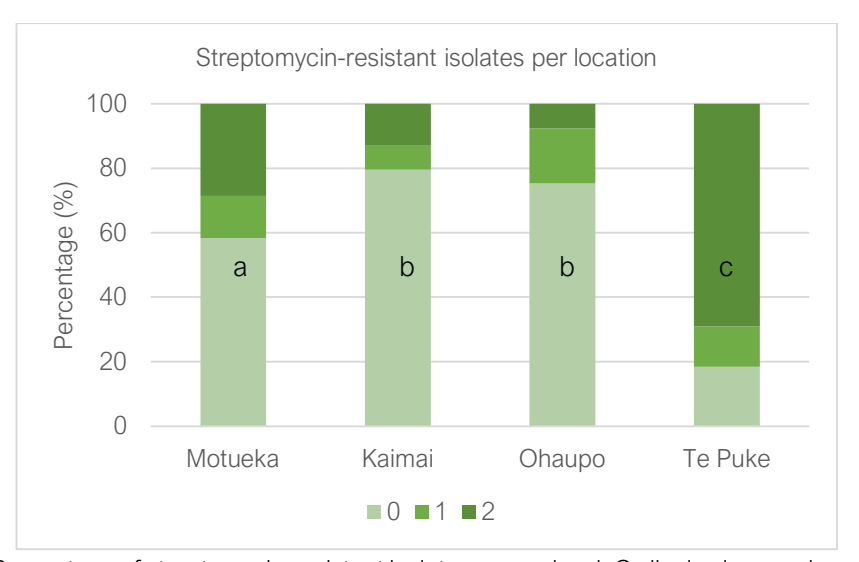


**Figure 26**. Percentage of streptomycin-resistant isolates per orchard. Ordinal values assigned to strains: (0) No resistance, (1) low/moderate resistance and (2) strong resistance to streptomycin at 100 ppm. Different lowercase letters indicate a significant difference according to one-way analysis of variance (ANOVA) (p < 0.05), n = 1,056.

# 3.3.2.12. Kasugamycin resistance

The aim of this assay was to screen kasugamycin-resistance isolates, the distribution of resistant isolates across locations and how this antibiotic may have impacted the development of potential resistant isolates (**Figure 27**).

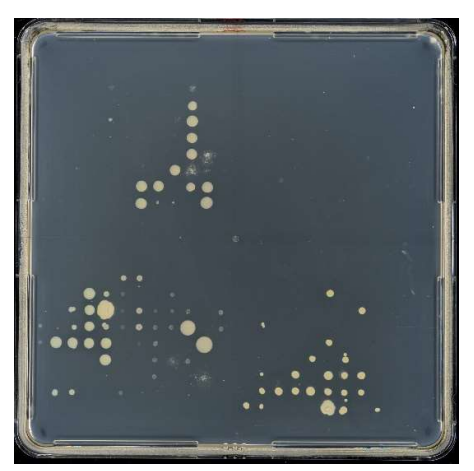
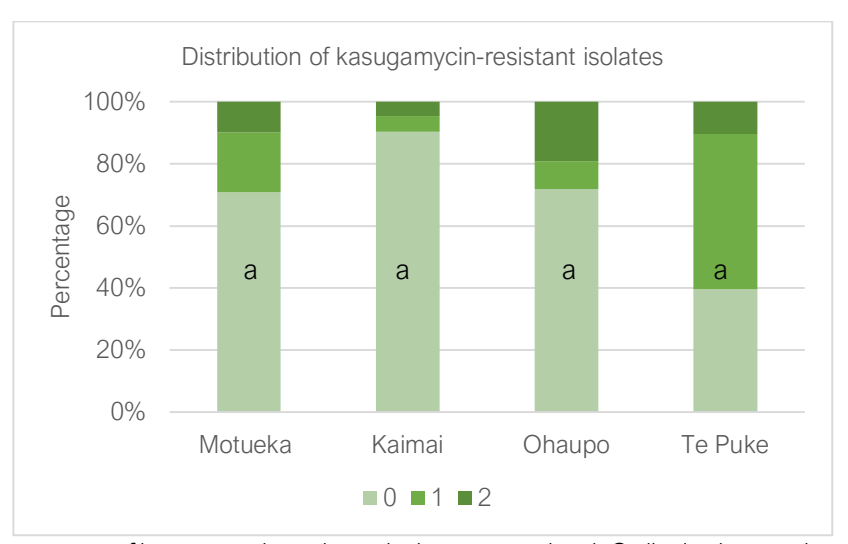
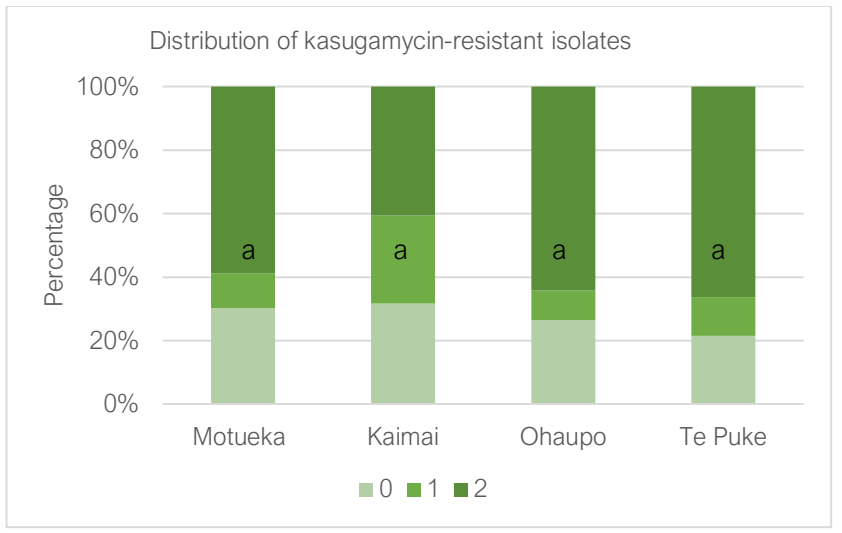


Figure 27. Example of high-throughput screening for kasugamycin-resistant strains 48 hpi.

Statistically there were no significant differences (p < 0.05) between orchard's isolates (**Figure 28**). Nonetheless, in descending order, Ohaupo's isolates had a higher proportion of kasugamycin-resistant isolates than other locations (19.10%). Then, Te Puke's (10.42%) and Motueka's (9.90%) orchards and lastly, Kaimai's orchard with only 4.51% of its isolates showing resistance. Te Puke's orchard had a significantly higher proportion of low/moderate tolerant isolates to kasugamycin (50%). When this assay was repeated with 20% of the recommended kasugamycin spraying dose a similar trend was seen when using the fully rate (**Figure 29**). Kaimai still contained a smaller proportion of kasugamycin-tolerant isolates while the other three orchards showing similar proportions to one another, albeit with Te Puke showing the highest percentage of tolerant isolates.



**Figure 28.** Percentage of kasugamycin-resistant isolates per orchard. Ordinal values assigned to strains: (0) No resistance, (1) low/moderate resistance and (2) strong resistance to kasugamycin at 100 ppm. Different lowercase letters indicate a significant difference according to one-way analysis of variance (ANOVA) (p < 0.05), n = 1,056.



**Figure 29**. Percentage of kasugamycin-resistant isolates per orchard. Ordinal values assigned to strains: (0) No resistance, (1) low/moderate resistance and (2) strong resistance to kasugamycin at 20 ppm. Different lowercase letters indicate a significant difference according to one-way analysis of variance (ANOVA) (p < 0.05), n = 1,056.

### 3.3.3. Phenotypic correlations

Examining the phenotypic correlations among groups of bacteria enables both the detection of environmental selection (e.g., by agrochemical resistance) and the identification of phenotypically/genetically linked traits. Often, phenotypic correlations reflect genotypic correlations. Therefore, this information could be of value in cases where resources do not allow sequencing of thousands of individual samples. However, for correlation analysis to be representative, large sample sets are required (Sodini, Kemper et al. 2018). Pearson's correlation coefficient shows how strongly two or more variables are related to each other and that fit is represented with values between -1 and 1 within a correlation matrix.

# 3.3.3.1. Phenotypic correlation for isolates from all four locations

From this matrix, at first sight, it can be identified that some strong positive and negative correlations (+/-0.3) exist between traits (**Figure 30**). *S. scabies* and *S. venezuelae* inhibitory strains were strongly positively correlated (above 0.3) with swarming motility and protease production. Other traits that were strongly correlated were resistance to copper sulphate and streptomycin, swarming motility, production of proteases, and inhibition of *S. scabies* and *S. venezuelae*. There is also an interesting 0.32 correlation coefficient between strains that were resistant to copper sulphate and were able to inhibit RT594. Additionally, a strong positive correlation coefficient of 0.49 between *S. scabies* and *S. venezuelae* was found as well as between strains that inhibited 10627 and RT594, with a correlation coefficient of 0.52. Similarly, between kasugamycin resistance, copper sulphate resistance and streptomycin resistance with correlation coefficients of 0.49 and 0.48. Finally, an extremely strong and unexpected 0.94 positive correlation was found between strains that were resistant to both copper sulphate and streptomycin.

In contrast, we found a lower number of strong negative correlations among other traits. Yellow-pigmented colonies tend to correlate moderately negatively with siderophore production and inhibition to *S. scabies*, but few other correlations of note were seen.

# 3.3.3.2. Phenotypic correlation per location

For further investigation, phenotypic datasets were split according to location. For the Motueka isolates' matrix, we observed a high number of zeros within the 'infected' sample set (**Supplementary 1**). All the isolates from Motueka were from a non-infected orchard and it was assumed that there were no *Psa*-infected samples due to the absence of the pathogen in South Island. In support of this, when Motueka leaf washings were plated on CFC media no *Psa* isolates were found.

Regarding Motueka's correlation matrix, most of the strong positive correlations seen within the 1,056-isolate matrix were absent here. However, the positive correlation between isolates that inhibit *S. scabies*, were swarming motile, produced proteases and inhibited *Psa* (10627) as well as the positive correlations between isolates that resist copper, streptomycin and kasugamycin experienced a

moderate increase compared to the 1,056-isolate matrix. The HCN-producing coefficient was 0 due to none of the isolates from this location producing the compound.

Within Kaimai's correlation matrix an interesting strong positive correlation arises between HCN-producing isolates and kasugamycin resistance (**Supplementary 2**). Similarly, the strong positive correlation between the inhibition of *Psa* 10627 and *Psa* RT954, inhibition of both *Psa* strains with resistance to copper and streptomycin or resistance to copper, streptomycin and kasugamycin, showed an increase in this location. Lastly, we observed a strong negative correlation between isolates that produced siderophores and had yellow-like colour.

Within the Ohaupo's correlation matrix, we observed a new and strong correlation between isolates that produced siderophores and inhibited both *S. scabies* and *S. venezuelae* (**Supplementary 4**). In general, most strong positive correlations matched with the previously explained 1,056-isolate matrix, with most of these moderately increasing. Some of these mentioned traits were within strains that are swarming motile, produced proteases, inhibited both *Psa* 10627 and RT594 and were resistant to both copper and streptomycin. Conversely, as it was seen within the Kaimai's correlation matrix, a strong negative correlation between isolates that produced siderophores and had yellow-like colour could be observed.

Finally, Te Puke's correlation matrix showed a high similarity when compared to Ohaupo's correlation matrix - with exception of the strong correlation between isolates that produced siderophores and inhibited both *S. scabies* and *S. venezuelae* (Supplementary 5).

### 3.3.3. Phenotypic correlation between *Psa*-infected and uninfected orchards

When comparing the only *Psa* biovar 3-free orchard correlation matrix (**Supplementary 2**) against the combined correlation matrix of the three infected ones (**Supplementary 6**), marked differences were observed. The *Psa*-free orchard (Motueka) showed a strong negative correlation between yellow-like strains and protease production as well as to inhibition of *S. scabies*. Additionally, both infected and non-infected orchards maintained some strong positive trait correlations such as protease production and inhibition to *S. scabies* or copper and streptomycin resistance. In contrast, there were some positively correlated traits that were exclusive to infected orchards only. For example, correlation between swarming motility, protease production, inhibition to both *S. scabies* and *S. venezuelae* and copper and streptomycin resistance.

### 3.3.3.5. Phenotypic correlation between visually symptomatic and asymptomatic samples

The phenotypic data compared in this section belonged to infected orchards only, with the aim of understanding whether visually symptomatic samples differed from visually asymptomatic or not infected ones. After a visual comparison, no striking differences were seen between the visually symptomatic correlation matrix (**Supplementary 7**) and the visually asymptomatic correlation matrix (**Supplementary 8**). Most of the common correlations described until now, specifically in the 1,056-correlation matrix, are preserved within these two matrices. However, within the symptomatic matrix, positive correlations tend to have coefficients of 0.05 to 0.1 higher compared to the visually asymptomatic correlation matrix. Also,

among these stands out the correlation between inhibition of *Psa* 10627 and RT594, which experienced the highest increase among the matrix, with a 40% increase when compared to the asymptomatic correlation matrix.

This last statement opens the idea of comparing the proportion of *Psa* biovar 3 inhibitory strains that were isolated from symptomatic and non-symptomatic samples according to the location where they were isolated (**Figure 31**). Statistical analysis showed that no big differences existed between symptomatic and non-symptomatic samples, although visually there appears to be a trend towards more strongly inhibitory bacteria within symptomatic or infected samples.

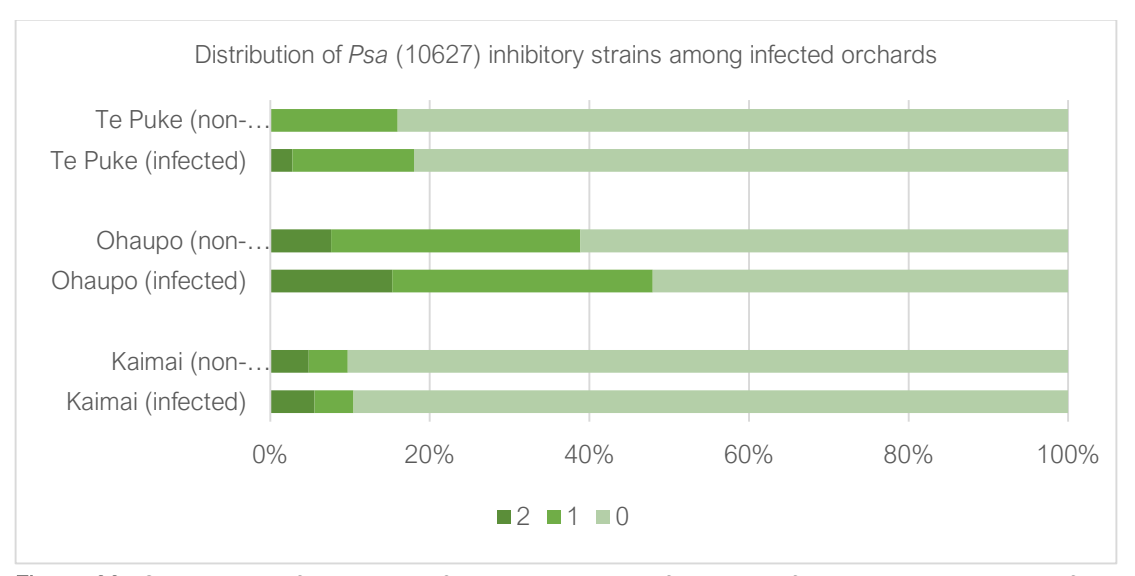


**Figure 30**. Comparison of *Psa* biovar 3 inhibitory isolates from *Psa*-infected orchards isolated from symptomatic (inf.) and non-symptomatic (no-inf.) samples (leaves and buds). (0) No inhibition, (1) low/moderate inhibition and (2) strong inhibition.

## 3.3.3.6. Phenotypic correlation between Psa-inhibitory and non-inhibitory strains

Several major trends were observed between the phenotypic correlation matrices. Inhibitory strains to *Psa* 10627 highly correlated with swarming motility, protease production, inhibition to both *S. scabies* and *S. venezuelae*, and copper, streptomycin and kasugamycin resistance (**Supplementary 9**). On the other hand, non-inhibitory strains to *Psa* 10627 still positively correlate with some of these trains but to a much lesser extent, with coefficients up to 0.45 lower compared to the inhibitory correlation matrix (**Supplementary 10**). Additionally, yellow-like inhibitory isolates seemed to negatively correlate with siderophore production, swarming motility, production of proteases and resistance to copper and streptomycin.

Kasuga															1.00
Strepto														1.00	0.48
CuSO4													1.00	0.95	0.49
Protease Congo R Inh scabies Inh venez Inh Psa Inh Psa Cu CuSO4												1.00	0.32	0.31	0.20
Inh Psa											1.00	0.52	0.16	0.13	0.12
Inh venez										1.00	0.12	0.23	0.41	0.38	0.16
nh scabies									1.00	0.49	90.0	0.13	0.41	0.39	0.15
Congo R								1.00	-0.03	0.04	90.0	0.03	0.03	0.01	0.01
Protease							1.00	0.01	0.54	0.39	60.0	0.13	0.37	0.33	0.14
Motility						1.00	0.33	0.05	0.43	0.41	0.16	0.28	0.47	0.47	0.22
HCN					1.00	0.27	0.08	-0.01	0.19	0.08	-0.01	0.08	0.29	0.30	0.16
$\geq$				1.00	0.17	0.09	0.21	0.03	0.28	0.12	-0.02	-0.02	0.15	0.13	0.00
Colour			1.00	-0.27	-0.16	-0.14	-0.15	0.03	-0.23	-0.13	-0.07	-0.10	-0.15	-0.15	-0.19
Inf sample		1.00	00.00	-0.01	-0.07	0.03	0.03	0.11	-0.01	-0.01	0.13	0.01	-0.07	-0.08	0.05
Inforchard Inf sample Colour	1.00	0.39	90.0	90.0	0.10	0.19	0.17	0.10	0.26	0.14	0.18	0.05	0.02	0.01	0.03
_	Inf orchard	Inf sample	Colour	ΛN	HCN	Motility	Protease	Congo R	Inh scabies	Inh venez	Inh Psa	Inh Psa Cu	CuSO4	Strepto	Kasuga

0.00

Figure 31. Correlation analysis with all phenotypic assays and orchards together from four locations. In order, margins abbreviations are infected orchard, infected sample, colour, UV or siderophore production, HCN production, swarming motility, protease production, Congo Red binding, S. scabies, S. venezuelae, Psa (10627) and Psa (RT594) inhibition and copper sulphate, streptomycin and kasugamycin resistance. Values between -1 and 1 indicate negative and positive correlations (Pearson's correlation coefficient).

### 3.4. Genome sequencing

To gain a deeper understanding of the kiwifruit *Pseudomonas* spp. population and the evolutionary traits acting upon it, 103 strains were whole genome sequenced. *Pseudomonas* spp. were specifically chosen based on their ability to suppress *Psa* 10627 together with 70 additional non-*Psa* inhibitory *Pseudomonas* isolates chosen based on their ability to tolerate copper sulphate and streptomycin at farming spraying concentrations, selected at random to reduce bias.

### 3.4.1. Phylogenetic trees

These 103 sequenced genomes were arranged in a phylogenetic tree based on a concatenation of the *atpD*, *dnaE*, *guaA*, *gyrB* and *rpoD* housekeeping genes (**Figure 32**). A preliminary visual analysis of this tree shows some clustering between orchards. It was not a strong correlation but by the distribution of the labels with coloured background, can be seen how some colours tend to be distributed across one region but not the opposite one. For example, most of Motueka's *Pseudomonas* spp. sit at the beginning of the phylogenetic tree with exception of four isolates. Similarly, Te Puke's *Pseudomonas* spp. are distributed across two main regions while Kaimai's isolates are distributed across the tree without following any obvious pattern. The relatively even distribution of genotypes across four orchards in different geographical locations might suggest that bacteria have moved across New Zealand. One hypothesis is that this could be due to anthropomorphic reasons. Zespri International Ltd. provides kiwifruit clonal cuttings to all growers that pay the royalty. Highly likely, those cuttings have been distributed by the same or a few nurseries, with bacterial isolates distributed alongside plant material.

When we compare the phylogenetic tree with the phenotypic data, we see clustering of certain phenotypic traits. For example, resistance to copper, streptomycin and kasugamycin strongly clustered on the left side of the phylogenetic tree (**Figure 33**). This pattern suggests the potential presence of MGEs such as ICEs or conjugative transposons that could confer resistance to the strains (Colombi, Straub et al. 2017). Some other phenotypes that clustered together were protease production, inhibition to *S. scabies*, *S. venezuelae*, *Psa* 10627 and RT594 and resistance to copper, streptomycin and kasugamycin, with remarkably high clustering seen between these last three phenotypes and genotypes. Interestingly, all the phenotypes that particularly cluster together are traits that correlate with the ability to strongly inhibit *Psa* 10627 (**Supplementary 9**). Further analysis of the genomic datasets will take place in the next chapter.

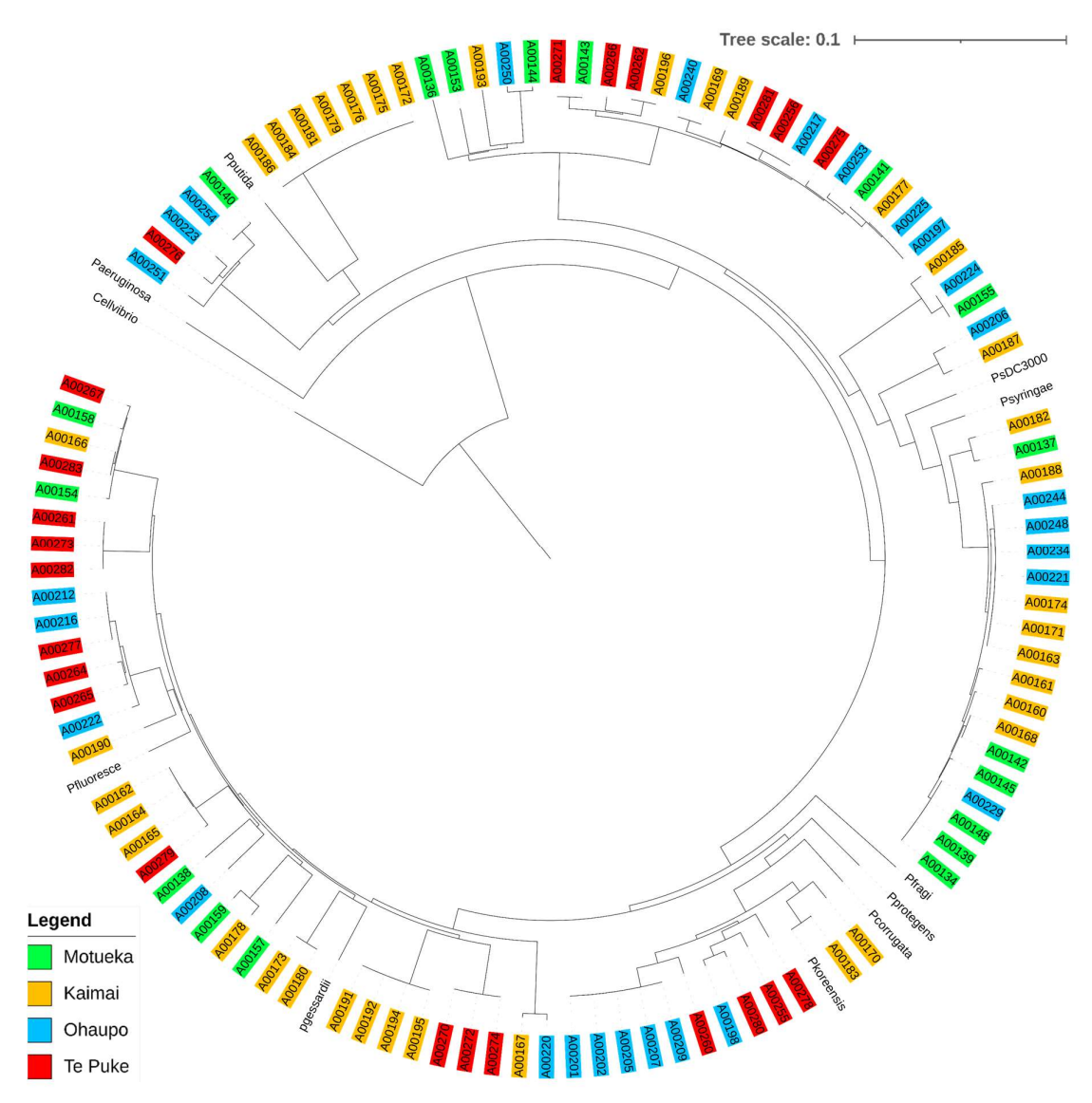
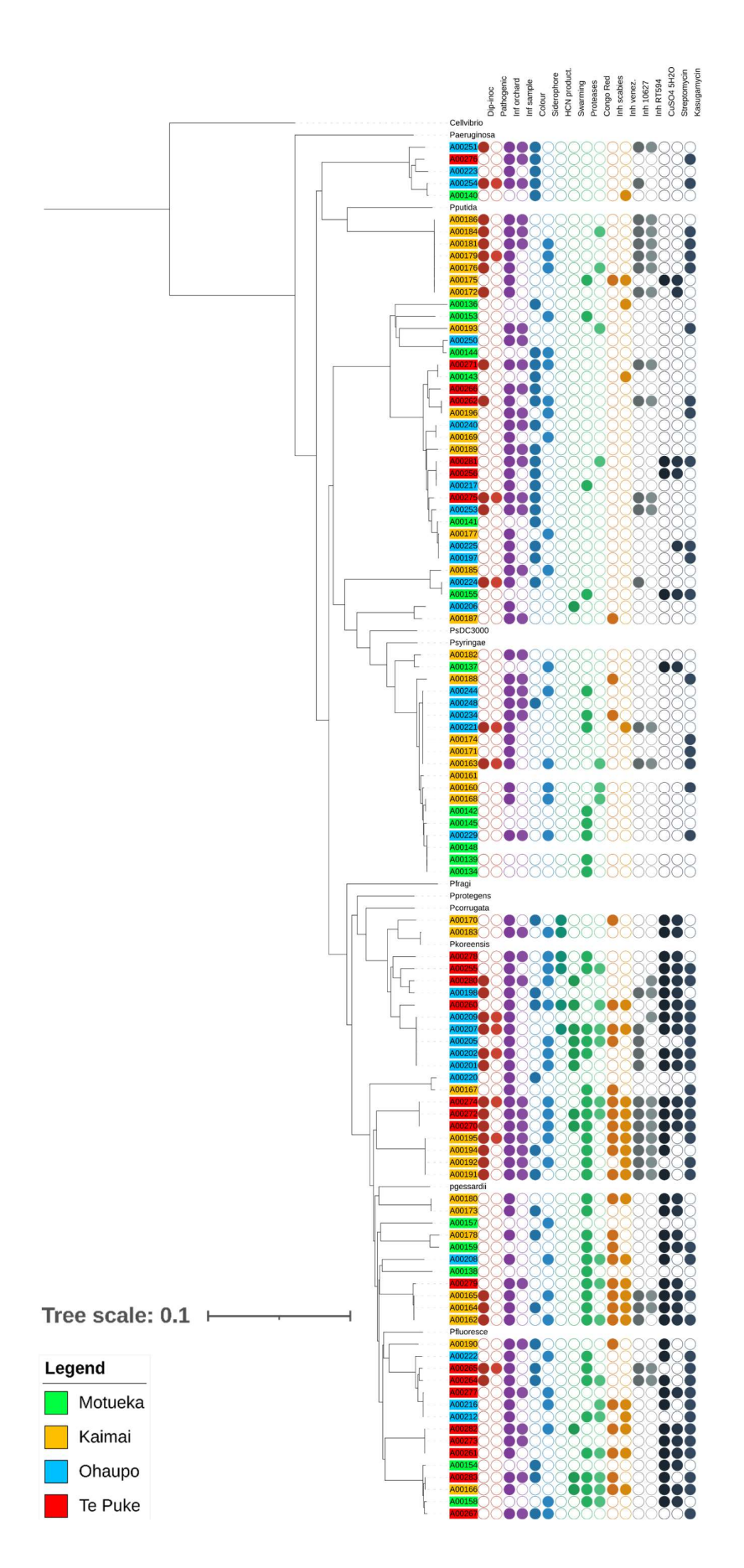


**Figure 32**. Maximum likelihood phylogenetic NJ tree of 103 *Pseudomonas* spp. with 1,000 bootstraps, based on a concatenation of *atpD*, *dnaE*, *guaA*, *gyrB* and *rpoD* housekeeping genes. Ten reference bacterial genomes are included for comparison. Strains are coloured according to their orchard of origin, as shown in the legend. Tree scale units represent represents the evolutionary time between nodes.



rpoD protein encoding genes with key phenotypic traits. Labels are dip-inoculation assay, pathogenic, sample origin, sample health, presence of irrigation, siderophore and HCN production, motility, protease production, inhibition against S. scabies, S. venezuelae, Psa 10627 and RT594 and copper, streptomycin and kasugamycin resistance. Filled, coloured circles represent presence of the trait. Tree scale units represent represents the evolutionary time between nodes. Figure 33. Maximum likelihood phylogenetic NJ tree of 103 Pseudomonas spp. with 1,000 bootstraps, based on a concatenation of atpD, dnaE, guaA, gyrB and

### 3.5. Discussion

Marked differences were observed in the phenotypic profiles between the different orchards in our study. Interestingly, we saw no strong *Psa* biovar 3-suppressive or HCN-producing isolates in our uninfected, South Island (Motueka) samples. For the three infected orchards, the phenotypic profile of Te Puke stood out. A higher frequency of Te Puke isolates produced hydrogen cyanide (HCN) and proteases, were motile, inhibited Gram-positive bacteria such as *S. scabies* and *S. venezuelae* and were resistant to copper sulphate (500 mg/L), streptomycin (100 ppm) and kasugamycin (100 ppm). Suggesting the potential presence of MGEs that could confer resistance to the strains, as seen with agrochemicals such as copper and streptomycin (Colombi, Straub et al. 2017). Positively, a total of 33 strains from Te Puke, Ohaupo and Kaimai were identified as being able to effectively fight back against *Psa* biovar 3 (both 10627 and RT594) under *in vitro* conditions.

Correlation analysis with the phenotypic data corroborated our previous conclusions. We observed a series of strong correlations between specific phenotypic datasets. Specifically, *Psa* biovar 3 inhibitory strains are more likely to produce HCN, be motile, to secrete proteases and to inhibit *Streptomyces* spp. *in vitro*. Bacteria coming from orchards where *Psa* biovar 3 is present showed a stronger positive correlation with bacteria presenting swarming motility, producing HCN and proteases, inhibiting *Streptomyces* spp. and being resistant to heavy metals and antibiotics. Similarly, we saw a strong positive correlation between the ability to suppress the *Psa* variant 10627 and the copper and streptomycin resistant strain RT594. This was something expected, as both strains are genetically highly related.

Interestingly, the strongest positive correlation coefficient was found between resistance to copper sulphate and streptomycin (0.94). We also saw a strong correlation between these two phenotypes and kasugamycin resistance. In contrast, among infected orchards, no big differences were found between isolates coming from visually asymptomatic when compared with visually symptomatic samples. The only exception was for the correlation between *Psa* variant 10627 and RT594 since the positive correlation was significantly higher among symptomatic samples.

Reading through these results, we can conclude that the naturally occurring *Pseudomonas* spp. population is phenotypically distinct when *Psa* biovar 3 is present or absent as has been proven and observed by other scientist (Purahong, Orru et al. 2018). The presence of the plant pathogen shapes the kiwifruit microbial community in a specific manner. For *Pseudomonas* spp. being able to survive within this context, extra genes or a 'survival machinery' is required, if compared to the isolated *Pseudomonas* spp. where the pathogen is not present. This might explain why a high proportion of *Pseudomonas* spp. from infected orchards contain several traits strongly correlated with biocontrol activity. The naturally occurring bacterial populations are exposed to continual threats, such as *Psa* invasion and bactericide sprays. Such differences may explain why no strong *Psa*-inhibitory strains of the variant 10627 were found in Motueka. Similar results have been seen with other crops, where disease-suppressive

environments are linked with the disease presence (Goh, Zoqratt et al. 2022). The environment is like a filter, removing species that lack traits for persisting under a particular set of conditions (Keddy 1992).

In planta, kiwifruit Pseudomonas spp. survive in the presence of Psa by producing secondary metabolites, biofilms or simply by combining these with being resistant to the active substances used for controlling Psa. Sometimes, to be resistant to those pesticides, upgrades in the 'survival machinery' naturally happen due to the presence of ICEs and conjugative plasmids (Colombi 2017, Colombi, Straub et al. 2017). The unusually high correlation between copper and streptomycin could be due to the presence of these MGEs. This connection will be analysed in more detail in subsequent chapters. Nonetheless, it is interesting that copper and streptomycin resistance correlate so well in most of the strains used in this thesis but not as highly with kasugamycin. Usually, bacteria that can tolerate bactericidal compounds do so after long-term exposure and/or presence of MGEs. However, the fact that more than 80% of Te Puke's isolates are moderately or fully resistant to copper, more than 80% to streptomycin and more than 60% to kasugamycin at spraying rates, is rather concerning. These results are foreseeing that spraying copper, streptomycin or kasugamycin to control Psa is at best a short-term solution.

Phylogenetic analysis helped in finding clustering between locations and phenotypic traits such as resistance to copper, streptomycin and kasugamycin clustering as well as revealing an integrated view of the complex structures of these communities. Results suggest that *Pseudomonas* spp. competition against *Psa* can generate phenotypic and phylogenetic clustering when it operates through environmentally mediated differences such as orchard location. Other traits that clustered were swarming motility, production of proteases and inhibition to *S. scabies*, *S. venezuelae*, 10627 and RT594. The phenotypic and phylogenetic structure of these communities are highly complex because of their condition evolution (e.g., exposure frequency to pesticides or *Psa* exposure). It would be interesting to further study such evolution, whether is conserved or convergent, to understand the dominant assembly process and the coexistence of different bacteria species (location filtering or limiting similarity) (MacArthur and Levins 1967).

Additionally, for this thesis were used Hayward kiwifruit samples only. It would be interesting to investigate if the findings described in this chapter also apply to Zespri Gold 3, the yellow flesh kiwifruit. Would *Psa* shape the natural-occurring *Pseudomonas* spp. population on Gold 3? Could we identify new or different phenotypic correlations linked to biocontrol against *Psa* biovar 3 in Gold 3? Can we identify new different correlations between genotypes, phenotypic traits, and the metadata within the Gold 3 microbiome? These questions are not covered further here but are interesting possibilities for future research.

# **CHAPTER 4**

GENOME MINING AND BIOINFORMATIC ANALYSIS OF AGROCHEMICAL RESISTANT GENES

# CHAPTER 4: GENOME MINING AND BIOINFORMATIC ANALYSIS OF AGROCHEMICAL RESISTANT GENES

#### 4.1. Introduction

Environmental pressures can lead to the development of new characteristics and rapid evolutionary changes. In New Zealand, copper sprays have been used to protect kiwifruit from *Psa* since the identification of the pathogen in the country. However, continuous exposure to copper and streptomycin for the control of plant pathogens can lead to selecting copper and streptomycin-resistant strains of the pathogens (Vanneste, Cornish et al. 2008). In 2014, the first copper resistant strain of *Psa* was isolated by VLS, it is known as biovar 3 (RT594). In 2015, it was revealed that a quarter of the strains of *Psa* biovar 3 isolated from Te Puke and other North Island locations were copper resistant (Colombi, Straub et al. 2017).

Colombi, Straub et al. (2017) helped unearth the genes that were responsible for copper resistance in New Zealand and by which mechanisms these were acquired. Copper resistance is typically conferred by operons encoding either copper efflux pumps, such as *cusAB* or *czcD*, and/or by sequestration systems such as *copABCD* that are regulated by *copRS*. The *copABCD* complex helps bacteria to survive in environments with high copper concentrations, such as those found in some industrial settings. They showed that in *P. aeruginosa*, *copABCD* is critical for the survival of under copper stress. Mutants lacking *copABCD* were highly sensitive to copper and had reduced growth and survival compared to wild-type bacteria. Additionally, *copABCD* is involved in the regulation of copper homeostasis in *P. aeruginosa* and contributes to copper resistance in general. The system helps to maintain a balance between copper uptake and efflux, allowing the bacteria to adapt to changing copper concentrations in the environment and is able to modify the bacterial cell envelope, which may help to prevent copper from entering the cell or promote its efflux from the cell.

CopA is a copper-transporting ATPase that helps to remove excess copper from the cytoplasm and prevent copper toxicity and plays a crucial role in copper homeostasis and resistance in *P. aeruginosa*. Further analysis showed that the expression of the *copA* gene is regulated by the transcriptional regulator *cueR*, which is activated by copper ions. This suggests that *copA* is part of a regulatory network that helps the bacteria to maintain a balance between copper uptake and efflux. Additionally, *copA* interacts with other copper resistance mechanisms, such as the *copB* and *copC* proteins, to ensure efficient copper efflux from the cell. the role of the copper-binding protein CopB was investigated in the bacterium Pseudomonas aeruginosa. *CopB* is a periplasmic protein that binds copper ions and helps to prevent copper toxicity. It plays an important role in copper resistance and homeostasis in *P. aeruginosa*. Also, it interacts with other copper resistance mechanisms, such as the *copA* and *copC* proteins, to ensure efficient copper efflux from the cell. Additionally, *copB* is part of a regulatory network that helps the bacteria to maintain a balance between copper uptake and efflux. The expression of the *copB* gene is controlled by the transcriptional regulator *cueR*, which is activated by copper ions, suggesting that *copB* 

is part of a larger system that helps the bacteria to adapt to changing copper concentrations in the environment (Colombi, Straub et al. 2017).

The periplasmic copper-binding protein copC is a small protein that binds copper ions and helps to prevent copper toxicity. It plays an important role in copper resistance and homeostasis. Also, copC interacts with other copper resistance mechanisms, such as the copA and copB proteins, to ensure efficient copper efflux from the cell. The expression of the copC gene is regulated by the transcriptional regulator cueR, which is activated by copper ions. Lastly, the periplasmic copper-binding protein copD is a small protein that binds copper ions and helps to prevent copper toxicity. CopD plays an important role in copper resistance and homeostasis in P. aeruginosa and interacts with other copper resistance mechanisms, such as the copA and copB, to ensure efficient copper efflux from the cell (Colombi, Straub et al. 2017).

CusAB is an efflux system comprised of a cytoplasmic membrane secondary transporter (enabling protein-driven substrate translocation from the cytoplasm (cusA)), a periplasmatic membrane fusion protein (cusB) and an outer membrane channel exporting substrate outside the cell (cusC). CusF is a chaperone protein that is required for full resistance (Kim and Yun 2010, Bondarczuk and Piotrowska-Seget 2013). Horizontal gene transfer is a powerful evolutionary tool that can affect the diversity of bacterial populations. It can involve the transfer of genes across broad phylogenetic distances, disrupting the niche preferences of bacteria and eventually leading to species differentiation (Polz, Alm et al. 2013). The czc/cusABC and copABCD operons are acquired via uptake of ICEs but can also be acquired through conjugative plasmids. As well as copper resistance, arsenic and cadmium resistant genes can also be acquired in this manner.

ICEs or conjugative transposons are distinguished from other types of vectors by their ability to distribute genetic elements both vertically and horizontally, and they are usually 4,000-500,000 base pairs in length (Daniel, Goldlust et al. 2020). The transfer of DNA is a critical component for antimicrobial resistance within bacterial cells (Gyles and Boerlin 2014). Following their excision from the chromosome, ICEs can be transferred by conjugation, a process initiated by a single-stranded DNA break at a specific locus called the origin of transfer (*oriT*) (Ceccarelli, Daccord et al. 2008). *oriT* is essential for plasmid mobilisation (Coupland, Brown et al. 1987). Among the mobilised elements, some are essential, and some are involved in multiple unrelated functions. Essential ones are those involved in excision/integration and conjugation (Johnson and Grossman 2015). On the other hand, ICEs carry a multitude of additional non-essential genes, for example, genes implicated in resistance to heavy metals or these with unrelated ones, such as heavy metal and antibiotic resistance together in the same MGE (Gullberg, Albrecht et al. 2014).

### 4.2. Aims

In this chapter, the following biological questions will be addressed:

Can we identify published copper and streptomycin resistance genes within the *Pseudomonas* strain collection?

Can we identify a molecular-level explanation for the high correlation between copper and streptomycin resistant strains?

Can we identify any novel mechanisms for copper and streptomycin resistance within the *Pseudomonas* strain collection? If so, are these present across the *Pseudomonas* strain collection?

### 4.3. Results

### 4.3.1. Correlation analysis of copper and streptomycin resistance genes

To investigate the potential presence of ICEs and plasmids within the *Pseudomonas* strain collection, 103 isolates were examined for resistance to both copper and streptomycin. Of these isolates, 43 isolates were copper resistant, and 36 streptomycin resistant. These isolates were whole genome sequenced to examine the distribution of known copper resistance operons *czc/cusABC* and *copABCD*. This set of genes are known to be acquired via integrative conjugative elements, but also are present on plasmids and are thought to be a major source of copper resistance.

The 103 whole genome sequenced strains were examined for presence of *czc/cusABC* and *copABCD* using a reciprocal blast analysis (**Supplementary 11**). Interestingly, only 20 (41%) of the 43 copper resistant strains contained the published essential genes for copper resistance (**Table 17**). In total, 48 strains were found to have *copABCD* across the collection. Among these, a high number of copper sensitive strains were found (58.3%) while 23 out of the 43 copper resistant strains had one or more missing genes from the *copABCD* operon. Furthermore, although 16 strains out of 103 *Pseudomonas* spp. had *copAB* only 1 of these strains was copper resistant (6.3%). Similarly, 32 strains out of the 103 *Pseudomonas* strains we examined had *copCD*, while 18 of them were copper resistant (56.3%).

To interrogate the obtained data in detail, a correlation analysis was carried out as previously described (Figure 34). *copAB* and *copCD* appear to be organised as two separate operons, contrasting previous scientific findings. If *copAB* is present, *copCD* is likely to be absent. *copCD* tends to be dominant in within the bacterial population, with more than 50% of the copper resistant strains having this operon but lacking *copAB*. Similarly, the correlation coefficient between *copC* and *copD* is positive and very high (0.85), suggesting both genes work together to enable copper resistance and are present as a single operon. The correlation coefficient between copper and streptomycin resistance in this matrix is lower than in Figure 31. However, the coefficient is still very high, at 0.78. This is due to the reduction of samples used for this matrix, where only 103 strains were used instead of 1,056 strains.

**Table 17**. Results of blasting analysis with *copABCD*. In order, genes used as query, number of strains with the queried genes, number of strains that are copper resistant *in vitro*, and percentage of strains with the queried genes that are copper resistant *in vitro*.

Cop	oper res	istant ge	enes	Number or strains	Copper resistant	% Copper resistant
copA	copB	copC	copD	48	20	41.7
copA	copB	сорС		2	2	100
	copB	copC	copD	2	0	0
copA	сорВ			16	1	6.3
		copC	copD	32	18	56.3
		сорС		2	1	50
			copD	1	1	100

Another operon that was found in all the copper resistant strains by Colombi, Straub et al. (2017) was *copRS*. This operon is commonly found in ICEs and plasmids. Assuming it is essential for copper resistance, it is striking that none of the 103 *Pseudomonas* strains investigated here had present the six genes (*copABCD* and *copRS*) across any of the copper resistant strains. Similarly, when we looked for *strAB*, it was expected that both genes would be found in the 36 streptomycin resistant strains. However, only five streptomycin resistant strains had both *strAB* genes.

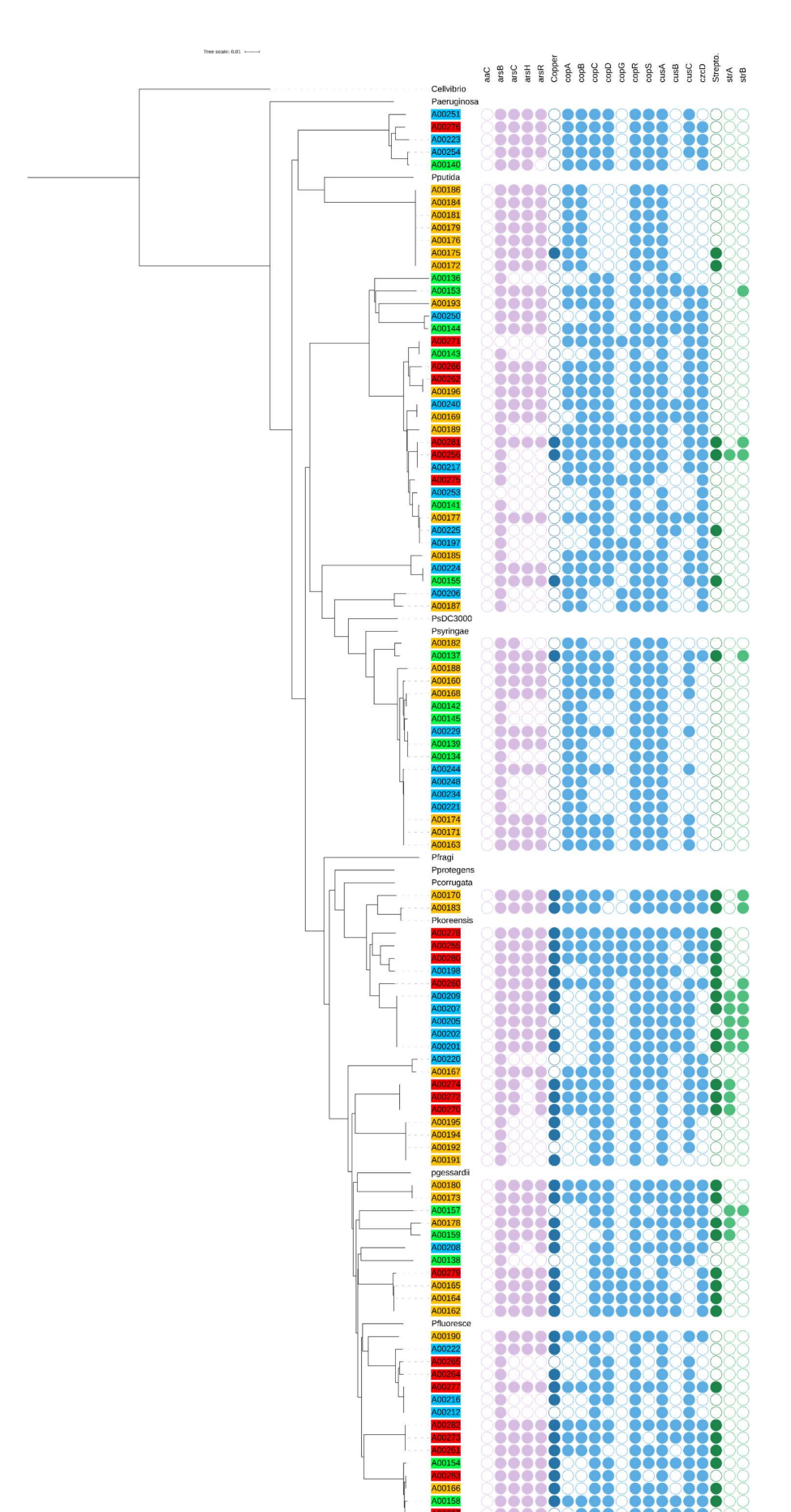
# 4.3.2. Phylogenetic tree

A phylogenetic tree was created combining the 103 *Pseudomonas* spp. strains genomes with the presence/absence of *czc/cusABC*, *copABCD* and *strAB* gene data (**Figure 35**). A high proportion of strains that did not contain the complete *strAB* operon were still resistant to streptomycin. A similar phenomenon was seen for copper resistant strains. Additionally, a degree of clustering was observed at the bottom of the phylogenetic tree coinciding with the clustering of phenotypic traits of copper and streptomycin resistance.

strB																				1.00
strA																			1.00	0.50
Strepto.																		1.00	0.37	0.33
czcD																	1.00	0.30	-0.01	0.01
cusC																1.00	0.27	0.10	0.18	0.26
cusB															1.00	0.17	0.19	0.36	0.29	0.32
cusA														1.00	90.0	0.15	-0.08	0.07	0.04	0.04
copS													1.00	-0.05	0.01	0.08	0.07	0.12	-0.09	0.14
copR												1.00	0.00	0.00	0.00	0.00	0.00	0.00	0.00	0.00
Sdoo											1.00	0.00	0.11	-0.23	-0.05	-0.23	0.29	0.19	-0.16	-0.08
CopD										1.00	0.08	0.00	-0.16	-0.05	0.28	09.0	0.43	0.17	0.18	0.12
copC									1.00	0.85	90.0	0.00	-0.19	-0.05	0.25	69.0	0.41	0.18	60.0	0.17
copB								1.00	-0.28	-0.26	-0.03	0.00	0.62	-0.07	-0.29	60.0	0.13	-0.08	-0.25	-0.10
copA							1.00	96.0	-0.29	-0.28	-0.01	0.00	0.59	-0.07	-0.35	0.07	60.0	-0.05	-0.23	-0.08
Copper						1.00	-0.23	-0.27	0.29	0.23	0.13	00.00	-0.09	0.08	0.26	0.19	0.21	0.78	0.31	0.27
arsR					1.00	0.31	0.20	0.23	0.19	0.18	-0.12	00.00	0.37	0.15	0.30	0.32	0.18	0.40	0.18	0.19
arsH				1.00	0.89	0.19	0.19	0.22	0.16	0.15	-0.09	0.00	0.43	0.14	0.29	0.23	0.13	0.31	0.00	0.21
arsC			1.00	0.89	0.95	0.28	0.23	0.26	0.16	0.15	-0.14	0.00	0.40	0.15	0.28	0.26	0.18	0.38	0.17	0.18
arsB		1.00	0.22	0.20	0.21	0.12	0.04	0.05	-0.06	-0.07	-0.13	0.00	60.0	-0.01	0.09	90.0	-0.11	0.10	0.05	0.05
aaC	1.00	0.00	0.00	0.00	0.00	0.00	0.00	0.00	0.00	0.00	0.00	0.00	0.00	0.00	0.00	0.00	0.00	0.00	0.00	0.00
	aaC	arsB	arsC	arsH	arsR	Copper	copA	copB	copC	CopD	Sdoo	copR	Sdoo	cusA	cusB	cusC	czcD	Strepto.	strA	strB

0.00

Figure 34. Correlation analysis between czc/cusABC and copABCD and other relevant genes involved in chemical resistance together with copper, and streptomycin phenotypic traits. Values between -1 and 1 indicate negative and positive correlations (Pearson's correlation coefficient).



genes known to be responsible for arsenic, copper, streptomycin and kasugamycin resistance together with Psa biovar 3 inhibition, copper resistance, streptomycin and kasugamycin frait (darker shades) or gene (lighter shades). Gene detection cut-off at 0.8 Figure 35. Maximum likelihood phylogenetic analysis based on a concatenation of atpD, dnaE, guaA, gyrB and rpoD protein encoding genes with presence/absence of identity. Tree scale units represent represents the evolutionary time between nodes.

### 4.3.3. Investigating the distribution of copper and streptomycin resistance genes

To further investigate the relationship between copper and streptomycin resistance, transposon mutagenesis was conducted with 10A5 (JM5412 in the NZ collection), a *Pseudomonas graminis* strain. This strain is resistant to 500 ppm of copper sulphate, encodes the *copABCD* operon and has a moderate tolerance to streptomycin at 100 ppm despite the absence of *strAB* operon. The Tn5 transposon was used to generate a mutant library, which was screened against copper and streptomycin to identify colonies with an altered capacity of survival.

In parallel, and with the aim of identifying and confirming the genetic determinants of copper and streptomycin resistance in 10A5, an Illumina/MinION re-sequencing was carried out providing four contigs: one of 5.8 million bp, another of 127,000 bp, a third of 118,000 bp and a final contig of 75,000 bp. According to the literature, *P. graminis* has a 5.8 million bp genome (Schoch, Ciufo et al. 2020). Therefore, the smaller three contigs (127,000-75,000 bp) are likely to be part of its accessory genome (genetic elements from non-parental lineages). Out of more than 2,000 transposon mutants, 15 were selected due to their copper and streptomycin sensitivity from which 12 were copper sensitive only and 3 were both copper and streptomycin sensitive. Selected transposons were sequenced and their location within the sequenced genome of 10A5 was determined (**Table 18**).

**Table 18**. Transposon candidates for potential copper and streptomycin resistant genes. Gene function predictions were derived based on BLAST using PROKKA. Cut-off for sequence similarity was 80%.

Name	Screening	Contig	inGene	inProduct
Tn 1	Cu	1	A00264_00659	HTH-type transcriptional activator rhaR
Tn 2	Cu	3	A00264_05358 a	Putative deoxyribonuclease <i>rhsC</i>
Tn 3	Cu	1	A00264_03023	Zinc import ATP-binding protein znuC
Tn 4	Cu	1	A00264_03024	Zinc uptake regulation protein
Tn 5	Cu	1	A00264_01974	hypothetical protein
Tn 6	Cu	1	A00264_02591	Protein Ves
Tn 7	Cu	1	A00264_01327	hypothetical protein
Tn 8	Cu	1	A00264_01468	Efflux pump subunit aaeA
Tn 9	Cu	1	A00264_04740	Efflux pump subunit aaeA
Tn 10	Cu/Str	1	A00264_01374	hypothetical protein
Tn 11	Cu/Str	1	A00264_02561	Primosomal protein N'
Tn 12	Cu	2	A00264_05228 a	Copper resistance protein A
Tn 13	Cu	1	A00264_03471	6,7-dimethyl-8-ribityllumazine synthase
Tn 14	Cu/Str	1	A00264_00033	hypothetical protein
Tn 15	Cu	2	A00264_05292	hypothetical protein

<sup>&</sup>lt;sup>a</sup> Transposon inserted in intragenic region to the left/right of this gene.

Across the 15 transposon mutants, 12 copper mutants were distributed across contigs one to three and the three dual copper and streptomycin mutants were only found to have transposons inserted into contig number one. From the 12 copper sensitive transposons, results showed that several different genes were disrupted by the transposon. For example, Tn 1 hit an HTH-type transcriptional activator

*rhaR* within the bacterial core genome (contig 1) Then, *rhaR* regulates the level of mRNA produced from the four L-rhamnose-inducible promoters of the rhamnose operon (Tobin and Schleif 1990). In contrast, Tn 2 was the only transposon inserted in contig number 3. It targeted the intragenic region of the *rhsBCD* operon.

Tn 3 and 4 hit the same operon, *znuABC*. Zinc ion is a critical cofactor for many metalloenzymes and is also important in the regulation of bacterial cells. However, loss of function due to transposon insertions, decreased tolerance of copper compared to the wild-type strain. Similarly, Tn 8 and 9 had transposons inserted within *aaeA*, an efflux system which has been previously reported to be involved in exporting harmful metabolic intermediates to prevent toxic accumulation (De Kievit, Parkins et al. 2001, Dyk, Templeton et al. 2004, Alav, Kobylka et al. 2021).

Lastly, from the copper sensitive transposons, Tn 12 was inserted in an unknown region. No significant similarity was found, probably due to the transposon being located just 43 bp from the very beginning of contig number 2. However, we know the left gene is *copA*, a copper-exporting type of ATPase previously identify among *Psa* resistant strains (Colombi, Straub et al. 2017). Tn 13 hit another unknown region, but it was surrounded by riboflavin producing genes. These genes are unlikely to be behind the copper resistance ability although *in vivo*, copper (II) is known to bind with riboflavin binding proteins (Smith, Pala et al. 2006).

Then, the three transposons mutants that had a dual sensitivity to both copper and streptomycin were all inserted in contig 1, within the bacterial core genome. Tn 10 hit was identified as a hypothetical protein, but it was surrounded by D-inositol-3-phosphate glycosyltransferase genes. This enzyme catalyses the biosynthesis of mycothiol which is used to maintain the intracellular redox homeostasis, to act as an electron acceptor/donor and serves as a cofactor in detoxification reactions for alkylating agents, free radicals and antibiotics (Newton and Fahey 2002, Rawat and Av-Gay 2007). Tn 11 was an unusual hit. The affected region was identified as primosomal protein N', also known as ATP-dependent helicase *priA*, an essential component of cell replication, repair, and recombination (Manhart and McHenry 2013). Lastly, Tn 14 was identified as hypothetical protein. When blasted against the NCBI database, none of the neighbouring proteins nor the one where the transposon was inserted had a query cover percentage above 40%.

Although no obvious novel proteins were linked with copper and/or streptomycin resistance, there were potential traits that could be further investigated. For example, Tn 2 was found to match with several locations within contig 3. Tn 2 matched with several *rhs* genes. The *rhs* genes are a family of genes, widespread among Gram-negative bacteria. Previous studies have suggested that *rhs* genes could encode factors that facilitate bacterial-host interactions. Among them, *rhsA* in *Escherichia coli* was previously identified in a transposon insertion mutagenesis screen for genes required for calf intestine colonization (Kung, Khare et al. 2012). Together with these genetic fragments, could have been inserted

other genetic elements downregulated that may encode the information required, in this case, for copper resistance.

Under the hypothetical presence of plasmids within 10A5 due to the existence three small contigs (127,000-75,000 bp), the sequences of contigs 2-4 were examined using automated software that predicts origin-of-transfer (*oriT*) regions. One of the prediction tools used was OriTfinder, a web server that facilitates the rapid identification of the *oriT* of a conjugative plasmid or chromosome-borne integrative and conjugative element (Li, Xie et al. 2018). Contig number 2 was predicted to have a similar *oriT* to the one present in *Pseudomonas alcaligenes*, the *oriT\_pRA2* with 68% identity (145/213 bp) and 7% gaps (16/213 bp) according OriTfinder (Yeo, Tham et al. 1998). Neither contig number 3 nor 4 had a predicted *oriT*.

To know more about these genes and their distribution across the population, a phylogenetic tree was created by using the targeted genes in Tn 1 – Tn 15 in 10A5 to identify their presence or absence across the sequenced *Pseudomonas* strain collection (**Figure 36**). No obvious clustering was identified, especially across genes targeted in Tn 3, Tn 4, Tn 5, Tn 6, Tn 8, Tn 9, and Tn 13, which were generally genes responsible for zinc uptake, efflux and copper resistance. Interestingly, Tn 7 and Tn 12 were mostly present among non-copper resistant strains only.

Next, to further understand the connection between copper and streptomycin resistance *in vitro* and at genotypic level, a correlation matrix was created (**Figure 37**). Tn 7 and Tn 12 was strongly negatively correlated with those isolates that showed a strong copper resistance phenotype *in vitro*. Similarly, Tn 10 showed a strong negative correlation with streptomycin resistance, meaning these targeted genes are highly unlikely to be responsible for copper resistance. On the other hand, genes targeted in Tn 1 and Tn 15 are strongly correlated with copper resistance. In contrast, transposons that were both streptomycin and copper sensitive had no positive correlations with streptomycin resistance phenotypical data.

Another question that arises when analysing these transposons is, how close are they from each other and where did they get inserted within the contigs. The sequenced region next to the transposon (1,000-1,200 bp) was marked within each targeted contig. In contig 1 transposons were quite spread out with no areas or regions heavily targeted by the transposon (**Supplementary 12**). The only area that was targeted twice by different transposons were genes responsible for zinc uptake. Contig 2 was only hit by Tn 12 and Tn 15. One was *copA*, a very well-characterised gene responsible for copper resistance and the other one, 70,000 bp forward, a hypothetical protein (**Supplementary 13**).

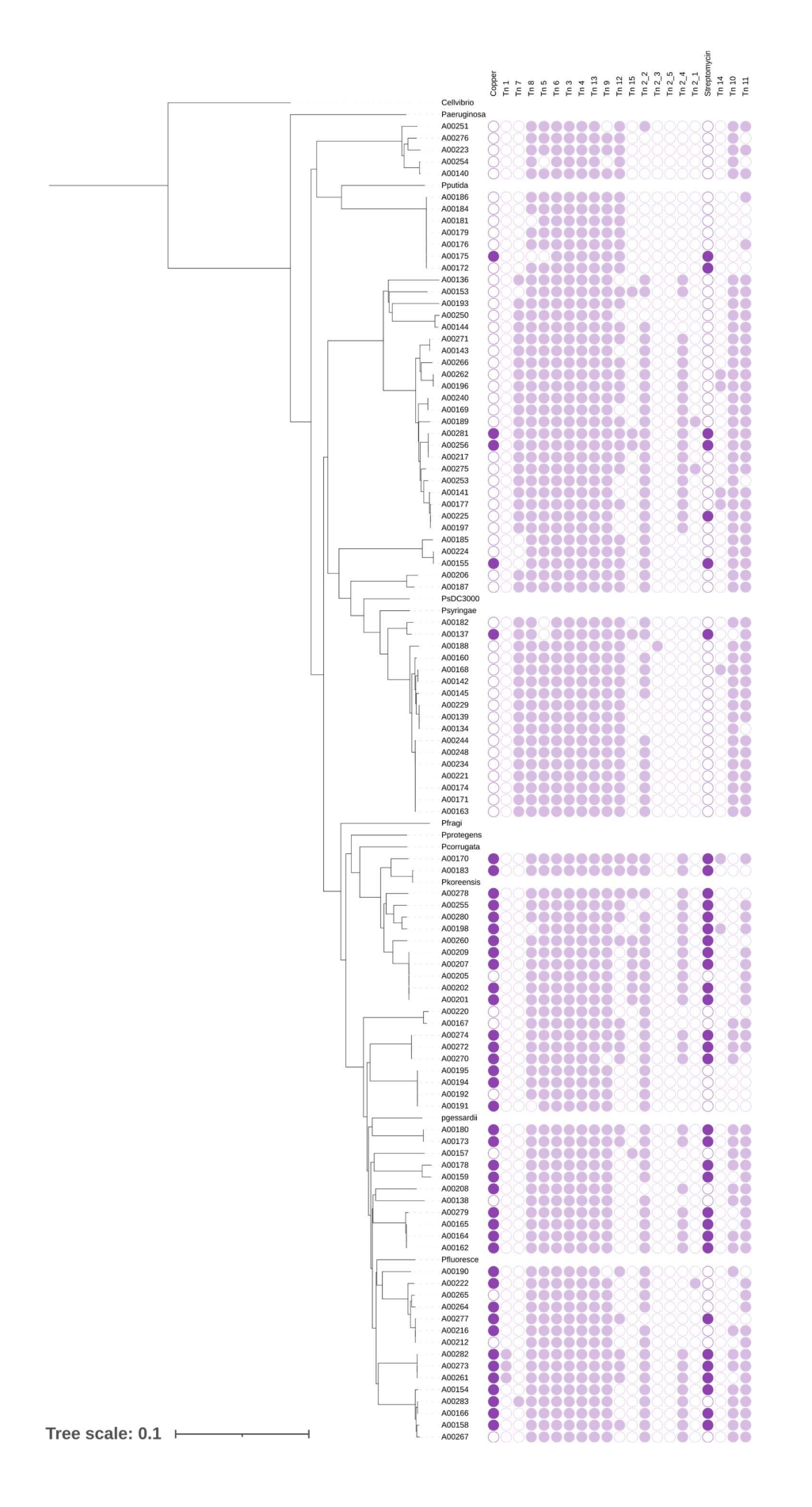


Figure 36. Maximum likelihood phylogenetic NJ tree of 103 Pseudomonas strains with 1,000 bootstraps, based on a concatenation of atpD, dnaE, guaA, gyrB and rpoD protein housekeeping genes. Ten reference bacterial genomes are included for comparison. Labels are copper phenotypic data, genes hit by transposon mutants sensitive to copper in 10A5, streptomycin phenotypic data and genes hit by transposon mutants sensitive to both copper and streptomycin in 10A5. Filled, coloured circles represent presence of the trait or gene. Tree scale units represent represents the evolutionary time between nodes.

	Copper	Streptomycin
Copper	1.00	, ,
Tn 1	0.20	
Tn 7	-0.53	
Tn 8	-0.14	
Tn 6	0.00	
Tn 3	0.00	
Tn 4	0.00	
Tn 13	0.00	
Tn 9	-0.03	
Tn 12	-0.23	
Tn 15	0.30	
Tn 2	-0.03	
Streptomycin	0.78	1.00
Tn 14	-0.07	-0.04
Tn 10	-0.37	-0.31
Tn 11	-0.08	0.00
-1.00	0.00	1.00

**Figure 37.** Correlation analysis with copper and streptomycin genes targeted by transposon mutagenesis in 10A5. In order, margins abbreviations are copper phenotypic data, genes targeted by transposon mutants sensitive to copper in 10A5, streptomycin phenotypic data and genes targeted by transposons mutants sensitive to both copper and streptomycin in 10A5. Values between -1 and 1 indicate negative and positive correlations (Pearson's correlation).

## 4.4. Discussion

Correlation analysis showed that copper sulphate and streptomycin resistance *in vitro* are strongly positively correlated suggesting that they might be genetically linked. However, when examining the presence of essential copper genes among copper resistant strains, most strains are missing one or more *copABCD* genes and tend to have *copABCD* split in two separate operons, with *copCD* being the operon most positively correlated with copper resistance. This is a typical pattern in plasmid evolution, where certain genes will be left behind and some novel ones will be acquired across lineages in order to bypass sensitivity to heavy metals (Wein and Dagan 2020). With time, those gained genes will also as acquire compensatory mutations which not only reduces both the fitness cost associated with plasmid acquisition as well as continually responding to the current environment of the host, for example, a heavy metals rich soil.

This work has aimed to elucidate the novel mechanisms for copper and streptomycin resistance, concluding with unexpected but interesting results. The kiwifruit microbiome is constantly evolving and adapting to agricultural treatments to survive (in a process known as the arms race). The transposon mutagenesis screening brings enough evidence to prove that there is a pool of potential novel genes that may be behind these resistances. Simultaneously, these genes will play a key role in how *Psa* evolves as many of these genes will eventually get transferred by conjugative plasmids or transposons.

Therefore, further research would be required to provide robust answers. Not only to demonstrate the presence of novel genetic elements across the naturally associated kiwifruit *Pseudomonas* responsible of copper and streptomycin resistance but also to investigate other resistances that may emerge on *Psa* due to exposure to kasugamycin.

Screening of transposon mutants has helped us to understand how complex copper and streptomycin resistances are at a genetic level and that a good proportion of the targeted genes are now newly linked with copper and/or streptomycin resistance. However, they were targeted only once. Screening more transposon mutants would considerably increase the robustness of these results. Same principle applies to uncover the dual copper and streptomycin resistance as none of the three genes targeted by the transposon were positively correlated with streptomycin nor copper resistance *in vitro*. Clearly, not enough transposons were identified, and a greater number would be required. However, judging from the phenotypic and genotypic correlation, I hypothesise that novel resistant genes to streptomycin and copper are present among the sequenced contigs.

Lastly, further work to clarify the role of the *rhs* gene family as transposons would involve, for example, the use of software to detect repetitive sequences although still would be challenging to detect completely novel elements (Lerat 2010). *Rhs* element contains several distinct components, some of which are highly conserved with respect to other members of the *rhs* family. The *rhs* elements are considered accessory genetic elements because is not present across all bacteria of the same species, although no extensive research has been done on these genes and therefore remains open their potential linkage with copper resistance (Zhao and Hill 1995, Alderley, Greenrod et al. 2022). Similarly, it could be possible that *znuABC* participates in copper homeostasis. Although the hypothesis of dual function of the zinc uptake system is unlikely according to other research studies (Gatti, Mitra et al. 2000, Gabbianelli, Scotti et al. 2011, Porcheron, Garenaux et al. 2013).

Presence of one or more plasmids for antibiotic and heavy metal resistance is a common phenomenon and something that has been observed among the *Pseudomonas* strain collection (**Figure 38**). To overcome this issue and as a future perspective, it would be interesting to sequence all the plasmids observed among this 103 *Pseudomonas* strain collection and then repeat the BLAST analysis. Perhaps, it would be easier to identify correlations among the collection and draw more robust conclusions. Similarly, that sequencing data could be used for future projects such as looking for potential kasugamycin resistance. Since very recently, new companies have entered the market that sequence plasmids of up to 300 kb at a very affordable price and high depth (1 bp error per 100 kb).

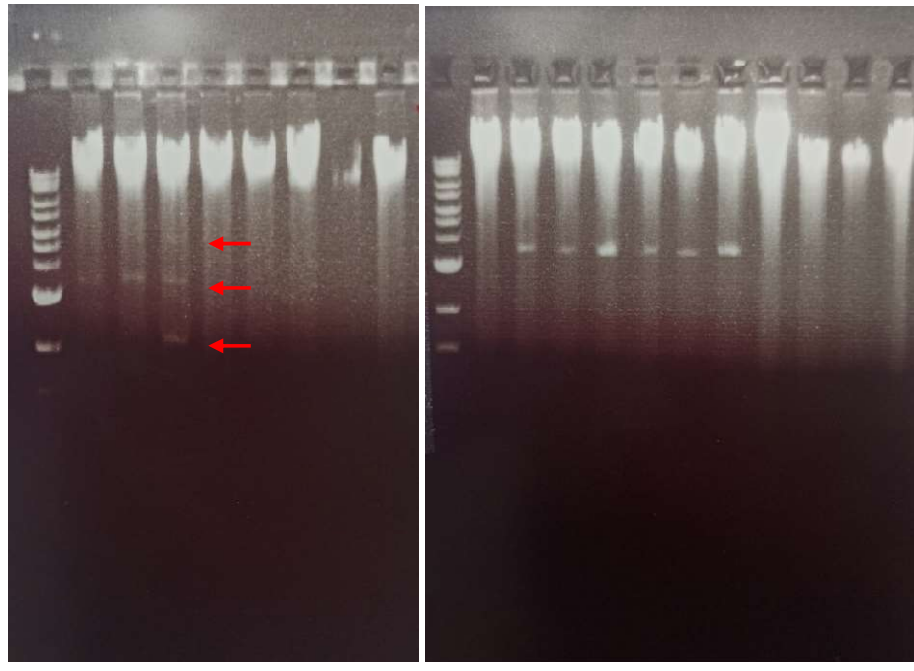


**Figure 38**. Gels run with gDNA extracted from the 103 *Pseudomonas* strains where several of them showed presence of predicted plasmids. Arrows show example of a strain detected with three small potential plasmids. Reference band: Quick-Load® 1 kb Extend DNA ladder.

# CHAPTER 5 BIOCONTROL AND PATHOGENICITY EXPERIMENTS

### CHAPTER 5: BIOCONTROL AND PATHOGENICITY EXPERIMENTS

#### 5.1. Introduction

Currently, agriculture is adapting due to the numerous challenges it is facing such as the continuous increase in the world's population, climate change, the emergence of new plant diseases and a rising educated population that demands sustainable production. Consequently, the number of active substances available to farmers is rapidly decreasing while the number of effective and efficient biopesticides and biofertilisers has become now more prevalent (Mitter, Pfaffenbichler et al. 2016). The demand of consumers to produce sustainable food products, the appearance of agrochemical resistance and the urgent need to look for longer-term solutions to protect kiwifruit vines has made companies shift their research interests towards eco-friendly and sustainable solutions. That is why major agricultural companies have been focusing on this research field, a business area with a 15% compound annual growth rate (CAGR) by 2027 (Mordor Intelligence 2021).

Biopesticides or BCAs are able to alter the plant microbiome in a way that can help decrease the incidence of plant disease and increase agricultural production (Andrews 1992). After the isolation of environmental inhibitory microbes, they need to pass through several distinct research stages. A biocontrol pipeline refers to the research progression of these microbes from the isolation stage to the commercialisation stage. Despite their natural origin, BCAs require rigorous tests to ensure that when they become registered biopesticides they will not harm people nor the environment. The process starts with culturing the microbes and evaluating their efficacy against the desired pathogen. This could involve overlay assays, such as dual culturing (water overlays), agar well diffusion assays or disc diffusion assays in vitro, for example. Then, the BCAs are tested under a controlled environment such a greenhouse in small scale (in planta and in vivo experiments). Next, secondary metabolites responsible for controlling the pathogen are purified, identified, characterised, and tested in small scale for toxicology, identification of potential non-targets and minimum lethal dosage. Carrier materials or spread enhancers as well as stabilisers or surfactants are also brought into trials with the BCAs to ensure that the maximum potential efficacy of the products is achieved. Finally, applications are sent to the relevant regulatory authorities for them to verify the biocontrol pipeline data and approve the registration (Lengai and Muthomi 2018, Dietz-Pfeilstetter, Mendelsohn et al. 2021). In the UK the relevant authority is the Department for Environment, Food & Rural Affairs (DEFRA), in the EU the European Food Safety Authority (EFSA) and in New Zealand the Ministry for Primary Industries (MPI).

In New Zealand, due to its commercial significance, Hort16A and Hayward, a yellow and green-fleshed kiwifruits, were the two major cultivars. It was not long before *Psa* arrived to New Zealand in 2010 when the biggest fears became true (Everett, Taylor et al. 2011). Hort16A, one of the most promising cultivars of the world leading kiwifruit company was highly sensitive to *Psa* biovar 3 (Ferrante and Scortichini 2009). Therefore, new cultivars had to be propagated. Currently, Hayward and Gold 3 (Zesy002), marketed as Zespri® SunGold are the two most commercially relevant cultivars. Since *Psa* became a

global problem, scientists from across the world started looking for ways to prevent or fight back against *Psa* infection. After 12 years of *Psa* in New Zealand, most of the spraying treatments are currently copper and bactericide based. Despite the environmental risks, they remain in use as no novel highly effective alternatives have been provided to kiwifruit growers to guarantee high fruit yield and the health status of the vines.

One of the relatively new BCAs approved with a BioGro Organic Certification in New Zealand is Aureo®Gold (*Aureobasidium pullulans*), a naturally present yeast on many plants and fruits in New Zealand. To provide protection frequent sprayings are required (every 7-14 days). Its efficacy is moderate high, depending on weather conditions, and it is not compatible with copper treatments (de Jong, Reglinski et al. 2019). Aureo®Gold cannot be sprayed within 14 days before or after a copper spray. Therefore, there is still room for improvement on efficacy, compatibility, and spraying frequency on the current BCA treatments available for kiwifruit growers. It would be ideal to find new BCAs that are highly effective against *Psa*, copper spraying compatible, synergetic with other BCAs and stable on kiwifruit for more than two weeks.

### 5.2. Aims

In this chapter, the following biological questions will be addressed:

Can we identify *Pseudomonas* strains that are *Psa*-inhibitory *in vitro* and are non-pathogenic against kiwifruit?

Can *Psa*-inhibitory *Pseudomonas* strains effectively fight back against *Psa* biovar 3 *in planta* as well as *in vitro*?

Can our *Pseudomonas* strains effectively antagonise *Psa* biovar 3 on kiwifruit vines under greenhouse conditions?

### 5.3. Results

As described in the introduction to this chapter, the BCAs discovery pipeline includes several steps. After the isolation of bacterial strains, the first step is to test if they can affect plant health. For this reason, we carried out pathogenicity assays using both model plants and kiwi vines under greenhouse conditions.

# 5.3.1. Pathogenicity assay by dip-inoculation

This test was critical for the identification of pathogenic *Psa*-inhibitory *Pseudomonas* strains. This is a common and essential step to identify potential plant bacterial pathogens and requires the inoculation of host plants. The test, also referred as hypersensitivity response test (HR), is commonly carried out on tobacco plants (*Nicotiana tabacum*) (Atkinson, Huang et al. 1985). It is known to work very well for the

identification of some pathogens such as phytopathogenic *Pseudomonas* spp. and *Erwinia amylovora*, but not for others such as *Xanthomonas* spp., where only little or no response is seen (Scala, Pucci et al. 2018).

Initially, there were performed a series of small tests using different plants, to identify the best model plant to use in larger assays, (e.g., biocontrol assays *in planta*). Among them, we tested kiwifruit (*Actinidia deliciosa*) seedlings in six-well plates with FP-agar. This test was thought to be promising due to its convenient sterile format and potential for dip inoculation, although it was ultimately discarded due to long germinating period, low germination ratio of the seeds, long wait for infection symptoms to appear and variability in infection symptoms, when inoculated with *Psa* biovar 3. Tobacco (*Nicotiana benthamiana*) was also tested but *Psa* biovar 3 did not create a large immune response and necrosis symptoms typical on kiwifruit were not visible, even when after infiltration inoculation. The assay performed with wheat (*Triticum* spp.) seedlings was promising due to their easy handling, contained and sterile growing environment. The use of transparent 25 mL tubes also allowed evaluation the impact that bacteria had on root growth. Unfortunately, it was discarded due to low HR and absence of necrosis symptoms once inoculated with *Psa* biovar 3. Finally, tomato (*Solanum lycopersicum* var. Moneymaker) plants were used and dip-inoculated showing a good HR response, necrosis spots and chlorosis halos around the dark spots as showed in **Figure 5**. For these reasons, it was decided to adopt tomato as a model plant for future experiments.

After three repetitions with 4-week-old tomato plants with 33 biocontrol candidates selected from the *in vitro* biocontrol assays, dip-inoculation pathogenicity assays revealed that approximately one third of the strains were pathogenic against tomato (**Table 19**). Among the pathogenic species were found *P. graminis*, *P. fluorescens*, *P. poae*, *P. coleopterum*, *P. syringae*, *P.* sp. BS3759, *P. chlororaphis* and *P.* sp. 34 E 7.

**Table 19.** Dip-inoculation visual assessment 7 dpi of 33 biocontrol *Pseudomonas* spp. candidates. Values of 0 represent absence of necrotic spots and 1 presence of necrotic spots.

NZ reference			ence	Pathogenic	Species
JM0149	3	С	5	0	Pseudomonas poae
JM0151	3	С	6	1	Pseudomonas sp. BS3759
JM0223	3	D	5	0	Pseudomonas poae
JM0225	3	D	6	0	Pseudomonas poae
JM0501	4	Α	9	0	Pseudomonas putida
JM0944	4	С	10	0	Pseudomonas putida
JM1064	4	D	10	1	Pseudomonas putida
JM0564	4	Е	10	0	Pseudomonas putida
JM0601	4	G	11	0	Pseudomonas putida
JM0626	4	Н	12	0	Pseudomonas putida
JM1087	5	F	8	0	Pseudomonas sp. 34 E 7
JM1088	5	F	9	0	Pseudomonas sp. 34 E 7
JM1123	5	G	9	0	Pseudomonas sp. 34 E 7
JM1168	5	Н	9	1	Pseudomonas sp. 34 E 7
JM1987	6	В	4	0	Pseudomonas koreensis
JM2054	6	С	7	0	Pseudomonas chlororaphis
JM2056	6	С	8	1	Pseudomonas chlororaphis
JM2107	6	D	7	0	Pseudomonas spp.
JM2169	6	Е	7	1	Pseudomonas chlororaphis
JM2206	6	F	7	1	Pseudomonas chlororaphis
JM2713	7	С	8	1	Pseudomonas sp. BS3759
JM2732	7	D	3	1	Pseudomonas syringae
JM2841	8	Н	1	0	Pseudomonas coleopterorum
JM2875	8	Н	7	0	Pseudomonas graminis
JM2885	8	Н	8	1	Pseudomonas coleopterorum
JM5353	9	Н	3	0	Pseudomonas graminis
JM5412	10	Α	5	0	Pseudomonas poae
JM5469	10	В	10	1	Pseudomonas poae
JM5665	10	F	12	0	Pseudomonas fluorescens
JM5693	10	G	10	0	Pseudomonas graminis
JM5705	10	G	12	0	Pseudomonas fluorescens
JM5738	10	Н	10	1	Pseudomonas fluorescens
JM5760	11	Α	8	1	Pseudomonas graminis
JM5955	11	F	1	0	Pseudomonas koreensis

# 5.3.2. Biocontrol assays with model plants

Following the identification of pathogenic *Pseudomonas* strains, *in planta* biocontrol assays were performed on tomato plants with the 22 non-pathogenic *Pseudomonas* biocontrol candidates. Eight non-*Psa* inhibitory *Pseudomonas* strains were used as negative controls (**Figure 41**). With this assay we aimed to screen *Pseudomonas* spp. bioactivity against *Psa* biovar 3 *in planta*. *Psa* biovar 3 was recovered from all the plant treatments and compared among each other as well as with the *Psa*-only control to see if their bacterial load increased or decreased when sprayed with biocontrol candidates and negative controls. To recover bacteria, antibiotic gene markers were introduced to differentiate *Psa* from the rest of the *Pseudomonas* strains. For this reason, biocontrol candidates were screened against copper, tetracycline, and gentamycin (

**Figure 39**). The obtained results concluded that the 22 biocontrol candidates were sensitive to either copper sulphate or gentamicin (**Figure 40**). The biocontrol strains resistant to copper were sprayed with 10627, strain carrying the *pME6032 vector*, conferring 12.5 mg/mL tetracycline resistance to *Psa*, while biocontrol strains resistant to tetracycline were sprayed with RT594, the *Psa* biovar 3 variant that is resistant to copper and streptomycin.

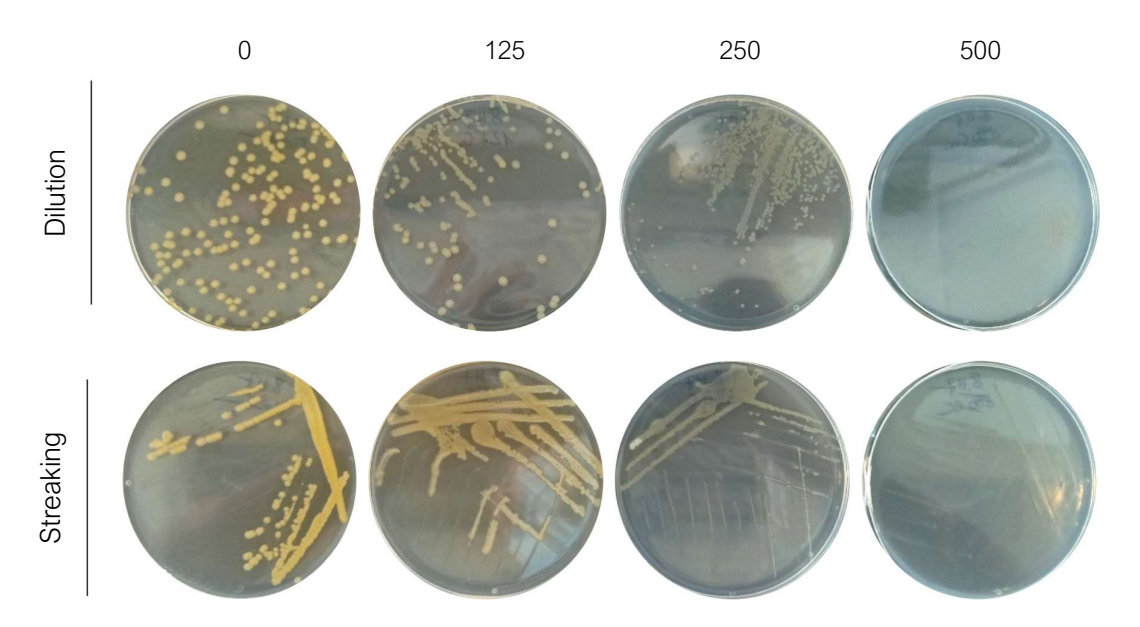


**Figure 39.** Screening representation to determine the minimum inhibitory concentration (MIC) of copper with a biocontrol candidate (8H7). On the top (0-500), amount of copper in ppm used to supplement KB-agar. Horizontally I on the left, method used to screen. Dilution (spreading 100  $\mu$ L of a 10<sup>-9</sup> dilution of the biocontrol candidate) or streaking (from overnight culture at 1 = OD<sub>600</sub>) on 90 mm-wide plates 48 hpi. Growth cannot be seen at 500 ppm of copper sulphate.

Strikingly most of the biocontrol strains were strongly resistant to copper sulphate and the remaining ones were resistant to antibiotics but to a lesser extent. At least 50% of the recommended spraying rate of copper was needed to control the growth of the biocontrol candidates. Additionally, very few biocontrol

strain candidates were completely sensitive to tetracycline and/or gentamycin. At certain degree, most of the strains were resistant to tetracycline and/or gentamycin (**Figure 40**).

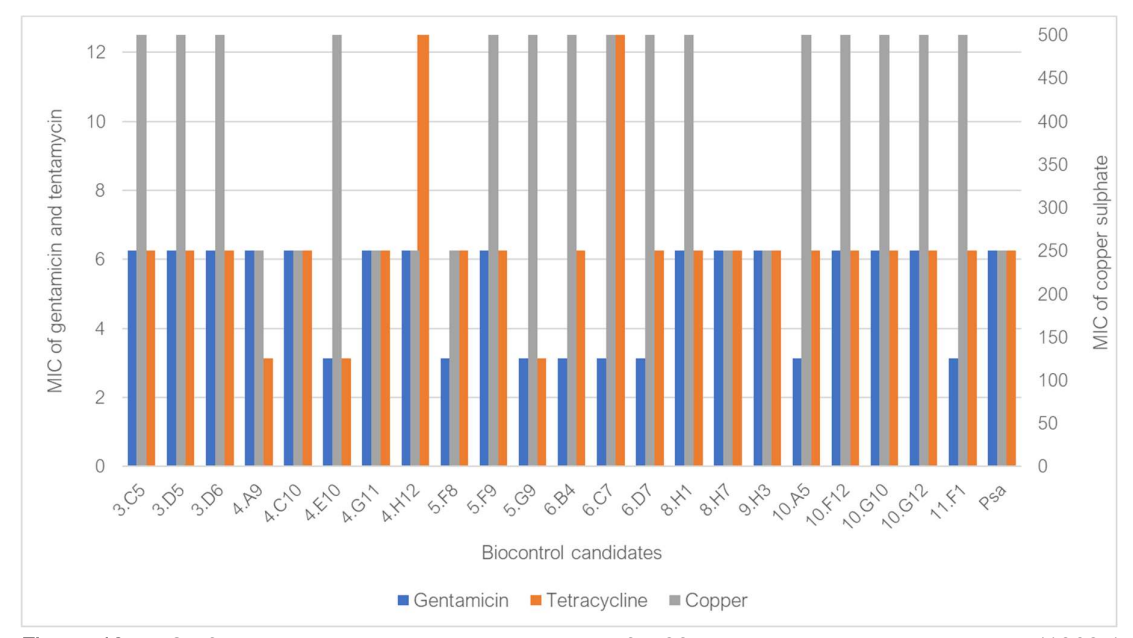
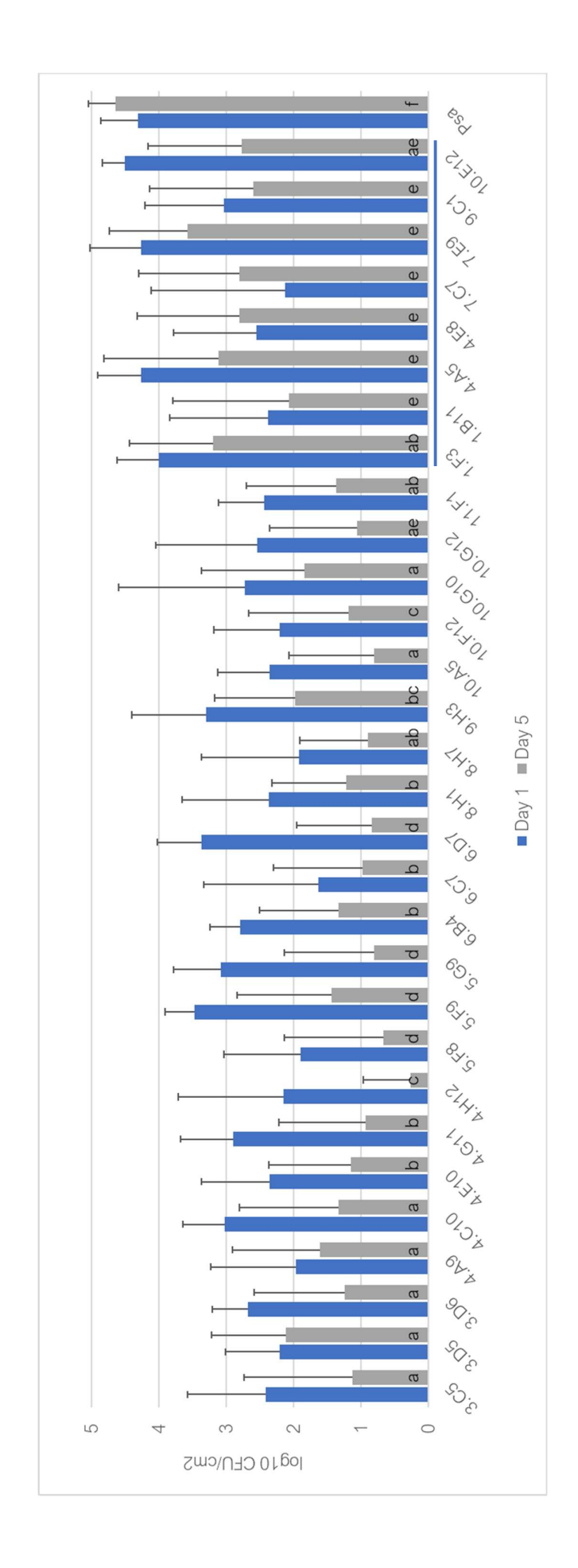


**Figure 40**. MIC of gentamicin, copper, and tetracycline for 22 biocontrol candidates and Psa (10627) between streaking and plating dilutions ( $\mu$ g/mL). On the x axis are shown the 22 biocontrol candidates and Psa.

Not all biocontrol candidates that effectively suppressed *Psa in vitro* performed well *in planta*. A few exceptions such as 4H12 (JM0626), 5G9 (JM1123), 8H7 (JM5412) and 10A5 (JM2875) stood out as very strong suppressors of *Psa* biovar 3 *in planta*. Each of these approximately reduced the pathogen presence in CFU/cm² by around 3-log. In other words, there was 99.99% less *Psa* biovar 3 on tomato plants treated with these biocontrol strains when compared to the untreated controls. Also, by testing randomly chosen non *Psa*-inhibitory strains alongside the biocontrol candidates, it was confirmed that not all *Pseudomonas* isolates were naturally *Psa*-inhibitory *in planta*.

The tomato plants that were sprayed with the effective biocontrol candidates visually corroborated the biocontrol effect (**Figure 421** and **Figure 42**). Plants treated with biocontrol candidates did not show visual disease symptoms and appeared to be as healthy as the untreated controls. The next step in the biocontrol pipeline will be to investigate whether these effective biocontrol strains can combat *Psa* infection on kiwifruit.



the right end of the graph. Different lowercase letters indicate a significant difference at 5 dpi according to one-way analysis of variance (ANOVA, p < 0.05). Values are Figure 41. Colony-forming units (CFU) per cm<sup>2</sup> leaf tissue recovered from tomato plants 1- and 5-days post inoculation (dpi). Horizontal axis contains 22 non-pathogenic Psa-inhibitory Pseudomonas strains (left side, 3.C5 to 11.F1), 8 non Psa-inhibitory Pseudomonas strains (horizontal blue line) and Psa biovar 3 as a negative control at given as mean ± s.d.

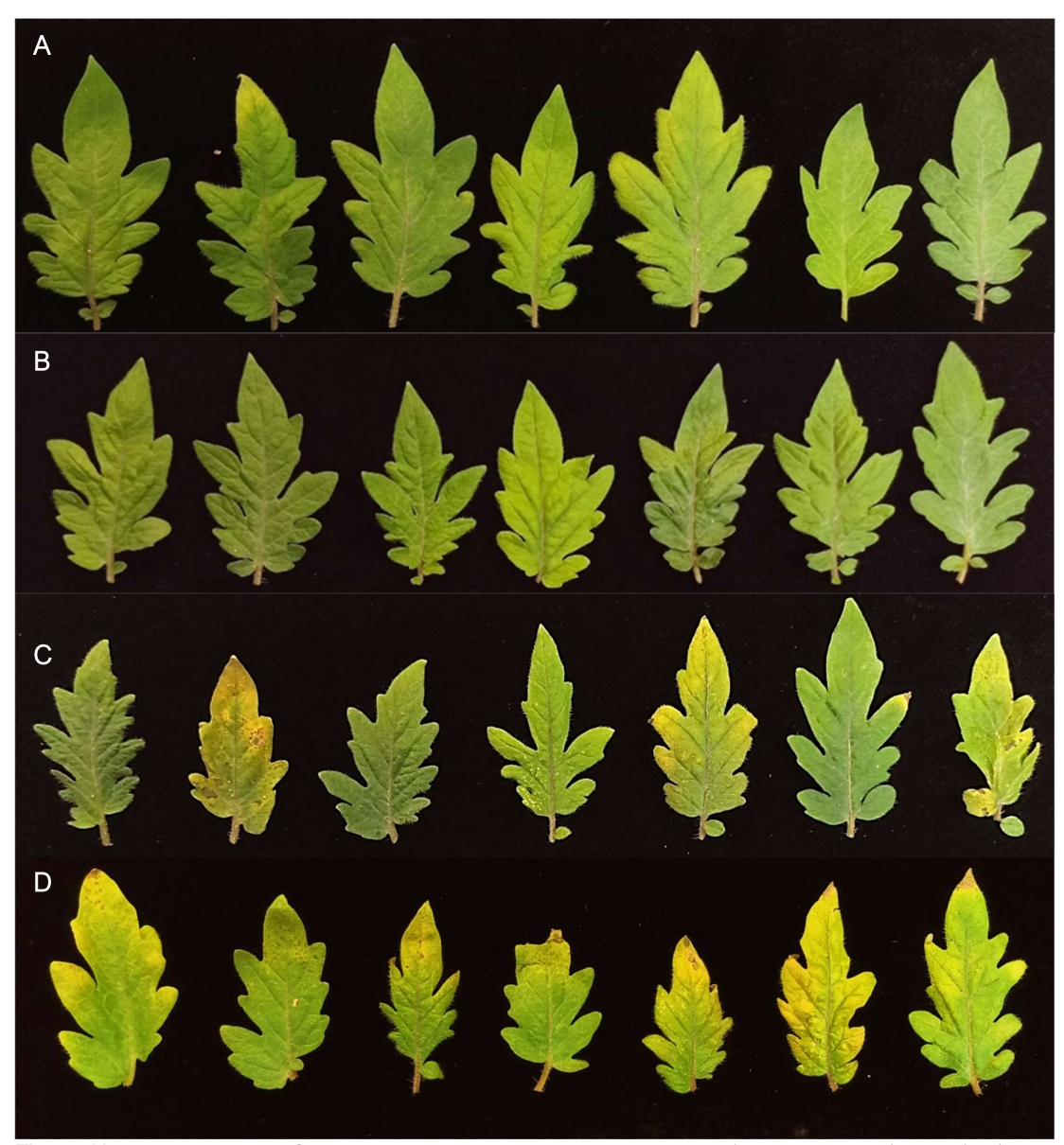


**Figure 42**. Representation of biocontrol assays on tomato plants 7 dpi. A) Uninoculated (control), B) *Psa*-inhibitory *Pseudomonas* strain (8H7 biocontrol candidate), C) Non-inhibitory *Pseudomonas* strain (negative control) and D) *Psa* biovar 3 only. Tomato leaves showing leaf brown spots (necrosis) with a thin yellow halo around it (chlorosis) are due to *Psa* biovar 3 infection.

# 5.3.4. Biocontrol assays with kiwifruit vines

Four of the most promising *Psa*-inhibitory biocontrol candidates (4.H12, 5.G9, 8.H7 and 10.A5), together with a water control, untreated control, a commercial treatment, Aureo®Gold, and Actigard® were tested on kiwifruit vines in New Zealand under greenhouse conditions. In collaboration with Joel Vanneste (P&FR), his team carried out all in planta biocontrol experiments, leaf assessments and statistical analysis while I was involved in the experimental planning, data analysis and interpretation stages (Supplementary 15). With this assay it was aimed to determine if the most effective biocontrol strains can protect kiwifruit as well as model tomato plants. These assays were carried out in Hamilton in New

Zealand, to mimic real climatic conditions where the biocontrol bacteria would be sprayed. The experimental site is geographically and commercially relevant for kiwifruit growth (central belt of the North Island) and experiments were conducted with identical plants as grown in commercial orchards (Hayward and Gold3 clones). The experiments were conducted under greenhouse conditions due to regulatory restrictions and to enable easier management of the experiment. The first two experiments were carried out with Hort16A kiwifruit vines, the most sensitive yellow kiwifruit cultivar. This assay was carried out twice, with *Psa* biovar 3 (10627), inoculated but unprotected negative control (Water) and a non-inoculated treatment (NiI), referring to the control group that receives no treatment or intervention (Figure 43 and Figure 44).

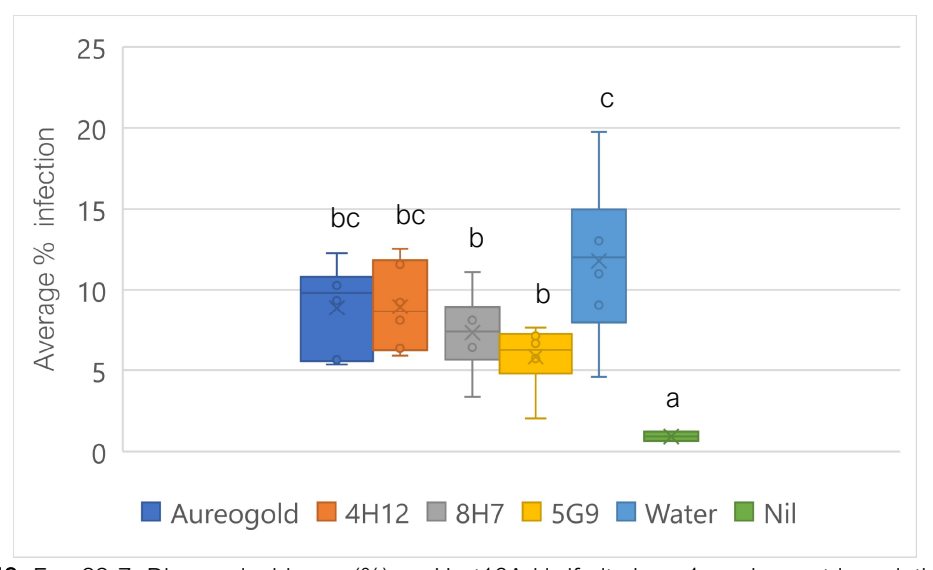


**Figure 43**. Exp 22-7. Disease incidence (%) on Hort16A kiwifruit vines 4 weeks post inoculation (wpi) assessed by Leaf Doctor. Boxes show median (horizontal lines inside the boxes), mean (crosses), observations (circles) and maximum and minimum values (whiskers). Letters on top of the whiskers represent a pairwise comparison. Same letters represent no significant difference of the means (p = 0.05), n = 32.

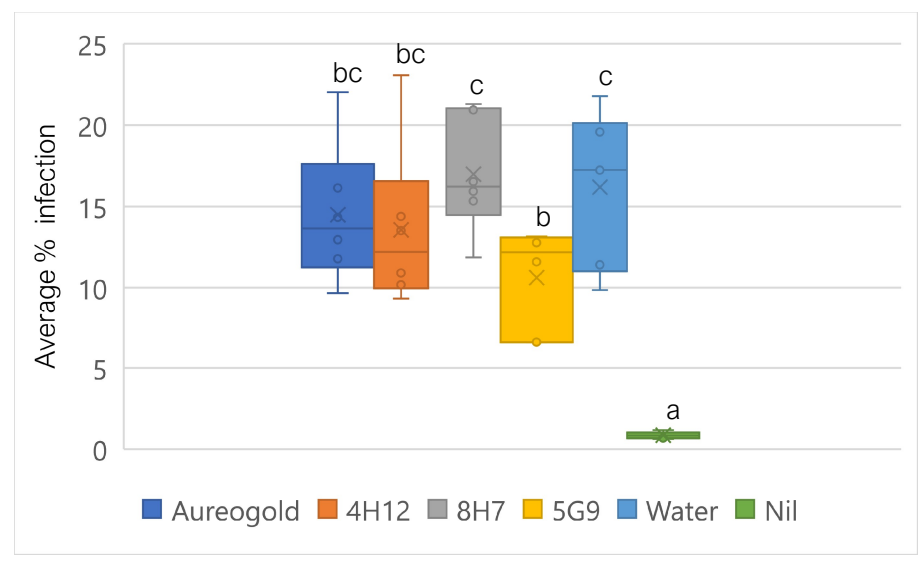


**Figure 44.** Exp 22-8. Disease incidence (%) on Hort16A kiwifruit vines 4 wpi assessed by Leaf Doctor. Boxes show median (horizontal lines inside the boxes), mean (crosses), observations (circles) and maximum and minimum values (whiskers). Letters on top of the whiskers represent a pairwise comparison. Same letters represent no significant difference of the means (p = 0.05), n = 36.

From these two repetitions, no significant differences in *Psa* suppression were observed between Aureo®Gold and 4H12. 5G9 performed better than both Aureo®Gold and 4H12, with a median approximately 25% lower in average infection compared to Aureo®Gold. However, the appreciated difference in the results were not statistically significant to conclude that 5G9 was better than the commercially available Aureo®Gold. Finally, there was a dispute between 8H7 and the Water treatment, with no statistical difference between them. During the first repetition, 8H7 performed similarly to 5G9 but here, 8H7 perform as the water control.

A similar assay was carried out with Hayward kiwifruit vines, a green flesh cultivar that is still grown not only in New Zealand but also all around the world. This assay was carried out twice (**Figure 45** and **Figure 46**). These assays showed that all treatments were significantly different to the water treatment (10627 only). However, repetitions did not show consistent results. First repetition showed that 4H12 and 8H7 performed the same way against *Psa*, Aureo®Gold performed the best, while 5H9 had an effect against *Psa* between Aureo®Gold and 4H12 and 8H7. The non-inoculated treatment was significantly different to all bacterial treatments.

Second repetition showed that all treatments performed better than water treatment. Among the three biocontrol candidates and Aureo®Gold, 5G9 and Aureo®Gold performed best against *Psa*. In contrast, water treatment had an average of infection of approximately 7.5%, the lowest registered across the biocontrol assays with Hort16A and Hayward, reducing the robustness of the results shown.

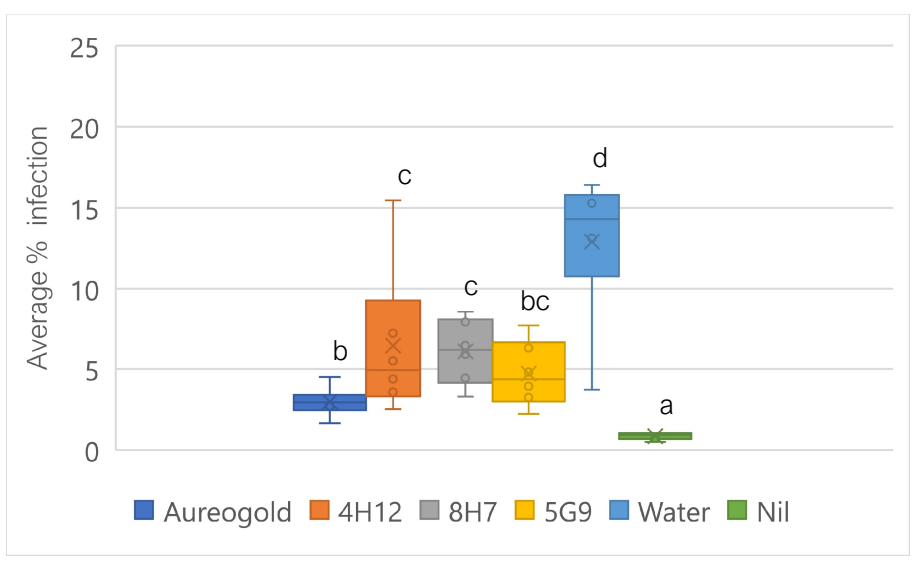


**Figure 45**. Exp 22-9. Disease incidence (%) on Hayward kiwifruit vines 4 wpi assessed by Leaf Doctor. Boxes show median (horizontal lines inside the boxes), mean (crosses), observations (circles) and maximum and minim values (whiskers). Letters on top of the whiskers represent a pairwise comparison. Same letters represent no significant difference of the means (p = 0.05), n = 36.

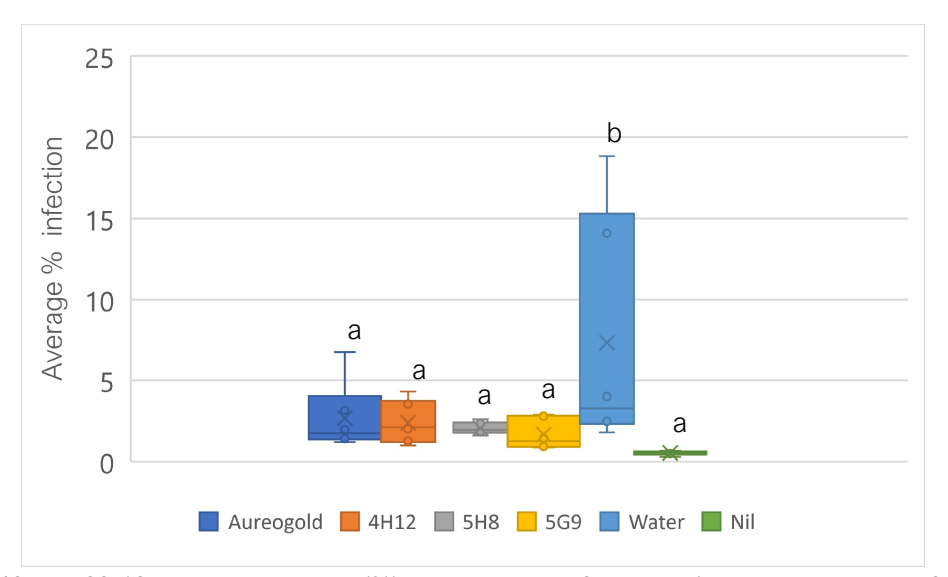


**Figure 46**. Exp 22-12. Disease incidence (%) on Hayward kiwifruit vines 4 wpi assessed by Leaf Doctor. Boxes show median (horizontal lines inside the boxes), mean (crosses), observations (circles) and maximum and minim values (whiskers). Letters on top of the whiskers represent a pairwise comparison. Same letters represent no significant difference of the means (p = 0.05), n = 36.

Finally, there were investigated if the biocontrol candidates would perform better in combination with Actigard®, an acibenzolar-S-methyl (ASM) elicitor. Based on published data, the combination of Aureo®Gold with Actigard® provides a synergistic effect, producing a stronger protective effect against *Psa* biovar 3 than when sprayed alone (de Jong, Reglinski et al. 2019).

RT594, the *Psa* resistant variant to copper was used for this assay on Hayward. Biocontrol candidates and Aureo®Gold were sprayed in combination to Actigard®, alongside the respective controls (**Figure** 

**47**). The combination of RT594 (Water), 4H12, 5G9 and 8H7 and Aureo®Gold with Actigard® showed high protection against *Psa*, showing significantly the same average infection as the untreated control. 4H12 sprayed alone was the worst performing biocontrol candidate when compared with both those strains sprayed in combination with Actigard® and those sprayed alone.

We can confirm 4H12, 5G9 and 4H12 reduce disease incidence of RT594. These results are very positive, and it would be interesting to repeat experiment 22-13 at least once more to confirm these positive results. My data suggest that 4H12, 5G9 and 4H12 are compatible with Actigard® and are as capable as the commercially available Aureo®Gold at suppressing *Psa*. However, further repetitions would be necessary to confirm synergy between Actigard® and the biocontrol candidates. This could not be proven in this study time due to time limitations of the project.

Statistically, the binomial generalised linear models indicated significant differences between the six treatments (Aureo®Gold, 4H12, 5G9, 8H7, Water and Nil) for all trials. For most of the trials the significant difference was between Nil and the other treatments. When Nil was excluded, only Exp 22-7 and Exp 22-9 had significant differences among the other treatments.

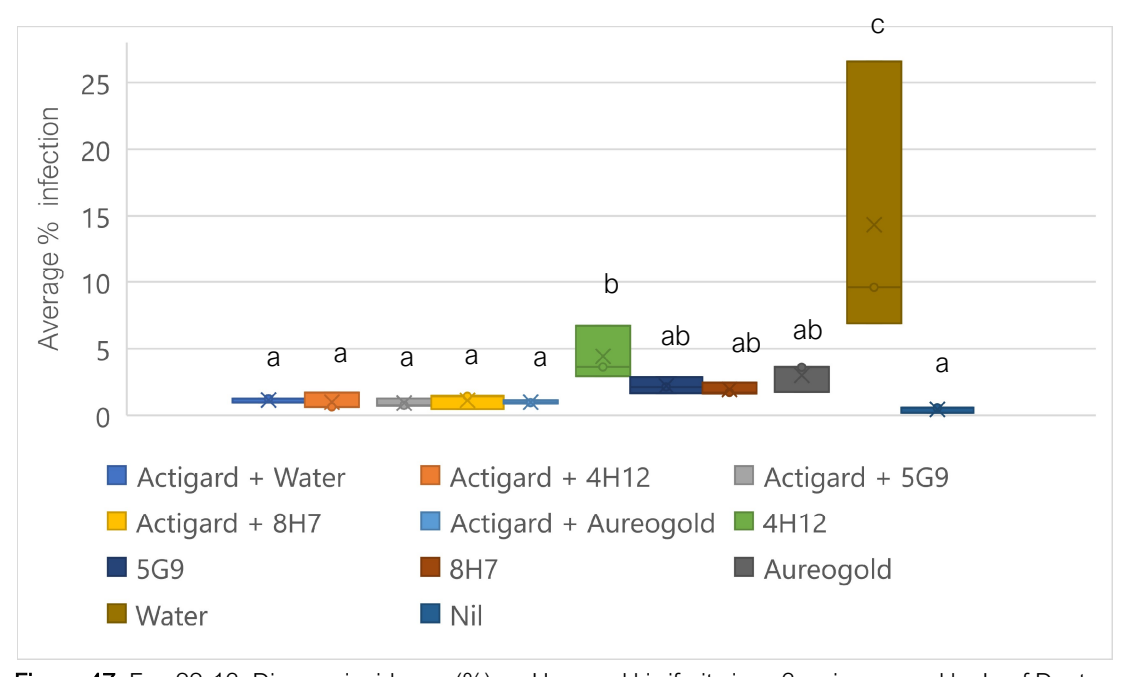


**Figure 47**. Exp 22-13. Disease incidence (%) on Hayward kiwifruit vines 3 wpi assessed by Leaf Doctor. Boxes show median (horizontal lines inside the boxes), mean (crosses), observations (circles) and maximum and minim values (box extremes). Letters on top of the whiskers represent a pairwise comparison. Same letters represent no significant difference of the means ( $\rho$  = 0.05), n = 33.

# 5.4. Discussion

Biocontrol experiments with model tomato plants helped to screen out pathogenic bacteria. Dipinoculation assays showed that one third of the *Psa*-inhibitory *Pseudomonas* spp. were pathogenic. It is common that pathogenic bacteria live together with other plant pathogens competing for an ecosystem niche, as previously observed on kiwifruit and other crops such as rice (Akter, Kadir et al. 2016, Yasmin, Hafeez et al. 2017, Purahong, Orru et al. 2018). These identified pathogenic bacteria cannot be used as BCAs but still can be taken forward for antiSMASH biosynthetic gene cluster mining as they may produce interesting novel bioactive molecules.

Twenty-two non-pathogenic biocontrol candidates were taken forward for biocontrol assays *in planta* using tomato plants as model plants. Up to four isolates were highly effective against *Psa* by reducing the presence of the pathogen on leaf by 99%. This ratio of successful biocontrol bacteria is not unusual. Often, biocontrol *in vitro* assay results do not correlate with *in planta* ones. Multiple studies have demonstrated that sometimes, *in vitro* selection of biocontrol agents does not guarantee success *in planta* (Burr, Matteson et al. 1996, Besset-Manzoni, Joly et al. 2019). However, more biocontrol candidates showed effective control despite not being at such a great extent as 4H12, 5G9, 8H7 or 10A5. All tomato plants treated with biocontrol or non-biocontrol isolates showed a significantly lower amount of *Psa* 5 dpi when compared to *Psa* sprayed only. However, they didn't meet the required level to protect kiwifruit vines. This phenomenon is not surprising. Bacteria compete for ecological niches, to colonise surfaces, and to quickly access nutrients.

Regarding kiwifruit *in planta* assays, 5G9 was the biocontrol strain that performed best at fighting back *Psa*, even better than Aureo®Gold. Similarly, on Hayward, the results were not robust enough due to one of the repetitions with an average of infection lower-than-expected in the control group (Water treatment). Despite that, the three biocontrol candidates provided good protection against *Psa*. In general, what these four trials had in common was that *Psa* infection was slightly lower than expected. This is likely to have been because of seasonality issues. These experiments were carried out in June-August 2022, which is wintertime in New Zealand. Based on previous experience in Joel Vanneste's lab, during wintertime, it is challenging to get high infection on kiwifruit vines. Due to COVID-19 restrictions, this was the only time that experimental work could be carried out. Finally, some early suggestions of synergy were observed between the biocontrol candidates or Aureo®Gold with Actigard® (de Jong, Reglinski et al. 2019). As a future perspective, it would be ideal to repeat the assays described here at least one more time to confirm the conclusions stated in this chapter, include more plants per treatment to reduce variability of the results and increase robustness, and carry out these assays during summertime when higher infection rates of *Psa* are expected.

In future, it would be interesting to test the synergetic effect of the biocontrol candidates when sprayed together as a synthetic community, with or without Actigard® and to check their compatibility with Aureo®Gold, copper, and streptomycin sprays. 5G9 and 10A5 were shown to be resistant to copper sulphate while 4H12, 5G9 and 10A5 showed moderate resistance to streptomycin *in vitro*. Would we see the same result *in planta*? Antagonism assays showed that 4H12 was antagonistic against 8H7 *in vitro* (

**Supplementary 16**). Would we see the same effect *in planta*? Ultimately, it would be interesting to see these strains move beyond greenhouse trials into orchard trials, and to commercial exploitation if results seen at greater scale are as promising.

After the successful discovery of 33 *Psa*-inhibitory *Pseudomonas* spp. and the selection of the highly effective biocontrol candidates against *Psa*, the next step involves the identification of the genetic elements that underpin the inhibitory response in each case. This will be investigated in the following chapter.

# **CHAPTER 6**

GENETIC MANIPULATION AND IDENTIFICATION OF BIOSYNTHETIC GENE CLUSTERS

# CHAPTER 6: GENETIC MANIPULATION, AND IDENTIFICATION OF BIOSYNTHETIC GENE CLUSTERS

## 6.1. Introduction

Microorganisms produce a wide variety of metabolites that have important uses in agriculture, medicine, and food production (Baltz 2019). These are produced by secondary metabolic biosynthetic pathways encoded in discrete gene arrangements called biosynthetic gene clusters (BGCs), whose activity is conditioned by the nutritional state of the organism among other stimuli (Ruiz, Chávez et al. 2010, Medema, Kottmann et al. 2015). One of the most common ways to discover these BGCs nowadays is through bioinformatics. Thanks to the rapid emergence and evolution of sequencing technologies over the past three decades, more than 600,000 bacterial genomes are currently available in public databases (Blackwell, Hunt et al. 2021). This abundance of sequence information has allowed scientists to develop a variety of bioinformatic platforms that directly help improving research outputs. These include tools for genome analysis and mapping, protein function prediction tools (Carver, Harris et al. 2012) and genome mining tools. Genome mining consists of a set of algorithms that are designed to analyse genome sequencing data to identify new BGCs as well as helping to identify the metabolic potential of the producer microorganisms (Hutchings, Truman et al. 2019, Russell and Truman 2020). Due to the increase in antimicrobial resistance and the dwindling number of discovery opportunities, the development of new compound strategies is becoming more challenging (Baltz 2017). However, the potential of genome mining to reinvigorate the pipeline of bioactive molecules against plant pathogens is immense (Hutchings, Truman et al. 2019).

One of the most widely used genome mining tools is the antibiotics and Secondary Metabolite Analysis Shell (antiSMASH). A tool released in 2011 for mining microbial genomes that has the capacity to identify up to 71 types of secondary metabolite BGCs. It works by comparing encoded gene products with a library of profile Hidden Markov Models (HMMs) for known biosynthetic enzymes. Gene clusters are then assigned to different biosynthetic classes according to antiSMASH's BGC detection profiles (Medema, Blin et al. 2011, Blin, Shaw et al. 2019, Blin, Shaw et al. 2021). In parallel to bioinformatic tools, the use of molecular methods such as transposon mutagenesis have proven to be highly effective at identifying BGCs across bacterial collections, allowing for the experimental identification of novel BGCs not belonging to any known classes that would not be easily discovered with traditional tools (Matuszewska, Maciąg et al. 2021, Moffat, Elliston et al. 2021).

Liquid chromatography-mass spectrometry (LC-MS) has also become a key part in research and discovery of secondary metabolites. As well as assisting classic genetic screening of mutants that may exhibit absence of predicted secondary metabolites (Covington and Seyedsayamdost 2022), its ability to analyse complex extracts and molecules has been used in various genome mining tools to improve the discovery of new natural products (NPs) (Jarmusch, van der Hooft et al. 2021). Particularly in NP discovery, the analysis of metabolomic data and molecular fragmentation patterns from tandem mass spectrometry (MS/MS) data can provide information on the structure of a given metabolite and assist in the discovery of families of related molecules through mass spectral molecular networking (Wang,

Carver et al. 2016, Leipoldt, Santos-Aberturas et al. 2017). Additionally, diverse tailoring modifications present in a metabolite can be traced to particular mass losses or gains, providing additional information regarding its biosynthesis (Crone, Vior et al. 2016, Russell, Vior et al. 2021).

#### 6.2. Aims

In this chapter, the following biological questions will be addressed:

Can we find correlations between the *Pseudomonas* spp. phenotypes and their BGC profiles?

Can we identify the NPs that are produced by the best performing biocontrol candidates which are responsible for both biocontrol *in vitro* and *in planta* against *Psa* biovar 3?

Can we identify novel BGCs that produce effective anti-Psa compounds?

#### 6.3. Results

Following the successful identification of four *Pseudomonas* strains highly effective against *Psa in planta*, the next steps in the biocontrol pipeline consisted of the identification of the BGCs that were responsible for the inhibitory effect *in planta* and to investigate the NPs that those biocontrol candidates were producing to effectively supress *Psa*.

# 6.3.1. Transposon mutagenesis library

The following sections describe the results for each of the transposon mutant libraries created to identify the potential BGCs in strains 4H12, 5G9, 8H7 and 10A5 that were responsible for *Psa* inhibition *in vitro* as well as *in planta*. Transposon systems were chosen based on the natural resistances present in the investigated strains. The kanamycin resistant and transposon Tn5 was introduced via electroporation or conjugation and used to generate random mutant libraries in strains 4H12, 8H7 and 10A5, which were screened to identify colonies with a negatively altered *Psa*-inhibitory activity based on biocontrol assays *in vitro*. Similarly, 5G9 was used to generate random mutant libraries but using *pALMAR3*, a host independent transposon that unlike the random insertion transposons such as Tn5 is known to specifically insert into an organism's genome at thymine-adenine motifs (Plasterk, Izsvák et al. 1999).

## 6.3.1.1. Identification of potential BGCs responsible for Psa biocontrol in strain 4H12

The Tn5 transposon mutant library for strain 4H12 contained over 6,000 mutants that were screened for their suppressor activity against *Psa*. Twenty-four of these mutants had lost their suppressor activity and were sequenced to assess the location of the transposon (**Table 20**).

**Table 20.** 4H12 mutants with Tn5 that have lost bioactivity. In order, qname: transposon reference, hname: targeted contig, hstart: start of the sequenced region within the contig, hend: end of the sequenced region within the contig, hstrand: direction of the transposon insertion (-1, to the left, 1 to the right), fracid: fraction of the positions in the alignment which are identical in the two compared sequences, inGene: locus number of targeted gene and inProduct: targeted gene name according NCBI database.

uatabase.							
qname	hname	hstart	hend	hstrand	fracid	inGene	inProduct
Tn 16	56	15870	17129	-1	0.97	2735	Isobutylamine N-hydroxylase
Tn 17	56	13402	14458	-1	0.99	2732	hypothetical protein
Tn 18	56	17553	17781	-1	1	2737	Putrescine aminotransferase
Tn 19	56	11472	12766	-1	0.98	2729 a	Outer membrane protein TolC
Tn 20	96	1471	2229	-1	0.99	3613 a	hypothetical protein
Tn 21	56	12278	13069	-1	0.96	2732	hypothetical protein
Tn 22	56	13919	15159	-1	0.99	2732	hypothetical protein
Tn 23	56	12121	13028	-1	0.98	2733	hypothetical protein
Tn 24	56	16303	17369	-1	0.96	2735	Isobutylamine N-hydroxylase
Tn 25	56	13438	14754	-1	0.97	2732	hypothetical protein
Tn 26	56	11630	12908	-1	0.96	2731	Colistin resist. protein EmrA
Tn 27	56	17721	19079	-1	0.98	2737	Putrescine aminotransferase
Tn 28	56	14080	15137	-1	0.98	2732	hypothetical protein
Tn 29	56	15789	17050	-1	0.97	2735	Isobutylamine N-hydroxylase
Tn 30	56	12238	12996	-1	0.98	2731	Colistin resist. protein EmrA
Tn 31	56	15473	16494	-1	0.99	2734	hypothetical protein
Tn 32	56	13397	14211	-1	1	2732	hypothetical protein
Tn 33	56	13399	14140	-1	1	2731	Colistin resist. protein EmrA
Tn 34	56	17564	18584	-1	1	2735	Isobutylamine N-hydroxylase
Tn 35	16	9645	10195	1	0.85	1291	Chaperone protein dnaK
Tn 36	56	14401	15571	-1	0.97	2733	hypothetical protein
Tn 37	56	14049	15239	-1	0.97	2733	hypothetical protein
Tn 38	56	13397	13622	-1	0.99	2732	hypothetical protein
Tn 39	56	15005	16016	-1	1	2733	hypothetical protein
3 T					1 - 61 / -! - 1- 1	. ( (). '	

<sup>&</sup>lt;sup>a</sup> Transposon inserted in intragenic region to the left/right of this gene.

It was fascinating that 22 out of 24 mutants had the transposon inserted in contig 56 and that within that contig, the 22 transposons were inserted across nine genes only (2729-2737). According to Operonmapper (Taboada, Estrada et al. 2018), the genes targeted by the transposon within contig 56 belong to one cluster containing ten open reading frames (ORFs) (2729-2738) (**Table 21**), which are likely organised as a single operon (**Figure 48**). Interestingly among them, genes 2730, 2736 and 2738 were

not targeted in any the transposon mutants identified in the screening experiment. When these ten genes were investigated further, it was found that they were recently identified as part of a novel BGC in *P. donghuensis* P482 called Cluster 17 and the product of this cluster is not yet known (Matuszewska, Maciąg et al. 2021).

Table 21. Annotation of genes from Cluster 17 found in 4H12.

Gene	Length (bp)	Product size (aa)	Annotation <sup>a</sup>	Cover <sup>b</sup>	Identity °
2729	1,350	449	Outer membrane protein TolC	99	72
2730	1,515	504	DHA2 family efflux transporter subunit	99	82
2731	1,068	355	HlyD family secretion protein	99	82
2732	810	269	DUF3050-like protein	97	83
2733	315	948	Fatty acid desaturase enzyme	93	75
2734	828	275	SDR NAD(P)-dependent oxidoreductase	99	85
2735	1,143	380	Isobutylamine N-hydroxylase	99	80
2736	465	154	SRPBCC-like protein	96	73
2737	1,269	422	Putrescine aminotransferase	99	81
2738	1,074	357	MupV-like SDR oxidoreductase protein	95	79
2735 2736 2737	1,143 465 1,269	380 154 422	oxidoreductase Isobutylamine N-hydroxylase SRPBCC-like protein Putrescine aminotransferase MupV-like SDR oxidoreductase	99 96 99	80 73 81

<sup>&</sup>lt;sup>a</sup> NCBI annotations, <sup>b</sup> maximum GenBank query coverage and <sup>c</sup> highest GenBank percentage identity with strains from the global database.



**Figure 48**. Graphic representation of Cluster 17. Above, first identified Cluster 17 (Krzyzanowska, Ossowicki et al. 2016, Matuszewska, Maciąg et al. 2021). Bellow, Cluster 17 found in *P. putida* 4H12. Arrows represent gene organisation and strand direction.

Cluster 17 was found across several *Pseudomonas* strains within the *P. putida* clade, specifically A00162, A00164, A00175 and A00176 (**Figure 33**). However, it is highly likely that this cluster is present in all the strains of the mentioned clade (A00186, A00184, A00181, A00179, A00176, A00175 and A00172). Assembly quality for these strains was not high and lead to fragmented genomes, making difficult to determine whether the cluster was complete in them. 4H12 was studied and processed with AntiSMASH 5.0 and 6.0 for detecting potential BGCs. Cluster 17 was not found by these recent versions of the software; however, the cluster was identified when using AntiSMASH 2.0 (Krzyzanowska, Ossowicki et al. 2016). When using AntiSMASH 6.0, 4H12 was predicted to contain other BGCs which may add strength to the biocontrol potential of the strain (**Figure 49**).

Region	Туре	From	To	Most similar kno	own cluster	Similarity
Region 17.1	NRPS-like Z	20,759	45,130	Mangotoxin ☑	NRPS	100%
Region 88.1	NAGGN 🗹	3,498	16,615			
Region 92.1	arylpolyene 🗹	1	16,084	APE Vf Z	other	20%
Region 458.1	terpene <b>௴</b>	1	2,261	Carotenoid	terpene	33%

Figure 49. AntiSMASH 6.0 identified secondary metabolite regions in 4H12 using strictness 'relaxed' analysis.

Several genes of Cluster 17 are initially annotated as hypothetical proteins as they do not have a clear hit with previously investigated homologs. For these genes, nucleotide searches confirmed the low number of closely related genes available, suggesting that these genomic regions are not highly conserved. Similarly, there is no other highly similar BCG published to date and the NP that it produces is currently unknown.

Genes, 2732-2738 seem to configure the biosynthetic core of Cluster 17, while the last three genes, 2729-2731, seem to encode transport machinery. Genes 2729-2731 were targeted four times and genes 2732-2737 18 times by the Tn5 transposon.

Gene 2729 encodes a ToIC protein, an efflux protein (OEP) with a trimeric barrel structure that forms a channel in the outer membrane (Koronakis, Eswaran et al. 2004). It is involved in export of small molecules and toxins across the outer membrane of Gram-negative bacteria and commonly associated with multidrug resistance (Zgurskaya, Krishnamoorthy et al. 2011). It is present across both pathogenic and non-pathogenic bacteria. It can operate in synchrony with three types of transport system: ATP-binding cassette transporters, resistance-nodulation-division (RND) multidrug efflux pumps and a major facilitator superfamily transporters (Fernando and Kumar 2013).

Gene 2730 was not targeted by the transposon, but its product was identified as the 14-spanner DHA2 (Drug:H+ Antiporter family 2), a major facilitator superfamily (MFS) transporter permease subunit involved in multidrug resistance (MDR). This family of proteins are poorly characterised but are known to be associated in the export of structurally and functionally unrelated compounds or in the uptake of amino acids into the vacuole or the cell (Dias and Sá-Correia 2013). In Gram-negative bacteria, the DHA2 family transporters may assemble with periplasmic and outer membrane-bound proteins to form tripartite systems, akin to those commonly associated with RND exporters, potentiating high levels of drug resistance. For example, *E. coli* multidrug efflux system *EmrAB-TolC* (Hassan, Brzoska et al. 2011). This gene has a high similarity with the multidrug export protein *EmrB* found in *E. coli and FarB* encoding protein found in *Rhodopseudomonas palustris*.

The gene 2731 is identified as an efflux pump transport protein. The closest annotated gene to the submitted query is called *HlyD*, is a member of the membrane fusion protein (MFP) family, a large family of polypeptides. Spanning the periplasm, they link the inner and outer membranes as a periplasmic adaptor protein, an essential component of bacterial tripartite efflux pumps (Hinchliffe, Greene et al. 2014). Due to its conserved *HlyD* domain protein it is highly likely that this gene is part of an efflux pump

and functions as a multidrug export *EmrA*-like protein (Pimenta, Racher et al. 2005). This gene, in other studies with *P. donghuensis* has been directly linked with the export of molecule(s) responsible for antibacterial activity (Matuszewska, Maciąg et al. 2021).

The products of genes 2729-2631 seem to compose a well organised tripartite efflux pump spanning the cytosol, the periplasm, and the extracellular environment that could be involved in the secretion of the anti-*Psa* secondary metabolite(s), as suggested by the work carried out in *P. donghuensis*. It could also be an efficient self-resistance mechanism for the producer strain. Within Gram-negative bacteria such as *Pseudomonas aeruginosa*, the highly similar *EmrAB*-ToIC tripartite is the major driver of multiple antibiotic resistances (Hinchliffe, Greene et al. 2014) (**Figure 50**). Interestingly, within this *EmrAB*-ToIC-like complex of proteins, it has been hypothesised that the MFS-type transporter system *EmrAB* aids in the transport of a diverse array of structurally unrelated molecules and varied functions (Puértolas-Balint, Warsi et al. 2019). It has been proven that this versatile structure can transport pyoverdines and is also speculated that participates in *E. coli* siderophore enterobactin synthesis (Matuszewska, Maciag et al. 2021). Additionally, it has been shown that transport several small molecular weight drugs (Alav, Kobylka et al. 2021).

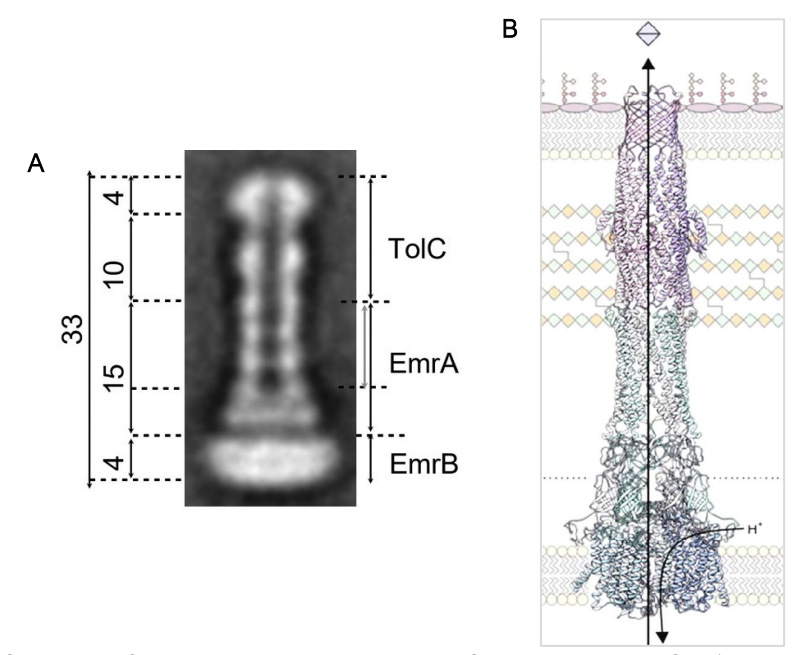


**Figure 50**. Structure of the multidrug transporter MFS-type EmrAB-TolC. A) Transmission electron microscopy (TEM) image of the EmrAB-TolC complex showing densities corresponding to TolC, EmrA and EmrB. Distances between these components are indicated in nm. The grey arrow indicates the  $\alpha$ -helical coiled-coil domains of EmrA. B) Representation of the single-component efflux transporter as an independent multidrug/H+ antiporters which transport the drugs from the cytoplasm to the periplasm. Substrate of the transporter is indicated as a purple-coloured double triangle. Adapted from: (Alav, Kobylka et al. 2021, Yousefian, Ornik-Cha et al. 2021).

Gene 2732 was not matched with any known homologs and therefore was originally annotated as a hypothetical protein, but it does contain a domain of unknown function (DUF3050). The closest investigated DUF3050 containing protein was found in *P. savastanoi*, previously *P. syringae*, a

pathogenic bacteria isolated from a kiwifruit leaf in Te Puke, New Zealand in 2011 (NCBI GenBank ID LKCI00000000.1) (Visnovsky, Fiers et al. 2016). DUF3050 is part of the heme oxygenase-like superfamily and has no clear known function. The heme oxygenase is an enzyme that catalyses the degradation of heme to produce biliverdin, ferrous ion, and carbon monoxide and is conserved across phylogenetic kingdoms (Li and Stocker 2009). These enzymes serve a variety of specific needs in different branches of life such as HMOX systems, facilitating iron acquisition (Frankenberg-Dinkel 2004, Lu, Wang et al. 2020).

Gene 2733, initially annotated as a hypothetical protein, has homology with fatty acid desaturase enzymes. There are not many close hits to this gene from 4H12 so it is difficult to elucidate the potential function of its product. Best fits are *desA*-like or *crtW*-like genes, both encoding fatty acid desaturase enzymes. These enzymes aid with lipid transport and metabolism. Fatty acid desaturases are divided into soluble and integral membrane classes. The membrane fatty acid desaturase (FADS)-like includes membrane FADSs, alkane hydroxylases, beta carotene ketolases (*CrtW*-like), hydroxylases (*CrtR*-like), and other related proteins. FADSs play an important role in the maintenance of the structure and functioning of cell membranes. These enzymes require iron and oxygen for activity and are involved in the initial oxidation of inactivated alkanes. Beta-carotene ketolase and beta-carotene hydroxylase are carotenoid biosynthetic enzymes for astaxanthin and zeaxanthin, respectively. Generally, they all share extensive hydrophobic regions that can span the polar membrane at least twice (Lu, Wang et al. 2020).

Gene 2734, annotated as a hypothetical protein has been proven to strongly contribute to the antibacterial activity against bacterial pathogens, as its inactivation results in a strong antibacterial activity reduction (Matuszewska, Maciąg et al. 2021). However, reductases are in multiple types of pathways, secondary and primary metabolism. Searches predict this protein is a short chain dehydrogenase/reductase SDR family NAD(P)-dependent oxidoreductase such as *fabG*-like dehydrogenase. The short-chain alcohol dehydrogenase family is involved in lipid transport and metabolism, secondary metabolites biosynthesis, transport and catabolism (Lu, Wang et al. 2020). The large superfamily of SDR is present in every living organism and catalyse various reactions belonging to both primary and secondary metabolism (Kallberg, Oppermann et al. 2002). SDRs have been reported to take part in biosynthesis pathways of several antimicrobial compounds, such as polyketide antibiotic kalimantacin *from P. fluorescens* or fusidic acid in *Aspergillus* spp. (Cao, Li et al. 2019). All this evidence suggests that this gene encodes one of the essential biosynthetic pathway enzymes that produces the antimicrobial metabolite.

Gene 2735 encodes a product identified as an acyl-CoA dehydrogenase (ACAD), and is highly similar gene to *fadE*, a gene encoding enzyme involved in the β-oxidation of fatty acids that has been identified as a key component of biosynthetic pathways within BCAs (Pliego, Crespo-Gómez et al. 2019). Dehydrogenases, and oxidases, catalyse the dehydrogenation of the corresponding trans-enoyl-CoA by FAD, which becomes reduced. The reduced form of ACAD is re-oxidised in the oxidative half-reaction

by electron-transferring flavoprotein, from which the electrons are transferred to the mitochondrial respiratory chain coupled with ATP synthesis (Lu, Wang et al. 2020).

Gene 2736 was not targeted by the transposon and initially annotated as a SRPBCC family protein, an acronym that stands for six proteins with a conserved domain (StART, RHOalphaC, PITP, Betv1, CoxG and CalC). SRPBCC domains have a deep hydrophobic ligand-binding pocket, and they bind diverse ligands. Closest annotated homolog is SRPBCC\_11, a ligand-binding SRPBCC domain of an uncharacterised subfamily of proteins. Some members of the superfamily are aromatase/cyclase (ARO/CYC) domains of proteins such as the ones needed to produce tetracenomycin by *S. glaucescens* (Lu, Wang et al. 2020). This family contains polyketide cylcases/dehydrases which are enzymes involved in polyketide synthesis. It also includes other proteins of the steroidogenic regulatory protein superfamily (lyer, Koonin et al. 2001).

Gene 2737 was identified as a putrescine aminotransferase, a *patA*-like gene which belongs to the class-III pyridoxal-phosphate-dependent aminotransferase family (Schneider and Reitzer 2012). The closest gene homologs found was PRK11522, a putrescine-2-oxoglutarate aminotransferase. Members of this pyridoxal phosphate enzymes are found in *E. coli, Erwinia carotovora* subsp. *atroseptica*, and other Gram-negative bacterial species (Samsonova, Smirnov et al. 2003). Other homologs found was an organic anion transporter (OAT)-like protein belonging to the pyridoxal phosphate-dependent aspartate aminotransferase superfamily. All the enzymes belonging to this family act on basic amino acids and their derivatives are involved in transamination or decarboxylation (Denessiouk, Denesyuk et al. 1999). Also, 2737 was identified as a *ArgD*-like gene, another acetylornithine/succinyldiaminopimelate/putrescine aminotransferase that may belong to a catabolic pathway.

Gene 2738 was not targeted by the transposon but is considered as part of the ten gene operon according to Operon-mapper. The gene encodes a *MupV*-like SDR family oxidoreductase homolog. Extended SDRs are distinct from classical SDRs. Extended SDRs are a diverse group of proteins, and include isomerases, oxidoreductases, epimerases and lyases. *MupV* in particular is a SDR protein from *P. fluorescens* involved in the biosynthesis of mupirocin, a polyketide-derived antibiotic (Cooper, Laosripaiboon et al. 2005). SDRs have a single domain with a structurally conserved Rossmann fold (tertiary protein fold), an NAD(P)(H)-binding region, and a structurally diverse C-terminal region. This subgroup of extended SDR family domains have the characteristic active site tetrad and a well-conserved NAD(P)-binding motif. They catalyse a wide range of activities including the metabolism of steroids, cofactors, carbohydrates, lipids, aromatic compounds, and amino acids, and act in redox sensing (Lesk 1995, Sellés Vidal, Kelly et al. 2018).

# 6.3.1.1.1. Preliminary results of next steps with 4H12

Next steps forward with 4H12 were identifying the powerful antimicrobial NP that produces Cluster 17 by using mass spectrometry and assessing whether knockout mutants of Cluster 17 can protect plants against *Psa* infection to confirm the biocontrol effect *in planta*. It was not possible to produce clean

knockout mutants even when several molecular techniques were tested such as gene synthesis and inverse PCR (primers used in **Supplementary 1**). Therefore, Tn 31, one of the 4H12 transposon mutants ( $\Delta$ 2734), was used to carry out a biocontrol assay *in planta* with model plants (tomato). Preliminary results of a single repetition experiment showed that no significant differences existed between plants inoculated with  $\Delta$ 2734+*Psa* and *Psa* only (**Figure 51**). Meanwhile, plants inoculated with wild type 4H12+*Psa* approximately reduced the presence of *Psa in planta* by around 2-log, preliminary confirming that this gene has an important role in *Psa*-suppression.

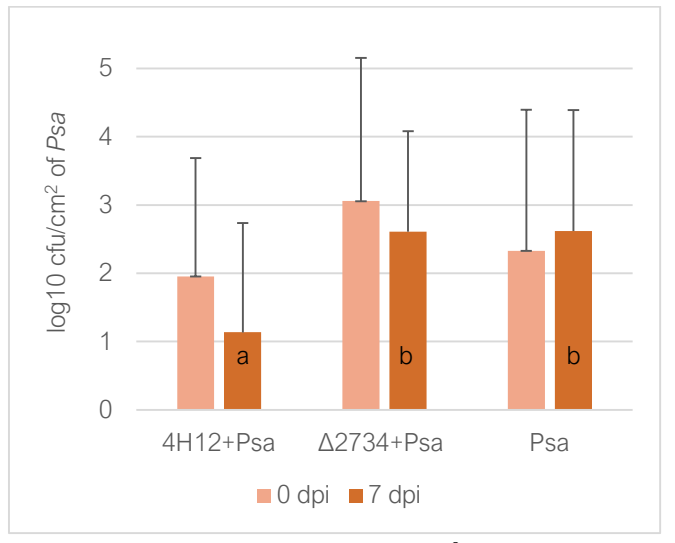


**Figure 51**. Colony-forming units (CFU) of Psa biovar 3 per cm² recovered from tomato plants 1- and 7 dpi. Horizontal axes represent different treatments: 4H12 sprayed before Psa biovar 3 (left,  $\Delta 2734$  (Tn 31), a 4H12 transposon mutant sprayed before Psa biovar 3 (centre) and Psa biovar 3 alone as a negative control (right). Different lowercase letters indicate a significant difference at 7 dpi according to one-way analysis of variance (ANOVA, p < 0.05). Values given as mean  $\pm$  s.d. (n=6).

Liquid cultures of 4H12 only, 4H12 together with *Psa*, *Psa* only and KB only were grown, concentrated three times, and tested for biocontrol *in vitro* as described in **section 0**. Biocontrol assays on KB-agar showed preservation of bioactivity post-sample concentration of the organic phase (**Figure 52**).

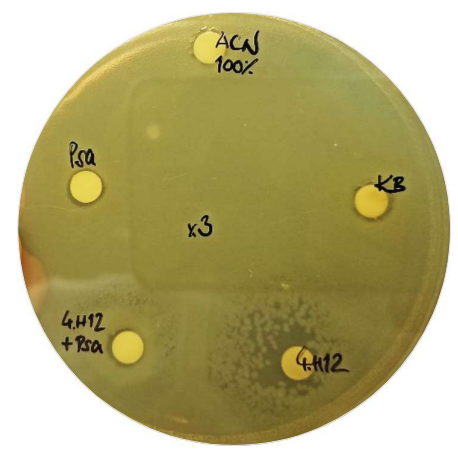


**Figure 52**. Biocontrol assay *in vitro*. Three times concentrated treatments (organic phase only) were tested against *Psa* used as overlay. Treatments were KB liquid medium (negative control), 4H12 only, 4H12 with *Psa*, *Psa* only (negative control) and acetonitrile (ACN) (negative control). Biggest inhibition zone was appreciated with 4H12 only and a mild inhibition in the 4H12 with *Psa* co-culture.

Dry organic phase was resuspended in 100% methanol while dry aqueous phase was resuspended in deionised sterile water. *Psa*, ACN and KB treatments did not show inhibition when placed on cellulose discs over a water overlay of *Psa*. This assay was repeated two times and results were consistent with the figure shown. Regarding the co-culture of *Psa* with 4H12, it was hypothesised that the exposure of 4H12 to *Psa* may induce the production of inhibitory molecules or would at least drastically reduce its growth as seen statically *in vitro*. Interestingly, little inhibition was appreciated, but still enough to identify single colonies around the proximities of the disc, showing moderate inhibition against *Psa*. In contrast, extracts of 4H12 grown alone had a greater *Psa*-inhibition effect with clear areas around the discs. Dry aqueous phase extracts did not show significant inhibition.

Once it was bioactivity was checked, LC-MS analysis was carried out with the concentrated extracts. Cultures of wild type 4H12 and the  $\Delta$ 2734 mutant (m4H12) showed the strains have a different metabolite profile, with some major peaks missing in the mutant (**Figure 53.**).

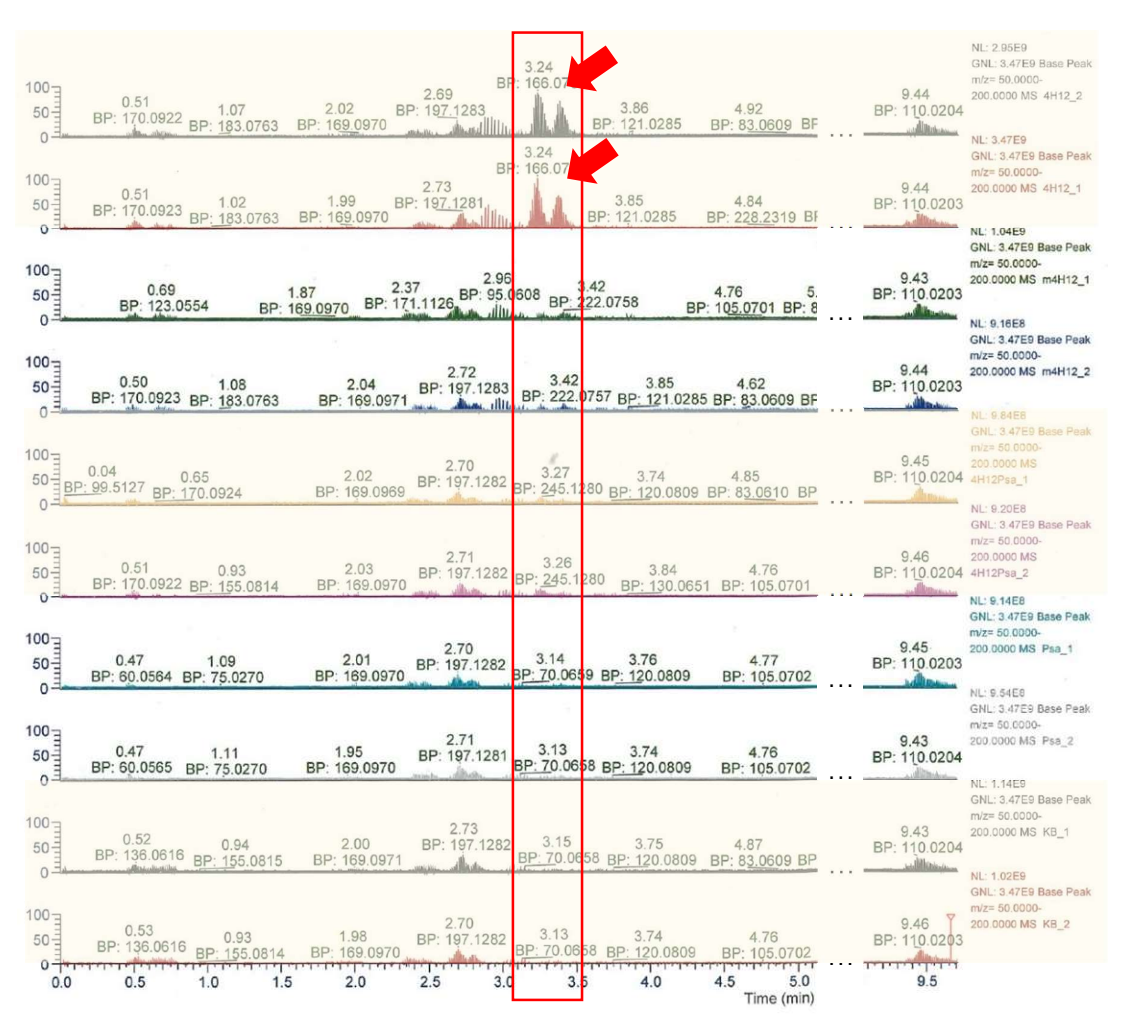


**Figure 53.** Mass spectra showing *in vitro* assays with 4H12 only (first and second chromatogram),  $\Delta 2734$  only (third and fourth chromatogram), 4H12 grown together with *Psa* (fifth and sixth chromatogram), *Psa* only (seventh and eighth chromatogram) and KB only (nineth and tenth chromatogram). Red arrows point at the only condition (two repetitions) that have two major peaks, both missing in the rest of conditions.

This preliminary result pointed to some candidate masses for the bioactive molecule/s in 4H12. Preliminary search of masses that stranded out such as m/z 166.0735 [M+H] in the public natural product databases such as Natural Product Atlas, MiBIG, PubChem and ChemSpider result in the identification of a potential neutral molecules such as  $C_8H_9N_2O_2$  or  $C_6H_7N_5O$ , within reasonable error there are other molecules with these formulae, including some possible natural compounds but with less likelihood to be the molecule/s produced by 4H12. Therefore, further work is required to assess whether those candidate peaks are indeed the bioactive molecule, as well as to characterise its structure.

# 6.3.1.2. Identification of potential BGCs responsible for Psa biocontrol in strain 5G9

The transposon screen of 5G9 with *pALMAR3* consisted of over 2,000 colonies from five separate transformation events. There were only three mutants which harboured transposon insertions within genes that affected the inhibition of *Psa* biovar 3 *in vitro*. These candidate genes are summarised in **Table 22**.

**Table 22**. Genes targeted by the *pALMAR3* transposon In order, qname: transposon reference, hname: targeted contig, hstart: start of the sequenced region within the contig, hend: end of the sequenced region within the contig, hstrand: direction of the transposon insertion (-1, to the left, 1 to the right), fracid: fraction of the positions in the alignment which are identical in the two compared sequences, inGene: locus number of targeted gene and inProduct: targeted gene name according NCBI database.

qname	hname	hstart	hend	hstrand	fracid	inGene	inProduct
Tn 40	56	27321	27421	1	0.81	3971	Cysteine synthase A
Tn 41	56	27310	27416	1	0.84	3970 a	Hypothetical protein
Tn 42	56	27310	27420	1	0.83	3970 a	Hypothetical protein

<sup>&</sup>lt;sup>a</sup> Transposon inserted in intragenic region to the left/right of this gene.

It was particularly challenging to identify mutants with its *Psa*-inhibition ability reduced due to all isolates remained inhibiting *Psa* in some extend (**Figure 54**).



**Figure 54**. Example of screening with two 5G9 transposons mutants. In the left, a mutant that produced as much *Psa*-inhibition as the wildtype *in vitro*. In the right, a mutant that had its ability to inhibit *Psa* reduced *in vitro*.

Interestingly, the only three transposons that were identified by their deficient *Psa* inhibition targeted the same gene or region and two of them were potentially clonal as the starting nucleotide (hstart) is the same. Transposon Tn 40 targeted a cysteine synthase A, while Tn 41-42 targeted the intragenic region at the left of the cysteine synthase A (**Figure 55**). *CysK* (O-acetylserine sulfhydrylase) is a phosphate-dependent enzyme which catalyses cysteine biosynthesis by converting O-acetyl serine into L-cysteine in the presence of sulphide. Other functions are in contact-dependent toxin activation in Gram-negative pathogens, in biofilm formation and, in ofloxacin and tellurite resistance among others (Joshi, Gupta et al. 2019). Additionally, cysteine synthase or *cysK* has been linked to anti-bacterial toxin activation (Shcherbakova, Odintsova et al. 2016, Benoni, Beck et al. 2017). Whether this gene or the surrounding ones such as *IpxO* (dioxygenase for synthesis of lipids) are related to biocontrol of *Psa* remains unknown. Additionally, antiSMASH 6.0 analysis was unable to detect any BGC in this genomic region, increasing the potential of discovering a novel NP.



**Figure 55.** Targeted operons by *pALMAR3* in 5G9. Orange stars next to genes represent transposon insertions.

# 6.3.1.3. Identification of potential BGCs responsible for Psa biocontrol in strain 8H7

Transposon Tn5 (kanamycin resistant), was used to generate a random mutant library of strain 8H7 via conjugation, yielding over 2,000 mutants, which were screened to identify colonies with a negatively altered *Psa*-inhibitory activity based on biocontrol assays *in vitro*. Only 12 positive mutants were obtained from the screening, which were then sequenced to identify the location of the insertion (**Table 23**).

**Table 23**. Genes targeted by the Tn5 Transposon. In order, qname: transposon reference, hname: targeted contig, hstart: start of the sequenced region within the contig, hend: end of the sequenced region within the contig, hstrand: direction of the transposon insertion (-1, to the left, 1 to the right), fracid: fraction of the positions in the alignment which are identical in the two compared sequences, inGene: locus number of targeted gene and inProduct: targeted gene name according NCBI database.

qname	hname	hstart	hend	hstrand	fracid	inGene	inProduct
Tn 43	1	1059448	1060464	-1	0.99	964	Succinate-CoA ligase [ADP- forming] subunit alpha
Tn 44	2	1058562	1058859	-1	0.99	2381	Hypothetical protein
Tn 45	2	1072018	1072350	-1	1	2395	Epimerase family protein
Tn 46	3	41713	42393	-1	1	2474	DNA polymerase I
Tn 47	3	203522	204122	1	0.97	2619	hypothetical protein
Tn 48	3	492944	493582	-1	0.98	2892	Na(+)/H(+) antiporter NhaA
Tn 49	3	72930	73498	-1	0.96	2508	HTH-type transcriptional regulator PerR
Tn 50	3	699518	700164	1	0.92	3051	Cyclic-di-GMP receptor FimW
Tn 51	3	77665	78305	-1	0.96	2512	Oxygen-dependent coproporphyrinogen-III oxidase
Tn 52	3	768632	769872	-1	0.95	3114	Phosphate starvation-inducible protein PsiF
Tn 53	3	763718	764301	1	1	3109	hypothetical protein
Tn 54	3	258282	258595	1	1	2672	D-amino acid dehydrogenase

8H7 is a *P. graminis*, another *Pseudomonas* species well known for their biocontrol activity against plant pathogens (Iglesias, Lopez et al. 2018). It is interesting that out of the 12 transposon mutants, they all sit in the first three contigs out of the 24 that this genome had when sequenced. Tn 43 was the only targeted gene hit by the transposon in contig 1 which was a succinate-CoA ligase-like gene (*sucC*), an essential gene for the central metabolism and is part of the *sucABCD* operon (Yu, Sung et al. 2006) (**Figure 56A**).

Despite Tn 44 and 45 being close to each other within the reference genome, they seem to not be part of a BGC. Gene 2381, targeted by the transposon (Tn 46), was initially annotated as a hypothetical protein, but it holds a high similarity with a 1-acyl-sn-glycerol-3-phosphate acyltransferase (99% query cover and 100% percentage identity). This type of phosphate acyltransferase gene potentially contributes to the generation of diversity in membrane phospholipids. In *E. coli, YihG*, a lysophosphatidic acid acyltransferase homolog, appears to regulate bacterial swimming motility through modulation of the

composition of fatty acyl groups in membrane phospholipids (Toyotake, Nishiyama et al. 2020). Additionally, gene 2381 sits next to an autotransporter domain-containing protein of more than 3,000 bp, a porin-like barrel that span cell membranes essential for import and export of nutrients, waste, and other products (Masi, Winterhalter et al. 2019) (**Figure 56B**). On the other hand, gene 2395 (targeted on Tn 45), is an epimerase family protein, which is essential for the construction of cell walls (Allard, Giraud et al. 2001).

Similarly, several targeted genes such as those in Tn 46-Tn 54 were identified as essential for metabolism and cell structure. Tn 46 was initially annotated as a hypothetical protein but was identified as a *polA*-like gene, an essential gene that encodes DNA polymerase I that is involved in DNA replication and repair (Quiñones, Wandt et al. 1997). Tn 47, which had gene 2619 targeted, was initially annotated as a hypothetical protein, but further analysis identified the gene as an ABC transporter permease subunit, a *pstC*-like gene and part of a phosphorous metabolism operon (*ptsABCS*) together with phosphatases and other genes such as *phoB*, *phoR* and *phoU* (**Figure 56C**) (Nouioui, Cortés-albayay et al. 2019). Also, *nhaA* was targeted by the transposon in Tn 48, which has an integral membrane protein that catalyse the exchange of H<sup>+</sup> for Na<sup>+</sup> and are critical for homeostasis and cell function (Padan 2014). In this case, this protein seems to be part of a several gene operon (**Figure 56D**). Some of them are *hutH*, *hutU*, *hutl* and *hutG* which regulate histidine utilization and degradation (Ormeño-Orrillo, Menna et al. 2012).

Tn 49 targeted gene 2508, a *perR*-like HTH domain-containing transcriptional regulator. Tn 51 targeted gene 2512, an oxygen-dependent coproporphyrinogen-III oxidase (*HemF*) which performs as cofactor-and in metal ion-independent catalysis (**Figure 56E**) (Breckau, Mahlitz et al. 2003, Seetharaman, Kumaran et al. 2006). Tn 52 and 53 targeted genes 3114 and *asmA* respectively (**Figure 56F**). They are annotated as a phosphate starvation-inducible protein *psiF* and *asmA*, respectively. Despite being so close within the genome, they seem to not have linked functions. The *psiF*-like protein is next to another hypothetical protein which no putative conserved domains were found. *asmA* is involved in the assembly of outer membrane proteins in *E. coli* and may have a role in lipopolysaccharide synthesis (Misra and Miao 1995, Deng and Misra 1996). Gene 3110 did not match with any putative conserved domains.

Tn 54 targeted gene 2672, a D-amino acid dehydrogenase (*dadA*) which is part of the *dadAX* operon (**Figure 56G**). The operon, regulated by (cyclic adenosine monophosphate) cAMP, encodes the D-amino acid dehydrogenase *dadA* and the amino acid racemase *dadX*, essential for D- and L-alanine catabolism (Wasserman, Walsh et al. 1983, Zhi, Mathew et al. 1998, Radkov and Moe 2013). It is known that D-alanine synthesis is involved in the production of peptidoglycan hydrolases which can work as biocontrol weapons against other bacteria (Szweda, Schielmann et al. 2012).

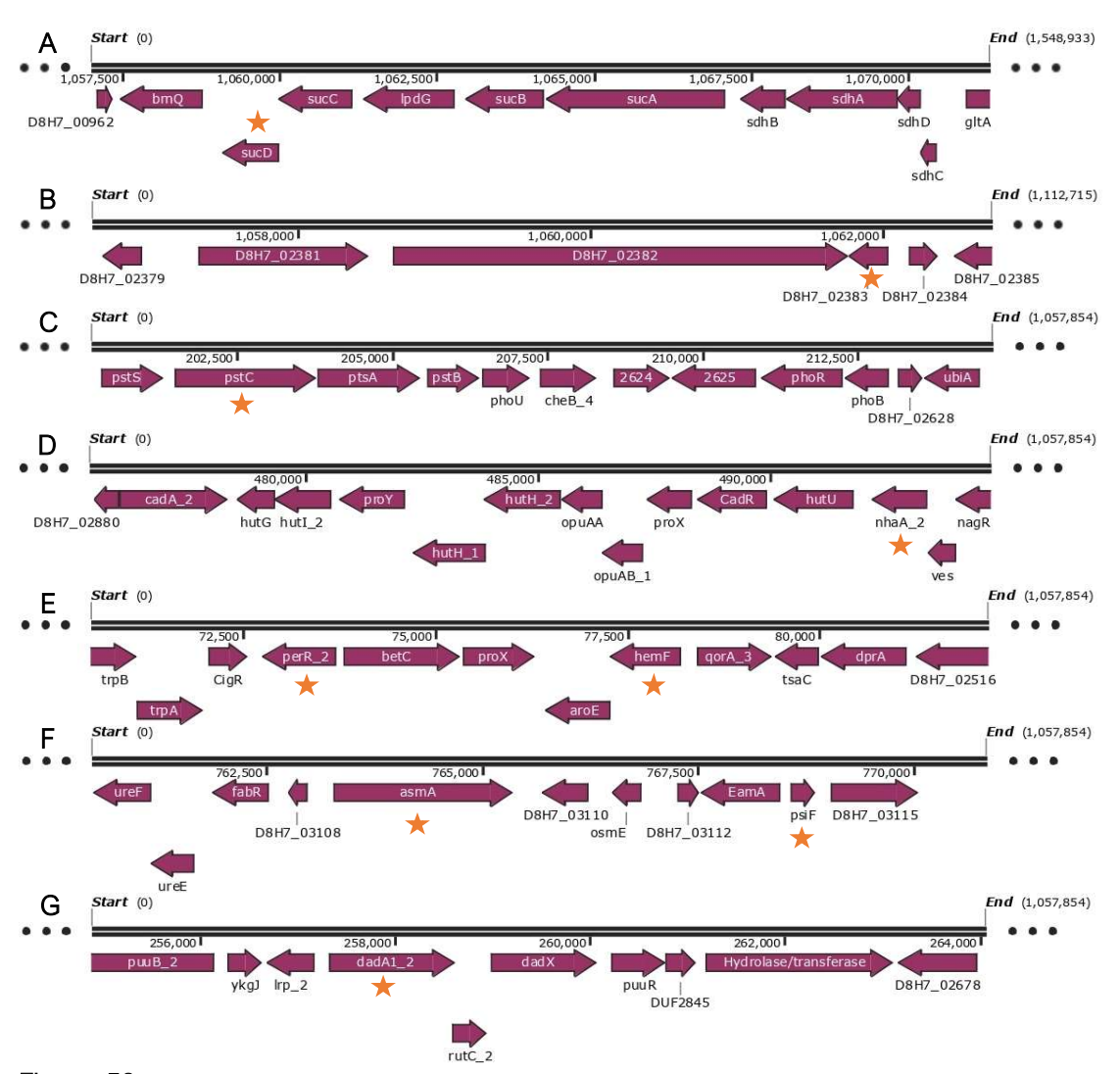


**Figure 56**. Targeted operons by Tn5 in 8H7. Orange stars next to genes represent transposon insertions.

AntiSMASH analysis of 8H7 showed that additional gene clusters were predicted to be within the bacterial genome. For example, in contig 1, two BGC were predicted to be present but none of them covered in any of the regions targeted by Tn5 transposons. One was a carotenoid-like terpene (100% similarity) and a cupriachelin-like NRPS. In contig 3, a complete arylpolyene-like was predicted but with a 40% similarity, in contig 5, a mangotoxin-like NRPS was predicted at the beginning of the contig with a 100% similarity and in contig 7, a NAGGN-like BGC.

# 6.3.1.4. Identification of potential BGCs responsible for Psa biocontrol in strain 10A5

Tn5 was introduced in strain 10A5 via conjugation to create a library of over 2,000 mutants from different conjugations that were screened *in vitro* and sequenced (**Table 24**). Screening of this library was particularly challenging as only 3 of the mutants had negatively affected inhibitory activity against *Psa*.

**Table 24.** Genes targeted by the Tn5 transposon in 10A5. In order, qname: transposon reference, hname: targeted contig, hstart: start of the sequenced region within the contig, hend: end of the sequenced region within the contig, hstrand: direction of the transposon insertion (-1, to the left, 1 to the right), fracid: fraction of the positions in the alignment which are identical in the two compared sequences, inGene: locus number of targeted gene and inProduct: targeted gene name according NCBI database.

qname	hname	hstart	hend	hstrand	fracid	inGene	inProduct
Tn 55	1	3202000	3203108	-1	0.95	2836	Deoxyuridine 5'-triphosphate nucleotidohydrolase protein
Tn 56	1	679880	681091	-1	0.98	607	Hypothetical protein
Tn 57	3	8888	9339	1	0.78	5358	Putative deoxyribonuclease

Tn 55 targeted a dut-like protein (Figure 57A). This protein is known to be involved in metabolic process such as the pyrimidine metabolism pathway. It produces dUMP, the immediate precursor of thymidine nucleotides and it decreases the intracellular concentration of dUTP so that uracil cannot be incorporated into DNA (National Center for Biotechnology Information 2022). This gene is surrounded by ysxA or radC, coaBC, a hypothetical protein and argB. The hypothetical protein, 2837, has gene homology with algC-like genes that enable organic substance metabolic processes, carbohydrate metabolic processes, magnesium ion binding and phosphotransferase activity which are highly linked to biosynthesis of antibiotics (Winsor, Griffiths et al. 2016). This five gene operon is believed to have a key role in motility (Qian, Fei et al. 2019). Meanwhile, 607, the second gene hit within contig 1 in the Tn 56 mutant encodes a hypothetical protein with no annotated homologues (Figure 57B). It can be appreciated that several genes from the same genomic area have no annotated homologues either. The only one that was annotated was 606 and it was identified as a rocR, rpfG, copR or adeR-like protein. All responsible for completely different functions according to what is annotated, from response regulator c-di-GMP phosphodiesterase, heavy metal response regulator or efflux system response regulator transcription factor. However, their specific function within 10A5 is pending to be determined. Gene 610 was annotated as a tyrosine-type recombinase/integrase which rearrange DNA duplexes by means of conservative site-specific recombination reactions (Esposito and Scocca 1997, Lu, Wang et al. 2020). Lastly, Tn 57, from contig 3, had targeted gene 5358, a putative deoxyribonuclease rhs family protein (Figure 57C). This gene was surrounded by both known and unknown proteins, as no gene homologs were found. Known proteins were rhsABCD-like proteins, together with a SMI1/KNR4 family protein.

Finally, 10A5 genome was processed with AntiSMASH for BGC identification. Six BGCs were predicted in contig 1 but none in contigs 2, 3 and 4. None of the predicted BGCs were targeted by the transposon mutagenesis screening (**Figure 58**).

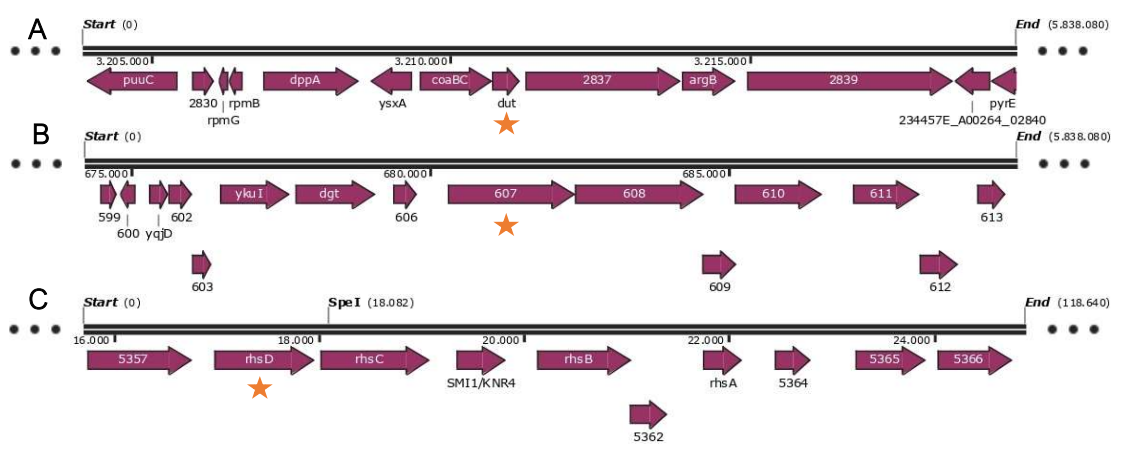


**Figure 57**. Targeted operons by Tn5 in 10A5. A) Gene targeted in Tn 55 was 2836, a dut-like protein, B) Gene targeted in Tn 56 was 607, a hypothetical protein and C) Gene targeted in Tn 57 was 5364, a hypothetical protein. Arrows represent gene organisation and strand direction. Unnamed genes are hypothetical proteins. Arrows at different levels show partial parallel gene overlap. Orange stars next to genes represent transposon insertions.

Region	Type	From	To	Most similar kn	own cluster	Similarity
Region 1.1	terpene 🗹	959,198	982,851	carotenoid 🗹	Terpene	100%
Region 1.2	NRPS 🗗	1,139,266	1,205,175	pyoverdin <b>☑</b> *	NRP	4%
Region 1.3	NAGGN 🗹	1,826,041	1,840,877			
Region 1.4	arylpolyene 🗹	2,852,557	2,896,170	APE Vf Z	Other	40%
Region 1.5	NRPS-like <b>☑</b> *	3,440,391	3,483,843	nematophin 2	NRP	12%
Region 1.6	redox-cofactor	3,729,089	3,751,275	lankacidin C 🗹	NRP + Polyketide	13%

**Figure 58**. Identified secondary metabolite regions in 10A5 using strictness 'relaxed' analysis. Region 1 shows contig 1 while second number of the region is the position within the contig.

# 6.3.2. AntiSMASH analysis for identification of BGCs

To get a greater understanding of the potential NP diversity within the isolated kiwifruit *Pseudomonas* strains, 103 strains were analysed with antiSMASH. From those, 33 strains were *Psa*-inhibitory under *in vitro* conditions and the rest, non-*Psa* inhibitory. The non-*Psa* inhibitory were randomly selected across the 1,056-strain collection. It is worth mentioning that the 33 biocontrol strains were re-sequenced at a higher depth for a better assembly quality and finer AntiSMASH prediction. Sequencing read lengths of 400-450 bp with NovaSeq PE250 significantly reduced the number of contigs for those assemblies

AntiSMASH output was recorded based on NP families with no identity cut off to allow further analysis to identify potential correlation patterns. The output was put together with the maximum likelihood phylogenetic tree and the *Psa*-inhibitory phenotypic data (**Figure 59**). A wide variety of BGCs were predicted across the 103 *Pseudomonas* strains. Most of them were non ribosomal peptide synthetase (NRPS) or hybrid polyketide synthase—non ribosomal peptide synthetase (PKS-NRPS) -like BGCs. For example, poaeamide, a novel lipopeptide rarely produced by some *Pseudomonas* that is involved in pathogen suppression and plant colonisation or viscosin-like lipopeptides that are commonly known for their anti-bacterial and anti-fungal activities (Zachow, Jahanshah et al. 2015, Pacheco-Moreno, Stefanato et al. 2021). Generally, no obvious correlation patterns were found between position in the

phylogenetic tree and inhibitory and non-inhibitory phenotype among the *Pseudomonas* strains. However, certain patterns in BGC content were found in some species clades. For example, certain BGCs for NPs such as siringafactin, syringolin A and syringomycin are more commonly found within the clade of *P. syringae* or terpene-like NPs within the *P. putida* clade. Further analysis revealed high positive correlations (coefficients above 0.2) between *Psa*-inhibitory strains and certain NPs such as pseudomonine, roseoflavin, pyochelin, terpenes, safracin and white line-inducing principles (WLIPs) (Supplementary 17).

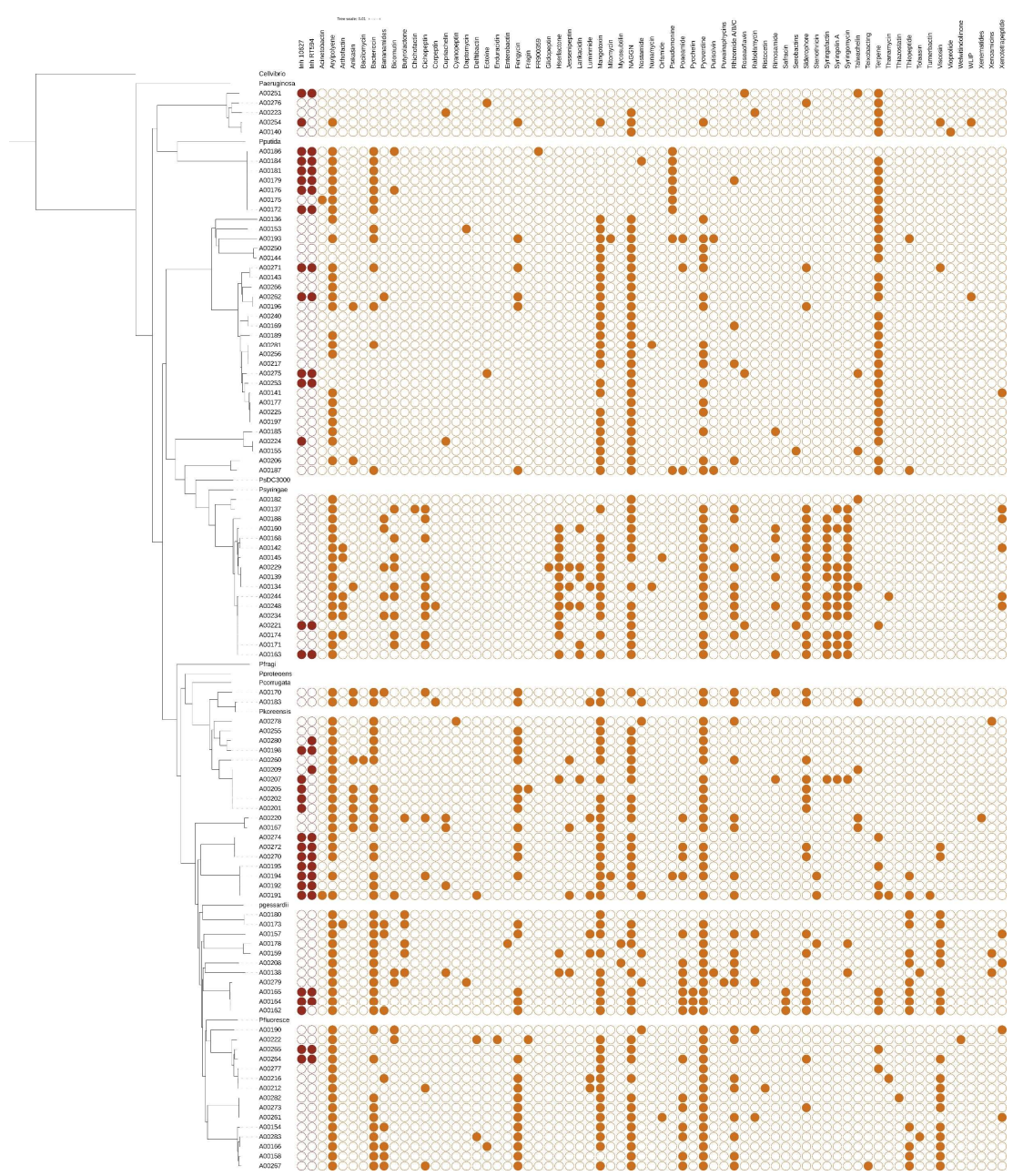


Figure 59. Maximum likelihood phylogenetic analysis combined with AntiSMASH analysis of 33 Psainhibitory Pseudomonas, 70 additional non-Psa inhibitory with reference strains. On the top margin, first two labels belong to the strains' ability to suppress Psa biovar 3 in vitro, together with the main families of NP or BGCs identified. In order, Acinetobactin, Arylpolyene, Arthofactin, Anikasin, Bacilomycin, Bacteriocin, Bananamides, Bicornutin, Butyrolactone, Chichofactin, Cichopeptin, Corpeptin, Cupriachelin, Cyanopeptin, Daptomycin, Delftibactin, Ectoine, Enduracidin, Enterobactin, Fengycin, Fragin, FR900359, Glidopeptin, Hserlactone, Jessenipeptin, Lankacidin, Luminmide, Mangotoxin, Mitomycin, Mycosubtilin, NAGGN, Nostamide, Nunamycin, Orfamide, Pseudomonine, Poaeamide Pyochelin, Pyoverdine, Putisolvin, Puwainaphycins, Rhizomide A/B/C, Roseaoflavin, Ralsolamycin, Ristocetin, Rimosamide, Safracin, Serobactins, Siderophore, Stenothricin, Syringafactin, Syringolin A, Syringomycin, Taiwachelin, Teixobacting, Terpene, Thanamycin, Thiazostatin, Thiopeptide, Tolaasin, Turnerbactin, Viscosin, Vioprolide, Welwitindolinone, WLIP, Xenematides, Xenoamicinsand Xenotetrapeptide. Coloured circles represent presence of the phenotype or NP BGC. No identity cut-off was used.

## 6.4. Discussion

The aim of the work described in this chapter is to determine the biosynthetic origin of the *Psa* suppressor activity observed in our *Pseudomonas* biocontrol isolates. By using transposon mutagenesis techniques and help of bioinformatics, four biocontrol candidates were investigated in this chapter.

In the case of strain 4H12 it was surprising that more than 90% of the selected transposon mutants targeted the same genomic area. The gene organisation and putative gene products of the targeted area strongly indicate that this locus contains a BGC for a secondary metabolite. This is supported by the work of Matuszewska and collaborators who identified the same BGC as responsible for biocontrol activity in P. donghuensis (Matuszewska, Maciąg et al. 2021). Interestingly, this BGC does not belong to any of the traditional classes of NPs and is not detected by genome mining tools such as antiSMASH, highlighting the novelty of the BGC. The conserved domain predictions of the BCG show that some enzymes are loosely related to fatty acid biosynthesis and modification, indicating this might be the substrate of the pathway. Several other enzymes, like oxidoreductases and an amino transferase could be involved in extra modifications, but there are no clear secondary biosynthetic enzymes in the pathway (e.g., NRPS or PKS), pointing to a product closely related to primary metabolites from the cell. The NP produced by this BGC remains uncharacterised, but preliminary analyses of transposon mutants culture extracts compared against 4H12 have shown promising candidate peaks and searches in databases suggest they are novel molecules. Clean knockout mutants would be required to guarantee robust mass spectrometry results without the potential polar effect that transposon mutants may cause as well as to characterise the biosynthesis of this NP. What I have observed from preliminary in planta assays is that the disruption of Cluster 17 has a significant impact on the biocontrol protection that 4H12 confers to plants against Psa. Further repetitions would be required to confirm this is correct. The powerful effect of 4H12 against Psa in vitro and in planta with both model plants and kiwifruit vines and the strong transposon library result suggest that further investigation of this cluster may be a promising opportunity for characterising a novel bioactive NP as well as for market purposes.

On the other hand, analysis of strains 8H7 and 10A5 did not have the same success as transposons targeted several genes quite distanced from each other within their genome. Many of them may not be relevant hits. Off-target hits are something expected to happen and that have been seen in other studies (Moffat, Elliston et al. 2021). Some of them are key genes for metabolism that affect the cell viability but others such as transporters (e.g., Tn 47, an ABC transporter), regulators (e.g., Tn 49, an HTH-type transcriptional regulator) and hypothetical proteins (e.g., genes surrounded by Tn 56) may have a great potential. It could be that they have not been described before or are part of completely novel clusters. A potential experiment would be to carry out LC-MS on extracts and try to identify any clear loss of secondary metabolites. In contrast with 4H12, none of the genes targeted by these transposons were recognised as part of any obvious BGC but does not mean they are not involved in NP biosynthesis in some way. A potential experiment would be to carry out LC-MS on extracts - any clear loss of specialised metabolites? Particularly in strain 10A5 it is striking the high number of targeted genes encoding

hypothetical proteins with no annotated homologs. The fact that these other strains the genes of interest were not targeted more times by the transposons shows that to increase the reliability of these results it would be required to screen more transposon mutants. Another problem in the case of strain 10A5 was the difficulty identifying non-inhibitory isolates in the screening. This could be due to two reasons: One, the potential bioactive BGC is relatively small and is statistically difficult to be targeted by the transposon; Two, the strain is highly complex and gene knockouts make no difference on its biocontrol effect due to having several copies of those key genes or having multiple and varied BGCs that are effective against *Psa*. These issues could partly be addressed by generating larger libraries with higher density of transposon insertion. Despite the challenges, the discovery of Cluster 17 and the high number of uncharacterised genes targeted indicate the potential of transposon mutant libraries to uncover novel biosynthetic diversity. Other examples of this are the discovery of the tropolone BGCs in *Pseudomonas* sp. 652 or thailandene A–C in *Burkholderia thailandensis* (Park, Moon et al. 2020, Moffat, Elliston et al. 2021).

To complement these results, antiSMASH analysis of the isolates genomes was carried out to identify putative BGCs as well as correlations between predicted NPs and inhibitory phenotypes. One of the conclusions obtained was that a wide variety of known and unknown NP potential was found across the 103 *Pseudomonas* strains. Secondly, that none of the BGCs identified by antiSMASH was targeted by any of the transposon mutants described in this chapter. This highlights the unexplored potential that these biocontrol strains have at the metabolic level, increasing the chances for identifying novel BGCs. This data was still of great use for identifying potential correlations between the *Psa*-inhibitory strains and production of potential NPs. Some of the NPs BGCs that were strongly correlated with *Psa*-inhibitory strains were those for pseudomonine, roseoflavin, pyochelin or safracin biosynthesis. All of them are well known types of NPs secreted by *Pseudomonas* spp. that have demonstrated their strong effect against phytopathogens (Lee, Blount et al. 2009, Daura-Pich, Hernández et al. 2020, Tienda, Vida et al. 2020, Kaplan, Musaev et al. 2021). It would be interesting to evaluate whether strains like 10A5 where non-suppressive phenotypes were found to find contain any of these BGCs, supporting one of the hypotheses described above.

Next steps will be to complete the identification of promising BGCs, in particular, Cluster 17, isolate and characterise their products and examine their ability to suppress *Psa* both *in vitro* and *in planta*. On preliminary assays culturing 4H12 alone in liquid media allowed bacteria to produce inhibitory metabolites while not in great amount when co-cultured with *Psa*. *Psa* may reduce this production due to several reasons. Perhaps 4H12 is unable to grow as fast as *Psa* in liquid media or does not grow as quick in solid than in liquid media, or inhibitory metabolites are not produced quickly enough to stop *Psa* growing. It also needs to be considered the CFU/mL on *in vitro* biocontrol assays. In solid media, plates are inoculated with a water overlay of *Psa* at 0.01 (OD<sub>600</sub>) against an undiluted drop of overnight culture of the biocontrol strain while in liquid media, co-cultures are inoculated with the same bacterial concentration and volume of both pathogen and biocontrol strain. Additionally, it would be of great use

carrying out heterologous expression of the BGCs in host bacteria and producing clean knockout mutants in the native strains, to help characterise the biosynthesis of any novel molecules.

The results in this chapter show that the combination of bioinformatics and molecular microbiology tools such as transposon mutant libraries complement each other very well and allow us to explore novel NP diversity and promising biocontrol candidates.

# CHAPTER 7

GENERAL DISCUSSION AND FUTURE PERSPECTIVES

# 7. GENERAL DISCUSSION AND FUTURE PERSPECTIVES

Twelve years after its identification, *Psa* biovar 3 remains as the major threat for the kiwifruit industry in New Zealand. Millions of pounds of profits are lost every year due to yield loss and disease prevention, when considering the expensive costs associated with spraying agrochemicals to contain *Psa*. Not to mention the environmental risks associated with copper and antibiotic use. Continuous use of these compounds might contribute to the appearance of new pesticide resistant bacteria. Not only *Psa* but other phytopathogens that can infect kiwifruit, putting at risk the national kiwifruit industry if current treatments become ineffective. Therefore, there is an urgent need for effective and environmentally friendly treatment options to control *Psa* on New Zealand's kiwifruit. In this thesis, I have interrogated representative naturally occurring *Pseudomonas* from New Zealand kiwifruit orchards, identified *Pseudomonas* strains that can effectively prevent *Psa* infection on kiwifruit and unlocked some of the genomic intricacies, such as previously uncharacterised BGCs that allow biocontrol kiwifruit *Pseudomonas* strains to control *Psa*.

# 7.1. Marked differences exist between strains' phenotypic profiles and orchard's locations

One of the particularities of this thesis is the high number of *Pseudomonas* strains characterised. Many academic research studies in the field of biocontrol employ low-throughput methods, often failing to unveil the full potential of plant microbiomes. For this thesis, with the isolation of over 6,000 strains and the characterisation of over 1,000 naturally occurring kiwifruit *Pseudomonas* strains from infected and uninfected orchards, a more modern commercial approach was achieved while using high-throughput screenings. Similarly, academic, and commercial approaches often fail at providing reliable BCAs. Often, BCAs are expected to be effective against several phytopathogens, under completely different environments and hosts from which they were isolated from. Here, bacteria were sampled from infected plants to enable effective colonisation and survival in the infected plant environment so their biocontrol performance can be optimum.

The characterisation of strains across the country from infected and non-infected kiwifruit orchards, allowed identifying highly effective strains against *Psa* and to understand that the presence of the pathogen shapes and conditions the development of the kiwifruit *Pseudomonas* epiphytic microbiome, due to selection pressures. No strong *Psa*-inhibitory isolates were found in Motueka, South Island, but in the North Island, where *Psa* was present. Furthermore, a significantly higher frequency of isolates from North Island were phenotypically more complex. They had a phenotypic profile associated with BCAs such as protease activity, HCN production or swarming motility (Ghods, Sims et al. 2015, Czajkowski, Maciag et al. 2020, Moffat, Elliston et al. 2021). Interestingly, when *in vitro* phenotypic results were analysed, a high positive correlation coefficient of 0.95 was found between isolates resistant to copper compounds and streptomycin. This co-occurrence and high correlation between copper and streptomycin resistant strains is likely due to a genetic linkage, mediated by MGEs (Colombi, Straub et al. 2017). Something that will be presented in further detail in the next section.

Next, over 100 *Psa*-inhibitory, non-*Psa* inhibitory and copper and streptomycin resistant *Pseudomonas* strains were selected for whole genome sequencing. Phylogenetic analysis of the sequenced *Pseudomonas* strain phylogenetic tree showed no strong clustering between strains across orchards. Most strains were evenly distributed across the sampled New Zealand orchards, except for Te Puke and Motueka samples that showed mild clustering. Strains from these last two orchards were mainly distributed within specific phylogenetic clades and nearly absent from the rest of the phylogenetic tree, highlighting the differences at evolutionary level between locations and exposure to *Psa*.

## 7.2. Published copper and streptomycin resistant genes are missing from most copper and streptomycin resistant *Pseudomonas* strains

Copper and streptomycin use within kiwifruit orchards is an extensive practice since *Psa* was detected in New Zealand. However, these treatments are environmentally damaging and in its due time their consequences may become self-evident. Copper and streptomycin resistance *in vitro* proved to be strongly positively correlated, despite no corresponding clustering at the genome level, foreseeing the presence of resistance-conferring MGEs across the *Pseudomonas* population. Presence of novel MGEs across the *Pseudomonas* strain population might mean these genetic elements could be transferred to *Psa* making current treatments ineffective.

Bioinformatic analysis revealed that *copABCD* genes tend to be missing from most copper resistant strains with *copAB* being the most common absent operon across copper resistant *Pseudomonas* strains. Similarly, some streptomycin resistant strains did not have *strAB*, suggesting that additional and not yet identified copper resistant genes may be conferring the copper and streptomycin resistance to these studied strains. To elucidate these hypothesised novel mechanisms for copper and streptomycin resistance, transposon mutagenesis was carried out. It was expected to target several times the same gene/s but instead, identified genes were targeted only once and were never observed as to be linked with copper and/or streptomycin resistance. This finding increases the potential of these genes to be novel resistant genes among *Pseudomonas* strains but simultaneously highlights the need of increasing the number of screened mutants to guarantee the robustness of the results. Some of the genes identified were known to be heavy metal efflux pumps. Potentially, these pumps may have a dual activity as described previously in Gram negative multi-drug resistant bacteria (Nikaido and Pagès 2012). Next, to verify the link of these potentially novel genes with copper resistance, more transposon mutants should be screened, and produce knockout mutants on those genes that are targeted the most.

Screening of transposon mutants has helped us understand better the deep genetic complexity of copper and streptomycin resistance. Future work to confirm the presence of MGEs like plasmids across the population could involve high-throughput, fast and cheap plasmid sequencing methods (e.g., Plasmidsaurus (<a href="www.plasmidsaurus.com">www.plasmidsaurus.com</a>)) and to confirm the potential duality of efflux pumps targeted by the transposon mutagenesis. Additionally, once the presence of novel MGEs that confer resistance has been confirmed, monitoring the spread of these in the environment could be conducted using

specifically designed primers. Similarly, kasugamycin is widely used within kiwifruit orchards. Kasugamycin-resistant *Pseudomonas* strains were identified across the collection; phenotypic clustering and high correlation between copper, streptomycin and kasugamycin resistance was identified. However, kasugamycin resistance mechanism/s remain unknown and kasugamycin-resistant *Psa* strains have never been identified. Further work is required to understand kasugamycin resistance and if may be conferred by MGEs. Exposure of *Psa* to a high frequency of kasugamycin-resistant isolates might lead to resistance. Transposon mutagenesis could be used to understand kasugamycin resistance idiosyncrasy, to develop in-field detection tools and to monitor the progress of kasugamycin-resistant strains across the kiwifruit orchards.

## 7.3. Pseudomonas strains strongly suppress Psa biovar 3 infection in planta

*Psa* biovar 3 remains as a problem for the kiwifruit industry in New Zealand. With the arising bacterial resistances that are increasing the chances of surging new *Psa* resistant variants, and the increasing population that is demanding organic products, it is critical that more effective, and environmentally friendly alternatives are provided to kiwifruit growers against *Psa*.

First, pathogenicity assays were carried out on tomato plants with 33 biocontrol candidates. This assay helped identify one third of the candidates as plant pathogenic. Then, *in planta* biocontrol experiments were carried out with 22 biocontrol candidates on tomato plants, resulting in the identification of up to four strong biocontrol candidates. Finally, *in planta* biocontrol experiments were carried out with 3 biocontrol candidates on kiwifruit. From the three *Pseudomonas* candidates, 5G9 was the best performing isolate, performing in most cases better than Aureo®Gold —the commercially available BCA against *Psa*—. Lastly, treatments were combined with Actigard®, to identify potential synergies. Positively, all treatments containing Actigard® had as much infection as the untreated or water control.

Biocontrol experiments on kiwifruit proved that a selection of naturally occurring kiwifruit *Pseudomonas* strains can strongly suppress *Psa* biovar 3 infection *in planta*, as well as Aureo®Gold. Further work would require repeating these experiments during New Zealand's Summer to achieve more consistent infections across control treatments. Then, it would be interesting to know if a bacterial consortia has the potential to raise the efficiency of the biocontrol strains against *Psa* as proved in several studies with other microbes and crops (Minchev, Kostenko et al. 2021, Mukherjee, Chouhan et al. 2021). Challenges of these approach involve, for example, potential antagonism between biocontrol strains. Other aspect worth studying is the *in-planta* establishment of these biocontrol strains. How may these strains perform against *Psa* when sprayed over vines that have an already stablished microbiome? Some of the most expensive agronomic costs are associated with frequency of spraying and costs of agrochemicals (Bourguet and Guillemaud 2016). It would be compelling to test in field trials how long these BCAs can provide protection against *Psa* on kiwifruit. Another benefit of a microbial consortia is that can be patented while native microorganisms on their own not. However, it should be considered that there are

circumstances that might derail these experiments such as weather heterogenicity, soil composition, performance on different kiwifruit varieties, and formulation challenges among others.

## 7.4. Kiwifruit Pseudomonas harbour a high diversity of NPs and biocontrol potential

New Zealand is an underexplored ecosystem from the antimicrobial point of view and harbours a huge potential for novel metabolite discovery (Tangestani, Broady et al. 2021). Kiwifruit *Pseudomonas* strains, also underexplored, might contain novel mechanisms that can help to fight back *Psa*. To unlock that potential, transposon mutagenesis techniques, combined with automated tools for BGCs identification, were used against more than a hundred *Pseudomonas* strains. Recent and promising advances in gene mining are unlocking the biosynthetic strains potential (Hannigan, Prihoda et al. 2019). Whole genome sequencing of 103 *Pseudomonas* strains at high depth combined with antiSMASH bioinformatic analysis led to the prediction of hundreds of BGCs that may produce novel anti-*Psa* chemicals. In parallel, transposon mutagenesis screenings were carried out resulting in the identification of novel genes that might be linked to *Psa* biocontrol, several of which were undetected by antiSMASH. With these results, the great potential of kiwifruit *Pseudomonas* bacteria for identifying novel BGCs has been unveiled.

The most striking result was that of 4H12. Most biocontrol-abolishing transposons targeted the same operon, resulting in the identification of a potential novel BGC, provisionally named as Cluster 17 in recent publications (Matuszewska, Maciąg et al. 2021). This BGC does not belong to any of the traditional known classes of NPs and is not detected by antiSMASH 6.0, highlighting its novelty. The metabolite that it produces remains unknown. Preliminary LC-MS analysis with a transposon mutant shows promising candidate peaks, and searches in databases suggest it is a novel molecule. Deletion knockout mutants would be required to confirm that what is observed is not product of polar effects. Polar effects due to transposon insertions in BGCs can affect the expression of adjacent genes, compromising the production of NPs. Something that is detrimental for mass-spectrometry analysis.

In planta preliminary experiments with model plants demonstrated that the disruption of Cluster 17 has a significant detrimental effect on the ability to protect the host against *Psa*. Other transposon targeted strains did not share the same fate. 5G9, 8H7 and 10A5 had several transposon insertions across their genomes, making it difficult to draw robust conclusions. This could have happened, for example, due to the presence of relatively small BGC and therefore are statistically more unlikely to be targeted. Another challenge associated with transposon screening of biocontrol bacteria is when they have multiple BGCs and despite having a disrupted BGC, still can provide biocontrol *in vitro* against the model pathogen, difficulting the identification of candidates. Screening bacteria with multiple BGCs against *Psa* can make it challenging for this strategy to work effectively. In general, even targeting genes that have not been described yet as part of BGCs, increases the probability of them being novel BGC genes.

Additionally, correlations between the traits of *Psa*-inhibitory strains and antiSMASH output data were explored. NPs such as pseudomonine, roseoflavin, pyochelin or safracin were positively linked to *Psa*-

inhibitory *Pseudomonas*. Next, it would be desirable, for the continuation of this research, to characterise and examine the impact of key NPs such as the one that might produce Cluster 17 and elaborating and testing deletion mutants in BGCs to prove the role of Cluster 17 in controlling *Psa in planta*. Simultaneously, it would be ideal to perform heterologous expression of Cluster 17 in host bacteria such as *Pseudomonas putida* KT2440 to isolate, overproduce and test the role of the NP produced *in planta* (Ankenbauer, Schäfer et al. 2020).

## 7.5. Final remarks, industrial applications, and future directions

Characterising and sequencing a representative number of *Pseudomonas* strains has helped to successfully identify phenotypic traces linked to biocontrol against *Psa*, to build phenotypic profiles based on location or exposure to *Psa*, and to identify resistances to agrochemicals across the natural occurring bacterial population of kiwifruit. As a result, effective BCAs against *Psa* have been identified, proving the success of this strategy. However, the use of robotics during phenotype and transposon mutant screening could have speeded up the early stages of the biocontrol process allowing more time working on compound discovery.

There is a remarkable industrial potential if these discoveries are further researched. Novel NPs can be patented and there are more than 11,600 hectares of kiwifruit in New Zealand that can benefit from novel and highly effective *Psa*-protectant treatments. But field trials, as well as additional laboratory assays, would be required. Similarly, knowing that antibiotic resistant *Pseudomonas* strains are emerging, providing primers for monitoring, and evaluating their development would be a highly useful tool for the future and success of the economically powerful New Zealand kiwifruit industry. Additionally, it could be explored if these BCAs alone or as consortia are able to protect other cash crops (e.g., wine grapes) and against other economically relevant diseases (e.g., *Fusarium* spp.) for a higher patent profitability.

Further down the line, it would be interesting to explore the potential use of the NPs produced by these BCAs in other industries such as the pharmaceutical. For example, some of the antibiotics used as anti-tumour drugs are produced by *Pseudomonas* spp. (e.g., exotoxin A for pancreatic cancer or azurin for breast cancer) (Karpiński and Adamczak 2018).



Supplementary 1. List of primers used for genetic manipulations, arbitrary PCR, and sequencing.

Oligos name	Primer sequence	Length	Target
Arb 1b	GGCCAGCGAGCTAACGAGACNN NNGATAT	29	Random PCR - Tn5/ <i>pAMLAR3</i>
Arb 1	GGCCAGCGAGCTAACGAGAC	20	Random PCR - Tn5/ <i>pAMLAR3</i>
ALMAR3-seq	ACATATCCATCGCGTCCGCC	20	Random PCR - pAMLAR3
ALMAR3-PCR	CGCAAACCAACCCTTGGCAG	20	Random PCR - pAMLAR3
16S Amplicon PCR fwd	TCGTCGGCAGCGTCAGATGTGTA TAAGAGACAGCCTACGGGNGGC WGCAG	55	16s rRNA
16S Amplicon PCR rev	GTCTCGTGGGCTCGGAGATGTGT ATAAGAGACAGGACTACHVGGGT ATCTAATCC	50	16s rRNA
Tn5 Ext	GAACTGCCTCGGTGAGTTT	19	For random PCR - Tn5
Tn5 seq	CCACCTACAACAAGCTCTCAT	22	For random PCR - Tn5
up02732_fwd	AGTCGACCTGCAGGCATGCAGCA GACGGGTGGCGCGCT	38	Target: isolate genomic regions from 4H12
up02732_rev	TAGAAAAGATCCACAGGGCGTTG CCGTTGG	30	Target: isolate genomic regions from 4H13
KAN32-38_fwd	CGCCCTGTGGATCTTTTCTACGG GGTCTGACG	32	Target: isolate genomic regions from 4H14
KAN32-38_rev	AGCGACCTTCAAATGTGCGCGGA ACCCC	28	Target: isolate genomic regions from 4H15
DOWN02738_fwd	GCGCACATTTGAAGGTCGCTTCC TGCGC	28	Target: isolate genomic regions from 4H16
DOWN02738_rev	GACCAATTGACTACCTAGGACCC TCAATCTGCTGCGCC	28	Target: isolate genomic regions from 4H17
UPpatA_fwd	AGTCGACCTGCAGGCATGCACGA GCGCTGTGCGTGCGC	28	Target: isolate genomic regions from 4H18
UPpatA_rev	TAGAAAAGATACACTGGAGTCAC CATGAAACAAGTCAGC	39	Target: isolate genomic regions from 4H19
KANpatA_fwd	ACTCCAGTGTATCTTTTCTACGGG GTCTGACG	32	Target: isolate genomic regions from 4H20
KANpatA_rev	AATCAGGCGCAAATGTGCGCGGA ACCC	28	Target: isolate genomic regions from 4H21
DOWNpatA_fwd	GCGCACATTTGCGCCTGATTCATT GCA	28	Target: isolate genomic regions from 4H22
DOWNpatA_rev	GACCAATTGACTACCTAGGACGA TAACGGTCATGTCGAC	39	Target: isolate genomic regions from 4H23
PsaF1	TTTTGCTTTGCACACCCGATTTT	23	Psa identification
PsaR2	CACGCACCCTTCAATCAGGATG	22	Psa identification
Apal_rev	AGCGGGCCCTCGGGGAAATGTG CGCGGAACCC	32	pTS1. Gene deletion. Rev primer for pTS1 Apal restriction enzime
4H12typA_fwd	TAGCACCTCTCGAGGCATCATGC CAGGGCTGTATGGCG	38	P. putida NZ4H12
4H12emrA_rev	CCAAAGACAAGCTCATCAAGCTG ACAC	27	P. putida NZ4H12
4H12emrA_fwd	GTGTCAGCTTGATGAGCTTGTCTT TGG	27	P. putida NZ4H12
4H122738_rev	CACGCTCTCCAGCGAGCTCTCGT CTTGTAGCAAAAATGCAGCC	43	P. putida NZ4H12

pBBRtypA_fwd	GCTGGGTACCGGGCCCCCCCCCCCCCCCCCCCCCCCCCC	43	P. putida NZ4H12
pBBR2738_rev	CCACCGCGGTGGCGGCCGCTCT AGACGTCTTGTAGCAAAAATGCAG CC	48	P. putida NZ4H12
GApBBR2_fwd	GTCCTGGCCAGCGGCCACGCGC AAGG	27	PCR check C17 cloning 2 segments
GApBBR2_rev	GCGACATGGTCGACAACGCCCG CACTGCG	30	PCR check C17 cloning 2 segments

Kasuga														1.00
Strepto													1.00	0.54
CuSO4												1.00	0.94	0.53
Protease Congo R Inh scabies Inh venez Inh Psa Inh Psa Cu CuSO4											1.00	0.03	0.03	0.06
Inh Psa										1.00	0.44	0.05	0.03	-0.03
Inh venez									1.00	90.0	-0.05	0.01	-0.01	-0.03
Inh scabies								1.00	0.05	90.0	-0.08	0.13	0.10	0.04
Congo R							1.00	-0.10	90.0	0.07	0.09	-0.11	-0.12	-0.09
Protease						1.00	-0.07	0.65	0.05	0.11	00.00	0.13	0.08	0.03
Motility					1.00	0.23	0.01	0.31	0.19	0.31	0.01	0.22	0.21	0.15
HCN				1.00	00.0	00.0	0.00	00.0	0.00	00.0	0.00	00.0	0.00	0.00
ΛΠ			1.00	00.00	0.11	0.18	0.05	0.16	0.01	-0.03	-0.12	0.03	0.01	0.05
Colour		1.00	-0.03	0.00	-0.12	-0.26	-0.04	-0.34	0.16	-0.15	-0.17	-0.16	-0.19	-0.10
Inf sample Colour UV	1.00	00.00	00.0	00.00	00.00	00.00	00.00	00.00	0.00	00.00	00.0	00.00	0.00	0.00
	Inf sample	Colour	>	HCN	Motility	Protease	Congo R	Inh scabies	Inh venez	Inh Psa	Inh Psa Cu	CuSO4	Strepto	Kasuga

0.00

Supplementary 2. Correlation analysis with all phenotypic assays from Moteka. In order, margins abbreviations are infected sample, colour, UV or siderophore production, HCN production, swarming motility, protease production, Congo Red binding, S. scabies, S. venezuelae, Psa (10627) and Psa (RT594) inhibition and copper sulphate, streptomycin and kasugamycin resistance. Values between -1 and 1 indicate negative and positive correlations (Pearson's correlation coefficient).

Kasuga														1.00
Strepto													1.00	0.63
CuSO4												1.00	0.93	09.0
Inh Psa Cu											1.00	0.53	0.53	0.17
Protease Congo R Inh scabies Inh venez Inh Psa Inh Psa Cu CuSO4										1.00	0.83	0.39	0.39	0.08
Inh venez									1.00	0.33	0.26	0.29	0.26	0.02
nh scabies								1.00	0.38	0.13	0.15	0.35	0.30	0.07
Congo R							1.00	0.03	0.04	0.11	0.08	0.05	-0.08	-0.08
Protease						1.00	0.09	0.39	0.29	0.07	-0.02	0.10	90.0	0.03
Motility					1.00	0.16	0.02	0.33	0.26	0.22	0.24	0.41	0.42	0.11
HCN				1.00	0.11	-0.02	90.0-	0.10	0.05	0.07	0.15	0.33	0.34	0.46
ΛN			1.00	0.09	0.02	0.27	0.15	0.25	0.08	0.03	0.07	0.14	0.11	0.05
Colour		1.00	-0.43	-0.09	-0.19	-0.11	0.02	-0.15	-0.11	-0.04	0.01	-0.03	-0.03	-0.08
Inf sample Colour	1.00	-0.11	0.04	-0.06	-0.16	0.05	0.23	-0.21	-0.04	0.01	-0.10	-0.23	-0.29	-0.13
	Inf sample	Colour	>	HCN	Motility	Protease	Congo R	Inh scabies	Inh venez	Inh Psa	Inh Psa Cu	CuSO4	Strepto	Kasuga

0.00

Supplementary 3. Correlation analysis with all phenotypic assays from Kaimai. In order, margins abbreviations are infected sample, colour, UV or siderophore production, HCN production, swarming motility, protease production, Congo Red binding, S. scabies, S. venezuelae, Psa (10627) and Psa (RT594) inhibition and copper sulphate, streptomycin and kasugamycin resistance. Values between -1 and 1 indicate negative and positive correlations (Pearson's correlation coefficient).

Kasuga														1.00
Strepto													1.00	0.26
CuSO4												1.00	0.89	0.32
Protease Congo R Inh scabies Inh venez Inh Psa Inh Psa Cu CuSO4											1.00	0.42	0.40	0.18
Inh Psa										1.00	0.47	0.48	0.43	0.17
Inh venez									1.00	0.16	0.17	0.48	0.48	-0.04
nh scabies								1.00	0.56	90.0	0.01	0.33	0.37	0.01
Congo R I							1.00	-0.05	-0.04	0.08	0.00	-0.03	-0.03	0.05
Protease						1.00	0.04	0.50	0.53	0.16	0.22	0.40	0.40	-0.07
Motility					1.00	0.46	0.07	0.25	0.34	0.33	0.29	0.50	0.49	0.14
HCN				1.00	0.22	0.08	-0.04	0.12	0.16	0.12	0.07	0.14	0.16	-0.03
ΛN			1.00	0.13	0.10	0.29	-0.04	0.50	0.33	90.0	-0.07	0.29	0.26	-0.12
Colour		1.00	-0.38	-0.05	-0.18	-0.11	0.03	-0.31	-0.23	-0.16	-0.12	-0.24	-0.25	-0.28
Inf sample Colour	1.00	-0.16	-0.14	90.0-	0.00	-0.07	0.08	-0.06	-0.15	0.12	0.09	-0.06	-0.05	0.22
	Inf sample	Colour	>	HCN	Motility	Protease	Congo R	Inh scabies	Inh venez	Inh Psa	Inh Psa Cu	CuSO4	Strepto	Kasuga

0.00

Supplementary 4. Correlation analysis with all phenotypic assays from Ohaupo. In order, margins abbreviations are infected sample, colour, UV or siderophore production, HCN production, swarming motility, protease production, Congo Red binding, S. scabies, S. venezuelae, Psa (10627) and Psa (RT594) inhibition and copper sulphate, streptomycin and kasugamycin resistance. Values between -1 and 1 indicate negative and positive correlations (Pearson's correlation coefficient).

Kasuga														1.00
Strepto													1.00	0.42
CuSO4												1.00	0.93	0.42
Protease Congo R Inh scabies Inh venez Inh Psa Inh Psa Cu CuSO4											1.00	0.28	0.29	0.26
Inh Psa										1.00	0.52	0.11	0.14	0.13
Inh venez									1.00	0.07	0.35	0.42	0.37	0.32
nh scabies								1.00	0.55	0.13	0.31	0.49	0.47	0.33
Congo R I							1.00	-0.15	-0.02	-0.12	-0.06	-0.04	-0.03	-0.09
Protease						1.00	-0.19	0.51	0.36	0.11	0.18	0.45	0.38	0.32
Motility					1.00	0.22	-0.04	0.45	0.41	0.12	0.37	0.37	0.39	0.21
HCN				1.00	0.23	-0.03	-0.06	0.16	-0.04	-0.05	0.05	0.21	0.24	0.10
$\geq$			1.00	0.18	-0.01	0.00	-0.02	90.0	-0.05	60.0	0.00	-0.06	-0.07	0.01
Colour		1.00	-0.18	-0.31	-0.19	-0.23	0.03	-0.29	-0.24	-0.11	-0.17	-0.33	-0.29	-0.31
Inf sample Colour	1.00	0.18	-0.04	-0.21	-0.03	-0.12	-0.04	-0.14	-0.07	90.0	0.01	-0.13	-0.06	-0.03
	Inf sample	Colour	2	HCN	Motility	Protease	Congo R	Inh scabies	Inh venez	Inh Psa	Inh Psa Cu	CuSO4	Strepto	Kasuga

0.00

Supplementary 5. Correlation analysis with all phenotypic assays from Te Puke. In order, margins abbreviations are infected sample, colour, UV or siderophore production, HCN production, swarming motility, protease production, Congo Red binding, S. scabies, S. venezuelae, Psa (10627) and Psa (RT594) inhibition and copper sulphate, streptomycin and kasugamycin resistance. Values between -1 and 1 indicate negative and positive correlations (Pearson's correlation coefficient).

Kasuga															1.00
Motility Protease Congo R Inh scabies Inh venez Inh Psa Inh Psa Cu CuSO4 Strepto														1.00	0.16
CuSO4													1.00	0.88	0.18
Inh Psa Cu												1.00	0.14	0.10	0.18
Inh Psa											1.00	0.62	0.16	0.10	0.15
Inh venez										1.00	0.07	0.07	0.36	0.30	-0.03
Inh scabies									1.00	0.45	0.00	0.05	0.41	0.39	-0.01
Congo R								1.00	-0.02	0.03	0.05	0.03	0.07	0.03	-0.03
Protease							1.00	0.05	0.35	0.34	0.15	0.13	0.37	0.30	0.08
Motility						1.00	0.17	0.04	0.39	0.33	-0.01	-0.05	0.43	0.45	0.01
HCN					1.00	0.27	-0.04	0.01	0.23	0.07	-0.01	-0.04	0.20	0.22	0.09
N				1.00	0.09	0.07	0.20	0.02	0.19	0.08	0.02	0.00	0.14	0.10	-0.06
Colour			1.00	-0.32	-0.12	-0.10	-0.17	0.01	-0.16	-0.13	-0.05	-0.10	-0.13	-0.11	-0.14
Inf orchardInf sample Colour		1.00	-0.03	-0.04	-0.12	-0.07	-0.04	90.0	-0.10	-0.05	0.08	0.05	-0.06	-0.05	0.05
Inf orchard	1.00	0.00	00.00	0.00	00.00	0.00	00.00	00.00	0.00	00.00	00.00	00.00	00.00	0.00	0.00
	Inf orchard	Inf sample	Colour	3	HCN	Motility	Protease	Congo R	Inh scabies	Inh venez	Inh Psa	Inh Psa Cu	5H20	Strepto	Kasuga

0.00

**Supplementary 6**. Correlation analysis with all phenotypic assays from the infected orchards (Te Puke, Kaimai and Ohaupo). In order, margins abbreviations are infected orchard, infected sample, colour, UV or siderophore production, HCN production, swarming motility, protease production, Congo Red binding, S. scabies, S. venezuelae, Psa (10627) and Psa (RT594) inhibition and copper sulphate, streptomycin and kasugamycin resistance. Values between -1 and 1 indicate negative and positive correlations (Pearson's correlation coefficient).

Kasuga													1.00
Protease Congo R Inh scabies Inh venez Inh Psa Inh Psa Cu CuSO4 Strepto Kasuga												1.00	0.51
CuSO4											1.00	0.95	0.52
Inh Psa Cu										1.00	0.43	0.41	0.27
Inh Psa									1.00	0.63	0.21	0.17	0.22
Inh venez								1.00	0.15	0.38	0.47	0.48	0.22
Inh scabies							1.00	0.53	90.0	0.25	0.42	0.40	0.18
Congo R						1.00	-0.01	-0.02	0.01	0.03	-0.01	-0.03	0.00
Protease					1.00	-0.01	0.54	0.50	0.13	0.29	0.43	0.41	0.14
Motility				1.00	0.43	-0.03	0.44	0.46	0.14	0.32	0.52	0.53	0.25
HCN			1.00	0.15	0.04	-0.06	0.01	-0.02	-0.07	0.07	0.28	0.29	0.14
ΛN		1.00	0.19	0.11	0.28	00.00	0.27	0.13	-0.08	0.03	0.13	0.11	-0.04
Colour	1.00	-0.31	-0.14	-0.12	-0.16	0.09	-0.21	-0.18	-0.10	-0.05	-0.06	-0.05	-0.18
	Colour	<b>&gt;</b>	NOH	Motility	Protease	Congo R	Inh scabies	Inh venez	Inh Psa	Inh Psa Cu	CuSO4	Strepto	Kasuga

0.00

Supplementary 7. Correlation analysis with all phenotypic assays from visually infected samples. In order, margins abbreviations are infected sample, colour, UV or siderophore production, HCN production, swarming motility, protease production, Congo Red binding, S. scabies, S. venezuelae, Psa (10627) and Psa (RT594) inhibition and copper sulphate, streptomycin and kasugamycin resistance. Values between -1 and 1 indicate negative and positive correlations (Pearson's correlation coefficient).

Kasuga														1.00
Strepto													1.00	0.45
CuSO4												1.00	0.95	0.46
nh Psa Cu										1.00		0.32	0.32	0.19
Inh Psa									1.00	0.44		0.13	0.13	0.02
Inh venez								1.00	90.0	0.18		0.46	0.41	0.16
Protease Congo R Inh scabies Inh venez Inh Psa Inh Psa Cu CuSO4							1.00	0.52	-0.03	0.08		0.48	0.48	0.18
Congo R						1.00	-0.07	0.07	90.0	0.00		0.14	0.11	0.05
Protease (					1.00	0.04	0.45	0.37	-0.01	0.00		0.40	0.36	0.17
Motility				1.00	0.23	0.10	0.39	0.37	0.12	0.30		0.49	0.50	0.23
HCN			1.00	0.33	0.08	0.01	0.26	0.10	0.00	0.10		0.35	0.37	0.23
N		1.00	0.18	90.0	0.15	0.05	0.31	0.12	0.03	-0.03		0.20	0.18	0.02
Colour	1.00	-0.34	-0.23	-0.22	-0.12	-0.01	-0.30	-0.20	-0.05	-0.13		-0.26	-0.25	-0.23
	Colour	>	HCN	Motility	Protease	Congo R	Inh scabies	Inh venez	Inh Psa	Inh Psa Cu	CuSO4	5H20	Strepto	Kasuga

0.50 0.00 -0.50

sample, colour, UV or siderophore production, HCN production, swarming motility, protease production, Congo Red binding, S. scables, S. venezuelae, Psa (10627) and Psa (RT594) inhibition and copper sulphate, streptomycin and kasugamycin resistance. Values between -1 and 1 indicate negative and positive correlations (Pearson's correlation coefficient). Supplementary 8. Correlation analysis with all phenotypic assays from visually healthy samples from infected orchards. In order, margins abbreviations are infected

Kasuga													1.00
Strepto												1.00	0.36
CuSO4											1.00	0.79	0.47
Protease Congo R Inh scabies Inh venez CuSO4										1.00	0.45	0.40	0.15
Inh scabies									1.00	0.94	0.61	0.54	0.20
Congo R I								1.00	00.00	90.0	00.0	-0.16	-0.04
Protease							1.00	0.01	0.76	0.71	0.63	0.49	0.39
Motility						1.00	0.64	0.04	0.57	0.54	0.55	0.51	0.16
HCN					1.00	0.27	0.10	-0.09	0.20	0.19	0.10	0.13	-0.11
N				1.00	0.18	0.27	0.19	0.09	0.45	0.39	0.39	0.29	-0.22
Colour			1.00	-0.28	-0.08	-0.26	-0.23	0.03	-0.17	-0.19	-0.31	-0.34	-0.20
Inf sample		1.00	-0.01	-0.12	-0.19	0.05	0.27	0.14	0.14	0.07	0.08	90.0	0.28
Inforchard Infsample Colour	1.00	0.00	0.00	0.00	0.00	0.00	0.00	0.00	0.00	0.00	0.00	0.00	0.00
	Inf orchard	Inf sample	Colour	2	HCN	Motility	Protease	Congo R	Inh scabies	Inh venez	CuSO4	Strepto	Kasuga

0.00

Supplementary 9. Correlation analysis with all phenotypic assays from Psa-inhibitory strains. In order, margins abbreviations are infected sample, colour, UV or siderophore production, HCN production, swarming motility, protease production, Congo Red binding, S. scabies, S. venezuelae, Psa (10627) and Psa (RT594) inhibition and copper sulphate, streptomycin and kasugamycin resistance. Values between -1 and 1 indicate negative and positive correlations (Pearson's correlation coefficient).

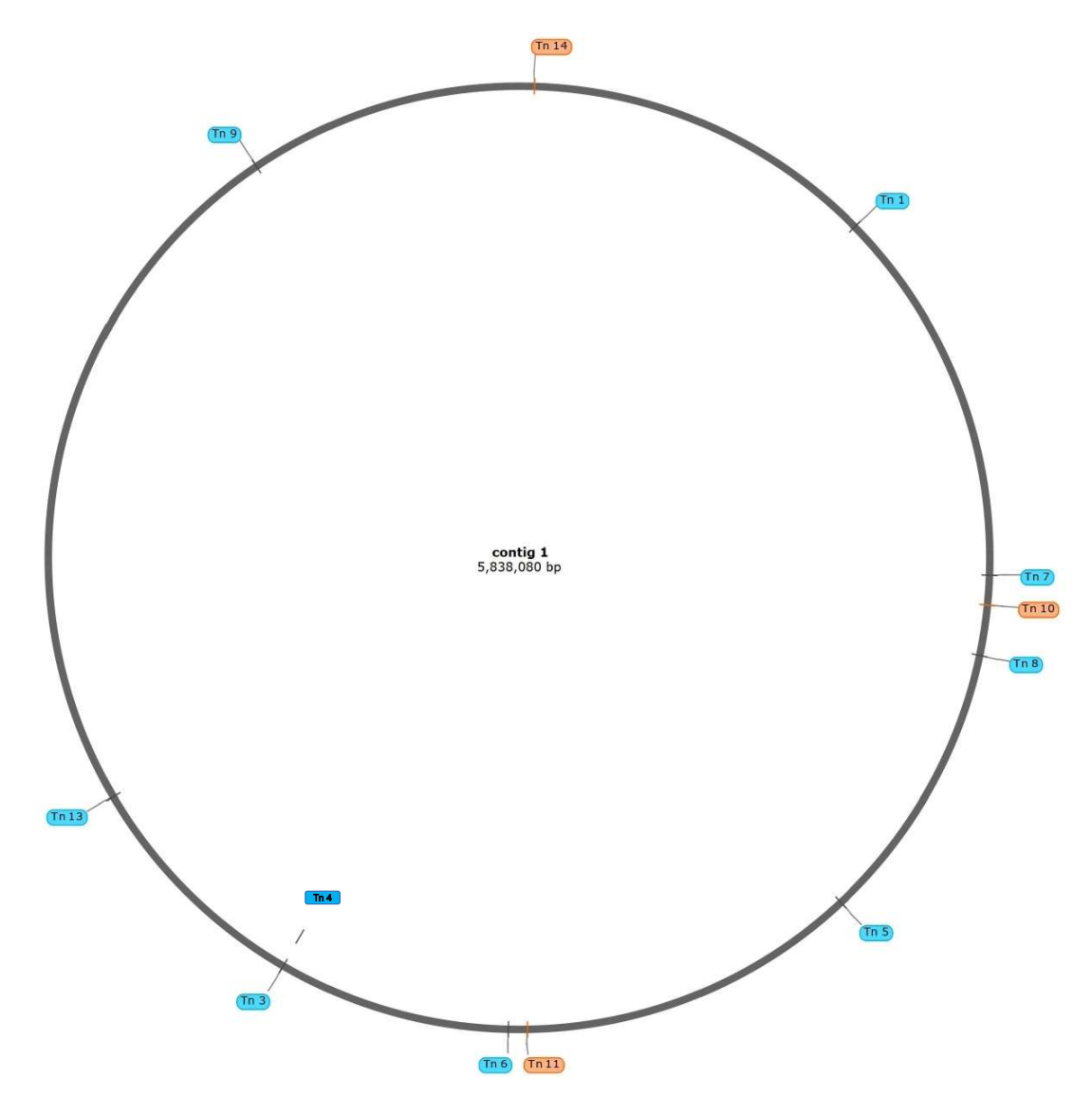
Kasuga													1.00
Strepto												1.00	0.49
CuSO4											1.00	0.95	0.49
Inh venez										1.00	0.39	0.36	0.14
nh scabies									1.00	0.47	0.40	0.38	0.15
Congo R I								1.00	-0.03	0.03	0.03	0.01	0.01
Protease Congo R Inh scabies Inh venez CuSO4							1.00	0.01	0.52	0.36	0.35	0.31	0.11
Motility						1.00	0.31	0.04	0.43	0.39	0.46	0.45	0.22
HCN					1.00	0.28	0.08	-0.01	0.19	0.08	0.31	0.32	0.18
ΛN				1.00	0.17	0.08	0.21	0.02	0.27	0.10	0.14	0.12	0.01
Colour			1.00	-0.27	-0.16	-0.14	-0.14	0.04	-0.24	-0.12	-0.14	-0.14	-0.18
nf sample		1.00	0.00	-0.01	-0.06	0.01	0.01	0.10	-0.02	-0.04	-0.10	-0.11	0.03
Inf orchardInf sample Colour	1.00	0.39	0.07	0.05	0.11	0.19	0.17	0.10	0.26	0.13	0.04	-0.01	0.02
_	Inf orchard	Inf sample	Colour	2	HCN	Motility	Protease	Congo R	Inh scabies	Inh venez	CuSO4	Strepto	Kasuga

0.00

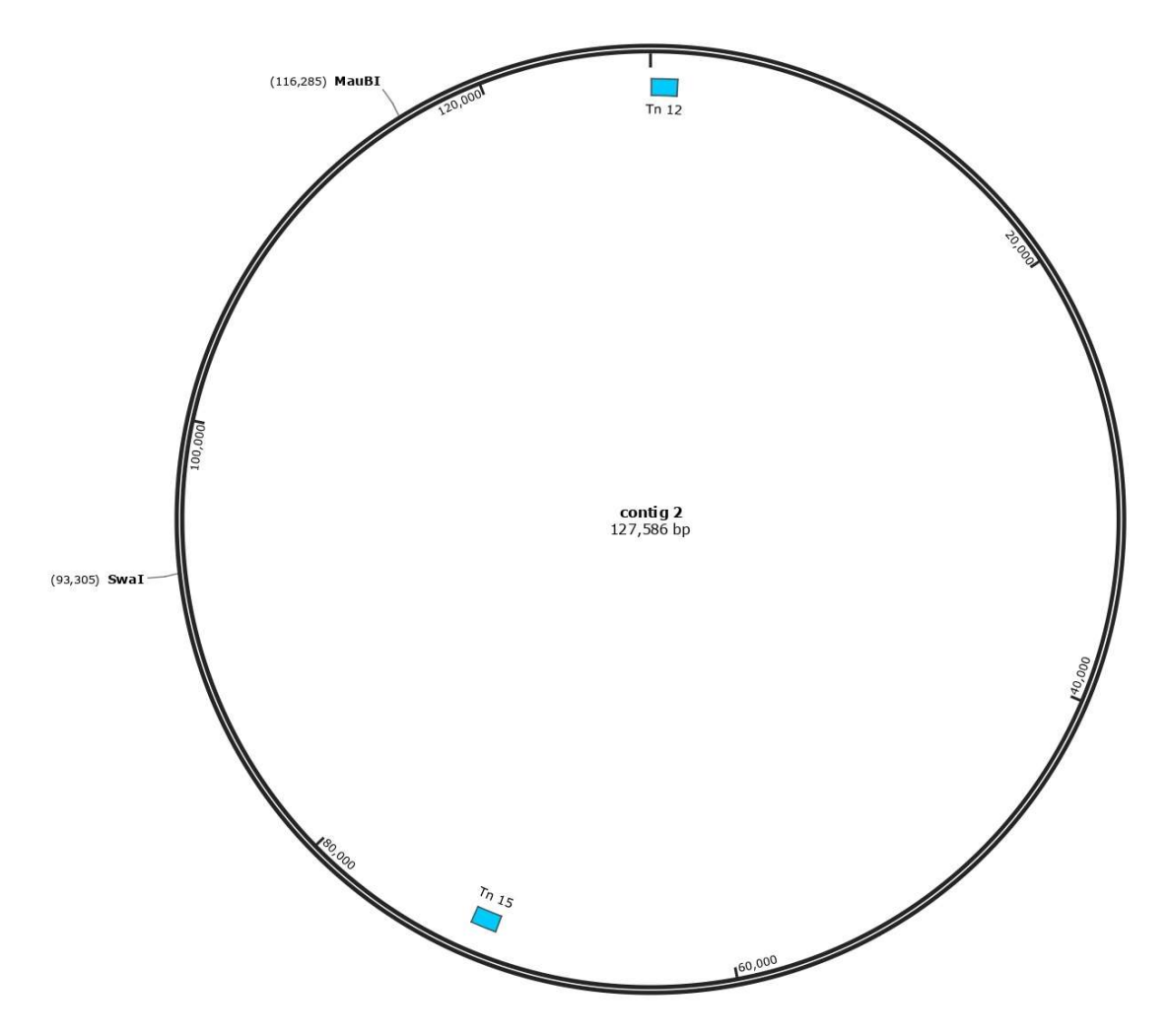
**Supplementary 10.** Correlation analysis with all phenotypic assays from non-inhibitory *Psa* strains. In order, margins abbreviations are infected sample, colour, UV or siderophore production, HCN production, swarming motility, protease production, Congo Red binding, S. scabies, S. venezuelae, Psa (10627) and Psa (RT594) inhibition and copper sulphate, streptomycin and kasugamycin resistance. Values between -1 and 1 indicate negative and positive correlations (Pearson's correlation coefficient).

**Supplementary 11**. Presence and absence of published essential copper resistant genes within the copper resistant *Pseudomonas* strains.

Gene	Copper	сорА	сорВ	сорС	copD	copG	copR	copS	cusA	cusB	cusC	czcD
A00137	1	1	1	1	1	0	1	1	1	0	1	1
A00154	1	0	0	1	1	0	1	1	1	1	1	1
A00155	1	1	1	1	1	0	1	1	1	0	1	1
A00158	1	1	1	1	1	0	1	1	1	1	1	1
A00159	1	0	0	0	1	0	1	0	1	1	0	1
A00162	1	0	0	1	1	1	1	1	1	1	0	1
A00164	1	0	0	1	1	1	1	1	1	1	0	1
A00165	1	0	0	1	1	1	1	1	1	0	0	1
A00166	1	0	0	1	1	0	1	1	1	0	1	1
A00170	1	1	1	1	1	0	1	1	1	1	1	1
A00173	1	1	1	1	1	0	1	1	1	1	1	1
A00175	1	1	1	0	0	0	1	1	1	0	0	0
A00178	1	0	0	1	1	0	1	1	1	1	1	1
A00180	1	1	1	1	1	0	1	1	1	1	1	1
A00183	1	1	1	1	0	0	1	1	1	1	1	1
A00190	1	1	1	1	1	0	1	1	1	0	1	1
A00191	1	0	0	1	1	0	1	0	1	0	0	0
A00194	1	0	0	1	1	0	1	0	1	0	1	0
A00195	1	0	0	1	1	0	1	0	1	0	1	0
A00198	1	0	0	1	1	1	1	1	1	1	0	0
A00201	1	0	0	1	1	0	1	1	1	1	1	0
A00202	1	0	0	1	1	0	1	1	1	1	1	0
A00207	1	0	0	1	1	0	1	1	1	1	1	0
A00208	1	0	0	1	1	0	1	1	1	1	1	1
A00209	1	0	0	1	1	0	1	1	1	1	1	0
A00216	1	0	0	1	1	0	1	0	1	0	1	0
A00222	1	0	0	1	0	0	1	0	1	0	0	0
A00255	1	1	1	1	1	1	1	1	1	0	1	1
A00256	1	1	1	1	1	0	1	1	1	0	1	1
A00260	1	1	1	1	1	0	1	1	1	0	1	1
A00261	1	1	1	1	0	0	1	1	1	0	1	1
A00264	1	0	0	1	1	0	1	0	1	0	1	0
A00270	1	1	1	1	1	0	1	0	1	0	1	1
A00272	1	1	1	1	1	0	1	0	1	0	1	1
A00273	1	1	1	1	1	0	1	0	1	1	1	1
A00274	1	1	1	1	1	0	1	1	1	0	1	1
A00277	1	1	1	1	1	0	1	1	1	0	1	1
A00278	1	1	1	1	1	1	1	1	1	1	1	1
A00279	1	0	0	1	1	1	1	0	1	0	0	1
A00280	1	1	1	1	1	1	1	1	1	0	1	1
A00281	1	1	1	1	1	1	1	1	1	0	1	1
A00282	1	1	1	1	1	0	1	1	1	1	1	1
A00283	1	0	0	1	1	0	1	0	1	0	1	1



**Supplementary 12**. Transposon insertion locations within *Pseudomonas* 10A5 in contig 1. In blue, copper sensitive transposons and in orange, dual copper, and streptomycin sensitive transposons.



**Supplementary 13**. Transposon insertion locations within *Pseudomonas* 10A5 in contig 2. In blue, copper sensitive transposons.

**Supplementary 14.** Biocontrol strains used for biocontrol assays in planta with model plants, bacteria recovered (CFU/cm²) 1 and 5 dpi, and their standard deviations (s.d.).

			B		
Strain L	IK reference	Day 1	Day 5	Day 1	Day 5
		(log10 CFU/cm²)	(log10 CFU/cm²)	(S.D.)	(S.D.)
Biocontrol	3.C5	2.408	1.122	1.162	1.614
Biocontrol	3.D5	2.200	2.111	0.812	1.104
Biocontrol	3.D6	2.675	1.245	0.532	1.334
Biocontrol	4.A9	1.968	1.606	1.256	1.300
Biocontrol	4.C10	3.026	1.329	0.614	1.471
Biocontrol	4.E10	2.358	1.154	1.014	1.218
Biocontrol	4.G11	2.900	0.929	0.773	1.287
Biocontrol	4.H12	2.150	0.260	1.562	0.709
Biocontrol	5.F8	1.891	0.666	1.146	1.472
Biocontrol	5.F9	3.472	1.440	0.435	1.393
Biocontrol	5.G9	3.080	0.801	0.695	1.334
Biocontrol	6.B4	2.795	1.337	0.443	1.165
Biocontrol	6.C7	1.628	0.981	1.706	1.313
Biocontrol	6.D7	3.366	0.844	0.656	1.106
Biocontrol	8.H1	2.369	1.217	1.281	1.103
Biocontrol	8.H7	1.913	0.891	1.455	1.010
Biocontrol	9.H3	3.296	1.974	1.103	1.199
Biocontrol	10.A5	2.350	0.801	0.781	1.262
Biocontrol	10.F12	2.208	1.182	0.970	1.484
Biocontrol	10.G10	2.721	1.839	1.870	1.527
Biocontrol	10.G12	2.541	1.055	1.501	1.300
Biocontrol	11.F1	2.434	1.363	0.681	1.331
Neg. control	1.F3	4.000	3.190	0.617	1.242
Neg. control	1.B11	2.380	2.073	1.460	1.717
Neg. control	4.A5	4.257	3.114	0.653	1.703
Neg. control	4.E8	2.555	2.807	1.223	1.513
Neg. control	7.C7	2.129	2.806	1.988	1.492
Neg. control	7.E9	4.260	3.576	0.759	1.163
Neg. control	9.C1	3.031	2.598	1.179	1.534
Neg. control	10.E12	4.506	2.767	0.333	1.391
Neg. control					

**Supplementary 15**. Kiwifruit cultivar, inoculum used per treatment (CFU/mL) of the kiwifruit biocontrol assay, disease incidence measured by Leaf Doctor (%) and standard deviation.

Reference	Cultivar	Treatment	Inoculum (CFU/mL)	Disease (%)	Standard deviation
		10627	1 · 10 <sup>8</sup>	11.87	5.04
		Aureo® Gold	1.33 · 10 <sup>6</sup>	8.87	2.78
Exp 22-7	Hort16A	JM0626	1 · 10 <sup>8</sup>	8.94	2.7
		JM2875	1.66 · 10 <sup>8</sup>	7.31	2.55
		JM1123	2 · 108	5.83	1.99
		Non inoculated	0	0.93	0.4
Exp 22-8	Hort16A	10627	1.6 · 10 <sup>8</sup>	16.19	4.64
		Aureo® Gold	1 · 10 <sup>6</sup>	14.49	4.3
		JM0626	1.7 · 10 <sup>8</sup>	13.56	5.04
		JM2875	2 · 108	16.98	3.59
		JM1123	1.3 · 108	10.63	3.17
		Non inoculated	0	0.85	0.2
Exp 22-9	Hayward	10627	1.6 · 10 <sup>8</sup>	12.91	4.68
		Aureo® Gold	1 · 10 <sup>6</sup>	2.97	0.9
		JM0626	1.7 · 10 <sup>8</sup>	6.44	4.7
		JM2875	2 · 108	6.08	1.99
		JM1123	1.3 · 108	4.7	2.01
		Non inoculated	0	0.86	0.21
	Hayward	10627	3.3 · 10 <sup>7</sup>	7.29	7.3
		Aureo® Gold	1.66 · 108	2.66	2.1
5 00 40		JM0626	3.43 · 10 <sup>8</sup>	2.38	1.29
Exp 22-12		JM2875	1.96 · 10 <sup>8</sup>	2.05	0.36
		JM1123	2.66 · 10 <sup>8</sup>	1.66	0.92
		Non inoculated	0	0.54	0.13
Exp 22-13		RT594	1 · 108	14.35	10.66
		Aureo® Gold	2.66 · 10 <sup>6</sup>	3	3
		JM0626	4.7 · 10 <sup>8</sup>	4.42	2
		JM2875	3.3 · 10 <sup>8</sup>	2.21	0.61
	Hayward	JM1123	7.3 · 10 <sup>8</sup>	1.93	0.45
		Non inoculated	0	0.45	0.21
		Actigard®	-	1.15	0.16
		Actigard® + Aureo® Gold	2.66 · 10 <sup>6</sup>	0.99	0.13
		Actigard® + JM0626	4.7 · 10 <sup>8</sup>	0.99	0.62
		Actigard® + JM2875	3.3 · 10 <sup>8</sup>	0.91	0.3
		Actigard® + JM1123	7.3 · 10 <sup>8</sup>	1.12	0.55

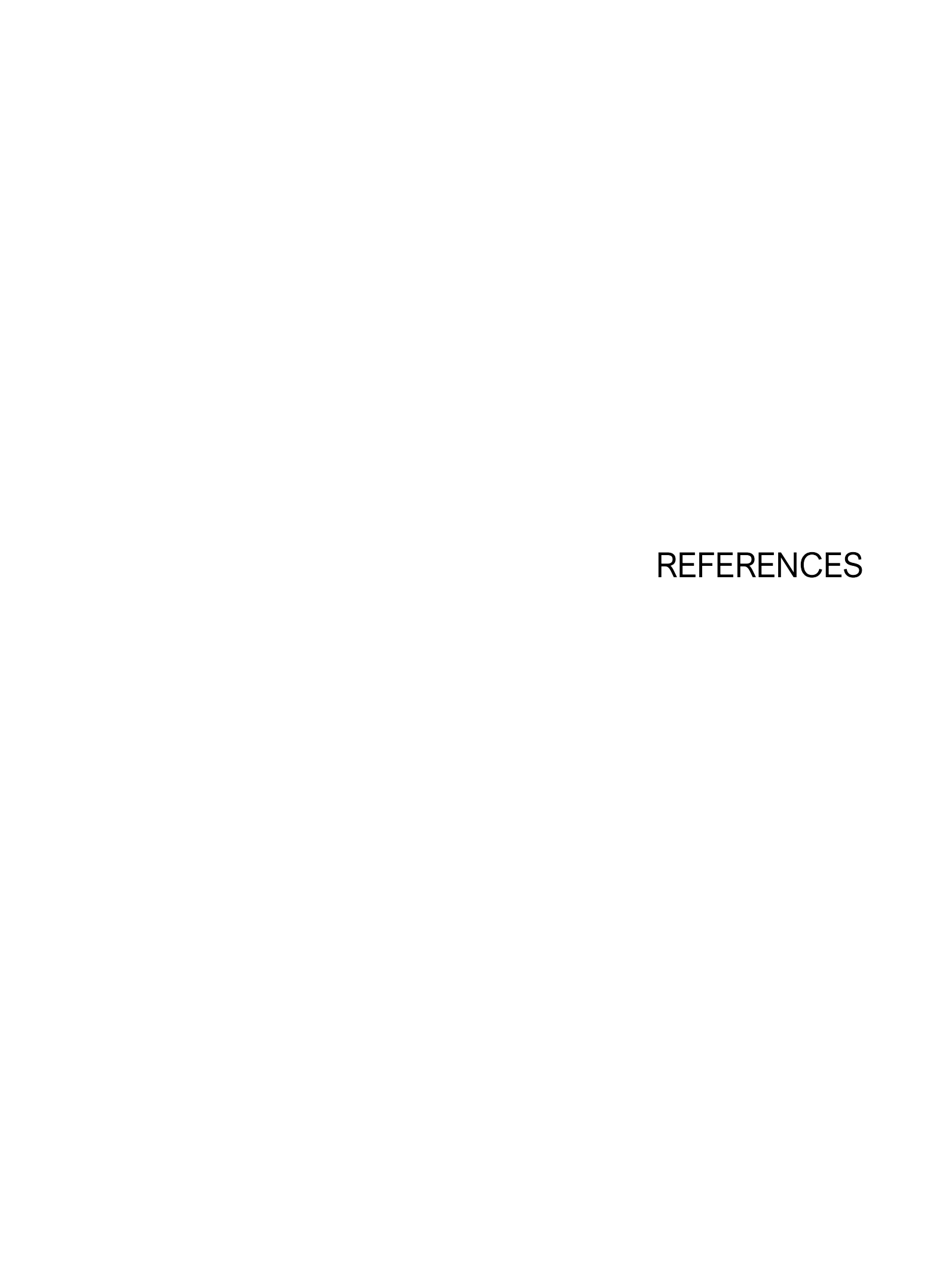


Supplementary 16. Antagonism assay between 4H12, inoculated as a water overlay (OD<sub>600</sub> = 0.01), and 8H7 as a 10  $\mu$ L drop in the middle of the 90 mm plate (OD<sub>600</sub> = 1) 72 hpi.

**Supplementary 17**. Correlation matrix summary from 103 *Pseudomonas* strains and all the predicted BGCs by AntiSMASH. Values between -1 and 1 indicate negative and positive correlations (Pearson's correlation coefficient).

NP	Inh 10627	Inh RT594	NP	Inh 10627	Inh RT594
Acinetobactin	0.058	0.076	Pseudomonine	0.276	0.326
Arylpolyene	-0.041	-0.092	Poaeamide	0.077	0.082
Arthofactin	-0.181	-0.161	Pyochelin	0.258	0.159
Anikasin	-0.028	-0.206	Pyoverdine	-0.156	-0.231
Bacilomycin	-0.066	-0.059	Putisolvin	-0.116	-0.103
Bacteriocin	0.174	0.160	Puwainaphycins	-0.066	-0.059
Bananamides	-0.158	-0.183	Rhizomide A/B/C	-0.337	-0.278
Bicornutin	-0.114	-0.073	Roseaoflavin	0.258	0.291
Butyrolactone	-0.167	-0.148	Ralsolamycin	-0.152	-0.135
Chichofactin	-0.066	-0.059	Ristocetin	-0.066	-0.059
Cichopeptin	-0.218	-0.183	Rimosamide	-0.059	-0.106
Corpeptin	-0.094	-0.084	Safracin	0.258	0.159
Cupriachelin	0.012	-0.054	Serobactins	0.058	0.076
Cyanopeptin	-0.066	-0.059	Siderophore	0.050	-0.101
Daptomycin	-0.094	-0.084	Stenothricin	0.133	0.159
Delftibactin	0.008	0.028	Syringafactin	-0.144	-0.172
Ectoine	0.008	0.028	Syringolin A	-0.113	-0.148
Enduracidin	-0.066	-0.059	Syringomycin	-0.198	-0.216
Enterobactin	-0.066	-0.059	Taiwachelin	-0.059	0.050
Fengycin	0.138	0.038	Teixobacting	-0.066	-0.059
Fragin	0.058	-0.084	Terpene	0.255	0.232
FR900359	0.147	0.166	Thanamycin	0.008	0.028
Glidopeptin	-0.066	-0.059	Thiazostatin	-0.066	-0.059
Hserlactone	-0.114	-0.134	Thiopeptide	0.002	-0.012
Jessenipeptin	-0.098	-0.073	Tolaasin	-0.094	-0.084
Lankacidin	-0.015	-0.073	Turnerbactin	0.147	0.166
Luminmide	-0.116	-0.090	Viscosin	0.060	0.013
Mangotoxin	-0.126	-0.194	Vioprolide	-0.066	-0.059
Mitomycin	0.058	0.076	Welwitindolinone	-0.066	-0.059
Mycosubtilin	-0.094	-0.084	WLIP	0.210	0.076
NAGGN	-0.077	-0.089	Xenematides	-0.066	-0.059
Nostamide	-0.015	0.014	Xenoamicins	-0.116	-0.103
Nunamycin	-0.094	-0.084	Xenotetrapeptide	-0.220	-0.195
Orfamide	-0.094	-0.084			





- Abelleira, A., A. Ares, O. Aguin, J. Penalver, M. C. Morente, M. M. Lopez, M. J. Sainz and J. P. Mansilla (2015). "Detection and characterization of Pseudomonas syringae pv. actinidifoliorum in kiwifruit in Spain." <u>Journal of Applied Microbiology</u> **119**(6): 1659-1671.
- Abelleira, A., A. Ares, O. Aguín, A. Picoaga, M. M. López and P. Mansilla (2014). "Current situation and characterization of Pseudomonas syringae pv. actinidiae on kiwifruit in Galicia (northwest Spain)." <u>Plant Pathology</u> **63**(3): 691-699.
- Abelleira, A., M. M. Lopez, J. Penalver, O. Aguin, J. P. Mansilla, A. Picoaga and M. J. Garcia (2011). "First Report of Bacterial Canker of Kiwifruit Caused by Pseudomonas syringae pv. actinidiae in Spain." <u>Plant Disease</u> **95**(12): 1583-1583.
- Aguín, O., A. Ares, A. Abelleira and P. Mansilla (2015). <u>Survival of Pseudomonas syringae pv. actinidiae in leaf-litter of actinidia deliciosa in Galicia (northwest Spain)</u>. I International Symposium on Bacterial Canker of Kiwifruit, Mt. Maunganui, New Zealand, International Society for Horticultural Science (ISHS), Leuven, Belgium.
- Ahmed, E. and S. J. Holmström (2014). "Siderophores in environmental research: roles and applications." <u>Microb Biotechnol</u> **7**(3): 196-208.
- Akter, S., J. Kadir, A. S. Juraimi and H. M. Saud (2016). "In vitro evaluation of Pseudomonas bacterial isolates from rice phylloplane for biocontrol of Rhizoctonia solani and plant growth promoting traits." <u>J Environ Biol</u> **37**(4): 597-602.
- Alam, K., M. M. Islam, C. Li, S. Sultana, L. Zhong, Q. Shen, G. Yu, J. Hao, Y. Zhang, R. Li and A. Li (2021). "Genome Mining of Pseudomonas Species: Diversity and Evolution of Metabolic and Biosynthetic Potential." Molecules **26**(24).
- Alav, I., J. Kobylka, M. S. Kuth, K. M. Pos, M. Picard, J. M. A. Blair and V. N. Bavro (2021). "Structure, Assembly, and Function of Tripartite Efflux and Type 1 Secretion Systems in Gram-Negative Bacteria." <a href="https://doi.org/10.1001/journal.com/">Chemical Reviews 121(9): 5479-5596</a>.
- Aldayel, M. F. (2019). "Biocontrol strategies of antibiotic-resistant, highly pathogenic bacteria and fungi with potential bioterrorism risks: Bacteriophage in focus." <u>Journal of King Saud University Science</u> **31**(4): 1227-1234.
- Alderley, C. L., S. T. E. Greenrod and V. P. Friman (2022). "Plant pathogenic bacterium can rapidly evolve tolerance to an antimicrobial plant allelochemical." Evolutionary applications **15**(5): 735-750.
- Allard, S. T., M. F. Giraud and J. H. Naismith (2001). "Epimerases: structure, function and mechanism." Cell Mol Life Sci **58**(11): 1650-1665.
- Alsohim, A. S., T. B. Taylor, G. A. Barrett, J. Gallie, X.-X. Zhang, A. E. Altamirano-Junqueira, L. J. Johnson, P. B. Rainey and R. W. Jackson (2014). "The biosurfactant viscosin produced by Pseudomonas fluorescens SBW25 aids spreading motility and plant growth promotion." <a href="Environmental Microbiology"><u>Environmental Microbiology</u></a> 16(7): 2267-2281.
- Andrews, J. H. (1992). "Biological control in the phyllosphere." Annu. Rev. Phytopathol. 30: 603-635.
- Ankenbauer, A., R. A. Schäfer, S. C. Viegas, V. Pobre, B. Voß, C. M. Arraiano and R. Takors (2020). "Pseudomonas putida KT2440 is naturally endowed to withstand industrial-scale stress conditions." <u>Microbial Biotechnology</u> **13**(4): 1145-1161.
- Antognozzi, E., F. Famiani, A. Palliotti and A. Tombesi (1993). <u>Effects of CPPU (cytokinin) on kiwifruit productivity.</u> VII International Symposium on Plant Growth Regulators in Fruit Production, Jerusalem, Israel, International Society for Horticultural Science (ISHS), Leuven, Belgium.
- Ares, A., J. Pereira, E. Garcia, J. Costa and I. Tiago (2021). "The Leaf Bacterial Microbiota of Female and Male Kiwifruit Plants in Distinct Seasons: Assessing the Impact of Pseudomonas syringae pv. actinidiae." <a href="Phytobiomes Journal">Phytobiomes Journal</a> 5(3): 275-287.

Arseneault, T., C. Goyer and M. Filion (2016). "Biocontrol of Potato Common Scab is Associated with High Pseudomonas fluorescens LBUM223 Populations and Phenazine-1-Carboxylic Acid Biosynthetic Transcript Accumulation in the Potato Geocaulosphere." <u>Phytopathology</u> **106**(9): 963-970.

Atkinson, M. M., J. S. Huang and J. A. Knopp (1985). "The Hypersensitive Reaction of Tobacco to Pseudomonas syringae pv. pisi: Activation of a Plasmalemma K/H Exchange Mechanism." <u>Plant Physiol</u> **79**(3): 843-847.

Atwood, J. L. (2017). Comprehensive supramolecular chemistry II, Elsevier.

Balestra, G. M., A. Mazzaglia, A. Quattrucci, M. Renzi and A. Rossetti (2009). "Current status of bacterial canker spread on kiwifruit in Italy." <u>Australasian Plant Disease Notes</u> **4**(1): 34-36.

Balestra, G. M., A. Mazzaglia and A. Rossetti (2008). "Outbreak of Bacterial Blossom Blight Caused by Pseudomonas viridiflava on Actinidia chinensis Kiwifruit Plants in Italy." Plant Dis **92**(12): 1707.

Balestra, G. M., M. Renzi and A. Mazzaglia (2010). "First report of bacterial canker of Actinidia deliciosacaused by Pseudomonas syringae pv. actinidiae in Portugal." New Disease Reports 22.

Balestra, G. M. M., A.; Quattrucci, A.; Spinelli, R.; Graziani, S.; Rossetti, A. (2008). Cancro batterico su Actinidia chinensis. Informatore Agrario. Verona, Edizioni l'Informatore Agrario Srl. **64:** 75-76.

Baltrus, D. A., H. C. McCann and D. S. Guttman (2017). "Evolution, genomics and epidemiology of Pseudomonas syringae: Challenges in Bacterial Molecular Plant Pathology." <u>Molecular Plant Pathology</u> **18**(1): 152-168.

Baltz, R. H. (2017). "Gifted microbes for genome mining and natural product discovery." <u>J Ind Microbiol</u> <u>Biotechnol</u> **44**(4-5): 573-588.

Baltz, R. H. (2019). "Natural product drug discovery in the genomic era: realities, conjectures, misconceptions, and opportunities." <u>Journal of Industrial Microbiology and Biotechnology</u> **46**(3-4): 281-299

Bastas, K. K. and A. Karakaya (2012). "First Report of Bacterial Canker of Kiwifruit Caused by Pseudomonas syringae pv. actinidiae in Turkey." <u>Plant Disease</u> **96**(3): 452-452.

Behnsen, J. and M. Raffatellu (2016). "Siderophores: More than Stealing Iron." <u>mBio</u> 7(6): e01906-01916.

Benoni, R., C. M. Beck, F. Garza-Sanchez, S. Bettati, A. Mozzarelli, C. S. Hayes and B. Campanini (2017). "Activation of an anti-bacterial toxin by the biosynthetic enzyme CysK: mechanism of binding, interaction specificity and competition with cysteine synthase." <u>Sci Rep</u> **7**(1): 8817.

Besset-Manzoni, Y., P. Joly, A. Brutel, F. Gerin, O. Soudière, T. Langin and C. Prigent-Combaret (2019). "Does in vitro selection of biocontrol agents guarantee success in planta? A study case of wheat protection against Fusarium seedling blight by soil bacteria." <u>PLOS ONE</u> **14**(12): e0225655.

Biondi, E., A. Galeone, N. Kuzmanović, S. Ardizzi, C. Lucchese and A. Bertaccini (2013). "Pseudomonas syringae pv. actinidiae detection in kiwifruit plant tissue and bleeding sap." <u>Annals of Applied Biology</u> **162**(1): 60-70.

Blackwell, G. A., M. Hunt, K. M. Malone, L. Lima, G. Horesh, B. T. F. Alako, N. R. Thomson and Z. Iqbal (2021). "Exploring bacterial diversity via a curated and searchable snapshot of archived DNA sequences." PLOS Biology 19(11): e3001421.

Blin, K., S. Shaw, A. M. Kloosterman, Z. Charlop-Powers, G. P. van Wezel, Marnix H. Medema and T. Weber (2021). "antiSMASH 6.0: improving cluster detection and comparison capabilities." <u>Nucleic Acids Research</u> **49**(W1): W29-W35.

Blin, K., S. Shaw, K. Steinke, R. Villebro, N. Ziemert, S. Y. Lee, M. H. Medema and T. Weber (2019). "antiSMASH 5.0: updates to the secondary metabolite genome mining pipeline." <u>Nucleic Acids Res</u> **47**(W1): W81-W87.

- Blumer, C. and D. Haas (2000). "Mechanism, regulation, and ecological role of bacterial cyanide biosynthesis." <u>Arch Microbiol</u> **173**(3): 170-177.
- Bondarczuk, K. and Z. Piotrowska-Seget (2013). "Molecular basis of active copper resistance mechanisms in Gram-negative bacteria." Cell Biol Toxicol **29**(6): 397-405.
- Bonnichsen, L., N. Bygvraa Svenningsen, M. Rybtke, I. de Bruijn, J. M. Raaijmakers, T. Tolker-Nielsen and O. Nybroe (2015). "Lipopeptide biosurfactant viscosin enhances dispersal of Pseudomonas fluorescens SBW25 biofilms." <u>Microbiology (Reading, England)</u> **161**(12): 2289-2297.
- Bourguet, D. and T. Guillemaud (2016). The Hidden and External Costs of Pesticide Use. <u>Sustainable Agriculture Reviews: Volume 19</u>. E. Lichtfouse. Cham, Springer International Publishing: 35-120.
- Boyd, A. and A. M. Chakrabarty (1995). "Pseudomonas aeruginosa biofilms: role of the alginate exopolysaccharide." Journal of Industrial Microbiology **15**(3): 162-168.
- Breckau, D., E. Mahlitz, A. Sauerwald, G. Layer and D. Jahn (2003). "Oxygen-dependent coproporphyrinogen III oxidase (HemF) from Escherichia coli is stimulated by manganese." <u>J Biol Chem</u> **278**(47): 46625-46631.
- Brown, S. D., S. M. Utturkar, D. M. Klingeman, C. M. Johnson, S. L. Martin, M. L. Land, T.-Y. S. Lu, C. W. Schadt, M. J. Doktycz and D. A. Pelletier (2012). "Twenty-One Genome Sequences from Pseudomonas Species and 19 Genome Sequences from Diverse Bacteria Isolated from the Rhizosphere and Endosphere of Populus deltoides." <u>Journal of Bacteriology</u> **194**(21): 5991-5993.
- Bull, C. T., S. H. De Boer, T. P. Denny, G. Firrao, M. Fischer-Le Saux, G. S. Saddler, M. Scortichini, D. E. Stead and Y. Takikawa (2010). "Comprehensive List of Names of Plant Pathogenic Bacteria, 1980-2007." Journal of Plant Pathology **92**(3): 551-592.
- Burr, T. J., M. C. Matteson, C. A. Smith, M. R. Corral-Garcia and T.-C. Huang (1996). "Effectiveness of Bacteria and Yeasts from Apple Orchards as Biological Control Agents of Apple Scab." <u>Biological Control</u> **6**(2): 151-157.
- Butler, M. I., P. A. Stockwell, M. A. Black, R. C. Day, I. L. Lamont and R. T. M. Poulter (2013). "Pseudomonas syringae pv. actinidiae from Recent Outbreaks of Kiwifruit Bacterial Canker Belong to Different Clones That Originated in China." Plos One **8**(2).
- Cameron, A. and V. Sarojini (2014). "Pseudomonas syringae pv. actinidiae: chemical control, resistance mechanisms and possible alternatives." <u>Plant Pathology</u> **63**(1): 1-11.
- Cao, Z., S. Li, J. Lv, H. Gao, G. Chen, T. Awakawa, I. Abe, X. Yao and D. Hu (2019). "Biosynthesis of clinically used antibiotic fusidic acid and identification of two short-chain dehydrogenase/reductases with converse stereoselectivity." Acta Pharmaceutica Sinica B **9**(2): 433-442.
- Carver, T., S. R. Harris, M. Berriman, J. Parkhill and J. A. McQuillan (2012). "Artemis: an integrated platform for visualization and analysis of high-throughput sequence-based experimental data." <u>Bioinformatics</u> **28**(4): 464-469.
- Ceccarelli, D., A. Daccord, M. René and V. Burrus (2008). "Identification of the origin of transfer (oriT) and a new gene required for mobilization of the SXT/R391 family of integrating conjugative elements." <u>J Bacteriol</u> **190**(15): 5328-5338.
- Chang, Q., W. Wang, G. Regev-Yochay, M. Lipsitch and W. P. Hanage (2015). "Antibiotics in agriculture and the risk to human health: how worried should we be?" <u>Evolutionary applications</u> **8**(3): 240-247.
- Chapman, J. R., R. K. Taylor, B. S. Weir, M. K. Romberg, J. L. Vanneste, J. Luck and B. J. R. Alexander (2012). "Phylogenetic Relationships Among Global Populations of Pseudomonas syringae pv. actinidiae." <a href="https://pxyco.org/phytopathology@102">Phytopathology@102</a>(11): 1034-1044.
- Chen, L., H. Jiang, Q. Cheng, J. Chen, G. Wu, A. Kumar, M. Sun and Z. Liu (2015). "Enhanced nematicidal potential of the chitinase pachi from Pseudomonas aeruginosa in association with Cry21Aa." <u>Sci Rep</u> 5: 14395.

- Collina, M., I. Donati, E. Bertacchini, A. Brunelli and F. Spinelli (2016). "Greenhouse assays on the control of the bacterial canker of kiwifruit (Pseudomonas syringae pv. actinidiae)." <u>Journal of Berry Research</u> 6(4): 407-415.
- Colombi, E. (2017). The role of integrative conjugative elements in evolution of the kiwifruit pathogen Pseudomonas syringae pv. actinidiae: a thesis submitted in partial fulfilment of the requirements for the degree of Doctor of Philosophy in Genetics at Massey University, Albany Campus, New Zealand. Doctor of Philosophy (PhD) Doctoral, Massey University.
- Colombi, E., C. Straub, S. Kunzel, M. D. Templeton, H. C. McCann and P. B. Rainey (2017). "Evolution of copper resistance in the kiwifruit pathogen Pseudomonas syringae pv. actinidiae through acquisition of integrative conjugative elements and plasmids." <u>Environ Microbiol</u> **19**(2): 819-832.
- Compant, S., A. Samad, H. Faist and A. Sessitsch (2019). "A review on the plant microbiome: Ecology, functions, and emerging trends in microbial application." <u>Journal of Advanced Research</u> **19**: 29-37.
- Cornish, D., M. Schipper, J. Oldham and J. Vanneste (2017). "Effect of peptones on the ability of plant pathogenic bacteria to grow on media supplemented with copper sulphate." <u>New Zealand Plant Protection(70)</u>: 265-271.
- Coupland, G. M., A. M. C. Brown and N. S. Willetts (1987). "The origin of transfer (oriT) of the conjugative plasmid R46: Characterization by deletion analysis and DNA sequencing." <u>Molecular and General Genetics MGG</u> **208**(1): 219-225.
- Covington, B. C. and M. R. Seyedsayamdost (2022). "Guidelines for metabolomics-guided transposon mutagenesis for microbial natural product discovery." Methods Enzymol **665**: 305-323.
- Crone, W. J., N. M. Vior, J. Santos-Aberturas, L. G. Schmitz, F. J. Leeper and A. W. Truman (2016). "Dissecting Bottromycin Biosynthesis Using Comparative Untargeted Metabolomics." <u>Angew Chem Int Ed Engl</u> **55**(33): 9639-9643.
- Cunnac, S., M. Lindeberg and A. Collmer (2009). "Pseudomonas syringae type III secretion system effectors: repertoires in search of functions." Current Opinion in Microbiology **12**(1): 53-60.
- Cunty, A., S. Cesbron, M. Briand, S. Carrère, F. Poliakoff, M.-A. Jacques and C. Manceau (2016). "Draft genome sequences of five Pseudomonas syringae pv. actinidifoliorum strains isolated in France." Brazilian journal of microbiology: [publication of the Brazilian Society for Microbiology] 47(3): 529-530.
- Cunty, A., F. Poliakoff, C. Rivoal, S. Cesbron, M. L. Saux, C. Lemaire, M. A. Jacques, C. Manceau and J. L. Vanneste (2015). "Characterization of Pseudomonas syringae pv. actinidiae (Psa) isolated from France and assignment of Psa biovar 4 to a de novo pathovar: Pseudomonas syringae pv. actinidifoliorum pv. nov." <u>Plant Pathology</u> **64**(3): 582-596.
- Cycoń, M., A. Mrozik and Z. Piotrowska-Seget (2019). "Antibiotics in the Soil Environment—Degradation and Their Impact on Microbial Activity and Diversity." <u>Frontiers in Microbiology</u> **10**(338).
- Czajkowski, R., T. Maciag, D. M. Krzyzanowska and S. Jafra (2020). Biological Control Based on Microbial Consortia From Theory to Commercial Products. <u>How Research Can Stimulate the Development of Commercial Biological Control Against Plant Diseases</u>. A. De Cal, P. Melgarejo and N. Magan. Cham, Springer International Publishing: 183-202.
- Dagher, F., A. Nickzad, J. Zheng, M. Hoffmann and E. Déziel (2021). "Characterization of the biocontrol activity of three bacterial isolates against the phytopathogen Erwinia amylovora." <u>Microbiologyopen</u> **10**(3): e1202.
- Daniel, S., K. Goldlust, V. Quebre, M. Shen, C. Lesterlin, J. Y. Bouet and Y. Yamaichi (2020). "Vertical and Horizontal Transmission of ESBL Plasmid from Escherichia coli O104:H4." <u>Genes (Basel)</u> 11(10).

Dastogeer, K. M. G., F. H. Tumpa, A. Sultana, M. A. Akter and A. Chakraborty (2020). "Plant microbiome—an account of the factors that shape community composition and diversity." <u>Current Plant Biology</u> **23**: 100161.

Daura-Pich, O., I. Hernández, L. Pinyol-Escala, J. M. Lara, S. Martínez-Servat, C. Fernández and B. López-García (2020). "No antibiotic and toxic metabolites produced by the biocontrol agent Pseudomonas putida strain B2017." <u>FEMS Microbiol Lett</u> **367**(9).

de Jong, H., T. Reglinski, P. A. G. Elmer, K. Wurms, J. L. Vanneste, L. F. Guo and M. Alavi (2019). "Integrated Use of Aureobasidium pullulans Strain CG163 and Acibenzolar-S-Methyl for Management of Bacterial Canker in Kiwifruit." <u>Plants</u> **8**(8): 287.

De Kievit, T. R., M. D. Parkins, R. J. Gillis, R. Srikumar, H. Ceri, K. Poole, B. H. Iglewski and D. G. Storey (2001). "Multidrug efflux pumps: expression patterns and contribution to antibiotic resistance in Pseudomonas aeruginosa biofilms." <u>Antimicrob Agents Chemother</u> **45**(6): 1761-1770.

DeBoy, R. T., E. F. Mongodin, D. E. Fouts, L. E. Tailford, H. Khouri, J. B. Emerson, Y. Mohamoud, K. Watkins, B. Henrissat, H. J. Gilbert and K. E. Nelson (2008). "Insights into plant cell wall degradation from the genome sequence of the soil bacterium Cellvibrio japonicus." J Bacteriol 190(15): 5455-5463.

Denessiouk, K. A., A. I. Denesyuk, J. V. Lehtonen, T. Korpela and M. S. Johnson (1999). "Common structural elements in the architecture of the cofactor-binding domains in unrelated families of pyridoxal phosphate-dependent enzymes." <u>Proteins</u> **35**(2): 250-261.

Deng, J. J., W. Q. Huang, Z. W. Li, D. L. Lu, Y. Zhang and X. C. Luo (2018). "Biocontrol activity of recombinant aspartic protease from Trichoderma harzianum against pathogenic fungi." <a href="Enzyme Microb Technol"><u>Enzyme Microb Technol</u> 112: 35-42.</a>

Deng, M. and R. Misra (1996). "Examination of AsmA and its effect on the assembly of Escherichia coli outer membrane proteins." Mol Microbiol 21(3): 605-612.

Dias, P. J. and I. Sá-Correia (2013). "The drug:H+ antiporters of family 2 (DHA2), siderophore transporters (ARN) and glutathione:H+ antiporters (GEX) have a common evolutionary origin in hemiascomycete yeasts." BMC Genomics 14: 901.

Dietz-Pfeilstetter, A., M. Mendelsohn, A. Gathmann and D. Klinkenbuß (2021). "Considerations and Regulatory Approaches in the USA and in the EU for dsRNA-Based Externally Applied Pesticides for Plant Protection." Frontiers in Plant Science 12.

Donati, I., G. Buriani, A. Cellini, S. Mauri, G. Costa and F. Spinelli (2014). "New insights on the bacterial canker of kiwifruit (Pseudomonas syringae pv. actinidiae)." Journal of Berry Research 4(2): 53-67.

Donati, I., A. Cellini, D. Sangiorgio, J. L. Vanneste, M. Scortichini, G. M. Balestra and F. Spinelli (2020). "Pseudomonas syringae pv. actinidiae: Ecology, Infection Dynamics and Disease Epidemiology." <u>Microb Ecol</u>.

Donot, F., A. Fontana, J. C. Baccou and S. Schorr-Galindo (2012). "Microbial exopolysaccharides: Main examples of synthesis, excretion, genetics and extraction." <u>Carbohydrate Polymers</u> **87**(2): 951-962.

Dreo, T., M. Pirc, M. Ravnikar, I. Zezlina, E. Poliakoff, C. Rivoal, F. Nice and A. Cunty (2014). "First Report of Pseudomonas syringae pv. actinidiae, the Causal Agent of Bacterial Canker of Kiwifruit in Slovenia." <u>Plant Disease</u> **98**(11): 1578-1578.

Durairaj, K., P. Velmurugan, J. H. Park, W. S. Chang, Y. J. Park, P. Senthilkumar, K. M. Choi, J. H. Lee and B. T. Oh (2017). "Potential for plant biocontrol activity of isolated Pseudomonas aeruginosa and Bacillus stratosphericus strains against bacterial pathogens acting through both induced plant resistance and direct antagonism." <u>FEMS Microbiol Lett</u> **364**(23).

Dyk, T., L. Templeton, K. Cantera, P. Sharpe and F. Sariaslani (2004). "Characterization of the Escherichia coli AaeAB Efflux Pump: a Metabolic Relief Valve?" <u>Journal of bacteriology</u> **186**: 7196-7204.

Elnashar, M. (2010). Biopolymers, BoD-Books on Demand.

Embaby, A. M., Y. Heshmat and A. Hussein (2016). "Unusual non-fluorescent broad spectrum siderophore activity (SID EGYII) by Pseudomonas aeruginosa strain EGYII DSM 101801 and a new insight towards simple siderophore bioassay." <u>AMB Express</u> **6**(1): 26.

EPPO (2014). "First report of Pseudomonas syringae pv. actinidiae in Australia." EPPO Bulletin 6(130).

EPPO (2014). "PM 7/120 (1) Pseudomonas syringae pv. actinidiae." EPPO Bulletin 44(3): 360-375.

Esposito, D. and J. J. Scocca (1997). "The integrase family of tyrosine recombinases: evolution of a conserved active site domain." Nucleic Acids Res **25**(18): 3605-3614.

European Commission (2020). Communication from the commission to the European Parliament, the Council, the European Economic and Social Committee and the Committee of the Regions. A Farm to Fork Strategy for a fair, healthy and environmentally-friendly food system. <u>E. Comission</u>. Brussels, Belgium, European Comission: 6-11.

Everett, K. R., R. K. Taylor, M. K. Romberg, J. Rees-George, R. A. Fullerton, J. L. Vanneste and M. A. Manning (2011). "First report of Pseudomonas syringae pv. actinidiae causing kiwifruit bacterial canker in New Zealand." <u>Australasian Plant Disease Notes</u> **6**(1): 67-71.

Fan, H. Y., Z. W. Zhang, Y. Li, X. Zhang, Y. M. Duan and Q. Wang (2017). "Biocontrol of Bacterial Fruit Blotch by Bacillus subtilis 9407 via Surfactin-Mediated Antibacterial Activity and Colonization." <u>Frontiers in Microbiology</u> **8**.

FAO. (2017, January 18, 2019). "Kiwifruit production in 2017." Retrieved April 4, 2019, 2019, from <a href="http://www.fao.org/faostat/en/#data/QC">http://www.fao.org/faostat/en/#data/QC</a>.

Feigl, F. and V. Anger (1966). "Replacement of Benzidine by Copper Ethylacetoacetate and Tetra Base as Spot-Test Reagent for Hydrogen Cyanide and Cyanogen." <u>Analyst</u> **91**(1081): 282-&.

Fernando, D. M. and A. Kumar (2013). "Resistance-Nodulation-Division Multidrug Efflux Pumps in Gram-Negative Bacteria: Role in Virulence." <u>Antibiotics (Basel)</u> **2**(1): 163-181.

Ferrante, P. and M. Scortichini (2009). "Identification of Pseudomonas syringae pv. actinidiae as causal agent of bacterial canker of yellow kiwifruit (Actinidia chinensis Planchon) in central Italy." <u>Journal of Phytopathology</u> **157**(11-12): 768-770.

Ferrante, P. and M. Scortichini (2010). "Molecular and phenotypic features of Pseudomonas syringae pv. actinidiae isolated during recent epidemics of bacterial canker on yellow kiwifruit (Actinidia chinensis) in central Italy." Plant Pathology **59**(5): 954-962.

Firrao, G., E. Torelli, C. Polano, P. Ferrante, F. Ferrini, M. Martini, S. Marcelletti, M. Scortichini and P. Ermacora (2018). "Genomic Structural Variations Affecting Virulence During Clonal Expansion of Pseudomonas syringae pv. actinidiae Biovar 3 in Europe." <u>Frontiers in Microbiology</u> **9**.

Flores, O., C. Prince, M. Nuñez, A. Vallejos, C. Mardones, C. Yañez, X. Besoain and R. Bastías (2018). "Genetic and Phenotypic Characterization of Indole-Producing Isolates of Pseudomonas syringae pv. actinidiae Obtained From Chilean Kiwifruit Orchards." Frontiers in Microbiology **9**(1907).

Frankenberg-Dinkel, N. (2004). "Bacterial Heme Oxygenases." <u>Antioxidants & Redox Signaling</u> **6**(5): 825-834.

Froud, K., K. Everett, J. Tyson, R. Beresford and N. Cogger (2015). "Review of the risk factors associated with kiwifruit bacterial canker caused by Pseudomonas syringae pv. actinidiae." <u>New Zealand Plant Protection</u> **68**: 313-327.

Fujikawa, T. and H. Sawada (2016). "Genome analysis of the kiwifruit canker pathogen Pseudomonas syringae pv. actinidiae biovar 5." <u>Scientific Reports</u> **6**(1): 21399.

Fujikawa, T. and H. Sawada (2019). "Genome analysis of Pseudomonas syringae pv. actinidiae biovar 6, which produces the phytotoxins, phaseolotoxin and coronatine." Sci Rep **9**(1): 3836.

- G. M. Balestra, G. B., A. Cellini, I. Donati, A. Mazzaglia, and F. Spinelli (2018). "First Report of Pseudomonas syringae pv. actinidiae on Kiwifruit Pollen from Argentina." <u>Plant Disease</u> **102**(1): 237-237.
- Gabbianelli, R., R. Scotti, S. Ammendola, P. Petrarca, L. Nicolini and A. Battistoni (2011). "Role of ZnuABC and ZinT in Escherichia coliO157:H7 zinc acquisition and interaction with epithelial cells." <u>BMC Microbiology</u> **11**(1): 36.
- Gallelli, A., S. Talocci, A. L'Aurora and S. Loreti (2011). "Detection of Pseudomonas syringae pv. actinidiae, causal agent of bacterial canker of kiwifruit, from symptomless fruits and twigs, and from pollen." <a href="https://phytopathologia.org/">Phytopathologia Mediterranea</a> 50(3): 462-472.
- Gao, S., H. Wu, W. Wang, Y. Yang, S. Xie, Y. Xie and X. Gao (2013). "Efficient colonization and harpins mediated enhancement in growth and biocontrol of wilt disease in tomato by Bacillus subtilis." <u>Lett Appl Microbiol</u> **57**(6): 526-533.
- Gao, S. F., H. J. Wu, X. F. Yu, L. M. Qian and X. W. Gao (2016). "Swarming motility plays the major role in migration during tomato root colonization by Bacillus subtilis SWR01." Biological Control **98**: 11-17.
- Gao, X., Q. Huang, Z. Zhao, Q. Han, X. Ke, H. Qin and L. Huang (2016). "Studies on the Infection, Colonization, and Movement of Pseudomonas syringae pv. actinidiae in Kiwifruit Tissues Using a GFPuv-Labeled Strain." <u>PloS one</u> **11**(3): e0151169-e0151169.
- Garcia, E., L. Moura, A. Abelleira, O. Aguin, A. Ares and P. Mansilla (2018). "Characterization of Pseudomonas syringae pv. actinidiae biovar 3 on kiwifruit in north-west Portugal." <u>Journal of Applied Microbiology</u> **125**(4): 1147-1161.
- Garrido-Sanz, D., J. P. Meier-Kolthoff, M. Göker, M. Martín, R. Rivilla and M. Redondo-Nieto (2016). "Genomic and Genetic Diversity within the Pseudomonas fluorescens Complex." <u>PLOS ONE</u> **11**(2): e0150183.
- Gatti, D., B. Mitra and B. P. Rosen (2000). "Escherichia coli Soft Metal Ion-translocating ATPases." <u>Journal of Biological Chemistry</u> **275**(44): 34009-34012.
- Geng, X., L. Jin, M. Shimada, M. G. Kim and D. Mackey (2014). "The phytotoxin coronatine is a multifunctional component of the virulence armament of Pseudomonas syringae." <u>Planta</u> **240**(6): 1149-1165.
- Geudens, N. and J. C. Martins (2018). "Cyclic Lipodepsipeptides From Pseudomonas spp. Biological Swiss-Army Knives." <u>Frontiers in Microbiology</u> **9**(1867).
- Ghods, S., I. M. Sims, M. F. Moradali and B. H. Rehm (2015). "Bactericidal Compounds Controlling Growth of the Plant Pathogen Pseudomonas syringae pv. actinidiae, Which Forms Biofilms Composed of a Novel Exopolysaccharide." <u>Appl Environ Microbiol</u> **81**(12): 4026-4036.
- Goh, Y. K., M. Z. H. M. Zoqratt, Y. K. Goh, Q. Ayub and A. S. Y. Ting (2022). "Discovering naturally-occurring microbiota in disease suppressive soil: Potential role of biological elements in suppressing Ganoderma boninense." <u>Biological Control</u> **165**: 104787.
- Greer, G. and C. M. Saunders (2012). The costs of Psa-V to the New Zealand kiwifruit industry and the wider community, Agribusiness and Economics Research Unit. **327**.
- Gross, H. and J. E. Loper (2009). "Genomics of secondary metabolite production by Pseudomonas spp." Nat Prod Rep **26**(11): 1408-1446.
- Gullberg, E., L. M. Albrecht, C. Karlsson, L. Sandegren and D. I. Andersson (2014). "Selection of a multidrug resistance plasmid by sublethal levels of antibiotics and heavy metals." <u>mBio</u> **5**(5): e01918-01914.
- Gurevich, A., V. Saveliev, N. Vyahhi and G. Tesler (2013). "QUAST: quality assessment tool for genome assemblies." <u>Bioinformatics</u> **29**(8): 1072-1075.

- Gyles, C. and P. Boerlin (2014). "Horizontally Transferred Genetic Elements and Their Role in Pathogenesis of Bacterial Disease." <u>Veterinary Pathology</u> **51**(2): 328-340.
- Haas, D. and G. Défago (2005). "Biological control of soil-borne pathogens by fluorescent pseudomonads." Nature Reviews Microbiology **3**(4): 307-319.
- Hall, T., I. Biosciences and C. Carlsbad (2011). "BioEdit: an important software for molecular biology." GERF Bull Biosci **2**(1): 60-61.
- Han, H.-S., Y.-J. Koh, J.-S. Hur and J.-S. Jung (2003). "Identification and characterization of coronatine-producing Pseudomonas syringae pv. actinidiae." <u>Journal of microbiology and biotechnology</u> **13**(1): 110-118.
- Han, H.-S., H.-Y. Nam, Y.-J. Koh, J.-S. Hur and J.-S. Jung (2003). "Molecular Bases of High-Level Streptomycin Resistance in Pseudomonas marginalis and Pseudomonas syringae pv. actinidiae." <u>The Journal of Microbiology</u> **41**(1): 16 21.
- Hannigan, G. D., D. Prihoda, A. Palicka, J. Soukup, O. Klempir, L. Rampula, J. Durcak, M. Wurst, J. Kotowski, D. Chang, R. Wang, G. Piizzi, G. Temesi, D. J. Hazuda, C. H. Woelk and D. A. Bitton (2019). "A deep learning genome-mining strategy for biosynthetic gene cluster prediction." <u>Nucleic Acids Res</u> **47**(18): e110.
- Hassan, K. A., A. J. Brzoska, N. L. Wilson, B. A. Eijkelkamp, M. H. Brown and I. T. Paulsen (2011). "Roles of DHA2 family transporters in drug resistance and iron homeostasis in Acinetobacter spp." <u>J Mol Microbiol Biotechnol</u> **20**(2): 116-124.
- Heimpel, G. E. and N. J. Mills (2017). <u>Biological Control: Ecology and Applications</u>. Cambridge, Cambridge University Press.
- Hennessy, R. C., C. B. W. Phippen, K. F. Nielsen, S. Olsson and P. Stougaard (2017). "Biosynthesis of the antimicrobial cyclic lipopeptides nunamycin and nunapeptin by Pseudomonas fluorescens strain In5 is regulated by the LuxR-type transcriptional regulator NunF." <u>Microbiologyopen</u> **6**(6).
- Henrichsen, J. (1972). "Bacterial Surface Translocation Survey and a Classification." <u>Bacteriological Reviews</u> **36**(4): 478-503.
- Hinchliffe, P., N. P. Greene, N. G. Paterson, A. Crow, C. Hughes and V. Koronakis (2014). "Structure of the periplasmic adaptor protein from a major facilitator superfamily (MFS) multidrug efflux pump." <u>FEBS Lett</u> **588**(17): 3147-3153.
- Hirose, K., Y. Ishiga and T. Fujikawa (2020). "Phytotoxin synthesis genes and type III effector genes of <em>Pseudomonas syringae</em> pv. <em>actinidiae</em> biovar 6 are regulated by culture conditions." <a href="mailto:bioRxiv">bioRxiv</a>: 2020.2004.2025.060921.
- Hug, J. J., D. Krug and R. Müller (2020). "Bacteria as genetically programmable producers of bioactive natural products." Nature Reviews Chemistry.
- Hutchings, M. I., A. W. Truman and B. Wilkinson (2019). "Antibiotics: past, present and future." <u>Current Opinion in Microbiology</u> **51**: 72-80.
- laneva, O. D. (2009). "Mechanisms of bacteria resistance to heavy metals." Mikrobiol Z 71(6): 54-65.
- Iglesias, M. B., M. L. Lopez, G. Echeverria, I. Vinas, L. Zudaire and M. Abadias (2018). "Evaluation of biocontrol capacity of Pseudomonas graminis CPA-7 against foodborne pathogens on fresh-cut pear and its effect on fruit volatile compounds." <u>Food Microbiol</u> **76**: 226-236.
- Ishiga, T., N. Sakata, V. T. Nguyen and Y. Ishiga (2020). "Flood inoculation of seedlings on culture medium to study interactions between Pseudomonas syringae pv. actinidiae and kiwifruit." <u>Journal of General Plant Pathology</u>: 1-9.
- Ishiga, Y., T. Ishiga, S. R. Uppalapati and K. S. Mysore (2011). "Arabidopsis seedling flood-inoculation technique: a rapid and reliable assay for studying plant-bacterial interactions." <u>Plant methods</u> **7**: 32-32.

- lyer, L. M., E. V. Koonin and L. Aravind (2001). "Adaptations of the helix-grip fold for ligand binding and catalysis in the START domain superfamily." Proteins **43**(2): 134-144.
- Jahanshah, G., Q. Yan, H. Gerhardt, Z. Pataj, M. Lämmerhofer, I. Pianet, M. Josten, H.-G. Sahl, M. W. Silby, J. E. Loper and H. Gross (2019). "Discovery of the Cyclic Lipopeptide Gacamide A by Genome Mining and Repair of the Defective GacA Regulator in Pseudomonas fluorescens Pf0-1." <u>Journal of Natural Products</u> **82**(2): 301-308.
- Jarmusch, S. A., J. J. van der Hooft, P. C. Dorrestein and A. K. Jarmusch (2021). "Advancements in capturing and mining mass spectrometry data are transforming natural products research." <u>Natural Product Reports</u> **38**(11): 2066-2082.
- Jing, X., Q. Cui, X. Li, J. Yin, V. Ravichandran, D. Pan, J. Fu, Q. Tu, H. Wang, X. Bian and Y. Zhang (2020). "Engineering Pseudomonas protegens Pf-5 to improve its antifungal activity and nitrogen fixation." <u>Microb Biotechnol</u> **13**(1): 118-133.
- Johnson, C. M. and A. D. Grossman (2015). "Integrative and Conjugative Elements (ICEs): What They Do and How They Work." Annu Rev Genet **49**: 577-601.
- Joshi, P., A. Gupta and V. Gupta (2019). "Insights into multifaceted activities of CysK for therapeutic interventions." 3 Biotech 9(2): 44.
- Kallberg, Y., U. Oppermann, H. Jörnvall and B. Persson (2002). "Short-chain dehydrogenases/reductases (SDRs)." European Journal of Biochemistry **269**(18): 4409-4417.
- Kang, B. R., A. J. Anderson and Y. C. Kim (2018). "Hydrogen Cyanide Produced by Pseudomonas chlororaphis O6 Exhibits Nematicidal Activity against Meloidogyne hapla." Plant Pathol J **34**(1): 35-43.
- Kaplan, A. R., D. G. Musaev and W. M. Wuest (2021). "Pyochelin Biosynthetic Metabolites Bind Iron and Promote Growth in Pseudomonads Demonstrating Siderophore-like Activity." <u>ACS Infect Dis</u> **7**(3): 544-551.
- Kapp, J. R., T. Diss, J. Spicer, M. Gandy, I. Schrijver, L. J. Jennings, M. M. Li, G. J. Tsongalis, D. G. de Castro, J. A. Bridge, A. Wallace, J. L. Deignan, S. Hing, R. Butler, E. Verghese, G. J. Latham and R. A. Hamoudi (2015). "Variation in pre-PCR processing of FFPE samples leads to discrepancies in BRAF and EGFR mutation detection: a diagnostic RING trial." Journal of Clinical Pathology **68**(2): 111-118.
- Karpiński, T. M. and A. Adamczak (2018). "Anticancer Activity of Bacterial Proteins and Peptides." <u>Pharmaceutics</u> **10**(2).
- Keddy, P. A. (1992). "Assembly and response rules: two goals for predictive community ecology." <u>Journal of Vegetation Science</u> **3**(2): 157-164.
- Khan, N. H. and M. Nafees (2017). "Comparative Study of Copper Accumulation and Distribution in Soil of Selected Orchard and NonOrchard Fields." <u>Agricultural Research and Technology Open Access Journal</u> **7**(3).
- Kim, G. H., K. H. Kim, K. I. Son, E. D. Choi, Y. S. Lee, J. S. Jung and Y. J. Koh (2016). "Outbreak and Spread of Bacterial Canker of Kiwifruit Caused by Pseudomonas syringae pv. actinidiae Biovar 3 in Korea." Plant Pathology Journal **32**(6): 545-551.
- Kim, G. H., Y.-S. Lee, J. S. Jung, Y.-J. Koh, R. T. M. Poulter and M. Butler (2020). "Genomic analyses of Pseudomonas syringae pv. actinidiae isolated in Korea suggest the transfer of the bacterial pathogen via kiwifruit pollen." <u>Journal of Medical Microbiology</u> **69**(1): 132-138.
- Kim, H. and J. Yun (2010). "Copper-Catalyzed Asymmetric 1,4-Hydroboration of Coumarins with Pinacolborane: Asymmetric Synthesis of Dihydrocoumarins." <u>Advanced Synthesis & Catalysis</u> **352**(11-12): 1881-1885.
- Kim, M. J., D. H. Chae, G. Cho, D. R. Kim and Y. S. Kwak (2019). "Characterization of Antibacterial Strains against Kiwifruit Bacterial Canker Pathogen." <u>Plant Pathol J</u> **35**(5): 473-485.

Kim, M. J., C. W. Jeon, G. Cho, D. R. Kim, Y. B. Kwack and Y. S. Kwak (2018). "Comparison of Microbial Community Structure in Kiwifruit Pollens." <u>Plant Pathol J</u> **34**(2): 143-149.

King, E. O., Ward, M. K., & Raney, D. E. (1954). Two simple media for the demonstration of pyocyanin and fluorescin. The Journal of laboratory and clinical medicine, 44(2), 301-307.

Koronakis, V., J. Eswaran and C. Hughes (2004). "Structure and function of TolC: the bacterial exit duct for proteins and drugs." <u>Annu Rev Biochem</u> **73**: 467-489.

Krishna, P. S., S. D. Woodcock, S. Pfeilmeier, S. Bornemann, C. Zipfel and J. G. Malone (2021). "Pseudomonas syringae addresses distinct environmental challenges during plant infection through the coordinated deployment of polysaccharides." <u>Journal of Experimental Botany</u> **73**(7): 2206-2221.

Krzyzanowska, D. M., A. Ossowicki, M. Rajewska, T. Maciag, M. Jablonska, M. Obuchowski, S. Heeb and S. Jafra (2016). "When Genome-Based Approach Meets the "Old but Good": Revealing Genes Involved in the Antibacterial Activity of Pseudomonas sp. P482 against Soft Rot Pathogens." Front Microbiol **7**: 782.

Kung, V. L., S. Khare, C. Stehlik, E. M. Bacon, A. J. Hughes and A. R. Hauser (2012). "An rhs gene of Pseudomonas aeruginosa encodes a virulence protein that activates the inflammasome." <u>Proceedings of the National Academy of Sciences</u> **109**(4): 1275-1280.

KVH (2016). CPPU User Guide. <u>Kiwifruit International and Kiwifruit Vine Health</u>. New Zealand, Zespri & KVH. **1:** 2.

Labaer, J., Q. Qiu, A. Anumanthan, W. Mar, D. Zuo, T. V. Murthy, H. Taycher, A. Halleck, E. Hainsworth, S. Lory and L. Brizuela (2004). "The Pseudomonas aeruginosa PA01 gene collection." <u>Genome Res</u> **14**(10b): 2190-2200.

Lamichhane, J. R. and V. Venturi (2015). "Synergisms between microbial pathogens in plant disease complexes: a growing trend." Frontiers in Plant Science 6.

Le Hesran, S., E. Ras, E. Wajnberg and L. W. Beukeboom (2019). "Next generation biological control – an introduction." Entomologia Experimentalis et Applicata 167(7): 579-583.

Lee, E. R., K. F. Blount and R. R. Breaker (2009). "Roseoflavin is a natural antibacterial compound that binds to FMN riboswitches and regulates gene expression." RNA Biol 6(2): 187-194.

Leigh, J. A. and D. L. Coplin (1992). "Exopolysaccharides in plant-bacterial interactions." <u>Annu Rev Microbiol 46</u>: 307-346.

Leipoldt, F., J. Santos-Aberturas, D. P. Stegmann, F. Wolf, A. Kulik, R. Lacret, D. Popadić, D. Keinhörster, N. Kirchner, P. Bekiesch, H. Gross, A. W. Truman and L. Kaysser (2017). "Warhead biosynthesis and the origin of structural diversity in hydroxamate metalloproteinase inhibitors." <a href="Nature Communications">Nature Communications</a> 8(1): 1965.

Lengai, G. M. and J. W. Muthomi (2018). "Biopesticides and their role in sustainable agricultural production." <u>Journal of Biosciences and Medicines</u> **6**(06): 7.

Lerat, E. (2010). "Identifying repeats and transposable elements in sequenced genomes: how to find your way through the dense forest of programs." <u>Heredity (Edinb)</u> **104**(6): 520-533.

Lesk, A. M. (1995). "NAD-binding domains of dehydrogenases." <u>Current Opinion in Structural Biology</u> **5**(6): 775-783.

Letunic, I. and P. Bork (2021). "Interactive Tree Of Life (iTOL) v5: an online tool for phylogenetic tree display and annotation." <u>Nucleic acids research</u> **49**(W1): W293-W296.

Li, C. and R. Stocker (2009). "Heme oxygenase and iron: from bacteria to humans." Redox Report 14(3): 95-101.

Li, H. (2013). "Aligning sequence reads, clone sequences and assembly contigs with BWA-MEM." <u>arXiv preprint arXiv:1303.3997</u>.

- Li, H., B. Handsaker, A. Wysoker, T. Fennell, J. Ruan, N. Homer, G. Marth, G. Abecasis, R. Durbin and G. P. D. P. Subgroup (2009). "The Sequence Alignment/Map format and SAMtools." <u>Bioinformatics</u> **25**(16): 2078-2079.
- Li, X., Y. Xie, M. Liu, C. Tai, J. Sun, Z. Deng and H.-Y. Ou (2018). "oriTfinder: a web-based tool for the identification of origin of transfers in DNA sequences of bacterial mobile genetic elements." <u>Nucleic Acids Research</u> **46**(W1): W229-W234.
- Lindeberg, M., S. Cunnac and A. Collmer (2012). "Pseudomonas syringae type III effector repertoires: last words in endless arguments." <u>Trends Microbiol</u> **20**(4): 199-208.
- Lindow, S. E. and M. T. Brandl (2003). "Microbiology of the Phyllosphere." <u>Applied and Environmental Microbiology</u> **69**(4): 1875-1883.
- Loper, J. E., K. A. Hassan, D. V. Mavrodi, E. W. Davis, C. K. Lim, B. T. Shaffer, L. D. H. Elbourne, V. O. Stockwell, S. L. Hartney, K. Breakwell, M. D. Henkels, S. G. Tetu, L. I. Rangel, T. A. Kidarsa, N. L. Wilson, J. E. V. de Mortel, C. X. Song, R. Blumhagen, D. Radune, J. B. Hostetler, L. M. Brinkac, A. S. Durkin, D. A. Kluepfel, W. P. Wechter, A. J. Anderson, Y. C. Kim, L. S. Pierson, E. A. Pierson, S. E. Lindow, D. Y. Kobayashi, J. M. Raaijmakers, D. M. Weller, L. S. Thomashow, A. E. Allen and I. T. Paulsen (2012). "Comparative Genomics of Plant-Associated Pseudomonas spp.: Insights into Diversity and Inheritance of Traits Involved in Multitrophic Interactions." <u>PloS Genetics</u> 8(7).
- Loreti, S., A. Cunty, N. Pucci, A. Chabirand, E. Stefani, A. Abelleira, G. M. Balestra, D. A. Cornish, F. Gaffuri, D. Giovanardi, R. A. Gottsberger, M. Holeva, A. Karahan, C. D. Karafla, A. Mazzaglia, R. Taylor, L. Cruz, M. M. Lopez, J. L. Vanneste and F. Poliakoff (2018). "Performance of diagnostic tests for the detection and identification of Pseudomonas syringae pv. actinidiae (Psa) from woody samples." European Journal of Plant Pathology **152**(3): 657-676.
- Lu, S., J. Wang, F. Chitsaz, M. K. Derbyshire, R. C. Geer, N. R. Gonzales, M. Gwadz, D. I. Hurwitz, G. H. Marchler, J. S. Song, N. Thanki, R. A. Yamashita, M. Yang, D. Zhang, C. Zheng, C. J. Lanczycki and A. Marchler-Bauer (2020). "CDD/SPARCLE: the conserved domain database in 2020." <u>Nucleic Acids</u> <u>Res</u> **48**(D1): D265-d268.
- Lucena-Aguilar, G., A. M. Sanchez-Lopez, C. Barberan-Aceituno, J. A. Carrillo-Avila, J. A. Lopez-Guerrero and R. Aguilar-Quesada (2016). "DNA Source Selection for Downstream Applications Based on DNA Quality Indicators Analysis." <u>Biopreserv Biobank</u> **14**(4): 264-270.
- M. C. Holeva, P. E. G., and C. D. Karafla (2015). "First Report of Bacterial Canker of Kiwifruit Caused by Pseudomonas syringae pv. actinidiae in Greece." <u>Plant Disease</u> **99**(5): 723-723.
- MacArthur, R. and R. Levins (1967). "The limiting similarity, convergence, and divergence of coexisting species." The american naturalist 101(921): 377-385.
- Majumder, D., J. Kongbrailatpam, E. Suting, B. Kangjam and D. Lyngdoh (2014). Pseudomonas fluorescens: A Potential Biocontrol Agent for Management of Fungal Diseases of Crop Plants: 317-342.
- Malone, J. G., T. Jaeger, C. Spangler, D. Ritz, A. Spang, C. Arrieumerlou, V. Kaever, R. Landmann and U. Jenal (2010). "YfiBNR mediates cyclic di-GMP dependent small colony variant formation and persistence in Pseudomonas aeruginosa." PLoS Pathog 6(3): e1000804.
- Manhart, C. M. and C. S. McHenry (2013). "The PriA Replication Restart Protein Blocks Replicase Access Prior to Helicase Assembly and Directs Template Specificity through Its ATPase Activity \*<sup> </sup>." <u>Journal of Biological Chemistry</u> **288**(6): 3989-3999.
- Mankin, A. (2006). "Antibiotic blocks mRNA path on the ribosome." <u>Nature Structural & Molecular Biology</u> **13**(10): 858-860.
- Marcelletti, S., P. Ferrante, M. Petriccione, G. Firrao and M. Scortichini (2011). "Pseudomonas syringae pv. actinidiae Draft Genomes Comparison Reveal Strain-Specific Features Involved in Adaptation and Virulence to Actinidia Species." PLOS ONE **6**(11): e27297.

Martinez Perez, J. (2020). A pandemic kiwi fruit pathogen. <u>Microbiologist</u>. UK, Socienty for Applied Microbiology. **21**: 29.

Martins dos Santos, V. A. P., K. N. Timmis, B. Tümmler and C. Weinel (2004). Genomic Features of Pseudomonas putida Strain KT2440. <u>Pseudomonas: Volume 1 Genomics. Life Style and Molecular Architecture</u>. J.-L. Ramos. Boston, MA, Springer US: 77-112.

Masi, M., M. Winterhalter and J.-M. Pagès (2019). Outer Membrane Porins. <u>Bacterial Cell Walls and Membranes</u>. A. Kuhn. Cham, Springer International Publishing: 79-123.

Matuszewska, M., T. Maciąg, M. Rajewska, A. Wierzbicka and S. Jafra (2021). "The carbon source-dependent pattern of antimicrobial activity and gene expression in Pseudomonas donghuensis P482." <u>Sci Rep</u> **11**(1): 10994.

Mauchline, T. H., D. Chedom-Fotso, G. Chandra, T. Samuels, N. Greenaway, A. Backhaus, V. McMillan, G. Canning, S. J. Powers, K. E. Hammond-Kosack, P. R. Hirsch, I. M. Clark, Z. Mehrabi, J. Roworth, J. Burnell and J. G. Malone (2015). "An analysis of Pseudomonas genomic diversity in take-all infected wheat fields reveals the lasting impact of wheat cultivars on the soil microbiota." <a href="mailto:Environmental-microbiology">Environmental Microbiology 17(11): 4764-4778</a>.

Mauchline, T. H. and J. G. Malone (2017). "Life in earth - the root microbiome to the rescue?" <u>Curr Opin Microbiol</u> **37**: 23-28.

Mazzaglia, A., D. J. Studholme, M. C. Taratufolo, R. M. Cai, N. F. Almeida, T. Goodman, D. S. Guttman, B. A. Vinatzer and G. M. Balestra (2012). "Pseudomonas syringae pv. actinidiae (PSA) Isolates from Recent Bacterial Canker of Kiwifruit Outbreaks Belong to the Same Genetic Lineage." <u>Plos One</u> **7**(5).

McAtee, P. A., L. Brian, B. Curran, O. van der Linden, N. J. Nieuwenhuizen, X. Chen, R. A. Henry-Kirk, E. A. Stroud, S. Nardozza, J. Jayaraman, E. H. A. Rikkerink, C. G. Print, A. C. Allan and M. D. Templeton (2018). "Re-programming of Pseudomonas syringae pv. actinidiae gene expression during early stages of infection of kiwifruit." <u>BMC Genomics</u> **19**(1): 822.

McCann, H. C., L. Li, Y. F. Liu, D. W. Li, H. Pan, C. H. Zhong, E. H. A. Rikkerink, M. D. Templeton, C. Straub, E. Colombi, P. B. Rainey and H. W. Huang (2017). "Origin and Evolution of the Kiwifruit Canker Pandemic." <u>Genome Biology and Evolution</u> **9**(4): 932-944.

Medema, M. H., K. Blin, P. Cimermancic, V. de Jager, P. Zakrzewski, M. A. Fischbach, T. Weber, E. Takano and R. Breitling (2011). "antiSMASH: rapid identification, annotation and analysis of secondary metabolite biosynthesis gene clusters in bacterial and fungal genome sequences." <u>Nucleic Acids</u> Research **39**(suppl\_2): W339-W346.

Medema, M. H., R. Kottmann, P. Yilmaz, M. Cummings, J. B. Biggins, K. Blin, I. De Bruijn, Y. H. Chooi, J. Claesen and R. C. Coates (2015). "Minimum information about a biosynthetic gene cluster." <u>Nature chemical biology</u> **11**(9): 625-631.

Meena, K. R. and S. S. Kanwar (2015). "Lipopeptides as the antifungal and antibacterial agents: applications in food safety and therapeutics." <u>BioMed research international</u> **2015**: 473050-473050.

Melotto, M., W. Underwood, J. Koczan, K. Nomura and S. Y. He (2006). "Plant stomata function in innate immunity against bacterial invasion." <u>Cell</u> **126**(5): 969-980.

Meparishvili, G. G., L. Gorgiladze, Z. Sikharulidze, M. Muradashvili, L. Koiava, R. Dumbadze and N. Jabnidze (2016). "First Report of Bacterial Canker of Kiwifruit Caused by Pseudomonas syringae pv. actinidiae in Georgia." <u>Plant Disease</u> **100**(2): 517-517.

Mercier, J. and S. E. Lindow (2000). "Role of leaf surface sugars in colonization of plants by bacterial epiphytes." Applied and environmental microbiology **66**(1): 369-374.

Minchev, Z., O. Kostenko, R. Soler and M. J. Pozo (2021). "Microbial Consortia for Effective Biocontrol of Root and Foliar Diseases in Tomato." <u>Frontiers in Plant Science</u> 12.

Misra, R. and Y. Miao (1995). "Molecular analysis of asmA, a locus identified as the suppressor of OmpF assembly mutants of Escherichia coli K-12." Mol Microbiol 16(4): 779-788.

Mitter, B., N. Pfaffenbichler and A. Sessitsch (2016). "Plant-microbe partnerships in 2020." <u>Microbial biotechnology</u> **9**(5): 635-640.

Moffat, A. D., A. Elliston, N. J. Patron, A. W. Truman and J. A. Carrasco Lopez (2021). "A biofoundry workflow for the identification of genetic determinants of microbial growth inhibition." <u>Synth Biol (Oxf)</u> **6**(1): ysab004.

Mordor Intelligence (2021). BIOPESTICIDES MARKET - GROWTH, TRENDS, COVID-19 IMPACT, AND FORECASTS (2022- 2027).

Mota, M. S., C. B. Gomes, I. T. Souza Júnior and A. B. Moura (2017). "Bacterial selection for biological control of plant disease: criterion determination and validation." <u>Brazilian journal of microbiology</u>: [publication of the Brazilian Society for Microbiology] **48**(1): 62-70.

Mukherjee, A., G. K. Chouhan, A. K. Gaurav, D. K. Jaiswal and J. P. Verma (2021). Chapter 9 - Development of indigenous microbial consortium for biocontrol management. <u>New and Future Developments in Microbial Biotechnology and Bioengineering</u>. J. P. Verma, C. A. Macdonald, V. K. Gupta and A. R. Podile, Elsevier: 91-104.

Nakajima, M., M. Goto and T. Hibi (2002). "Similarity between Copper Resistance Genes from Pseudomonas syringae pv. actinidiae and P. syringae pv. tomato." <u>Journal of General Plant Pathology</u> **68**(1): 68-74.

National Center for Biotechnology Information, N. (2022). "PubChem Protein Summary for Protein Q4K3S2." Retrieved September 17, 2022 from <a href="https://pubchem.ncbi.nlm.nih.gov/protein/Q4K3S2">https://pubchem.ncbi.nlm.nih.gov/protein/Q4K3S2</a>.

Neale, H., N. Deshappriya, D. Arnold, M. E. Wood, M. Whiteman and J. T. Hancock (2017). "Hydrogen sulfide causes excision of a genomic island in Pseudomonas syringae pv. phaseolicola." <u>European Journal of Plant Pathology</u> **149**(4): 911-921.

Newton, G. L. and R. C. Fahey (2002). "Mycothiol biochemistry." <u>Archives of Microbiology</u> **178**(6): 388-394.

Nguyen, D. D., A. V. Melnik, N. Koyama, X. Lu, M. Schorn, J. Fang, K. Aguinaldo, T. L. Lincecum, Jr., M. G. Ghequire, V. J. Carrion, T. L. Cheng, B. M. Duggan, J. G. Malone, T. H. Mauchline, L. M. Sanchez, A. M. Kilpatrick, J. M. Raaijmakers, R. De Mot, B. S. Moore, M. H. Medema and P. C. Dorrestein (2016). "Indexing the Pseudomonas specialized metabolome enabled the discovery of poaeamide B and the bananamides." Nat Microbiol 2: 16197.

Nguyen, H. V., N. Nguyen, B. K. Nguyen, A. Lobo and P. A. Vu (2019). "Organic Food Purchases in an Emerging Market: The Influence of Consumers' Personal Factors and Green Marketing Practices of Food Stores." <u>International Journal of Environmental Research and Public Health</u> **16**(6): 1037.

Nikaido, H. and J. M. Pagès (2012). "Broad-specificity efflux pumps and their role in multidrug resistance of Gram-negative bacteria." <u>FEMS Microbiol Rev</u> **36**(2): 340-363.

Nouioui, I., C. Cortés-albayay, L. Carro, J. F. Castro, M. Gtari, F. Ghodhbane-Gtari, H.-P. Klenk, L. S. Tisa, V. Sangal and M. Goodfellow (2019). "Genomic Insights Into Plant-Growth-Promoting Potentialities of the Genus Frankia." <u>Frontiers in Microbiology</u> 10.

Ongena, M. and P. Jacques (2008). "Bacillus lipopeptides: versatile weapons for plant disease biocontrol." <u>Trends in Microbiology</u> **16**(3): 115-125.

Ormeño-Orrillo, E., P. Menna, L. G. Almeida, F. J. Ollero, M. F. Nicolás, E. Pains Rodrigues, A. Shigueyoshi Nakatani, J. S. Silva Batista, L. M. Oliveira Chueire, R. C. Souza, A. T. Ribeiro Vasconcelos, M. Megías, M. Hungria and E. Martínez-Romero (2012). "Genomic basis of broad host range and environmental adaptability of Rhizobium tropici CIAT 899 and Rhizobium sp. PRF 81 which are used in inoculants for common bean (Phaseolus vulgaris L.)." <u>BMC Genomics</u> 13: 735.

- Pacheco-Moreno, A., F. L. Stefanato, J. J. Ford, C. Trippel, S. Uszkoreit, L. Ferrafiat, L. Grenga, R. Dickens, N. Kelly, A. D. H. Kingdon, L. Ambrosetti, S. A. Nepogodiev, K. C. Findlay, J. Cheema, M. Trick, G. Chandra, G. Tomalin, J. G. Malone and A. W. Truman (2021). "Pan-genome analysis identifies intersecting roles for Pseudomonas specialized metabolites in potato pathogen inhibition." <u>eLife</u> 10: e71900.
- Padan, E. (2014). "Functional and structural dynamics of NhaA, a prototype for Na+ and H+ antiporters, which are responsible for Na+ and H+ homeostasis in cells." <u>Biochimica et Biophysica Acta (BBA) Bioenergetics</u> **1837**(7): 1047-1062.
- Park, J.-D., K. Moon, C. Miller, J. Rose, F. Xu, C. C. Ebmeier, J. R. Jacobsen, D. Mao, W. M. Old, D. DeShazer and M. R. Seyedsayamdost (2020). "Thailandenes, Cryptic Polyene Natural Products Isolated from Burkholderia thailandensis Using Phenotype-Guided Transposon Mutagenesis." <u>ACS Chemical Biology</u> **15**(5): 1195-1203.
- Passari, A. K., V. K. Mishra, V. V. Leo, V. K. Gupta and B. P. Singh (2016). "Phytohormone production endowed with antagonistic potential and plant growth promoting abilities of culturable endophytic bacteria isolated from Clerodendrum colebrookianum Walp." Microbiol Res **193**: 57-73.
- Pattemore, D. E., R. M. Goodwin, H. M. McBrydie, S. M. Hoyte and J. L. Vanneste (2014). "Evidence of the role of honey bees (Apis mellifera) as vectors of the bacterial plant pathogen Pseudomonas syringae." <u>Australasian Plant Pathology</u> **43**(5): 571-575.
- Peek, M. E., A. Bhatnagar, N. A. McCarty and S. M. Zughaier (2012). "Pyoverdine, the Major Siderophore in Pseudomonas aeruginosa, Evades NGAL Recognition." <u>Interdiscip Perspect Infect Dis</u> **2012**: 843509.
- Pethybridge, S. J. and S. C. Nelson (2015). "Leaf Doctor: A New Portable Application for Quantifying Plant Disease Severity." Plant Disease 99(10): 1310-1316.
- Pieterse, C. M., C. Zamioudis, R. L. Berendsen, D. M. Weller, S. C. Van Wees and P. A. Bakker (2014). "Induced systemic resistance by beneficial microbes." <u>Annu Rev Phytopathol</u> **52**: 347-375.
- Pimenta, A. L., K. Racher, L. Jamieson, M. A. Blight and I. B. Holland (2005). "Mutations in HlyD, part of the type 1 translocator for hemolysin secretion, affect the folding of the secreted toxin." <u>J Bacteriol</u> **187**(21): 7471-7480.
- Plasterk, R. H., Z. Izsvák and Z. Ivics (1999). "Resident aliens: the Tc1/mariner superfamily of transposable elements." <u>Trends in genetics</u> **15**(8): 326-332.
- Pliego, C., J. I. Crespo-Gómez, A. Pintado, I. Pérez-Martínez, A. de Vicente, F. M. Cazorla and C. Ramos (2019). "Response of the Biocontrol Agent Pseudomonas pseudoalcaligenes AVO110 to Rosellinia necatrix Exudate." Appl Environ Microbiol **85**(3).
- Pollex, J. (2017). "Regulating Consumption for Sustainability? Why the European Union Chooses Information Instruments to Foster Sustainable Consumption." European Policy Analysis **3**(1): 185-204.
- Polz, M. F., E. J. Alm and W. P. Hanage (2013). "Horizontal gene transfer and the evolution of bacterial and archaeal population structure." <u>Trends Genet</u> **29**(3): 170-175.
- Porcheron, G., A. Garenaux, J. Proulx, M. Sabri and C. Dozois (2013). "Iron, copper, zinc, and manganese transport and regulation in pathogenic Enterobacteria: correlations between strains, site of infection and the relative importance of the different metal transport systems for virulence." <u>Frontiers in Cellular and Infection Microbiology</u> 3.
- Prjibelski, A., D. Antipov, D. Meleshko, A. Lapidus and A. Korobeynikov (2020). "Using SPAdes De Novo Assembler." <u>Current Protocols in Bioinformatics</u> **70**(1): e102.
- ProMed. (2011, 2011-03-25). "Bacterial canker, kiwifruit Chile: first report: (O'Higgins, Maule). ." 20110325.0940. from <a href="http://www.promedmail.org/post/20110325.0940">http://www.promedmail.org/post/20110325.0940</a>.

Puértolas-Balint, F., O. Warsi, M. Linkevicius, P.-C. Tang and D. I. Andersson (2019). "Mutations that increase expression of the EmrAB-TolC efflux pump confer increased resistance to nitroxoline in Escherichia coli." <u>Journal of Antimicrobial Chemotherapy</u> **75**(2): 300-308.

Purahong, W., L. Orru, I. Donati, G. Perpetuini, A. Cellini, A. Lamontanara, V. Michelotti, G. Tacconi and F. Spinelli (2018). "Plant Microbiome and Its Link to Plant Health: Host Species, Organs and Pseudomonas syringae pv. actinidiae Infection Shaping Bacterial Phyllosphere Communities of Kiwifruit Plants." Frontiers in Plant Science 9.

Qian, G., S. Fei and M. Y. Galperin (2019). "Two forms of phosphomannomutase in gammaproteobacteria: The overlooked membrane-bound form of AlgC is required for twitching motility of Lysobacter enzymogenes." <a href="Environmental Microbiology">Environmental Microbiology</a> 21(11): 3969-3978.

Quinlan, A. R. and I. M. Hall (2010). "BEDTools: a flexible suite of utilities for comparing genomic features." <u>Bioinformatics</u> **26**(6): 841-842.

Quiñones, A., G. Wandt, S. Kleinstäuber and W. Messer (1997). "DnaA protein stimulates polA gene expression in Escherichia coli." Mol Microbiol **23**(6): 1193-1202.

Raaijmakers, J. M., I. De Bruijn, O. Nybroe and M. Ongena (2010). "Natural functions of lipopeptides from Bacillus and Pseudomonas: more than surfactants and antibiotics." <u>FEMS Microbiol Rev</u> **34**(6): 1037-1062.

Radkov, A. D. and L. A. Moe (2013). "Amino Acid Racemization in Pseudomonas putida KT2440." Journal of Bacteriology **195**(22): 5016-5024.

Rainey, P. B. and M. J. Bailey (1996). "Physical and genetic map of the Pseudomonas fluorescens SBW25 chromosome." Molecular Microbiology 19(3): 521-533.

Rawat, M. and Y. Av-Gay (2007). "Mycothiol-dependent proteins in actinomycetes." <u>FEMS Microbiology</u> <u>Reviews</u> **31**(3): 278-292.

Redondo-Nieto, M., M. Barret, J. Morrissey, K. Germaine, F. Martínez-Granero, E. Barahona, A. Navazo, M. Sánchez-Contreras, J. A. Moynihan, C. Muriel, D. Dowling, F. O'Gara, M. Martín and R. Rivilla (2013). "Genome sequence reveals that Pseudomonas fluorescens F113 possesses a large and diverse array of systems for rhizosphere function and host interaction." BMC Genomics **14**: 54.

Remminghorst, U., I. D. Hay and B. H. Rehm (2009). "Molecular characterization of Alg8, a putative glycosyltransferase, involved in alginate polymerisation." <u>Journal of biotechnology</u> **140**(3-4): 176-183.

Rojas, E. C., R. Sapkota, B. Jensen, H. J. L. Jorgensen, T. Henriksson, L. N. Jorgensen, M. Nicolaisen and D. B. Collinge (2019). "Fusarium Head Blight Modifies Fungal Endophytic Communities During Infection of Wheat Spikes." <u>Microb Ecol</u>.

Ruiz, B., A. Chávez, A. Forero, Y. García-Huante, A. Romero, M. Sánchez, D. Rocha, B. Sánchez, R. Rodríguez-Sanoja, S. Sánchez and E. Langley (2010). "Production of microbial secondary metabolites: regulation by the carbon source." <u>Crit Rev Microbiol</u> **36**(2): 146-167.

Russell, A. H. and A. W. Truman (2020). "Genome mining strategies for ribosomally synthesised and post-translationally modified peptides." <u>Comput Struct Biotechnol J</u> **18**: 1838-1851.

Russell, A. H., N. M. Vior, E. S. Hems, R. Lacret and A. W. Truman (2021). "Discovery and characterisation of an amidine-containing ribosomally-synthesised peptide that is widely distributed in nature." <u>Chemical Science</u> **12**(35): 11769-11778.

Sambrook, J., D. W. Russell, E. F. Fritsch and T. Maniatis (2001). <u>Molecular cloning: a laboratory manual</u>. Cold Spring Harbor, N.Y., Cold Spring Harbor Laboratory Press.

Samsonova, N. N., S. V. Smirnov, I. B. Altman and L. R. Ptitsyn (2003). "Molecular cloning and characterization of Escherichia coli K12 ygjG gene." <u>BMC Microbiol</u> **3**(1): 2.

Santos Kron, A., V. Zengerer, M. Bieri, V. Dreyfuss, T. Sostizzo, M. Schmid, M. Lutz, M. N. P. Remus-Emsermann and C. Pelludat (2020). "Pseudomonas orientalis F9 Pyoverdine, Safracin, and Phenazine

Mutants Remain Effective Antagonists against Erwinia amylovora in Apple Flowers." <u>Appl Environ Microbiol</u> **86**(8).

Sarker, S. D. and L. Nahar (2012). "An introduction to natural products isolation." <u>Methods Mol Biol</u> **864**: 1-25.

Sawada, H. and T. Fujikawa (2019). "Genetic diversity of Pseudomonas syringae pv. actinidiae, pathogen of kiwifruit bacterial canker." <u>Plant Pathology</u> **68**(7): 1235-1248.

Sawada, H., K. Kondo and R. Nakaune (2016). "Novel biovar (biovar 6) of Pseudomonas syringae pv. actinidiae causing -bacterial canker of kiwifruit (Actinidia deliciosa) in Japan." <u>Japanese Journal of Phytopathology</u> **82**(2): 101-115.

Sawada, H., F. Suzuki, I. Matsuda and N. Saitou (1999). "Phylogenetic analysis of Pseudomonas syringae pathovars suggests the horizontal gene transfer of argK and the evolutionary stability of hrp gene cluster." <u>J Mol Evol</u> **49**(5): 627-644.

Scala, V., N. Pucci and S. Loreti (2018). "The diagnosis of plant pathogenic bacteria: a state of art." <u>Front Biosci (Elite Ed)</u> **10**: 449-460.

Schneider, B. L. and L. Reitzer (2012). "Pathway and enzyme redundancy in putrescine catabolism in Escherichia coli." <u>J Bacteriol</u> **194**(15): 4080-4088.

Scortichini , M. (1994). "Occurrence of Pseudomonas syringae pv. actinidiae on kiwifruit in Italy." <u>Plant Pathology</u> **43**(6): 1035-1038.

Scortichini, M., S. Marcelletti, P. Ferrante, M. Petriccione and G. Firrao (2012). "Pseudomonas syringae pv. actinidiae: a re-emerging, multi-faceted, pandemic pathogen." <u>Molecular Plant Pathology</u> **13**(7): 631-640.

Seetharaman, J., D. Kumaran, J. B. Bonanno, S. K. Burley and S. Swaminathan (2006). "Crystal structure of a putative HTH-type transcriptional regulator yxaF from Bacillus subtilis." <u>Proteins</u> **63**(4): 1087-1091.

Sellés Vidal, L., C. L. Kelly, P. M. Mordaka and J. T. Heap (2018). "Review of NAD(P)H-dependent oxidoreductases: Properties, engineering and application." <u>Biochimica et Biophysica Acta (BBA) - Proteins and Proteomics</u> **1866**(2): 327-347.

Serizawa, S., T. Ichikawa, Y. Takikawa, S. Tsuyumu and M. Goto (1989). "Occurrence of Bacterial Canker of Kiwifruit in Japan: Description of Symptoms, Isolation of the Pathogen and Screening of Bactericides." <u>Japanese Journal of Phytopathology</u> **55**(4): 427-436.

Seth-Smith, H. M. B., F. Bonfiglio, A. Cuenod, J. Reist, A. Egli and D. Wuthrich (2019). "Evaluation of Rapid Library Preparation Protocols for Whole Genome Sequencing Based Outbreak Investigation." Front Public Health 7: 241.

Shcherbakova, L. A., T. I. Odintsova, A. A. Stakheev, D. R. Fravel and S. K. Zavriev (2016). "Identification of a Novel Small Cysteine-Rich Protein in the Fraction from the Biocontrol Fusarium oxysporum Strain CS-20 that Mitigates Fusarium Wilt Symptoms and Triggers Defense Responses in Tomato." <u>Frontiers in Plant Science</u> **6**.

Siddiqui, I. A., D. Haas and S. Heeb (2005). "Extracellular protease of Pseudomonas fluorescens CHAO, a biocontrol factor with activity against the root-knot nematode Meloidogyne incognita." <u>Applied and environmental microbiology</u> **71**(9): 5646-5649.

Simbolo, M., M. Gottardi, V. Corbo, M. Fassan, A. Mafficini, G. Malpeli, R. T. Lawlor and A. Scarpa (2013). "DNA Qualification Workflow for Next Generation Sequencing of Histopathological Samples." Plos One **8**(6).

Smith, S. R., I. Pala and M. Benore-Parsons (2006). "Riboflavin binding protein contains a type II copper binding site." <u>J Inorg Biochem</u> **100**(11): 1730-1733.

- Sodini, S. M., K. E. Kemper, N. R. Wray and M. Trzaskowski (2018). "Comparison of Genotypic and Phenotypic Correlations: Cheverud's Conjecture in Humans." <u>Genetics</u> **209**(3): 941-948.
- Sousa, A. M., I. Machado, A. Nicolau and M. O. Pereira (2013). "Improvements on colony morphology identification towards bacterial profiling." <u>Journal of Microbiological Methods</u> **95**(3): 327-335.
- Stajich, J. E., D. Block, K. Boulez, S. E. Brenner, S. A. Chervitz, C. Dagdigian, G. Fuellen, J. G. Gilbert, I. Korf and H. Lapp (2002). "The Bioperl toolkit: Perl modules for the life sciences." <u>Genome research</u> **12**(10): 1611-1618.
- Staunton, J. and K. J. Weissman (2001). "Polyketide biosynthesis: a millennium review." <u>Nat Prod Rep</u> **18**(4): 380-416.
- Stringlis, I. A., H. Zhang, C. M. J. Pieterse, M. D. Bolton and R. de Jonge (2018). "Microbial small molecules weapons of plant subversion." Nat Prod Rep **35**(5): 410-433.
- Surico, G. (2013). "The concepts of plant pathogenicity, virulence/avirulence and effector proteins by a teacher of plant pathology." <u>Phytopathologia Mediterranea</u> **52**(3): 399-417.
- Szweda, P., M. Schielmann, R. Kotlowski, G. Gorczyca, M. Zalewska and S. Milewski (2012). "Peptidoglycan hydrolases-potential weapons against Staphylococcus aureus." <u>Applied Microbiology and Biotechnology</u> **96**(5): 1157-1174.
- Taboada, B., K. Estrada, R. Ciria and E. Merino (2018). "Operon-mapper: a web server for precise operon identification in bacterial and archaeal genomes." <u>Bioinformatics</u> **34**(23): 4118-4120.
- Takikawa Y, S. S., Ichikawa T, Tsuyumu S, Goto M (1989). "Pseudomonas syringae pv. actinidiae pv. nov.: the causal bacterium of canker of kiwifruit in Japan." <u>Annals of the Phytopathological Society of Japan 55(4)</u>: 437-444.
- Tamura, K., M. Imamura, K. Yoneyama, Y. Kohno, Y. Takikawa, I. Yamaguchi and H. Takahashi (2002). "Role of phaseolotoxin production by Pseudomonas syringae pv. actinidiae in the formation of halo lesions of kiwifruit canker disease." <a href="Physiological and Molecular Plant Pathology">Physiological and Molecular Plant Pathology</a> **60**(4): 207-214.
- Tancos, K. A. and K. D. Cox (2017). "Effects of Consecutive Streptomycin and Kasugamycin Applications on Epiphytic Bacteria in the Apple Phyllosphere." Plant Disease **101**(1): 158-164.
- Tangestani, M., P. Broady and A. Varsani (2021). "An investigation of antibacterial activity of New Zealand seaweed-associated marine bacteria." <u>Future Microbiology</u> **16**(15): 1167-1179.
- Teixeira, M., E. Sanchez-Lopez, M. Espina, A. Calpena, A. Silva, F. Veiga, M. Garcia and E. Souto (2018). Emerging Nanotechnologies in Immunology, Elsevier Amsterdam, The Netherlands:.
- Tienda, S., C. Vida, E. Lagendijk, S. de Weert, I. Linares, J. Gonzalez-Fernandez, E. Guirado, A. de Vicente and F. M. Cazorla (2020). "Soil Application of a Formulated Biocontrol Rhizobacterium, Pseudomonas chlororaphis PCL1606, Induces Soil Suppressiveness by Impacting Specific Microbial Communities." Front Microbiol 11: 1874.
- Tobin, J. F. and R. F. Schleif (1990). "Purification and properties of RhaR, the positive regulator of the L-rhamnose operons of Escherichia coli." J Mol Biol **211**(1): 75-89.
- Tontou, R., D. Giovanardi and E. Stefani (2014). "Pollen as a possible pathway for the dissemination of Pseudomonas syringae pv. actinidiae and bacterial canker of kiwifruit." <u>Phytopathologia Mediterranea</u> **53**(2): 333-339.
- Toyotake, Y., M. Nishiyama, F. Yokoyama, T. Ogawa, J. Kawamoto and T. Kurihara (2020). "A Novel Lysophosphatidic Acid Acyltransferase of Escherichia coli Produces Membrane Phospholipids with a cisvaccencyl Group and Is Related to Flagellar Formation." <u>Biomolecules</u> **10**(5): 745.
- Tran, N. T., C. E. Stevenson, N. F. Som, A. Thanapipatsiri, A. S. B. Jalal and T. B. K. Le (2018). "Permissive zones for the centromere-binding protein ParB on the Caulobacter crescentus chromosome." <u>Nucleic Acids Res</u> **46**(3): 1196-1209.

Turner, T. R., E. K. James and P. S. Poole (2013). "The plant microbiome." Genome Biology 14(6): 209.

Upadhyay, A., M. Kochar, M. V. Rajam and S. Srivastava (2017). "Players over the Surface: Unraveling the Role of Exopolysaccharides in Zinc Biosorption by Fluorescent Pseudomonas Strain Psd." <u>Frontiers in Microbiology</u> **8**(284).

Vanneste, J. L. (2012). "Pseudomonas syringae pv. actinidiae (Psa): a threat to the New Zealand and global kiwifruit industry." New Zealand Journal of Crop and Horticultural Science **40**(4): 265-267.

Vanneste, J. L. (2013). "Recent progress on detecting, understanding and controlling Pseudomonas syringae pv. actinidiae: a short review." New Zealand Plant Protection, Vol 56 66: 170-177.

Vanneste, J. L. (2017). "The Scientific, Economic, and Social Impacts of the New Zealand Outbreak of Bacterial Canker of Kiwifruit (Pseudomonas syringae pv. actinidiae)." <u>Annual Review of Phytopathology.</u> Vol 55 **55**: 377-399.

Vanneste, J. L., D. A. Cornish, J. Yu, R. J. Boyd and C. E. Morris (2008). "Isolation of copper and streptomycin resistant phytopathogenic Pseudomonas syringae from lakes and rivers in the central North Island of New Zealand." New Zealand Plant Protection 61(0): 80-85.

Vanneste, J. L., D. Giovanardi, J. Yu, D. A. Cornish, C. Kay, F. Spinelli and E. Stefani (2011). "Detection of Pseudomonas syringae pv. actinidiae in kiwifruit pollen samples." <u>New Zealand Plant Protection</u> **64**: 246-251.

Vanneste, J. L., G. F. McLaren, J. Yu, D. A. Cornish and R. Boyd (2005). "Copper and streptomycin resistance in bacterial strains isolated from stone fruit orchards in New Zealand." <u>New Zealand Plant Protection, Volume 58, 2005. Proceedings of a conference, Wellington, New Zealand, 9-11 August 2005</u>: 101-105.

Vanneste, J. L., F. Poliakoff, C. Audusseau, D. A. Cornish, S. Paillard, C. Rivoal and J. Yu (2011). "First Report of Pseudomonas syringae pv. actinidiae, the Causal Agent of Bacterial Canker of Kiwifruit in France." <u>Plant Disease</u> **95**(10): 1311-1312.

Vanneste, J. L. and M. D. Voyle (2003). "Genetic basis of copper resistance in New Zealand strains of Pseudomonas syringae." New Zealand Plant Protection, Vol 56 56: 109-112.

Vanneste, J. L., J. Yu, D. A. Cornish, J. M. Oldham, F. Spinelli, D. E. Pattemore, B. Moffat and A. d'Accolti (2015). <u>Survival of Pseudomonas syringae pv. actinidiae in the environment</u>. I International Symposium on Bacterial Canker of Kiwifruit, Mt. Maunganui, New Zealand, International Society for Horticultural Science (ISHS), Leuven, Belgium.

Vanneste, J. L., J. Yu, D. A. Cornish, D. J. Tanner, R. Windner, J. R. Chapman, R. K. Taylor, J. F. Mackay and S. Dowlut (2013). "Identification, Virulence, and Distribution of Two Biovars of Pseudomonas syringae pv. actinidiae in New Zealand." <u>Plant Dis</u> **97**(6): 708-719.

Varivarn, K., L. A. Champa, M. W. Silby and E. A. Robleto (2013). "Colonization strategies of Pseudomonas fluorescens Pf0-1: activation of soil-specific genes important for diverse and specific environments." <a href="https://example.colorida.col

Visnovsky, S. B., M. Fiers, A. Lu, P. Panda, R. Taylor and A. R. Pitman (2016). "Draft Genome Sequences of 18 Strains of Pseudomonas Isolated from Kiwifruit Plants in New Zealand and Overseas." <u>Genome Announc</u> **4**(2).

Völksch, B. and R. May (2001). "Biological control of Pseudomonas syringae pv. glycinea by epiphytic bacteria under field conditions." <u>Microbial Ecology</u> **41**(2): 132-139.

Wang, M., J. J. Carver, V. V. Phelan, L. M. Sanchez, N. Garg, Y. Peng, D. D. Nguyen, J. Watrous, C. A. Kapono, T. Luzzatto-Knaan, C. Porto, A. Bouslimani, A. V. Melnik, M. J. Meehan, W. T. Liu, M. Crüsemann, P. D. Boudreau, E. Esquenazi, M. Sandoval-Calderón, R. D. Kersten, L. A. Pace, R. A. Quinn, K. R. Duncan, C. C. Hsu, D. J. Floros, R. G. Gavilan, K. Kleigrewe, T. Northen, R. J. Dutton, D. Parrot, E. E. Carlson, B. Aigle, C. F. Michelsen, L. Jelsbak, C. Sohlenkamp, P. Pevzner, A. Edlund, J. McLean, J. Piel, B. T. Murphy, L. Gerwick, C. C. Liaw, Y. L. Yang, H. U. Humpf, M. Maansson, R. A.

- Keyzers, A. C. Sims, A. R. Johnson, A. M. Sidebottom, B. E. Sedio, A. Klitgaard, C. B. Larson, C. A. B. P, D. Torres-Mendoza, D. J. Gonzalez, D. B. Silva, L. M. Marques, D. P. Demarque, E. Pociute, E. C. O'Neill, E. Briand, E. J. N. Helfrich, E. A. Granatosky, E. Glukhov, F. Ryffel, H. Houson, H. Mohimani, J. J. Kharbush, Y. Zeng, J. A. Vorholt, K. L. Kurita, P. Charusanti, K. L. McPhail, K. F. Nielsen, L. Vuong, M. Elfeki, M. F. Traxler, N. Engene, N. Koyama, O. B. Vining, R. Baric, R. R. Silva, S. J. Mascuch, S. Tomasi, S. Jenkins, V. Macherla, T. Hoffman, V. Agarwal, P. G. Williams, J. Dai, R. Neupane, J. Gurr, A. M. C. Rodríguez, A. Lamsa, C. Zhang, K. Dorrestein, B. M. Duggan, J. Almaliti, P. M. Allard, P. Phapale, L. F. Nothias, T. Alexandrov, M. Litaudon, J. L. Wolfender, J. E. Kyle, T. O. Metz, T. Peryea, D. T. Nguyen, D. VanLeer, P. Shinn, A. Jadhav, R. Müller, K. M. Waters, W. Shi, X. Liu, L. Zhang, R. Knight, P. R. Jensen, B. O. Palsson, K. Pogliano, R. G. Linington, M. Gutiérrez, N. P. Lopes, W. H. Gerwick, B. S. Moore, P. C. Dorrestein and N. Bandeira (2016). "Sharing and community curation of mass spectrometry data with Global Natural Products Social Molecular Networking." Nat Biotechnol 34(8): 828-837.
- Wasserman, S. A., C. T. Walsh and D. Botstein (1983). "Two alanine racemase genes in Salmonella typhimurium that differ in structure and function." <u>Journal of bacteriology</u> **153**(3): 1439-1450.
- Wein, T. and T. Dagan (2020). "Plasmid evolution." Current Biology 30(19): R1158-R1163.
- Weller, D. M. (2007). "Pseudomonas Biocontrol Agents of Soilborne Pathogens: Looking Back Over 30 Years." Phytopathology® **97**(2): 250-256.
- Wilfinger, W. W., K. Mackey and P. Chomczynski (1997). "Effect of pH and ionic strength on the spectrophotometric assessment of nucleic acid purity." <u>Biotechniques</u> **22**(3): 474-476, 478-481.
- Winsor, G. L., E. J. Griffiths, R. Lo, B. K. Dhillon, J. A. Shay and F. S. Brinkman (2016). "Enhanced annotations and features for comparing thousands of Pseudomonas genomes in the Pseudomonas genome database." <u>Nucleic Acids Res</u> **44**(D1): D646-653.
- Wood, D. E. and S. L. Salzberg (2014). "Kraken: ultrafast metagenomic sequence classification using exact alignments." <u>Genome Biology</u> **15**(3): R46.
- Woodcock, S. D. (2016). A Review of Research and Development Undertaken on Psa. New Zealand, Kiwifruit Vine Health: 49.
- Wu, X., S. Monchy, S. Taghavi, W. Zhu, J. Ramos and D. van der Lelie (2011). "Comparative genomics and functional analysis of niche-specific adaptation in Pseudomonas putida." <u>FEMS Microbiol Rev</u> **35**(2): 299-323.
- Xin, X. F. and S. Y. He (2013). "Pseudomonas syringae pv. tomato DC3000: a model pathogen for probing disease susceptibility and hormone signaling in plants." <u>Annu Rev Phytopathol</u> **51**: 473-498.
- Xin, X. F., B. Kvitko and S. Y. He (2018). "Pseudomonas syringae: what it takes to be a pathogen." <u>Nat Rev Microbiol</u> **16**(5): 316-328.
- Yasmin, S., F. Y. Hafeez, M. S. Mirza, M. Rasul, H. M. I. Arshad, M. Zubair and M. Iqbal (2017). "Biocontrol of Bacterial Leaf Blight of Rice and Profiling of Secondary Metabolites Produced by Rhizospheric Pseudomonas aeruginosa BRp3." <u>Frontiers in microbiology</u> **8**: 1895-1895.
- Yeo, C. C., J. M. Tham, S. M. Kwong, S. Yiin and C. L. Poh (1998). "Tn5563, a transposon encoding putative mercuric ion transport proteins located on plasmid pRA2 of Pseudomonas alcaligenes." <u>FEMS Microbiol Lett</u> **165**(2): 253-260.
- Yousefian, N., A. Ornik-Cha, S. Poussard, M. Decossas, M. Berbon, L. Daury, J.-C. Taveau, J.-W. Dupuy, S. Đorđević-Marquardt, O. Lambert and K. M. Pos (2021). "Structural characterization of the EmrAB-TolC efflux complex from E. coli." <u>Biochimica et Biophysica Acta (BBA) Biomembranes</u> **1863**(1): 183488.
- Yu, B. J., B. H. Sung, J. Y. Lee, S. H. Son, M. S. Kim and S. C. Kim (2006). "sucAB and sucCD are mutually essential genes in Escherichia coli." FEMS Microbiology Letters **254**(2): 245-250.
- Zachow, C., G. Jahanshah, I. de Bruijn, C. Song, F. Ianni, Z. Pataj, H. Gerhardt, I. Pianet, M. Lämmerhofer, G. Berg, H. Gross and J. M. Raaijmakers (2015). "The Novel Lipopeptide Poaeamide of

the Endophyte Pseudomonas poae RE\*1-1-14 Is Involved in Pathogen Suppression and Root Colonization." Mol Plant Microbe Interact 28(7): 800-810.

Zeng, H., W. Yang, C. Lu, W. Lin, M. Zou, H. Zhang, J. Wan and X. Huang (2016). "Effect of CPPU on Carbohydrate and Endogenous Hormone Levels in Young Macadamia Fruit." <u>PloS one</u> **11**(7): e0158705-e0158705.

Zgurskaya, H. I., G. Krishnamoorthy, A. Ntreh and S. Lu (2011). "Mechanism and Function of the Outer Membrane Channel TolC in Multidrug Resistance and Physiology of Enterobacteria." <u>Front Microbiol</u> **2**: 189.

Zhao, S. and C. W. Hill (1995). "Reshuffling of Rhs components to create a new element." <u>J Bacteriol</u> **177**(5): 1393-1398.

Zhi, J., E. Mathew and M. Freundlich (1998). "In vitro and in vivo characterization of three major dadAX promoters in Escherichia coli that are regulated by cyclic AMP-CRP and Lrp." <u>Molecular and General Genetics MGG</u> **258**(4): 442-447.